



Pedro Ferreira Da Mota Mónica De Oliveira

# CONTRIBUTION TO THE KNOWLEDGE OF DINOFLAGELLATE CYSTS FROM THE UPPER CRETACEOUS OF PORTUGAL: STUDY OF THE LAGOONAL ASSOCIATIONS FROM THE CENOMANIAN OF NAZARÉ

Dissertação de Mestrado em Geociências, na Área de Especialização em Geologia do Petróleo, orientada pelo Professor Doutor Pedro Callapez Tonicher e pela Professora Doutora Lúcia Sousa Castro e apresentada à Faculdade de Ciências e Tecnologia da Universidade de Coimbra

Fevereiro de 2017



UNIVERSIDADE DE COIMBRA

Foto: Pedro Miranda, Fevereiro 2014  
(retirada de <https://i.ytimg.com/vi/awjMSjic268/maxresdefault.jpg> com autorização do autor)



————— *Pedro Ferreira Da Mota Mónica De Oliveira* —————

CONTRIBUTION TO THE KNOWLEDGE OF  
DINOFLAGELLATE CYSTS FROM THE UPPER  
CRETACEOUS OF PORTUGAL: STUDY OF  
THE LAGOONAL ASSOCIATIONS FROM  
THE CENOMANIAN OF NAZARÉ

*Dissertação de Mestrado em Geociências, na Área de Especialização  
em Geologia do Petróleo, orientada pelo Professor Doutor Pedro Callapez Tonicher  
e pela Professora Doutora Lígia Sousa Castro e apresentada à Faculdade de Ciências  
e Tecnologia da Universidade de Coimbra*

COIMBRA – 2017



*A meus Pais e Avós.*



---

## *Agradecimentos*

Dirijo em primeiro lugar os meus sinceros e profundos agradecimentos aos meus orientadores, Professor Pedro Miguel Callapez e Professora Lúgia Castro, pela oportunidade que me deram, bem como à Doutora Zélia Pereira, pela sua colaboração inestimável.

Ao Professor Pedro Callapez, agradeço a disponibilidade para orientar um tema dentro da minha área de interesse, bem como toda a ajuda prestada, tanto no campo como com a bibliografia disponibilizada. Agradeço igualmente o facto de me ter dado a oportunidade de trabalhar e aprender com a Professora Lúgia Castro, na Universidade Nova de Lisboa, e com a Doutora Zélia Pereira, no Laboratório Nacional de Energia e Geologia (LNEG). Agradeço, por fim, a sua contagiante boa disposição e o acompanhamento continuado que me deu, bem como a confiança que depositou em mim e nesta Tese de Mestrado.

À Professora Lúgia Castro agradeço a hospitalidade com que me recebeu na Universidade Nova, em Lisboa, e a disponibilização das instalações do Departamento de Ciências da Terra, bem como de todo o material necessário para a concretização da parte prática da dissertação, além de toda a bibliografia complementar que colocou à minha disposição. Agradeço igualmente o seu empenho no acompanhamento do meu trabalho e os conhecimentos que me transmitiu ao longo dos meses em que tive oportunidade de trabalhar a seu lado.

À Doutora Zélia Pereira agradeço igualmente, em primeiro lugar, a hospitalidade com que fui recebido no seu local de trabalho, o Laboratório Nacional de Energia e Geologia, no Porto, e todo o conhecimento e paixão que me transmitiu pelas áreas da Micropaleontologia e Palinologia. Expresso também o meu agradecimento pela disponibilização de todo o material teórico e de laboratório, que muito ajudaram na elaboração da dissertação, bem como a revisão cuidada das estampas e capítulos. Foi, para mim, um prazer ter tido a oportunidade de trabalhar com a Doutora Zélia

Pereira, a quem agradeço uma vez mais toda a simpatia, paciência e empenho.

Deixo também um agradecimento à Marta Costa pelo cuidado e paciência com que me mostrou os procedimentos e etapas para a montagem de lâminas delgadas, que utilizou na sua dissertação de Mestrado, bem como pelos conselhos dados e pela sua simpatia.

Queria deixar ainda uma mensagem de gratidão ao Doutor Narciso Ferreira pela amável hospitalidade com que me recebeu no LNEG.

Ao Senhor Fernando, técnico de laboratório do LNEG, o meu sentido agradecimento pela demonstração dos procedimentos laboratoriais necessários para a montagem das lâminas posteriormente observadas ao microscópio. Terei saudades das nossas partidas de bilhar nas horas livres.

Aos meus colegas e amigos do Departamento de Ciências da Terra da Universidade de Coimbra deixo igualmente um reconhecido agradecimento, pelos anos e bons momentos que partilhámos durante a Licenciatura e Mestrado. Desejo sorte e sucesso a todos.

À minha família, deixo o meu maior agradecimento, pelo seu apoio incondicional e por estarem sempre presentes. Esta dissertação, tal como todas as etapas importantes da minha vida, é dedicada a vós.



---

## *Resumo*

A presente dissertação apresenta uma análise estratigráfica e palinológica integrada de uma secção de Cretácico Superior amostrada nos níveis basais da sucessão carbonatada exposta na arriba sul do promontório da Nazaré, com particular incidência no estudo quantitativo dos quistos de dinoflagelados de parede orgânica. Com uma idade Cenomaniano inferior terminal a médio, esta secção tem sido interpretada como registando a transição de um ambiente marinho aberto de plataforma interna a ambiente marginal marinho restrito (lagunar) entre o final do Cenomaniano inferior e o início do Cenomaniano médio. Onze amostras foram recolhidas em quatro níveis margosos selecionados ao longo do perfil estratigráfico e preparadas para análise ao microscópio, através de técnicas palinológicas normalizadas. Nove amostras ofereceram um conteúdo palinológico diversificado, incluindo quistos de dinoflagelados, esporos, grãos de pólen, foraminíferos, algas e acritarcas. As associações de dinoquistos apresentaram uma diversidade reduzida, sendo fortemente dominadas pelo peridinióide eurialino *Subtilisphaera* sp.. As inferências paleoambientais e paleoecológicas autorizadas pelos dinoquistos foram consistentes com reconstituições paleogeográficas de um ambiente lagunar propostas anteriormente para o Cenomaniano médio da região da Nazaré. A idade sugerida da sucessão estratigráfica, com base nas associações de dinoquistos, foi cenomaniana inferior a superior, mais tardia do que a idade cenomaniana inferior a média suportada pela convergência de vários outros indicadores bioestratigráficos. Não se verificaram ganhos de resolução bioestratigráfica relativamente à distinção entre subandares do Cenomaniano. As comparações com associações coevas de dinoquistos do Noroeste da Europa e com associações do Cretáceo Superior da Plataforma Castelhana acentuaram, sobretudo, a especificidade paleoambiental marcada do setor da Nazaré durante o Cenomaniano médio, com características de tipo lagunar.

**Palavras-Chave:** Quistos de Dinoflagelados, Bioestratigrafia, Palaeoecologia, Cenomaniano, Nazaré.



---

## *Abstract*

This work consists of an integrated stratigraphic and palynological analysis of an Upper Cretaceous section sampled at the base of the carbonate succession exposed on the south side of the Nazaré promontory, with a particular focus on the quantitative study of organic-walled dinocysts. The studied section has a proposed late early-middle Cenomanian age, and has been interpreted as recording a transition from an open inner shelf during the late early Cenomanian to a marginal-marine lagoonal environment at the early middle Cenomanian. A total of 11 bulk samples were collected from four marly layers selected along the section and subsequently prepared for microscopic analysis following standard palynological techniques. Nine of them yielded a diversified palynological content, including dinocysts, miospores, foraminifera test linings, blue-green algae and acritarchs. Dinocysts assemblages presented a relatively low diversity and were strongly dominated by the euryhaline peridinioid *Subtilisphaera* sp.. Dinocysts-based palaeoenvironmental and palaeoecological inferences were consistent with previous palaeogeographic reconstructions of a mid-Cenomanian lagoonal setting for the Nazaré range. The suggested age of the sampled succession, when based on dinocysts, is older than the upper Cenomanian, but higher than the lower to middle Cenomanian dating robustly supported by several other biostratigraphic markers. No improvement of the biostratigraphic resolution of Cenomanian substages could be obtained. Comparisons with coeval dinocysts assemblages of Northwest Europe and Upper Cretaceous assemblages of the Castilian Platform were mostly supportive of a highly specific local mid-Cenomanian palaeoenvironment in the Nazaré sector, with characteristics of a lagoonal type.

**Key-words:** Dinoflagellate cysts, Biostratigraphy, Palaeoecology, Cenomanian, Nazaré (West Portugal).



---

# Table of Contents

<b>13</b>	<b>1. Introduction</b>
13	1.1. Presentation and pertinence of the theme
16	1.2. Objectives of the study
17	1.3. Structure of the work
<b>19</b>	<b>2. Geological Setting</b>
<b>25</b>	<b>3. Stratigraphic Framework: the Portuguese Cenomanian-Turonian carbonate formations</b>
25	3.1. Historical overview of research
26	3.2. General lithostratigraphy and biostratigraphy
30	3.3. Local stratigraphic setting: the “Sítio da Nazaré Formation”
35	3.4. The surveyed stratigraphic profile
<b>39</b>	<b>4. Dinoflagellates Biology and Morphology</b>
39	4.1. Importance of the Dinoflagellates
40	4.2. Defining features
40	4.2.1. <i>Flagella</i>
41	4.2.2. <i>Dinokaryon</i>
42	4.2.3. <i>Other dinoflagellates ultrastructures</i>
44	4.3. Tabulation in dinoflagellates
45	4.4. Dinoflagellates lifecycle
47	4.5. Dinocysts morphology
47	4.5.1. <i>Cyst wall</i>
48	4.5.2. <i>Surface relief</i>
49	4.5.3. <i>Archeopyle</i>
50	4.5.4. <i>Paratabulation</i>
<b>51</b>	<b>5. Dinoflagellates taxonomy, stratigraphical distribution and palaeology</b>
51	5.1. Taxonomy

55	5.2. Dinocyst Biostratigraphy
55	5.2.1. <i>Relation to main geochronological units</i>
58	5.2.2. <i>Dinocyst biozonations</i>
60	5.2.3. <i>Dinocyst stratigraphic studies in Portugal (Mesozoic-Cenozoic)</i>
62	5.3. Ecology and Palaeology
63	5.3.1. <i>The ecological classification of organic-walled dinocysts: ground concepts</i>
66	5.3.2. <i>Dinocysts-based environmental signals and new sets of environmental factors</i>
68	5.3.3. <i>Dinocysts-based palaeology</i>
<b>71</b>	<b>6. Method and Procedures</b>
71	6.1. Sampling
73	6.2. Palynological processing
<b>79</b>	<b>7. Results</b>
79	7.1. Groups of palynomorphs and their relative abundance
85	7.2. Relevant palynological ratios
91	7.3. Characterization of dinocysts assemblages
100	7.4. Characterization of other palynomorphs assemblages
102	7.5. Dinocyst-based biostratigraphy
104	7.6. Comparison with other Cretaceous dinocysts assemblages
<b>111</b>	<b>8. Final Discussion</b>
111	8.1. Palaeoenvironmental and palaeoecological implications
115	8.2. Biostratigraphical implications
115	8.3. Comparative views with other Cretaceous dinocysts assemblages
<b>117</b>	<b>References</b>
<b>141</b>	<b>APPENDIX: Plates 1 to 42</b>

## *Chapter 1*

---

# INTRODUCTION

### **1.1. PRESENTATION AND PERTINENCE OF THE THEME**

The Western Portuguese Carbonate Platform (WPCP) is one of several European and North-African extended rimmed shelves that bordered the northern branch of the Tethyan Realm during a long term interval of worldwide sea level increase and eustatic highstand that occurred at the middle part of Cretaceous Period (e.g. Haq, 2014; Hancock & Kaufman, 1979; Hardenbol *et al.*, 1998; Hart, 1990). Its depositional setting is related to the Cretaceous development of the Estremadura and Beira Litoral onshore sectors of the West Iberian Margin, after the post-rifting stage of the Lusitanian Basin (Wilson, 1988; Wilson, Hiscott, Willis, & Gradstein, 1989; Pinheiro, Wilson, Reis, Whitmarsh, & Ribeiro, 1996; Kullberg, Rocha, Soares, Rey, Terrinha, *et al.*, 2006; Rey, Dinis, Callapez, & Cunha, 2006; Dinis, Rey, Cunha, Callapez, & Reis 2008). Gradually settled during the Albian and Cenomanian stages and persisting to the end of Lower Turonian, its carbonate facies are presently widely documented along the onshore of the Western Portuguese Margin or Mesozoic West Portuguese Border (Soares & Rocha, 1984), in between the parallels of Aveiro and Lisbon (Callapez, 2008). Due to its location between North and Central Atlantic and North Africa, the WPCP has been the subject of recurrent interest concerning the biotic differentiation and mixing across the Tethyan and Temperate realms, particularly as regards the biogeographical distribution of rudist reefs and reef building corals, other benthic faunas and ammonites (Callapez, 2008).

Among the Cenomanian-Turonian carbonate exposures, the one of Nazaré,

adjoining the fishing village by the same name (see Fig. 1A and B), occupies a hinge position between the northern and the southern domains of the WPCP which, especially after the middle Cenomanian, display rather distinct facies: limestones with rudists and coral buildups at the south, and marly limestones with ammonites at the north (Choffat, 1900; Berthou, 1973, 1984a, 1984b, 1984c, 1984d; Berthou, Chancellor, & Lauverjat, 1985; Berthou & Lauverjat, 1979; Lauverjat, 1982; Callapez, 1998).

This outcrop presents an extended Late Cretaceous sequence, ranging from “Bellasian” (Choffat’s (1900) sensu) layers of Albian/early Cenomanian age to the lower Turonian (still additionally overlain by Campanian–Maastrichtian siliciclastics) (Antunes, 1979), and its thick succession of Cenomanian lagoonal marls and limestones are particularly suitable to the study of fossil content (Callapez *et al.*, 2014). For those reasons, it has long been the subject of systematic stratigraphical and palaeontological studies (for a review, see Callapez, 1998, 2008; Hart *et al.*, 2005). Distinct macro and micro faunas have been considered in local biostratigraphical and palaeoenvironmental studies, or in regional ones that included Nazaré. After the pioneering monographs of Paul Choffat (1849–1919), whose datings were mainly based on ammonite assemblages (Choffat, 1898, 1900), the French workers Pierre-Yves Berthou (1973, 1984a, 1984b, 1984c, 1984d) and Jacques Lauverjat (1982) reviewed aspects of the biostratigraphical setting and resorted to foraminifera and ostracods as stratigraphical biomarkers integrated with ammonoids, echinoids and other additional biostratigraphical data. More recently, cephalopod (particularly ammonites) assemblages (Callapez, 1998, 1999, 2001, 2004, 2008; Callapez & Soares, 2001; Barroso-Barcenilla, Callapez, Soares, & Segura, 2011) and the foraminifera biostratigraphy (Hart *et al.*, 2005) were thoroughly revised from the 1990s onward, together with detailed analysis of macrobenthic invertebrate associations (Callapez, 1998, 2008) and vertebrate remains of the Cenomanian lagoonal levels, including fish, turtle, and crocodyliform specimens (Callapez, 1998; Callapez *et al.*, 2014), for biostratigraphic and palaeoecological purposes.



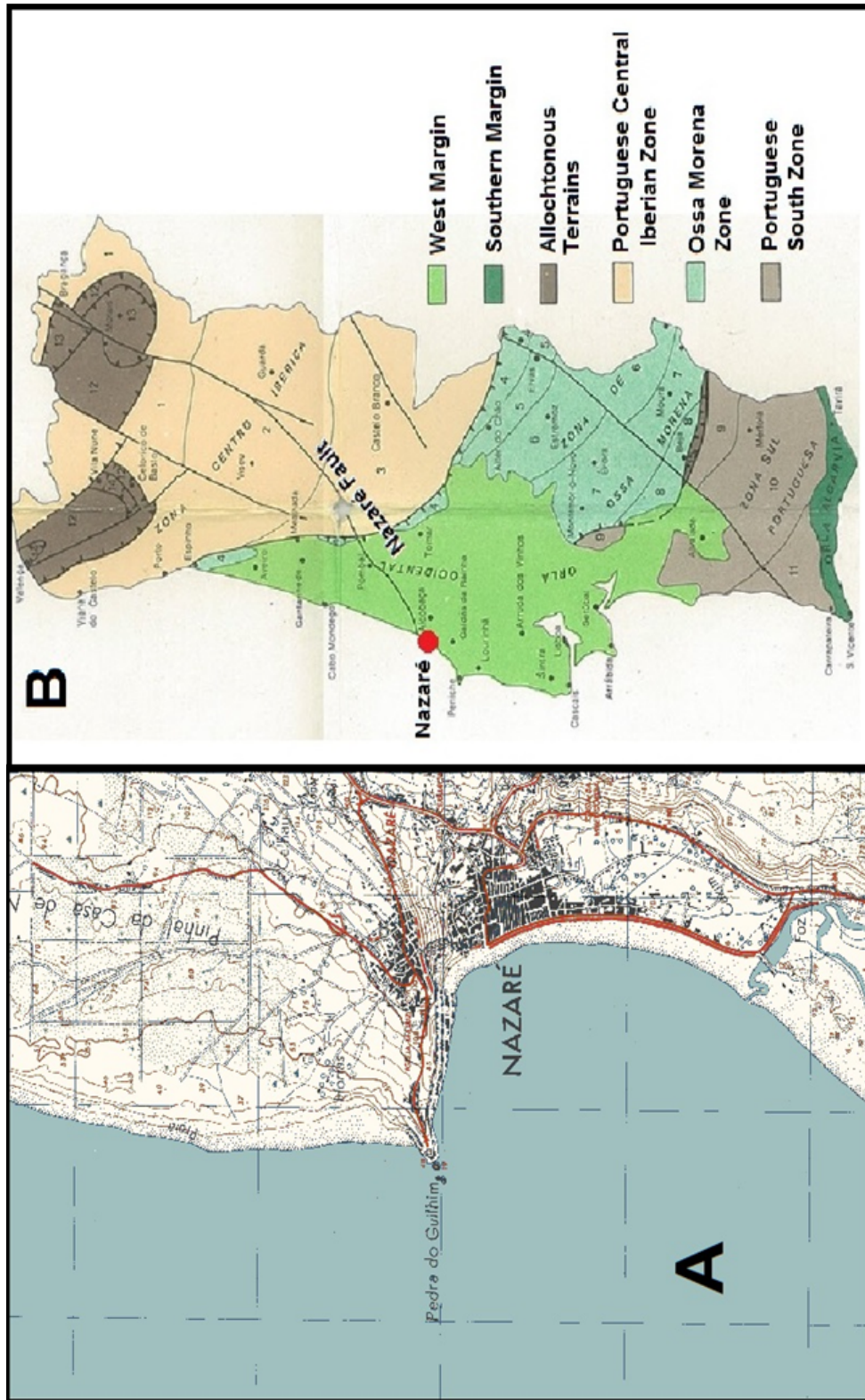


Figure 1 - A. Local topographic view of Nazaré. B. Tectono-stratigraphic scheme of Portugal (adapted from the Geological Map of Portugal -1:500000, 1992).

Despite several examples of the use of dinoflagellate cysts as biomarkers in Cenomanian deposits of the WPCP (*e.g.*, Berthou, Foucher, Lecocq & Moron, 1980; Moron, 1981; Berthou & Hasenboehler, 1982), there are no Cenomanian dinocyst studies specifically performed on the Nazaré outcrop, except for two samples collected by Moron (*op. cit.*) below the base of the marine carbonate units. The above mentioned studies are, to the best of our knowledge, the only ones tackling the Upper Cretaceous in Portugal, confirming the scarcity of dinocyst-based studies of the Portuguese, and more generally Iberian, Cenomanian-Turonian signaled in Peyrot (2011).

Considering the previous scenery, the present work arises as the first step of a new scientific project concerning the palynological research of dinoflagellates and dinocysts in the Upper Cretaceous of Portugal. Particularly, it focuses the study of a stratigraphical section sampled in the basal marl and limestone beds exposed in the south side of the Nazaré promontory, with an upper lower to basal middle Cenomanian record, and a particular focus on the preliminary quantitative study of organic-walled dinocysts. From a palaeoenvironmental and palaeoecological standpoint, this particular section has been interpreted as recording the transition from an open inner shelf during the late early Cenomanian to a more constrained lagoonal environment in the mid part of this stage (Callapez *et al.*, 2014).

## 1.2. OBJECTIVES OF THE STUDY

As an interdisciplinary work that focuses integrated aspects of general stratigraphy, taxonomy of organic-walled dinocysts and palaeoecology, the present study is centered on several general and specific main objectives.

The general aim of the research is to detail our knowledge on the dinoflagellate cysts from the early to lower Cenomanian transition in the shallow carbonate facies of the WPCP at the locality of Nazaré, one of the main sections for the study of this time span in the West Portuguese Margin.

Taken as specific objectives, the purported goals of the study are:

- (1) To complement previous local biostratigraphic analyses of the basal section of the carbonate formation by using dinocyst-based data as an additional biotic calibration;
- (2) To use the acknowledged potential of dinocyst assemblages as palaeoenvironmental tracers, and their marked provincialism, to enhance the reconstruction of local palaeogeographical domains and their associated palaeoecology in the

lower and middle Cenomanian (much less studied in the Iberian Peninsula than the upper Cenomanian and Cenomanian–Turonian boundary, associated with the Bonarelli Event; *e.g.*, Callapez, 2001, 2003; Hart *et al.*, 2005; Barroso-Barcenilla *et al.*, 2011);

- (3) To obtain an exploratory view of the similarities and differences with the associations of dinocysts *taxa* in stratigraphically equivalent regions in NW Europe (Lignum, 2009); as noticed in Berthou *et al.* (1980), dinocysts of the Mesogean (Tethyan) province are less known than those of the Boreal province and might contribute to an understanding of the palaeogeographical differentiation/articulation between them;
- (4) To contribute thereby to an integrated approach for a better knowledge of Tethyan carbonate platforms in the Iberian Peninsula, within the geodynamic context of the Atlantic and Mediterranean margins.

### 1.3. STRUCTURE OF THE WORK

The dissertation unfolds across 8 chapters, including the present one (Introduction) and a final discussion at the end. Chapter 2 presents the main geological setting, including an overall characterization of the Lusitanian Basin and the Western Portuguese Carbonate Platform (WPCP). Chapter 3 presents the stratigraphical framework at several levels, moving from a characterization of the Cenomanian–Turonian stratigraphy of the carbonate platform to a more focused stratigraphical description of the Nazaré sector, and finally narrowing down to the stratigraphic column elected for study, located at the base of the southern exposures of the Nazaré promontory. Chapter 4 conveys the essentials of dinoflagellates biology and morphology. Chapter 5 addresses the taxonomic, biostratigraphic (cyst zonations) and palaeoecological issues related to the use of dinocysts as biomarkers, while also including a quick overview of dinocyst-based studies conducted in Portugal. Chapters 6 and 7 constitute the empirical part of the dissertation. The methods (*e.g.*, the sampling of the geological column) and procedures (pre-laboratorial and laboratorial processing, leading to the microscopic analysis of the palynological content in the samples) are described in chapter 6. Chapter 7 presents the analyzed data under the form of tables, graphs, and summary statistics, and characterizes them with a view to their biostratigraphical and palaeoecological significance. Chapter 8, under the heading of “final discussion”, summarizes the main findings, discusses the limits and scope of the study, and tackles directions for future research.



## Chapter 2

---

# GEOLOGICAL SETTING

The Lower part of the Upper Cretaceous sedimentary record in Portugal is mainly represented by the West Portuguese Carbonate Platform (WPCP) in the West-Central part of the continental margin of Iberia (Berthou, 1984b; Callapez, 1998). From a geological standpoint, the WPCP is related to the the Cretaceous development of the onshore sector of the Western Iberian (Portuguese) Margin, after the end of the distensive phase of the Lusitanian Basin in the late Aptian (Kullberg, 2000; Kullberg *et al.*, 2006; Pinheiro *et al.*, 1996) and during a long-term Albian to Late Cenomanian eustatic sea-level rise leading to the formation of a number of European and North-African shallow marine carbonate platforms along the borders of the northern branch of the Tethyan Realm (Callapez, 2004, 2008).

This platform overlies a nearly 5000 m thick Triassic to Jurassic and Early Cretaceous sedimentary record reflecting the geotectonic evolution of the Lusitanian Basin (Fig. 1A) across several rifting and post-tectonic relaxation intervals (Rocha & Soares, 1984), until the formation of ocean crust which marks the transition of the Western Central Portuguese margin to a passive margin (Callapez, 2008; Kullberg *et al.*, 2014). While depositional processes occurring in the passive margin were no longer genetically associated with the rifting Basin (Kullberg *et al.*, 2014), they were still constrained by its deep structuring into several sectors on the basis of a system of inherited late-Variscan faults and salt tectonics (Ribeiro *et al.*, 1979).

The main lithostratigraphic units of these sectors (Northern, Central and Southern sectors, according to Rocha and Soares, 1984: see Fig. 2A) have been a longstanding subject of study from diverse standpoints (*e.g.*, lithological, stratigraphic,

sedimentary, palaeogeographical) and underwent consecutive revisions (see Kullberg, 2000, for an overview). Specifically for the Cretaceous onshore sedimentary record of the Western Central Portuguese Margin, a lithostratigraphic synthesis, along with an interpretation of the main allogenic controls, is provided by Dinis *et al.* (2008), ranging from Berrasian to Middle Campanian–Maastrichtian deposits (see Fig. 1C) and distinguishing between a Northern and a Southern sector (separated by the Caldas da Rainha parallel). Transgressive and regressive episodes, under both eustatic and tectonic control, played a fundamental role in the deposition history, with transgressive events usually marked by carbonate intercalations and carbonate platforms (Dinis *et al.*, 2008, Kullberg *et al.*, 2006). In particular, after a regressive trend during the late Aptian and the Aptian–Albian transition (Moron 1981), a long-term eustatic rise with an Albian onset gave way to the diachronic establishment of a carbonate platform in the southern domain (region of Lisbon), at first, and extending progressively up North all along the Cenomanian, to reach a maximum of carbonate sedimentation (full infill of the Lusitanian Basin) during the initial Upper Cenomanian (Callapez, 2008; Dinis *et al.*, 2008) (see Fig. 2B). After this maximal Cretaceous transgression, the carbonate platform underwent a regressive episode (associated with an uplift of the continental margin), with progradation and fluvial incision, but still persisted to the end of Lower Turonian, after which it consistently gave way to the progradation of micaceous alluvial sands over realms of the platform (Callapez, 2004, 2008).

The Cretaceous carbonate outcrops of the Western Portuguese Margin are irregularly spread along the coastline in between the parallels of Aveiro and Lisbon, following the overall NNE–SSW orientation of the passive margin (see Fig. 1B). Reflecting the additional role of NE–SW and E–W oriented reactivated Hercynian faults and regional halokynetic structures, leading to somewhat different tectonic–sedimentary evolutions for different regions, a northern and a southern domain can be distinguished, delimited by the tectonic axis Caldas da Rainha–Nazaré–Pombal (Callapez, 1998, 2008; Dinis, Rey, Cunha, Callapez, & Reis, 2008; Dinis *et al.*, 2015:). Lower Cretaceous sequences, namely Albian marine and lower Cenomanian, are only clearly identified in the southern domain, while the later phases of deposition, namely marine Lower Turonian, are only represented in the northern domain (Berthou *et al.*, 1980), with a broad representation of a middle Cenomanian to lower Turonian carbonate platform, and of later Turonian to Maastrichtian marine and fluvial siliciclastics (Dinis, Rey, Cunha, Callapez, & Reis, 2008).

GEOLOGICAL SETTING

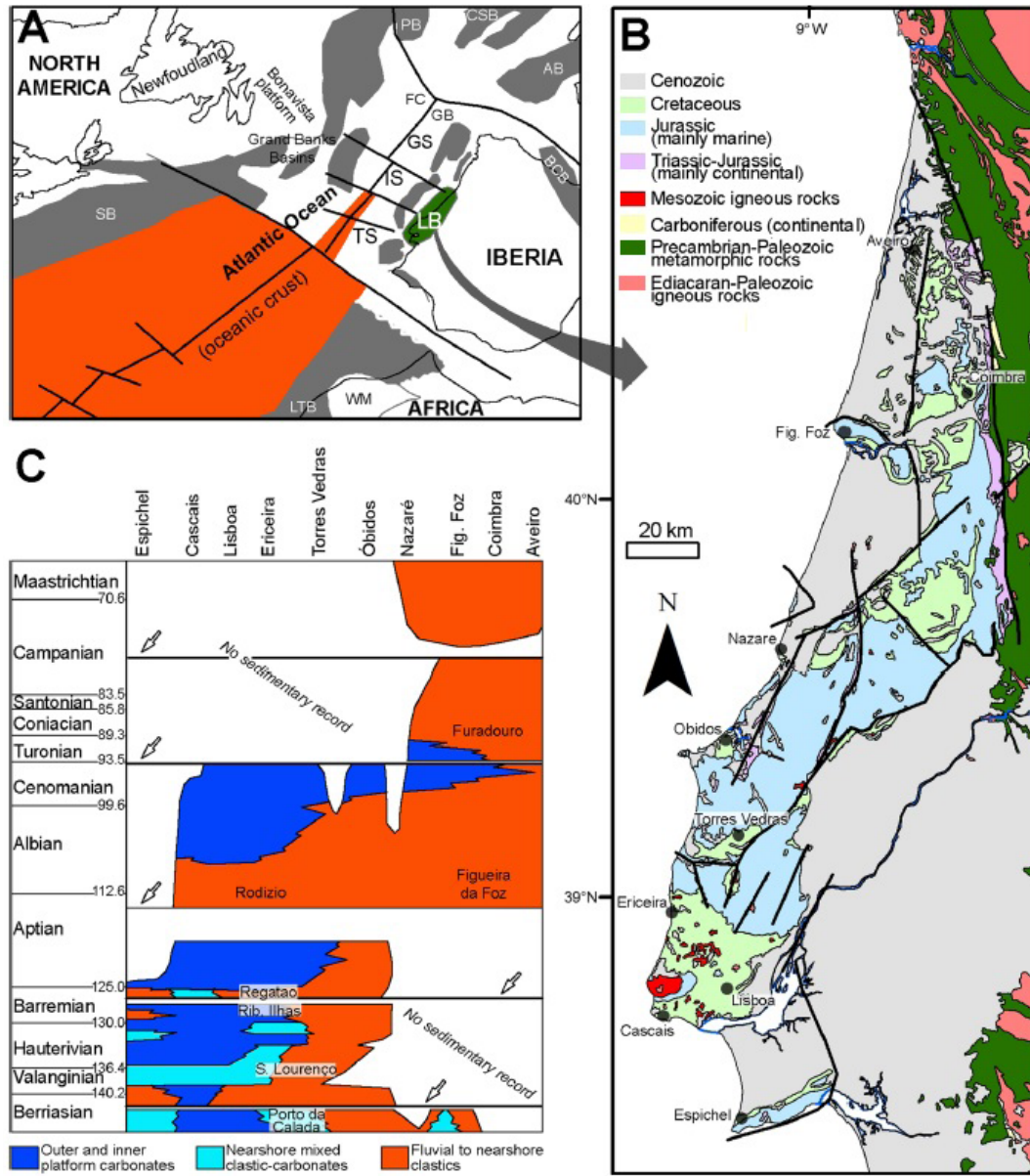


**Figure 2 - A.** Context of the Lusitanian basin within North Atlantic during the Cretaceous opening. GS: Galicia Sector. IS: Iberian Sector. TS: Tagus Sector. GB: Galicia Bank. FC: Flemish Cap. SB: Scotian basin. **B.** Geological outline of the Western Central Portuguese margin. **C.** Main Cretaceous lithostratigraphic units from western Portugal (adapted from Dinis *et al.*, 2015).

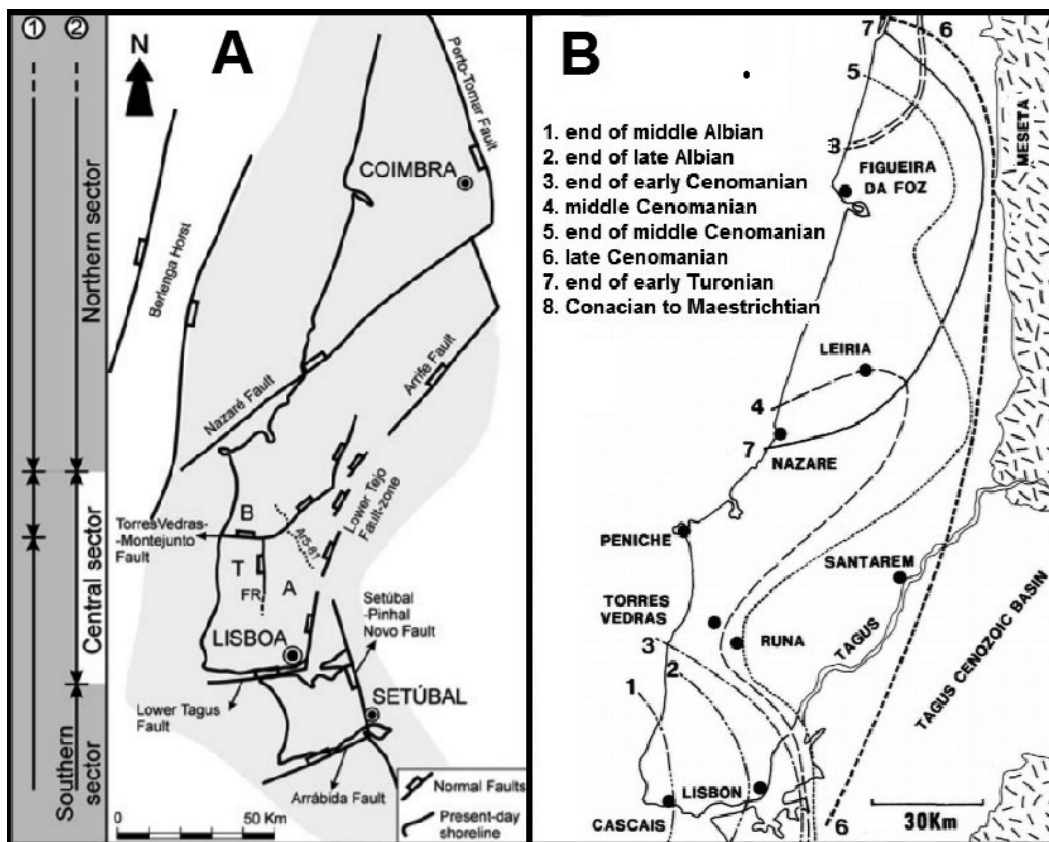


**Figure 3 - A.** Division of the West Portuguese margin into Northern, Central and Southern sectors on the basis of a system of inherited late-Variscan faults (adapted from Kullberg *et al.*, 2014). **B.** Palaeogeographic map of Late Cretaceous marine deposition; lines numbered 1 to 6 indicate the probable position of the shoreline from middle Albian to late Cenomanian (maximal Cretaceous transgression) (adapted from Montenat *et al.*, 1988).

In addition to their distinct ages and stratigraphic facies, these two domains have also been recognized as distinct palaeogeographic and palaeoclimate realms, with significant palaeoecological implications regarding the distribution and diversity of shallow-water marine biota (Callapez, 1998, 2008). Contrasting to the setting up of a rimmed platform displaying a predominance of coral reef complexes and rudist build-ups in the southern domain, open platform domains developed in the northern sector with a predominance of ammonite facies along with benthic faunas (Berthou, 1973, 1984b; Lauerjat, 1982; Callapez, 1998, 2004, 2008). Domain diversity, which was also favoured by local uplift movements along the diapiric axes, was greater in the northern sector after the initial upper Cenomanian major transgression, exhibiting strong lateral variation in facies (Callapez, 1998, 2003, 2004). Thanks to its palaeoenvironmental diversity (inner shelves, reefs, lagoons, alluvial plains, etc.) and its linkage to the evolution of the West Iberian Margin in between the Northern



and Central Atlantic and the African plate, the Cenomanian–Turonian Carbonate Platform has a distinctive importance for the overall articulation between the Tethyan and the Boreal realms (Berthou *et al.*, 1980; Dinis & Cunha, 2004), particularly as regards the understanding of faunal change and mixing between Northern Tethys, North–Africa and the Temperate Domain of West Europe (Callapez, 2008).

The present study will be concerned with the base of the Upper Cretaceous Cenomanian platform, with a focus on the region of Nazaré. As indicated above, Nazaré occupies a hinge position in between the northern and the southern palaeogeographic domains. The Lower Cretaceous series, best represented in the Lisbon Peninsula, can still be documented at the exposures of Nazaré, which additionally present a rich depositional series for the entire Cenomanian, including a brecciated endokarst correlative of the Cenomanian–Turonian transition that stands as a first sign of the future inversion of the basin (Berthou *et al.*, 1980; Corrochano, Reis, & Armenteros, 1998; Dinis & Cunha, 2004; Reis, Corrochano, & Armenteros, 1997; Callapez, 2014). The identity of this boundary region as regards both the Lisbon Peninsula and the northern subdomain has allowed for the further distinction between a northern and a central sector of the carbonate platform in the Cenomanian–Turonian successions (Callapez, 2008).



## *Chapter 3*

---

# STRATIGRAPHICAL FRAMEWORK: THE CENOMANIAN-TURONIAN PLATFORM CARBONATES OF WEST PORTUGAL

### **3.1. HISTORICAL OVERVIEW OF RESEARCH**

The study of the Portuguese Cenomanian–Turonian carbonate units has a century-old tradition. Research was initiated by Daniel Sharpe (1806–1856) during the decades of 1830–40, among other XIXth century pioneers, and continued by Paul Choffat (1849–1919) and collaborators, from 1880 until the beginning of XX century. As a Swiss geologist based in Portugal, Choffat collaborated with the Geological Commission of the Kingdom for the detailed description of the stratigraphy, palaeontology and cartography of the Portuguese Mesozoic (Antunes, 1986). His first major study on the Cretaceous System dates back to 1885, and the section of Nazareth was described in 1894 attached to the monograph by Gaston de Saporta (1823–1895) on palaeobotany.

From 1960s onwards the works of Soares (*e.g.*, 1966, 1972, 1980), focusing particularly on the region of Baixo Mondego, provided important contributions (França & Zbyszewski, 1963). In the 1970s and 1980s, studies by P.-Y. Berthou, J. Lauerjat and collaborators have allowed the establishment of new biostratigraphic scales for the Cenomanian–Turonian (*e.g.*, Berthou, 1984a, 1984b, Berthou *et al.*, 1980, 1985). Special note is due to the monographs by Berthou (1973) and Lauerjat (1982), where the outcrop of Nazaré was again taken up and its microfacies and associations of foraminifera and ostracods were addressed.

Starting in the 1990s, this study was resumed and the stratigraphy and invertebrates content revised north of Nazaré (*e.g.*, Callapez, 1998, 2008). Foraminifera

biostratigraphy was tackled by Hart *et al.* (2005) and the ammonite biostratigraphy synthesized in Barroso-Barcenilla *et al.* (2011). The section of Nazaré was remade by Callapez (1998, 2001) and Callapez *et al.* (2014), including the study of the vertebrates of Cenomanian lagoonal levels.

The vast majority of these and other studies to date addressed stratigraphic successions located across the onshore regions of Estremadura and Beira Litoral, from Lisbon to Figueira da Foz and Nazaré-Leiria-Coimbra, which may be classified into one of the three sectors mentioned above: northern, central and southern.

### 3.2. GENERAL LITOSTRATIGRAPHY AND BIOSTRATIGRAPHY

The Cenomanian-Turonian carbonate series is part of a megasequence ranging from Late Aptian to Early Campanian in age (Cunha, 1992; Cunha & Reis, 1995), which comprises a succession of (1) alluvial coarse siliciclastic sediments and interbedded lutites drained westwards from the Hercynian Massif of Iberia, (2) open and rimmed platform carbonates, (3) marine to alluvial micaceous sandstones (best represented in the northeast areas of the onshore, and (4) alluvial sandstones and conglomerates (Callapez, 2004). Within this general sequence, the carbonate platform facies are middle Albian-early Turonian in age and are in turn articulated in two megasequences delimited by clear unconformities (Callapez, 1998; Dinis *et al.*, 2008; Rey *et al.*, 2006). The first megasequence records Albian to Upper Cenomanian marginal marine facies and includes only a limited representation of Albian carbonate sedimentation, basically limited to the Lisbon/Sintra region. The second megasequence is Turonian and has its depocentre in the Northern sector.

The middle Albian-middle Cenomanian carbonate succession of the first megasequence was first studied in the southern region by Choffat, in 1885, who proposed the following units, defined by the marine fossils content, from base to the top: 1) the *Knemiceras uhligi* level; 2) the *Polyconites subverneuilli* recifal level; 3) the *Exogyra pseudaficana* [*Ilymatogyra*] level; 4) the *Pterocera incerta* [*Harpagodes*] level. These marl and limestone units, around 400 m thick, are overlain by a bed with the ammonite *Neolobites vibrayanus* and a further level with ‘rudist limestones’ (systematic update sensu Callapez, 2003) (Callapez, 2004, 2008), both upper Cenomanian in age. The designation of “Bellasian” was used by Choffat (1885, 1900) as a chronostratigraphic unit aggregating the four levels described beneath the bed with the ammonite *Neolobites vibrayanus*. More detailed biostratigraphic research led to the attribution of

an Albian age to the two lower levels (1 and 2), redefined as the Galé Formation (Rey, 1992, 2007), and to the dating of levels 3 and 4, redefined as the Caneças Formation, as, respectively, lower and middle Cenomanian (Rey, Dinis, Callapez & Cunha, 2006). The thickness of the old “Bellasian” unit of Choffat is strongly reduced towards north. Only the middle Cenomanian level with *Pterocera incerta*, displaying a mixed facies of sandy and marly limestones and sandy marls, can be found north of Torres Vedras, but associated with a marked retrogradation of the carbonate facies with ostreids and exogirinids (Callapez, 2004, 2008). However, the lower Cenomanian bed composed of marly limestones with biostromes of *Exogyra pseudaficana* still occurs across the Estremadura and in the exposures of Nazaré, in the Central sector (Callapez, 2008; Callapez *et al.*, 2014).

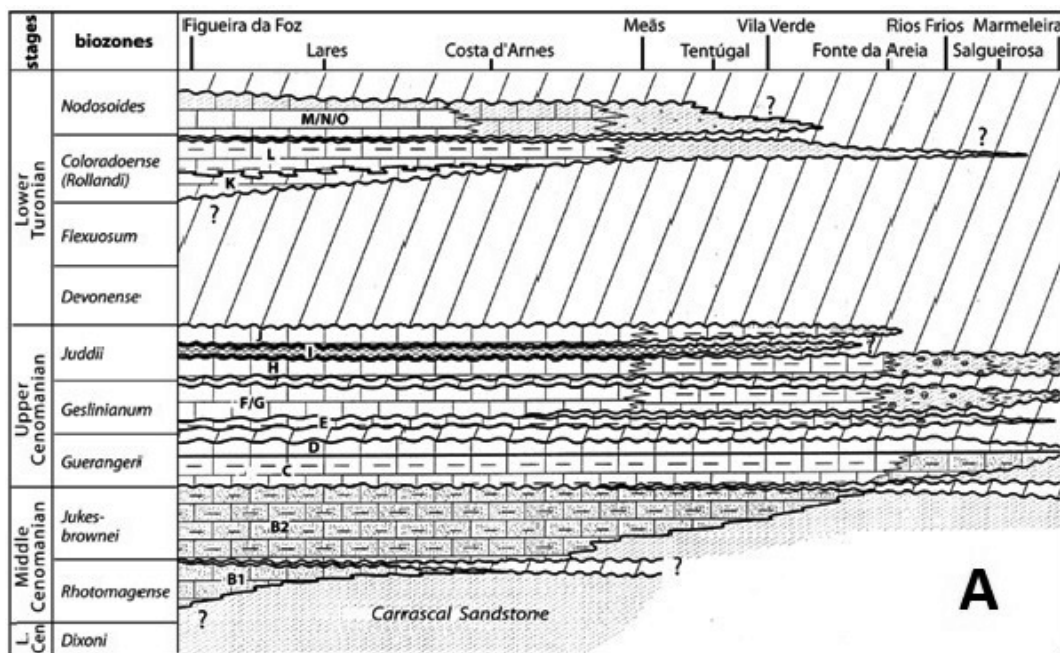
As for the middle Cenomanian-lower Turonian interval in the first megasequence, the basal upper Cenomanian is marked by a transgressive surface observable in all sectors of the onshore and recorded by a significant increase of fully carbonate facies of nodular limestone and marly limestone with ammonites, nautiloids and a diverse benthic fauna of open shelf environments (Callapez, 2004; Barcenilla *et al.*, 2011). The most expanded sequences for this interval (“Beds with *Neolobites vibrayeanus*” of Choffat, 1989, 1900), which also present the richest biostratigraphically significant fossil content, outcrop both in the northern sector, near Figueira da Foz (Soares, 1980; Callapez, 1998, 2004, 2008), and the southern sector, in Nazaré and near Runa and Lisbon (Berthou, 1973, 1984a; Lauerjat, 1982).

The type area for the upper Cenomanian carbonate succession was established by Choffat (1897, 1900) and followed by subsequent workers (*e.g.*, Berthou & Lauerjat, 1974; Soares, 1980) at the site of Salmanha, near Figueira da Foz (Costa d’Arnes Formation), due to the best individualization of ammonite rich stratigraphic levels easily correlated with sections from other areas of the carbonate platform. The original succession of Salmanha comprises 14 levels ordered from “B” to “O”, which can be individualized by their lithofacies, fossil content, including ammonites, inoceramids and foraminifera, and are most often bounded by discontinuities (Choffat, 1897, 1898, 1900; Berthou & Lauerjat, 1974; Soares, 1980; Rocha, Manuppella, Mouterde, Ruget, & Zbyszewski, 1981; Lauerjat, 1982; Berthou, 1984a, Berthou, 1973, 1984a, 1984b, 1984c, 1984d; Berthou *et al.*, 1985; Callapez, 1998, 2001, 2004; Callapez & Soares, 2001; Barcenilla *et al.*, 2011). According to the cumulated biostratigraphic evidence (*e.g.*, levels C to J are late Cenomanian in age, with “C” and “D” corresponding to the basal upper Cenomanian, and the first lower Turonian deposits (level “K”) laying on top of “J” (Callapez, 1998).

The lower part of the upper Cenomanian, displaying as a set of nodular and

marly limestones, occurs across the whole basin, corresponding to the beds with the Tethyan ammonite *Neolobites vibrayeanus* (Berthou, 1984a) which, together with an overlying thick succession of “rudists limestone”, constitute the Bica Formation (Rey *et al.*, 2006).

In the upper part of the upper Cenomanian record three geographic ranges with distinct associations of facies can be recognised: (1) Rimmed shelf limestones with rudists and coral buildups south of Leiria (towards Lisbon); (2) Open shelf marly limestones with ammonites north of Leiria (towards Figueira da Foz and Coimbra); and (3) inner shelf and lagoonal marls with echinoids and ostreids East of Leiria (around Ourém) (Choffat, 1900; Berthou *et al.*, 1980; Berthou, 1984a). The correspondences between these distinct ranges, particularly the two main ammonite and rudists associations of facies, have been the subject of a number of stratigraphic and palaeontological studies (*e.g.*, Choffat 1898, 1900; Berthou, 1973; Berthou & Lauerjat, 1979; Crosaz-Galletti, 1979; Moron, 1981; Lauerjat 1982; Callapez, 1998; Barcenilla *et al.*, 2011) and are now better understood (Berthou, 1984a), allowing for an overall stratigraphic framework (see Fig. 2 A and B).



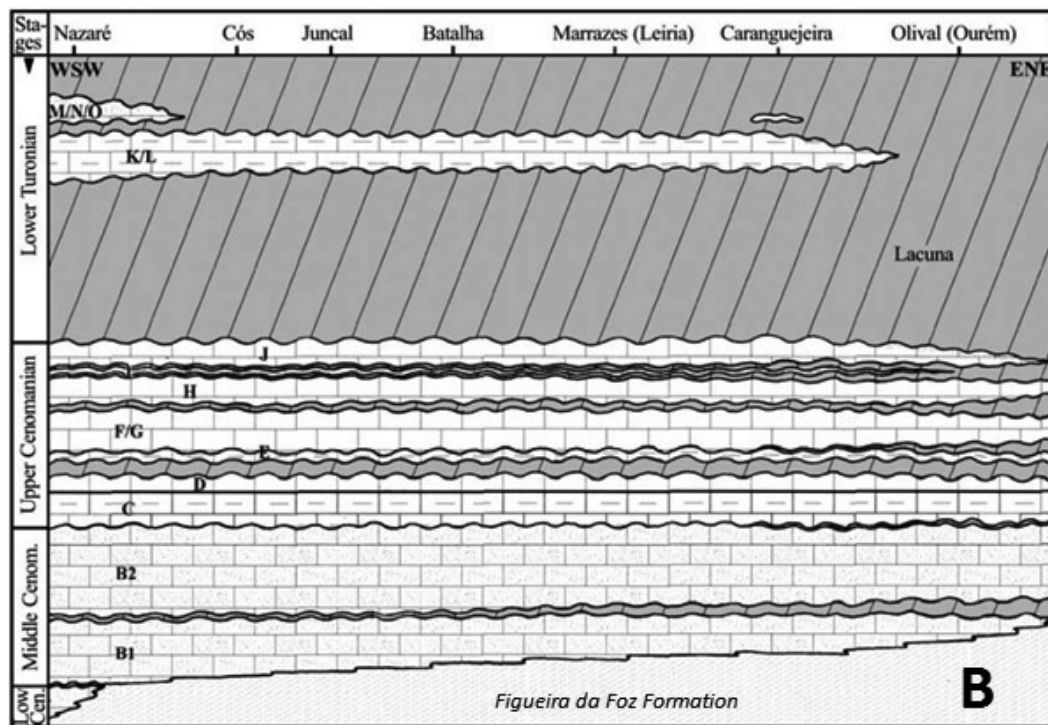


**Figure 4 - A.** General stratigraphy of the carbonate succession in the northern sector, from Figueira da Foz inward, with standard ammonites biozones (after Hart *et al.*, 2005, modified after Callapez, 1998). **B.** General stratigraphy of the Cenomanian-Turonian from the onshore sectors of the West Portuguese Margin eastwards of Nazaré (after Callapez, 2008).

This first Albian-upper Cenomanian megasequence presents a regressive facies at its top boundary (unit "J"), followed by a hiatus and a karstified surface (Baixo Mondego and Nazaré) marking the Cenomanian-Turonian transition unconformity (*e.g.*, Callapez, 2004; Dinis *et al.*, 2008): This discontinuity is related to the overall uplift of the continental margin, resulting in the emersion and subaerial exposure of the onshore sections of the carbonate platform (Callapez, 2008).

The second megasequence, which is entirely Turonian in age, is recorded by units "K" to "O" of Choffat (1897, 1900), with a maximal thickness of 18 m in the type area (Salmanha, Figueira da Foz). With the exception of a narrow set of exposures along the southeast block of the Cós-Leiria-Pombal fault (central sector), it is restricted to the northern sector. The "K" and "L" levels correspond to the basal lower Turonian, starting with dolomitic marls which evolve to platy marly limestones including abundant concentrations of reoriented turrilids (Callapez, 2004). Ammonite associations mainly occur in level "L", dominated by vascoceratids of the middle lower Turonian Tethyan biozone of *Thomasites rollandi* (Chancellor, Kennedy, & Hancock, 1994). This correlation concurs with the additional common occurrence

of inoceramids *Mytiloides* spp. among the fossil fauna (Callapez, 1998, 2003, 2004). The correlative depositional sequence in the central sector (southeast block of the Cós-Leiria-Pombal) consists in 2–3 m thick marls with rudist (*Radiolites peroni*) biostromes.

The upper part of the lower Turonian is represented by units “M”, “N” and “O”, consisting of a succession with cross-bedded inner shelf grainstones with coral and rudist debris and an increasing upwards content in micaceous sandstones (Soares, 1980; Lauverjat, 1982; Callapez, 1998, 2004, 2008; Hart *et al.*, 2005.) This late sequence shows no record of ammonites, but the occurrence of *Actaeonella caucasica grossouvrei* suggests a late early Turonian age (Callapez, 1993). Also, Berthou (1984b) inferred a possible correlation with the standard zone of *Mammmites nodosoides* based in palynological data provided by micaceous sandstones sampled at the region of Coimbra. This sequence presents a strong regressive character, documenting a transition to littoral plain and alluvial micaceous sandstones (Furadouro Formation), culminating with a withdrawal of the sea from the onshore sectors of the Western Portuguese margin (Callapez, 2008). The correlative sediments in the Central sector (recorded at the top of the exposures of Nazaré) correspond to coarse sands with abraded fragments of radiolitids and actaeonellids, consistent with a shallow littoral domain with prograding alluvial sandy bars (Callapez, 2004, 2008).

### 3.3. LOCAL STRATIGRAPHIC SETTING: THE “SÍTIO DA NAZARÉ FORMATION”

As mentioned before, tectonic activity associated with late Hercynian structural faults of diverse orientation led to the differentiation of several palaeogeographical regions in the carbonate platform (Callapez, 1998). The predominant NE-SW Cós-Leiria-Pombal flexure and fault system (“Nazaré fault”) (Dinis, Lopes, Rodrigues, & Cunha, 2012; Kullberg, 2000; Kullberg, Rocha, Soares, Duarte, & Marques, 2014) played a major role in the distinction between a northern, a central, and a southern region, but other sets of faults with NNW–SSE to NW-SE and with submeridian to meridian (N-S to NNE–SSW) orientations additionally contributed to the differentiation of structural domains within each region (Callapez, *op. cit.*). In the northern sector, the Cenomanian–Turonian outcrops of the Baixo-Mondego Region are thus commonly divided in different structural and palaeogeographical domains, displaying marked lateral facies variation (Choffat, 1900; Soares, 1966, 1968, 1980): Figueira da Foz, Montemor-o-Velho, Tentúgal and East of Ribeira de Ançã (Callapez, 1992, 1998).



In the Central sector, four structural domains have also been distinguished in the outcrops exposed over the southeast region of the Cós-Leiria-Pombal: (1) Nazaré; (2) Alpedriz syncline, (3) Pousos syncline and (4) Ourém (Choffat, 1900; Berthou, 1973; Crosaz, 1975, 1976; Lauerjat, 1982; Callapez, 1998, 2004). The stratigraphic succession analyzed in this study is included in the Nazaré sector, which constitutes the most western (external) domain of the Nazaré-Leiria-Ourém region, bordered at east by the northern end of the diapiric anticline of Caldas da Rainha, and presenting the most complete upper Cretaceous carbonate series in the central sector.

The single Cenomanian-Turonian outcrop found in the Nazaré sector corresponds to the large promontory which dominates the fishing village of Nazaré, located south, in the foothill (see Fig. 5A and B), with cliffs and slopes cutting Cenomanian massive limestones (*e.g.*, Choffat, 1900; Berthou, 1973; Lauerjat, 1982; Hart *et al.*, 2005; Callapez, 2004; Callapez *et al.*, 2014) (see Fig. 5C). As stated in section 2.1 (historical overview of research), both the stratigraphy and the fossil content of this outcrop have been the subject of much prior research since the pionnering works of Choffat (1886, 1900, 1901-02) and Saporta (1894, including an appendix with the first description of the stratigraphic section by Choffat), benefiting from cumulative contributions of further sedimentological, palynological, palaeoecological and micro- and macro-faunal analyses (*e.g.*, Antunes, 1979; Barroso-Barcenilla *et al.*, 2011; Berthou, 1973, 1984a; Berthou *et al.*, 1985; Reis, Corrochano, & Armentero, 1997; Callapez, 1998, 2001, 2004; Callapez & Soares, 2001; Callapez *et al.*, 2014; Lauerjat, 1982). An overall description of the stratigraphic setting of Nazaré is provided in the following.

The sedimentary succession from the base of the promontory upwards displays the following main sequences (description closely following Callapez, 1998; Callapez, 2004; Callapez *et al.*, 2014):

- 1) Albian to lower Cenomanian marine sandstones and lutites with plant remains (ca. 30 meters of exposure, recording the upper part of the Figueira da Foz Fm.);
- 2) Upper lower Cenomanian littoral plain mixed facies with *Ilymatogyra pseudoafricana* and *Ceratostreon flabellatum* biostromes, changing laterally to inner shelf carbonates rich in benthic invertebrates and occasional turtle remains (level with *Exogyra pseudoafricana* from Choffat's "Bellasian"; 1 to 8 meters thick);
- 3) Middle Cenomanian laminated marls and mudstones interbedded with oyster pavements and biostromes of *Gyrostrea ouremensis*, overlain at the top by massive dolomitic beds with fish remains; this unit, which also contains vertebrates remains and ichthyological fauna, crocodile and chelonians, is 39 meters thick and corresponds to unit "B" of Choffat, signaling a shift from an open inner platform environment to a lagoonal environment;

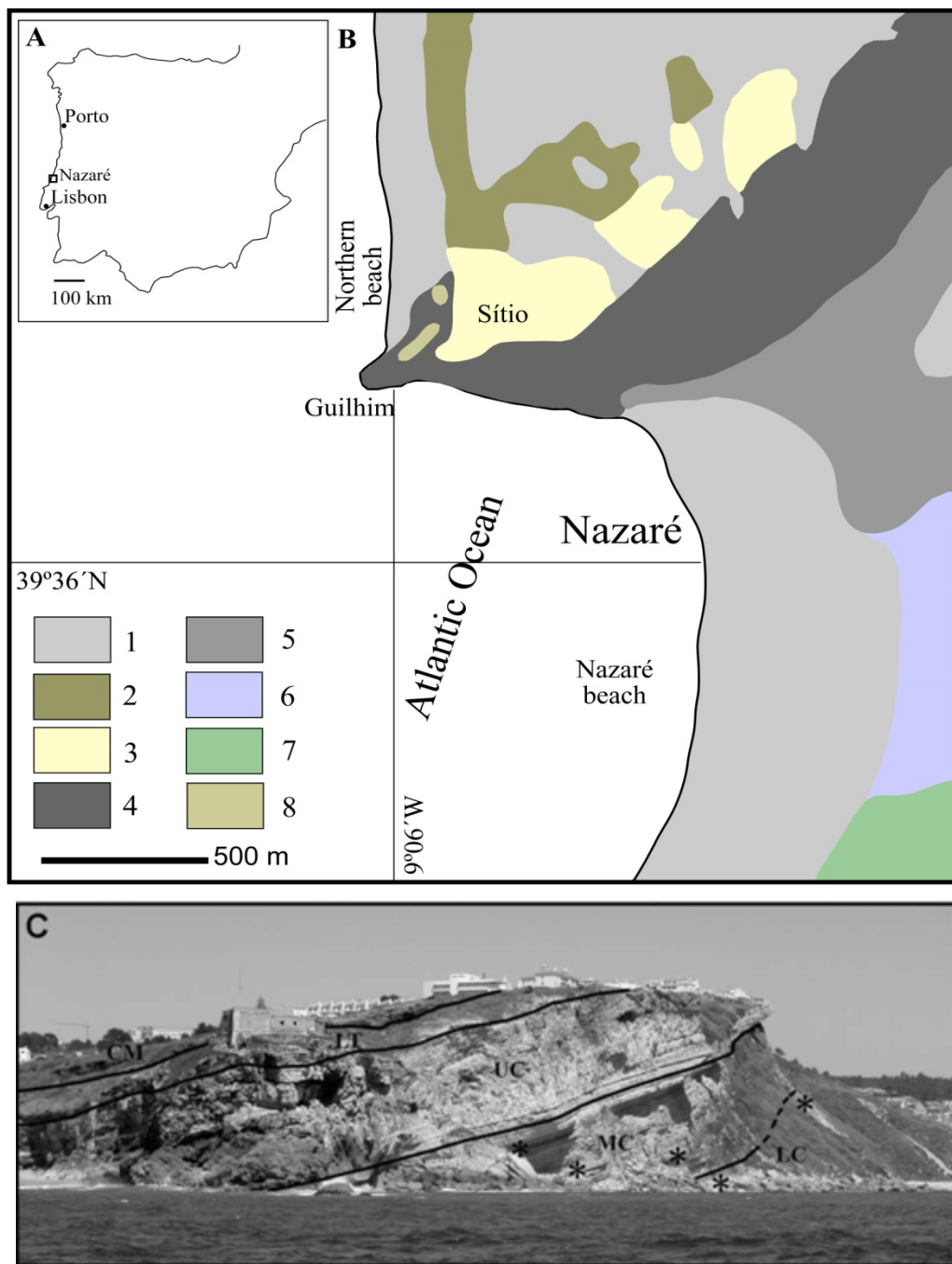


**Figure 5** – **A.** Location of Nazaré in the western Iberia Margin (West Central Portugal). **B** – Simplified geological map of Nazaré [1, beach sands; 2, dunes; 3, Campanian–Maastrichtian siliciclastics; 4, Cenomanian–Turonian platform carbonates; 5, Lower Cretaceous siliciclastics; 6, Upper Jurassic siliciclastics; 7, Upper Jurassic carbonates; 8, basaltic dykes]. **C** – The Nazaré promontory viewed from the west (i.e., from the seaside). Black lines delimitate chronostratigraphic boundaries: LC, upper lower Cenomanian; MC, middle Cenomanian; UC, upper Cenomanian; LT, lower Turonian; CM, Campanian–Maastrichtian; \*, location of main beds with vertebrate samples (adapted from Callapez *et al.*, 2014).

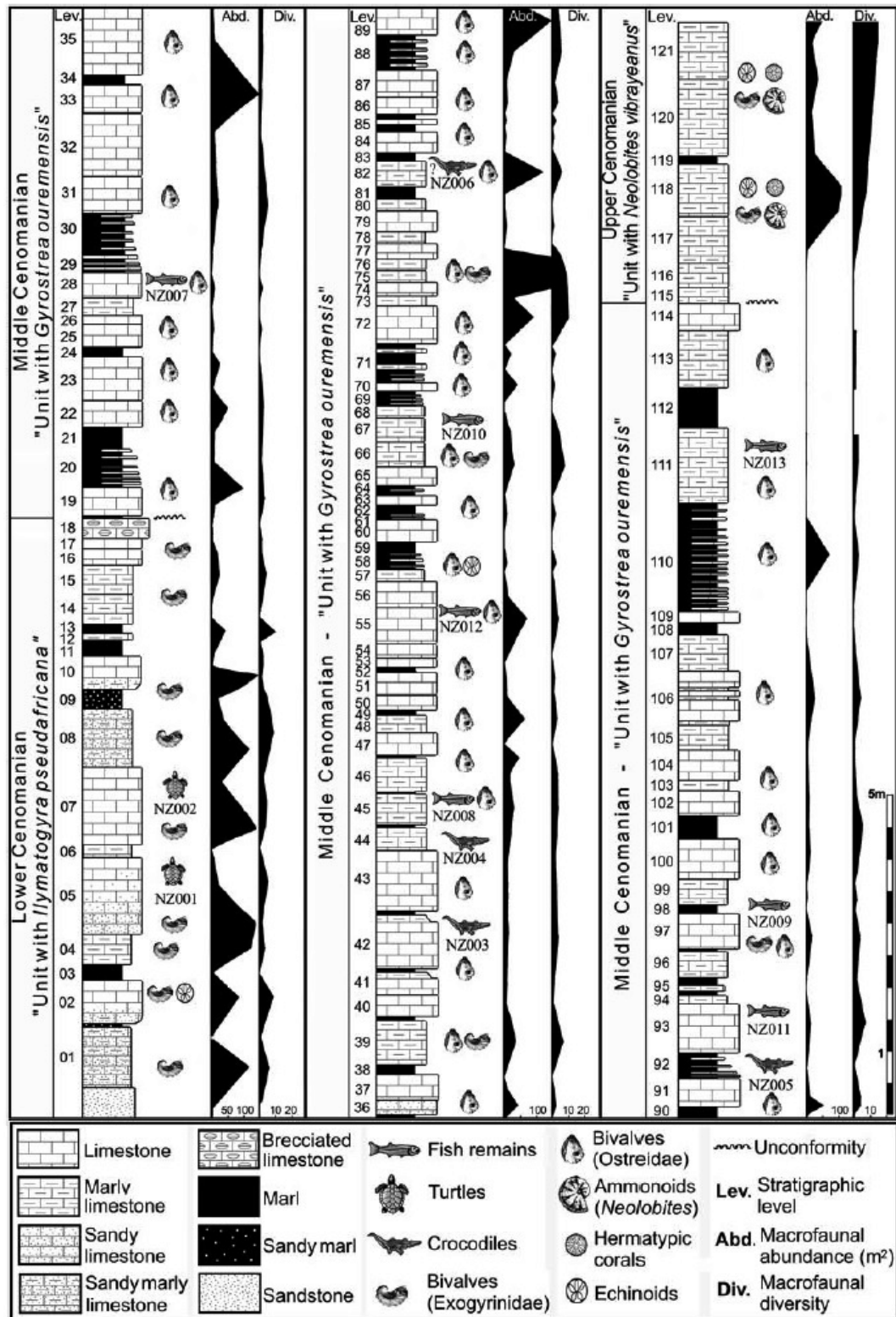


Figure 6 – Stratigraphic profile of the “Sítio da Nazaré Fm.”, ranging from upper lower to basal upper Cenomanian is illustrated below (taken from Callapez *et al.*, 2014).

- 4) Basal upper Cenomanian layers, composed of nodular limestones and marly limestones with *Neolobites vibrayeanus* and a fully marine benthic palaeofauna (11 meters thick), corresponding to unit “C” of Choffat (“Beds with *Neolobites vibrayeanus*”). This succession and the associated transgressive surface are easily identified in the whole carbonate platform, allowing an accurate stratigraphic correlation;
- 5) Upper Cenomanian massive beds of whitish calcarenitic limestone with a rich invertebrate fauna of bivalves, gastropods and echinoids (circa 4 m), corresponding to unit “D” of Choffat (“Bed with *Anorthopygus michelini*”).
- 6) On the top of the previous beds a narrow layer (few centimeters thick) of pinkish to beige yellowish nodular limestone including abundant *Tylostoma ovatum*, *Helicaulax* sp. and *Drepanocheilus* sp. can be observed, as a record of unit “E” (Callapez, 1998).

Units “D” and “E” constitute the easternmost part of the upper edge of the promontory on the south side, forming a cornice below the Sítio da Nazaré. More westward, still on the south side, Choffat’s levels “F”, “G” and “H” are represented by a succession of outer reef limestones with *Caprinula* debris, one of the most typical groups of rudists from the upper Cenomanian Tethyan faunas (circa 21 m);

- 7) The highest upper Cenomanian record, corresponding to levels “I”/“J” (more easily observable on the western cliff), is composed of laminated limestones and heavily bioturbated marls, probably correlative of the Bonarelli event and affected by the early development of a well exposed intra-Cretaceous endokarst (Callapez *et al.*, 2014; Corrochano, Reis, & Armentero, 1998; Reis *et al.*, 1997).

The units from the top part of the Cenomanian–Turonian succession are exposed on the western side of the promontory (light-house outcrop and north-beach), where their strata slightly dip northwards. Lower Turonian sequences are well documented on the northern corner of the cliffs, resting unconformably on upper Cenomanian limestones (unit “J”, which in this realm corresponds to a 7 m sequence of marls and limestones) (Callapez 2004). Basal lower Turonian (units K/L) is represented by white and pink limestone interbedded with layers of micaceous sandy limestone (5–6 m), containing abraded fragments of *Radiolites peroni*, *Apricardia* sp., scleractinian corals, and *Actaeonella caucasica grossowrei* (Callapez, 1998; Callapez *et al.*, 2014).

An erosional surface associated with an abrupt change in facies signals the boundary between the “K”/“L” and “M”/“O” sequences. Over the micaceous

limestones, 4,5 metres of yellow coarse sandstones with debris of *Acataeonella caucasica grossouvrei* and *Radiolites peroni* correspond to Choffat's unit "M", of middle lower Turonian age.

Finally, overlaying unconformably the Cenomanian-Turonian series, a layer of Coniacian-Santonian alluvial sandstones (circa 6 m), followed by a succession of Campanian-Maastichtian alluvial red mudstones interbedded with calciclastic conglomerates and red lutites with land gastropods (Antunes, 1979), closes at the top the Late Cretaceous exposures of Nazaré (Callapez, 2004; Callapez *et al.*, 2014).

A stratigraphic profile of the Nazaré carbonate succession, ranging from Lower to basal Upper Cenomanian is illustrated above (Fig. 6, taken from Callapez *et al.*, 2014). In addition to sedimentary data, the fossil content, characterized by its abundance and diversity, is indicated. The significant LEP (Level with *Exogyra pseudoafricana*)/B and B/C stratigraphic discontinuities, respectively at the boundaries between the lower and middle Cenomanian and the middle and upper Cenomanian, are signaled in between levels 18-19 and 114-115. This profile is part of a more extended one covering the entire Cenomanian-Turonian succession (until levels M/N/O) set up in Callapez (1998), starting at the base of the formation 400 meters west of the Northern end of the Nazaré's beach (U.T.M. NE 93450 83990).

### 3.4. SURVEYED STRATIGRAPHIC PROFILE

The succession considered for study in this work starts at the base of the carbonate exposures on the south cliffs of Nazaré, in between the Sítio and the Rock of Guilhim (39°36'15.11"N and 9°4'55.26"W) (see Fig. 7). It extends upwards for 13,5 meters, covering an exposure of inner shelf and lagoonal marls and limestones of late early to middle Cenomanian age, with a view to examining its fossil content in dinocysts and other palynomorphs.



**Figure 7** – Photograph of the outcrop signaling the location of the studied succession by means of a red frame. Lep = Level with *Exogyra pseudofriciana*; DS = discontinuity; “B1”, “B2”, “E”, “F”, “H” and “I” refer to the stratigraphic levels of Choifrat (1897).

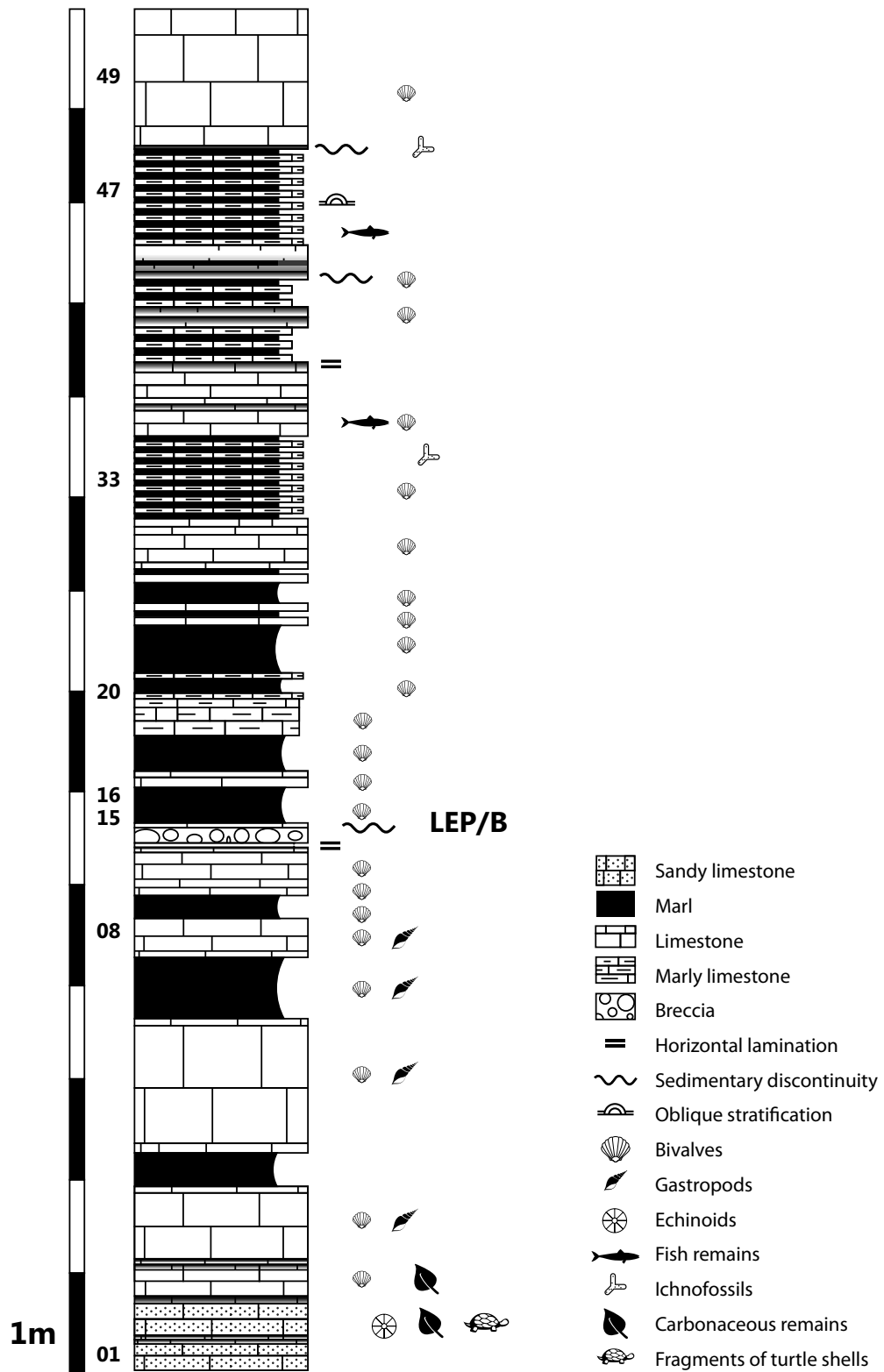


Figure 8 – Stratigraphic profile of the studied succession.

The selected stratigraphic profile is presented in Fig. 8, distinguishing 49 levels. The Lower-Middle Cenomanian boundary is signaled by the LEP/B discontinuity (12-13). Around 5,5 m of the profile lie below the LEP/B discontinuity, and the remaining 8 m above it, but without reaching the B1/B2 discontinuity, which delimits the early and latter middle Cenomanian (interval correlative to the standard ammonite zones of *Rhotomagense* and *Jukes-brownwei*, respectively) and occurs just below level 44 in the Callapez (1998) profile. This late early and early middle Cenomanian interval is coeval with the beginning of one of the most significant sea level rises in the Cretaceous Period (Callapez *et al.*, 2014; Gale *et al.*, 2002; Haq, Hardenbol & Vail, 1988) and has been interpreted as relating to a palaeoenvironmental evolution from an open inner shelf close to an intertidal flat in the lower Cenomanian to a more constrained lagoonal environment in the middle Cenomanian.

The section contains a succession of alternating limestones and marls with biostromes of *Ilymatogyra pseudoafricana*, followed by laminitic marly levels with *Gyrostrea ouremensis*. Upwards in the series the content in sands (sandy limestones) markedly decreases. From a lithostratigraphic point of view, the layers represented in the profile are partly equivalent to the Costa de Arnes Formation described by Rocha *et al.* (1981) for the Figueira da Foz and Baixo Mondego regions, thus representing the sector of the Cenomanian-Turonian carbonate located northward the Nazaré-Leiria-Pombal structural axis (Callapez, 1998; Dinis *et al.*, 2008).



## Chapter 4

---

# DINOFLAGELLATES BIOLOGY AND MORPHOLOGY

### 4.1. IMPORTANCE OF THE DINOFLAGELLATES

Dinoflagellates are unicellular microscopic organisms which, together with diatoms and coccolithophores, constitute an important part of the phytoplankton, closely following diatoms as primary marine producers (Hoppenrath & Saldarriaga, 2012). Since about half of dinoflagellates species are actually heterotrophic and not photosynthetic, they are also important members of the zooplankton, strongly contributing to their taxonomic diversity and biomass (Gaines & Elbrächter, 1987). They can be found in virtually all sorts of aquatic environments, ranging from marine (the predominant case), to brackish and freshwater ecosystems to sea ice (Taylor, Hoppenrath, & Saldarriaga, 2008). Besides the planktonic forms, there are also benthonic species. At particular stages of their life cycle Dinoflagellates may produce cysts with high potential to a successful fossilization, affording thereby important biostratigraphical and palaeoecological information (Sousa, Ribas-Carballo, & Pais, 1999).

Consistent fossil records of dinoflagellates have been established from Middle Triassic onwards (Fensome, Saldarriaga, & Taylor, 1999). Despite some evidence for the presence of the dinoflagellates lineage before the Mesozoic, the morphology of dinoflagellates as we know it today seems to have arisen from an evolutionary event occurred in the Early Mesozoic, thus making difficult to interpret fossils preceding that period as dinoflagellates (Fensome *et al.*, 1999). Around three quarters of the genders and half of the species that have been described thus far are fossils (Taylor *et al.*,

2008). Given the importance of dinoflagellate morphology for its identification and classification, and its close connection to the dinoflagellate biology and life cycle, we provide in this chapter a brief biological characterization of this important taxonomic group. The characterization offered is largely based on Evitt, Lentin, Millioud, Stover, and Williams (1977), Fensome *et al.* (1999), Medlin and Fensome (2013), and Sousa *et al.* (1999). The database DINOFLAJ2 (Fensome, MacRae, & Williams, 2008), in particular the Glossary section, based on Fensome, Taylor, Norris, Sarjeant, Wharton, and Williams (1993), was also used as a regular source for short definitions.

## 4.2. DEFINING FEATURES

### 4.2.1. Flagella

The defining trait of dinoflagellates is the presence, at some stage of their life cycle, of two dissimilar flagella typically emerging out of a flagellar pore in the conventionally termed ventral surface of the cell (see Fig. 9). These flagella allow for position stability and motility in the aquatic environment. A ribbon-like transverse flagellum lying in the *cingulum*, an equatorial furrow all around the cell, provides simultaneous forward and rotating propulsion through undulation from base to tip at the outer edge. A more conventional longitudinal flagellum, projecting outwards from a median groove termed *sulcus*, beats posteriorly and allows for translational motion (Gaines & Taylor, 1985).

The type of flagella insertion just described is predominant and known as dinokont flagellation. A number of dinoflagellate genus, such as the *Prorocentrum*, present what has been termed desmokont flagellation: flagella are still similarly differentiated, but they do not lie in grooves and are anterior relative to motion (Fensome *et al.*, 1999; Hoppenrath & Saldarriaga, 2012). In both cases, flagella and/or their associated structures provide a natural orientation to the cells.

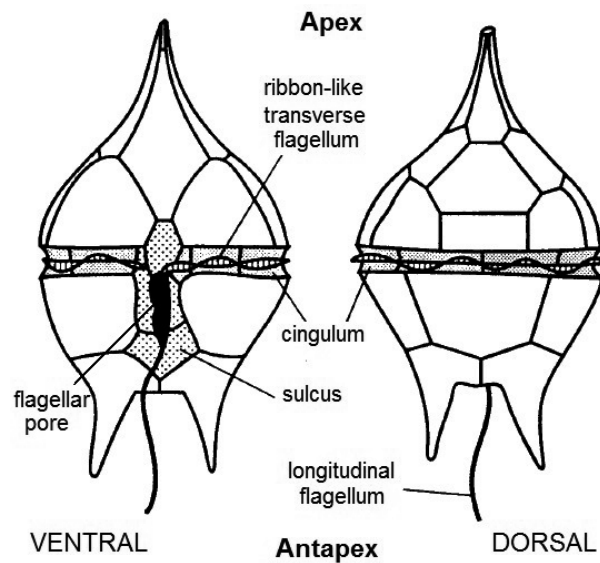


**Figure 9** - Morphology of a typical motile cell, illustrating the two dissimilar flagella and the axes defining the cell natural orientation: apex-antapex and ventral and dorsal surfaces (adapted from Fensome, Riding, and Taylor, 1996).

The *cingulum* (transverse groove) divides the cell in an upper and a lower part, generally designated as episome and hyposome, respectively. The highest point of the episome is called the apex, and lies at the front of the movement when the cell is swimming. The bottom of the hyposome is called the antapex. The upper and lower parts of the motile cell are for that reason also designated, respectively, as apical or anterior and antapical or posterior. The *sulcus* (longitudinal groove) conventionally defines a ventral surface of the cell, and thus also an opposite dorsal surface. For each surface, ventral and dorsal, right and left lateral sides can then be distinguished using the *sulcus* as a middle reference. Understanding of the cell orientation is essential both in describing a particular dinoflagellates species and in meaningfully interpreting descriptions made available in the literature.

#### 4.2.2. Dinokaryon

A second typical feature of most, though not all, dinoflagellates is the possession of a nuclear state known as dinokaryon (Fensome *et al.*, 1999). While both molecular phylogenetic and ultrastructural information establish dinoflagellates as eukaryotes, typically included in the Protist reign (division Dinoflagellata), dinokaryons (which determine the subdivision Dinokaryota) depart from conventional eukaryote nuclei

in several regards. They lack histones and nucleosomes, presenting a much lower ratio of proteins to DNA than other eukaryotes (Rizzo, 1991). Rather than decondensing during the interphase, chromosomes remain visible all along the mitotic cycle (Spector, Vasconcelos, & Triemer, 1981). Mitosis is also atypical, being dubbed as dinomitosis: the nucleus membrane is not ruptured during mitosis, which is thus “closed”, and the mitotic spindle is extranuclear, not linked to the centrioles (Dodge & Greuet, 1987). Dinoflagellates without a dinokaryon are classified as Syndiniales (subdivision Syndinia).

#### 4.2.3. Other dinoflagellate ultrastructures

As other eukaryotes, dinoflagellate cells contain in their cytoplasm different types of organelles, including mitochondria, vacuoles and pusules (a special kind of vacuoles opening up at the cellular bases), Golgi complex, pyrenoids and plastids (in photosynthetic and mixotrophic species, which are the vast majority: Schnepf & Elbrächter, 1992), besides microbodies and storage products. The most common sort of plastids are peridin plastids, and photosynthetic pigments include peridin, chlorophylls a and c<sub>2</sub>, b-carotene and small quantities of diadinoxanthin and dinoxanthin (Jeffrey, Sielicki, & Haxo, 1975; Sousa *et al.*, 1999). Heterotrophic dinoflagellates do not present chloroplasts and may exhibit a variety of feeding structures, dependent on the particular form of feeding (*e.g.*, direct phagocytosis, myzocytosis, or pallium feeding), such as cytostomes, peduncules or pallia (Jacobson and Anderson, 1992; Hackett, Anderson, Erdner, & Bhattacharya, 2004).

Especially important for the issue of dinoflagellates classification is the organization of the outer region of dinoflagellate cells, designated as cortex (Netzel & Dürr, 1984) or amphiesma (Morril & Loeblich III, 1983). The amphiesma is a complex structure composed of several membranes: underneath the plasmalemma, a membrane that coats the entire motile dinoflagellate cell, it typically includes a single layer of flat vesicles called alveolae or amphiesmal vesicles, which play a structural role. In many cases, these vesicles comprise tightly fit cellulosic plates (one per vesicle), which provide an external armor to the cell, known as theca. In other cases, the vesicles are either empty or filled with amorphous material. Dinoflagellates with thecal plates are thus known as armoured or techate and those without cellulosic plates as atehcate. Cell protection is ensured in atehcate dinoflagellates by a flexible protein coating, and some species may present an internal calcareous (or less often siliceous) skeleton (Morril & Loeblich III, 1983; Sousa *et al.*, 1999).

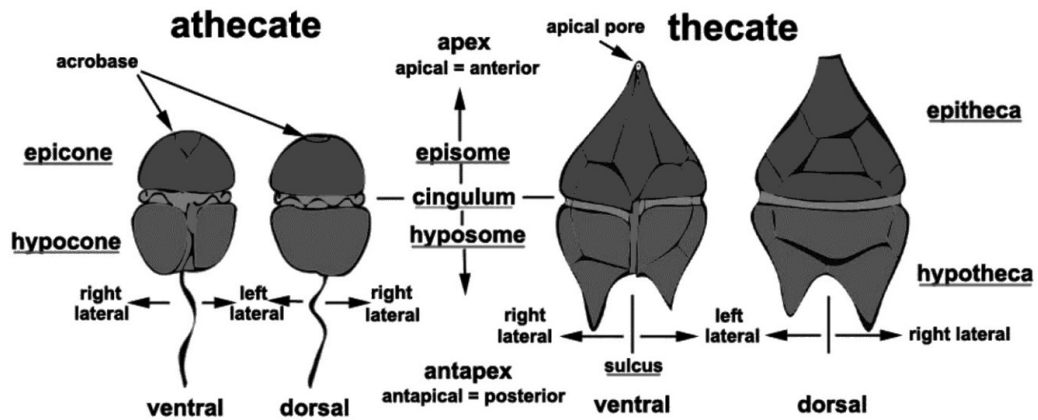


**Figure 10** - External morphology of an athecate and thecate motile cells: variations in the designation of anterior and posterior regions of the cell according to its thecate or athecate character are illustrated (after Hoppenrath, 2008, in Hoppenrath and Saldarriaga, 2012; changed to gray scale).

In some species a thin fibrous membrane, designated as dino-pellicle, chiefly made of cellulose and combined in varying degree with dinosporin, occurs under the alveolae. This pellicle can be the main strengthening layer of the amphiesma in some athecate dinoflagellates, which are then referred to as pelliculate dinoflagellates (Morris & Loeblich III, 1983). When present in thecate varieties, the pellicle lies under the theca and forms the wall of organic-walled cysts prone to fossilize. The more specific designations of the episome (apical part) and hyposome (antapical part) of the motile cell defined by the cingulum vary according to the naked or armoured character of the dinoflagellate (see Fig. 10).

The episome can be termed epicone or epitract in atechate cells and epitheca in thecate ones (or yet epicyst in dinocysts). The hyposome may be called hypocone or hypotract in atechate varieties and hypotheca in thecate ones (or yet hypocyst in dinocysts). Atechate cells may present a groove at the apex, known as acrobase, and thecate cells a pore at the top of the apical horn (apical pore).

The thecal plates form closely imbricated patterns, with sutures at their boundaries. These sutures grant flexibility and make possible for the cell to grow by adding wall material at the margins of the thecal plates. The arrangements of alveoles and thecal plates, known as tabulation, remain to this day the most information-rich morphological dataset for the classification (taxonomy) of dinoflagellates motile stages. Tabulation has long been shown to be highly conservative in each species (Fensome *et al.*, 1999).

### 4.3. TABULATION IN DINOFLAGELLATES

Six main systems of tabulation have been distinguished in dinoflagellates (Fensome *et al.*, 1993), respectively: Gymnodinioid, Suessioid, Gonyaulacoid-Peridinioid, Nannoceratopsioid, Dynophysoid and Prorocentroid. A brief characterization is given in the following of each of these systems (see Fig. 11):

*Gymnodinioid tabulation*: amphiesmal vesicles are numerous, often hexagonally-shaped, typically without theca plates, and either randomly organized or arranged in more than ten latitudinal series.

*Suessioid tabulation*: vesicles typically include delicate thecal plates (polygonal and of similar size) and are organized in an array of five to ten latitudinal series, with most often a not clearly differentiated cingulum.

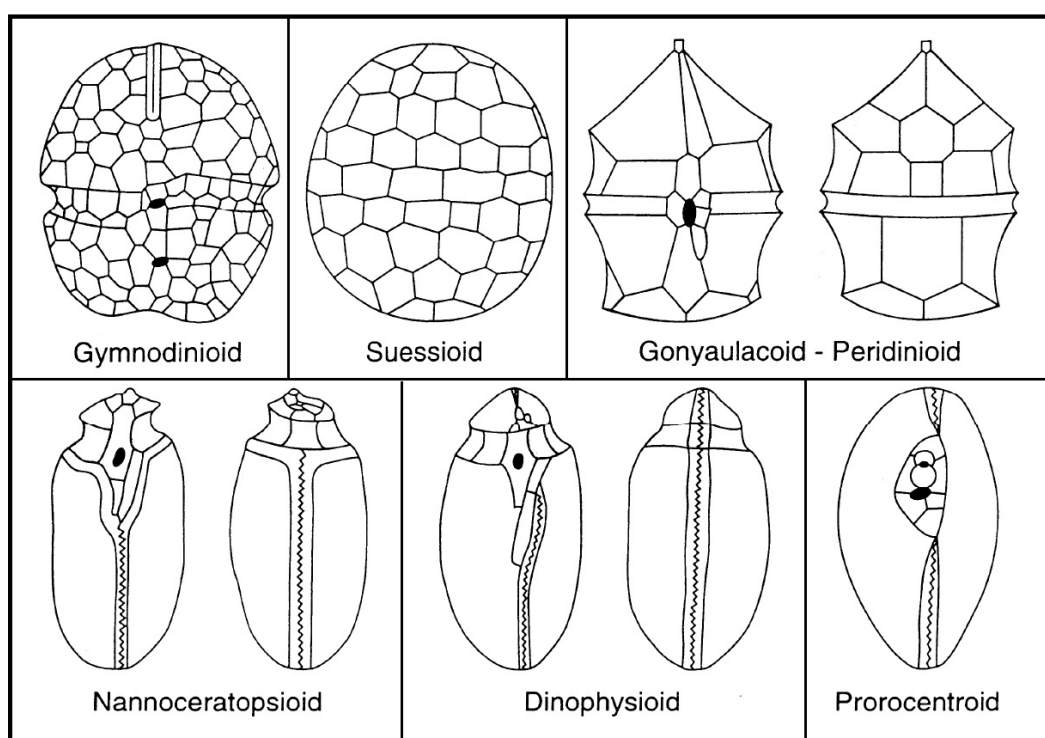


**Figure 11** - Schematic illustration of tabulation types (after Fensome *et al.*, 1999, modified from Fensome *et al.*, 1993).

*Gonyaulacoid-Peridinioid tabulation*: amphiesmal vesicles contain true thecal plates and are arranged in five or six primary latitudinal series and one longitudinal series, with a marked cingulum. Considered from the apex to the antapex poles, the thecal plates are classified as apicals (those contacting the apical pore complex), precingulars (immediately preceding the cingulum), cingulars (located on the

cingulum), postcingulars (immediately following the cingulum) and antapicals (lying on the antapex), with those lying in between these series termed intermediaries and those located within the sulcus as sulcal. As a difference between gonyaulocoid and peridionoid tabulations, the former is associated with a symmetrical first apical plate and the occurrence of two antapical plates, while the latter involves an asymmetrical first apical plate and two to four fundital plates (posterior to the first postcingular series and external to the sulcus).

*Dinophysoid tabulation*: the vesicles are arranged in four latitudinal series, with a clear cingulum and a saggital sulcus that splits the theca in two well-defined right and left halves. A simple apical pore occurs on the ventral surface of the epitheca.

*Nannoceratopsoid tabulation*: corresponds to a hybrid of the two preceding tabulations, combining a hyposoma which is dinophysoid and an episoma which is gonyaulacoid-peridinioid.

*Prorocentroid*: the teca comprises two large plates, named valves, separated by a saggital suture, without distinguishable cingulum or sulcus. Flagella are apically inserted (desmokonit flagellation) on one of two apical pores, surrounded by small plates lying mainly on an excavation of the right valve.

These tabulation systems are of critical importance not just to the taxonomy of living dinoflagellates as to the taxonomy of fossil species, to the extent that the surface of fossil cysts reflects the cortical organization of the motile cell. As this happens to a varying degree, and cyst-specific structures without a thecal equivalent (coined as cystomorphic structures by Gocht, 1983) can also occur, tabulation applied to fossils has been more specifically referred to as paratabulation. However, in its broad sense, the term tabulation conveniently encompasses the taxonomy of both living and fossile material (Fensome *et al.*, 1999). This issue will be more directly dealt with in the section devoted to the morphology of dyncocysts.

#### 4.4. DINOFLAGELLATES LIFECYCLE

With few exceptions, dinoflagellates present haplobiontic lifecycles (Fensome, Taylor, Norris, Sarjeant, Wharton, & Williams, 1993). Population growth is mostly obtained through asexual reproduction via binary division of biflagellate haploid motile cells (vegetative stage). Although it has only been observed on a small percentage of species (around 1%), sexual reproduction also occurs under given environmental conditions, calling for an increase in genetic variability. Gametes (either isogametes

or anisogametes) are then formed, similar to the regular haploid motile cells, which fuse to produce a diploid zygote motile cell, known as planozygote. Depending again on the environment, the planozygote can directly undergo meiosis, restoring the vegetative haploid stage of the life cycle, or can shift first into a dormant stage, the hypnozygote, before meiosis takes place after a variable period, controlled by surrounding conditions which trigger excystment (see Fig. 12).

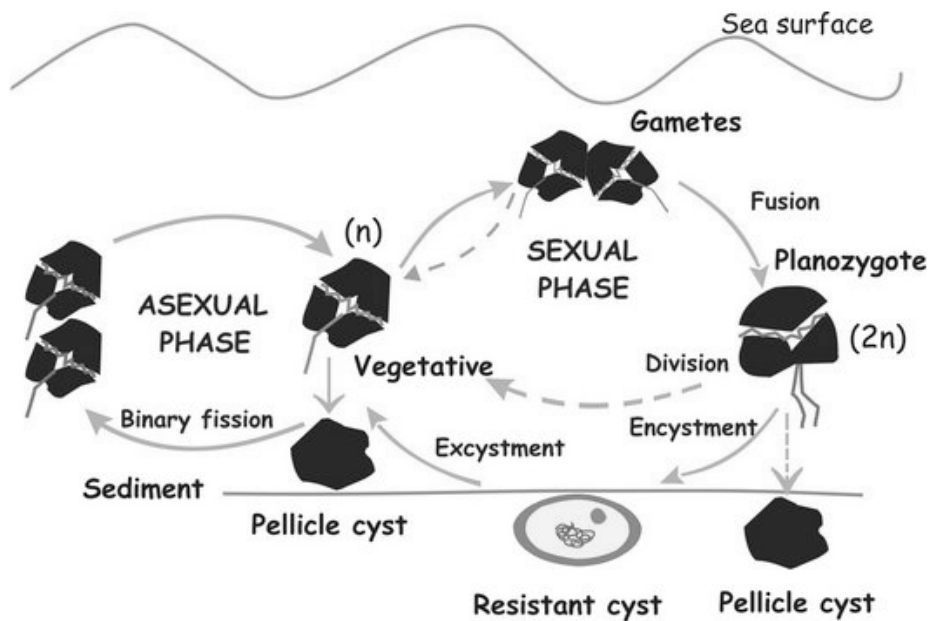


**Figure 12** - Dinoflagellates life cycle (after Figueiroa & Garcés, 2010, modified from Walker, 1984; changed to gray scaled).

This hypnozygote, also known as a resting cyst or dynocyst, is non-motile (it has no flagella) and is environmentally resistant through the building of a continuous thick wall below the theca. It naturally sinks into the sediments, behaving like a sedimentary particle. Another type of cysts, variedly known as pellicle, temporary, or ecdysal cysts, presents instead a thin wall which lasts only for a short period, and, just as the wall of vegetative (metabolic active) cysts, are easily destroyed by bacteria after death of the organism. By contrast, resistance cysts present organic walls typically made of dinosporine, a highly resistant material akin to sporopollenin, or sometimes inorganic, calcareous or (more rarely) siliceous walls, which all enable fossilization after the organism's death. Most fossil dinoflagellates are thus believed to correspond to fossilized resistance dinocysts.

It has been estimated that only 15-20 % of living dinoflagellates produce cysts which are prone to fossilization. As noted in Fensome *et al.* (1999), this may appear



at first sight to strongly limit the usefulness of microfossil records for highlighting dinoflagellate evolution. However, only a few number of dinoflagellate lineages are actually represented in the fossil record, mainly of the Gonyaulacoid-Perinioid system, so that the representation for these particular lineages is quite above the 15–20% overall threshold (Fensome *et al.*, 1999, p. 69). Critical to the biostratigraphic importance of fossil dinocysts is the way they reflect or not the external shape, particularly the tabulation, of the living motile cell. This depends on how the cyst wall is formed and opens way to the morphological classification of cysts.

#### 4.5. DINOCYSTS MORPHOLOGY

A resistant cyst may be formed either through building a continuous wall immediately within the theca (thus with a similar shape to the theca) or only after the contraction of the cell into a spherical body with projections (processes or crests), in which case the shape of the wall may significantly depart from the shape of the mother cell. Cysts of the former type are known as proximate and typically present no external projections. Cysts of the latter type are termed chorate or proximochorate, depending on the ratio of the length of the external projections to the shorter diameter of the central body (Sargeant, 1982). The length of these projections is in between ten and thirty percent of the central body diameter in proxichomorate and in excess of thirty percent in chorate cysts.

Among the chief morphological features of the cysts are the cyst wall, which can present different degrees of complexity, the surface ornamentation (relief or projections), the archeopyle (corresponding to the excystment aperture), and the tabulation or paratabulation system.

##### 4.5.1. Cyst wall

Dinocysts may have a single-layered wall enclosing a single cavity, in which case they are called autocysts, the wall being then termed autophragm and the enclosed cavity the autocoel. These dinocysts are also referred to as acavate and are often, though not exclusively, of the proximate type, reflecting the overall shape of the mother cell. Morphologically more complex dinocysts may in turn present a wall with several layers and enclosed cavities. When there are two layers, the inner one is

called endophragm and the outer one periphragm, with the innermost cavity named the endocoel and the cavity encircled by the two layers named the pericoel. When three layers occur, the one external to the periphragm is termed the ectophragm (typically structurally linked to the underlying layer via processes or other supporting formations) and the cavity between it and the periphragm is known as the ectocoel. Another kind of three-layered wall sometimes occurs, as in some peridinioid fossils, exhibiting an independent thin layer lying in between the periphragm and the endophragm. This layer, which is not structurally supported by any other, is known as the mesophragm and encircles a cavity termed the mesocoel. All cysts with multiple layers and cavities are known as cavate (Evitt *et al.*, 1977; De vertuil & Norris, 1966; Sousa *et al.*, 1999). Different types of cavate cysts can be distinguished, which constitute important morphological information (morphotypes) for species identification and dinocysts taxonomy. These include the holocavate, circumcavate, bicavate, cornucavate, suturocavate and camocavate forms, which differ concerning the form and distribution of the cavities in the cyst (Evitt, 1985). Procedures have been outlined for identifying the wall layers, largely based on the presence of regular processes and septa (Evitt *et al.*, 1977) which will be briefly addressed in the following subsection.

#### 4.5.2. Surface relief

The surface of dinocysts may be smooth or exhibit some relief, such as the patterns of parasutural lines (Evitt *et al.*, 1977) reflecting the arrangement of theca plates (thecamorphic structures), or cystemorphic structures such as processes (columnar formations arising from a specific point on an external structure), spines (acuminate processes) and septa (delicate linear projections which form circles or crests on the wall). These relief structures are highly variable in shape and distribution over the cyst (*e.g.*, from random to parasutural to intratabular) (see Evitt *et al.*, 1977; Evitt, 1985; Zonneveld & Pospelova, 2015). In many cysts, the relief patterns, namely the processes and septa, reflect in total or in part the tabulation system of the original cell, which turns them into a core morphological element for the dinoflagellate-cyst association (Fensome *et al.*, 1993). They are commonly highly regular structures, virtually constant across individuals in a given species. However, they may sometimes happen to be irregular, varying from specimen to specimen within a species, in which case they become mere incidental features. Besides their value for species identification, they may also, less contentiously than overall cyst shape, be the carriers

of important palaeoenvironmental information. For instance, a relation between shorter processes and growth in lower salinity environments has been consistently documented (Dale, 1996).

#### 4.5.3. Archeopyle

The archeopyle is an important morphological feature of dinocysts. It corresponds to the opening through which excystment takes place (Evitt *et al.*, 1977; Fensome *et al.*, 1993). Commonly, it is outlined by an archeopyle suture, visible at the microscope and believed to be formed at the time the cyst wall develops, but it may also result from the detachment of plates not delineated by a preexisting suture. The archeopyle suture typically runs along the boundaries of one or more paraplates (parasutures), defining this way a section of the cyst paratabulation. The opening left by the rupture of the wall along the archeopyle suture (or by plate detachment without a predetermined suture) is termed the archeopyle operculum. Opercula comprising one single paraplate are termed monoplacoid and those comprising several paraplates polyplacoid. When the operculum is completely encircled by the archeopyle suture, being thus entirely detachable from the cyst wall, it is said to be free (even if it may by accident be adherent to the wall at a point where the suture happened not to open). When the suture does not fully surround the operculum, which thus remains partly attached to the cyst, the operculum is known as adnate. Just as its shape and size, location of the archeopyle on the cyst may be highly variable, ranging from apical to intercalary and precingular, and even to postcingular and antapical, as is the case with siliceous cysts of Peridinites. Polyplacoid opercula may include paraplates belonging to one single series of paraplates, in which case they are simple, or to two or more series, in which case they are said to be compound. A particular case of a compound archeopyle is known as epicystal archeopyle (after Evitt *et al.*, 1977), who deem this designation preferable to the one of epittractal archeopyle), comprising all paraplates of the epicyst. Although the archeopyle morphology may be highly specific in some dinoflagellate species, as noticed in Evitt *et al.*, 1977, it only provides direct indications about a small fraction (usually restricted to very few plates) of the tabulation.

#### 4.5.4. Paratabulation

Paratabulation is by far the most important morphological classificatory feature of dinocysts. It designates the ensemble of characteristics of the apparent plates on the cyst, including their shape, number, size and mutual relationship (Evitt *et al.*, 1977). As mentioned previously, tabulation is currently used to encompass both the tabulation of living motile cells and of fossil cysts, the same main six tabulation systems described above (section “tabulation in Dinoflagellates”) being also used for the classification of patterns of plates in dinocysts. However, the expression paratabulation signals the circumstance that tabulation of the cyst will typically offer an incomplete view of the theca tabulation, the link between the two being thus inferential to some extent. Notwithstanding, just as tabulation for living motile cells, paratabulation has proven invaluable for the taxonomy of fossil dinocysts.

One important methodological aspect of tabulation has been the development of notational codes to describe it, known as tabulation formulae (or paratabulation formulae, when applied to paraplates). A popular tabulation formula was put forward by Kofoid as early as 1907/1909 and is still in use today in modified versions (Fensome *et al.*, 1993). Plates in each latitudinal series (apical, precingular, postcingular, antapical), indexed by specific symbols, are numbered from left to right starting from the midventral position and parallel to the transverse flagellum. While the tabulation formula for a theca includes the total number of thecal plates, the paratabulation formula for a cyst only expresses the number of observable plates and their disposition. As a consequence, the two formulae will only coincide when the thecal morphology happens to be fully expressed in the cyst morphology (see Evitt *et al.*, 1977). Tabulation and paratabulation formulae deal with only a selected portion of the information conveyed by the tabulation (paratabulation), as they concern the number and arrangement of plates with no consideration for their size, shape and mutual relationships. Useful as they are, they cannot thus be thought of as exhausting the morphological information of dinoflagellates or dinocysts tabulations.

One often useful complement to address cysts paratabulation is provided by the pattern of processes (see subsection “surface relief” above), whenever they happen to reflect thecal morphology (*e.g.*, when arranged along the parasutural lines, or presenting an intratabular distribution). Formulae for processes have also been developed, which may or not coincide with the paratabulation formula (Stover, 1975).

## Chapter 5

---

# DINOFLAGELLATES TAXONOMY, STRATIGRAPHICAL DISTRIBUTION AND PALAEOECOLOGY

### 5.1. TAXONOMY

An acceptable classification of dinoflagellates should be able to encompass both present and fossil forms and moreover reflect dinoflagellates phylogeny. Fensome *et al.* (1993) developed a phylogenetic tree of dinoflagellates based on ultrastructures, particularly tabulation, which was subsequently supported in many aspects by molecular studies (Medlin & Fensome, 2013). While molecular phylogenetic analyses successfully contributed to highlight the closest evolutionary relatives of dinoflagellates (e.g., Apicomplexa and Ciliata), they have failed to this day in decoding the internal relationships among classical orders of dinoflagellates (Gómez, 2012; Hackett *et al.*, 2004; Taylor, 2004). Nevertheless, they have supported overall morphologically based classifications (Hackett *et al.*, 2004), which thus remain at the centre of taxonomic efforts.

Despite progress made in the morphological characterization of dinoflagellates since the first attempts of a comprehensive taxonomy (Bujak & Williams, 1981; Taylor, 2004), several problems remain in the classification of this group, as part of a work in progress, particularly at the order levels (Gómez, 2012). One long acknowledged difficulty arises from the fact that species in a single living genus do not necessarily present uniform morphocysts, or that the cysts of two distinct species may be much more distinct than their theca armour (Sargeant, 1974). Nomenclature issues have also always been around, starting with the treatment of dinoflagellates by different authors under either the international zoological or the botanical nomenclature

codes (respectively, I.Z.C.N and I.B.C.N: Gómez, 2012). It is now widely accepted that the ICN, abbreviation for *International Code of Nomenclature for algae, fungi, and plants* (McNeill *et al.*, 2012) should be used for the classification of living Dinokaryota and of known fossil dinoflagellates (all in the Dinokaryota Subdivision) (Williams & Fensome, 2016).

In spite of that, evolutions of the code itself and the need to account for new fossil *taxa* and nomenclatural changes proposed in a fast growing literature have required the regular revision and updating of major classification systems. In the case of fossil dinoflagellates, the first systematic attempt at an inclusive index of genera and species (the Lentin and Williams Index: Lentin & Williams, 1973) has accordingly undergone numerous revisions (Lentin & Williams, 1975, 1977, 1981, 1985, 1989, 1993; Williams, Lentin, & Fensome., 1998; Fensome & Williams, 2004; Williams & Fensome, 2016). Some of these revisions were given a digital form and made generally available online, leading to DINOFLAJ2 (Fensome, MacRae, & Williams, 2008), which superseded the earlier DINOFLAJ database (Fensome, MacRae, & Williams, 1998) and incorporates the nomenclature and taxonomy of the 2004 edition of the Lentin and Williams Index. A major update of DINOFLAJ2 is in preparation for release during 2016 (DINOFLAJ3, upcoming: Fensome & Williams 2016).

Besides an index of fossil dinoflagellates at the levels of genera, species and subspecies (after Williams & Fensome, 2004), DINOFLAJ2 includes a joint classification of fossil and living dinoflagellates from the level of division (Dinoflagellates) down to genera (based on Fensome *et al.* 1993), where it becomes continuous with the index information. The general taxonomy presented below is based on Fensome *et al.* (1993) (see also Sousa *et al.*, 1999), and reproduced with adaptations from DINOFLAJ2 (see Table 1).

**Table 1** – Classification of dinoflagellates within the Kingdom Protist down to the suborder rank (reproduced with adaptations from DINOFLAJ2).

Kingdom	Division	Sub division	Class	Subclass	Order	Suborder
Protist	Dinoflagellata	Dinokaryota	Dinophyceae	Gymnodiniphyceidae	Gymnodiniales	Gymnodiniineae
						Actiniscineae
					Ptychodiscales	
				Suessiales		
				Peridiniphyceidae	Gonyaulacales	Rhaetogonyaulacineae
						Cladopyxiineae
						Goniodomineae
						Gonyaulacineae
						Ceratiineae
						Uncertain
				Peridinales	Heterocapsineae	
					Peridiniineae	
					Glenodiniineae	
					Uncertain	
		Uncertain	Uncertain			
Dinophysiphyceidae	<u>Nannoceratopsiales</u>					
	<u>Dinophysiales</u>					
Prorocentrophycidae	Prorocentrales					
Uncertain	Desmocapsales					
	Phytodinales					
	Thoracosphaerales					
	Uncertain					
Blastodiniphyceae	Blastodinales					
Noctiluciphyceae	Noctilucales					
Uncertain	Uncertain					
Syndinea	Syndiniophyceae	Syndiniales				
Uncertain						

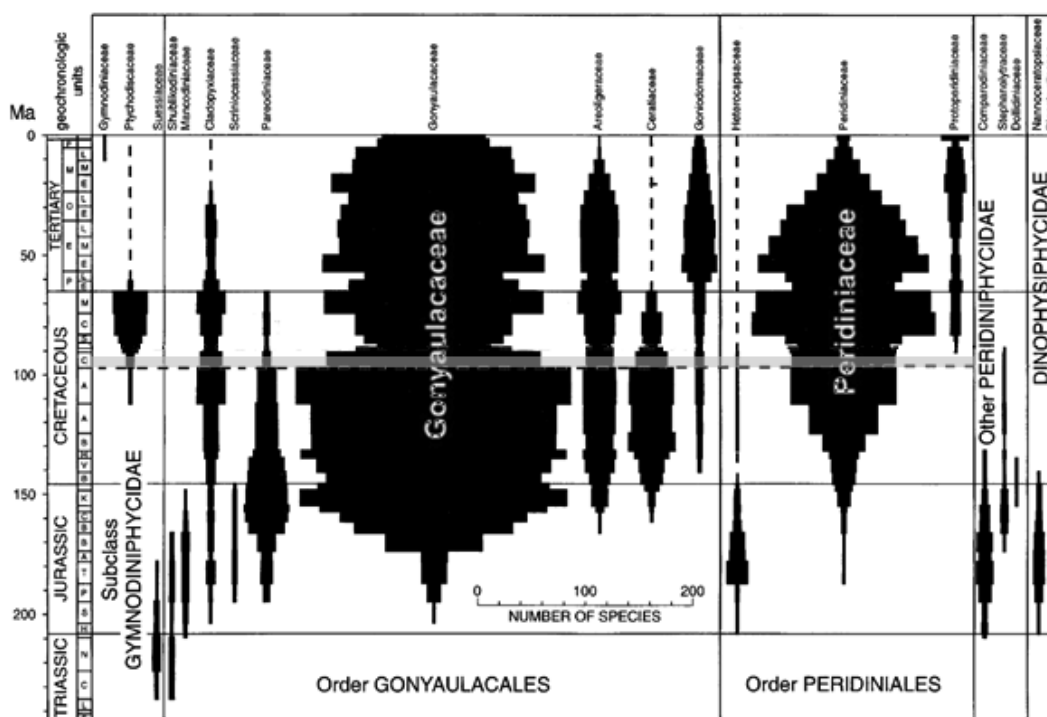


**Figure 13** - Number of known dinoflagellate fossil species per family and per time interval (Mezosoic stages and epochs) represented as spindle plots. The light-transparent blue rectangle corresponds to the Lower and Middle Cenomanian time interval (adapted from Fensome *et al.*, 1999).

Taxonomically, dinoflagellates constitute a division (Dinoflagellates) of the Kingdom Protist, comprising three subdivisions, of which one is uncertain. The remaining two are the Dinokaryota (dinoflagellates presenting a dinokaryon in at least one stage of their life-cycle) and the Syndiniae (dinoflagellates presenting dinokont flagellation and histones in the nucleus). While Syndiniae have a single class (Syndiniophyceae), Dinokaryota comprise four classes, one of them uncertain and, under the class Dinophyceae, five subclasses, with one uncertain (Table 1).

All known fossil dinoflagellates belong to the Dinokaryota subdivision. The Class Dinophyceae encompasses the six basic tabulation/paratabulation types described in the preceding chapter (gymnodinoid, suessioid, gonyaulacoid-peridinioid, dinophysoid, nannoceratopsioid and prorocentroid: Fensome *et al.*, 1993; Talyor, 1987), which provide the morphological basis for the distinction of subordinated main orders. These tabulation systems have distinct representations among extant and fossil forms.

The gonyaulacoid-peridinioid system, exemplified by a majority of fossil dinoflagellates (from the Jurassic onwards) is also commonly represented in motile dinoflagellate cells (Fensome *et al.*, 1999). Nannoceratopsioid tabulations are exclusive



of the fossil record (Jurassic). Prorocentroid tabulation is only found in living forms, which, to the exception of two questionable Jurassic fossil genera (*Nannoceratopsis* and *Ternia*), might also be said of the dinophysoid tabulation. The gymnodinioid and suessioid systems have a sporadic fossil representation and have both extant representatives. Fig. 13 relates the classification of dinoflagellates to geochronologic units (Mesozoic stages and epochs) by plotting the time of appearance of different taxonomic subclasses and orders and the number of species per family obtained in the fossil record. The time interval delimited by the two horizontal dashed lines in the Cretaceous corresponds to the lower and upper boundaries of the Cenomanian Stage, which is the stratigraphic interval focused in the present work.

A more detailed account, at the level of relevant genera and species, of the relation between fossil dinoflagellates taxonomy and main stratigraphic intervals, will be given in the section devoted to dinocyst biostratigraphy.

## 5.2. DINOCYST BIOSTRATIGRAPHY

### 5.2.1. Relation to main geochronological units

Despite biogeochemical evidence for a pre-Mesozoic occurrence of dinoflagellates, with ancestors possibly dating back to the Cambrian period (Moldowan & Talyzina, 1998), the earliest confirmed dinocysts were found in Middle-Late Triassic sediments, 240–200 Ma (Macrae, Fensome, & Williams, 1996; Medlin & Fensome, 2013). From then on, cyst-forming dinoflagellates are abundantly documented in the fossil record of marine Mesozoic–Cenozoic sediments, exhibiting noticeable species diversity (circa 2500 species: Taylor *et al.*, 2008). The pattern of diversity shows a rapid increase from Late Triassic to a maximum in the Cretaceous (local peaks in the Albian and the Maastrichtian), and a consistent decline all along the Cenozoic, starting in the Early Paleocene and with the single exception of a local increase in the Early Eocene (MacRae *et al.*, 1996: see Fig. 14).

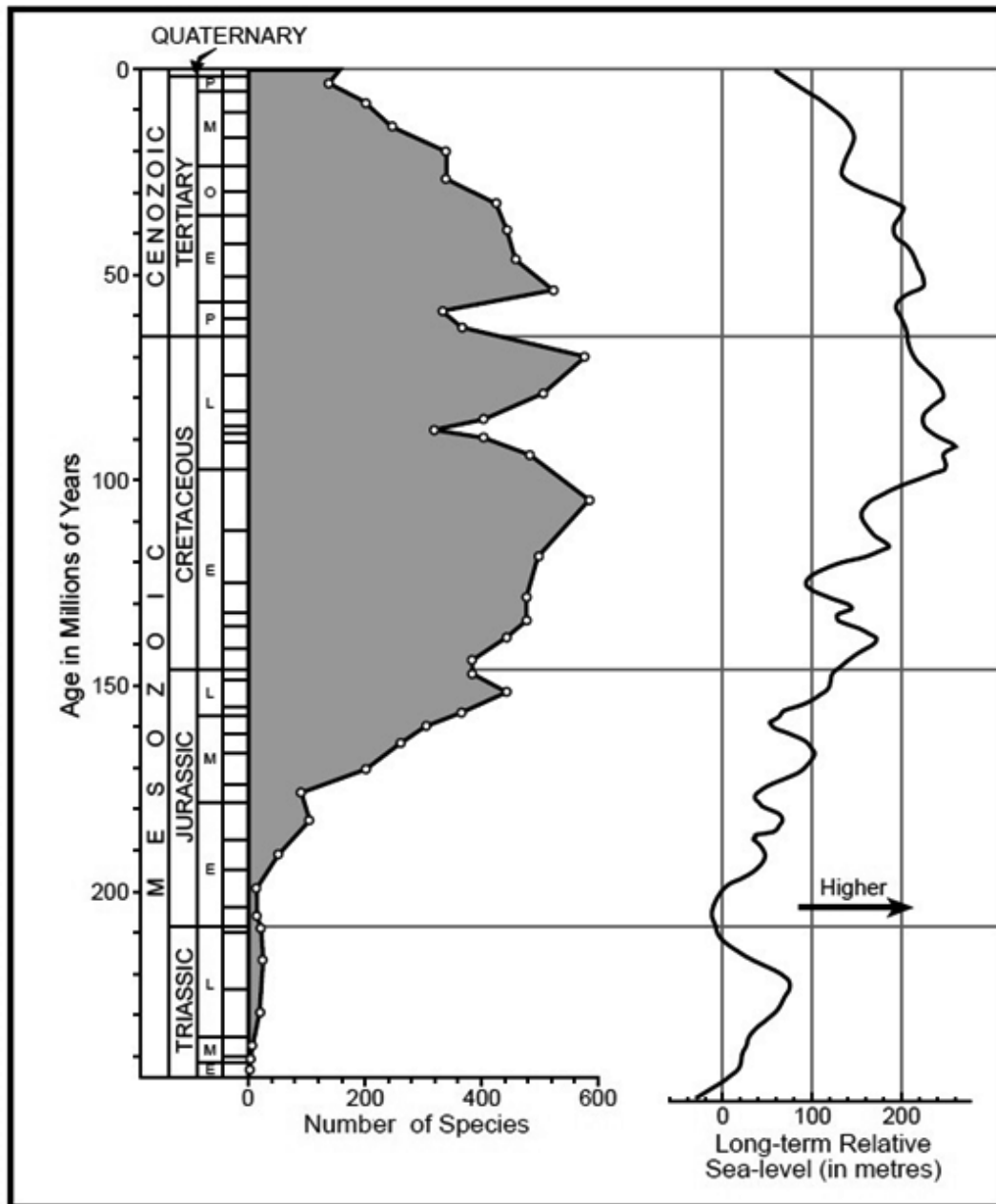


**Figure 14** - Fossil dinoflagellate diversity (number of species) during the Mesozoic and the Cenozoic (until the Quaternary) and its overall correlation with in long-term sea level (after MacCrae *et al.*, 1996).

Despite disagreement as to the precise number of dinocyst species in each chrono-geologic unit (see Macrae *et al.*, 1996, Pross & Brinkhuis, 2005 and Taylor *et al.*, 2008), the profile of diversity plots is strikingly similar across different studies, indicating that it reflects natural events, rather than sampling or methodological artifacts (Macrae *et al.*, 1996). Overall, the cyst-diversity plot correlates well with the long-term sea-level curve, with high diversity associated to periods of high sea levels

and large shelf seas, plausibly manifesting the preference of dinoflagellates for shelf environments (Macrae *et al.*, 1996; Pross & Brinkhuis, 2005). The declining trend from the Lower Cenozoic until the present day somewhat parallels the development of the Earth's cryosphere (Pross & Brinkhuis, 2005).

The rapid radiation of dinocysts from the Late Triassic into the Early Jurassic, characterized by a marked proliferation of morphological types (namely as regards tabulation) and followed, after the Middle Jurassic, by a relative stabilization of major lineages, was interpreted as a truly evolutionary event (Fensome *et al.*, 1999), despite early concerns over the incompleteness of the fossil record. This interpretation is strengthened by the occurrence of sequential appearances of individual families with a link provided by intermediate tabulations (*e.g.*, peridinioids appear to have derived from gonyaulacaleans via a cladopyxiinean ancestor already present in the Early Jurassic) (Fensome *et al.*, 1999). Available evidence that core structural features of the dinoflagellates as we know them today, such as the *cingulum* and the *sulcus*, may have evolved during the Late Triassic–Early Jurassic radiation also points in that same direction, having been supported by molecular analyses (Medlin & Fensome, 2013).

The first morphological (tabulation-based) groups to appear were suessioids and gonyaulacoids, followed by peridinioids, which underwent a quick expansion in the Cretaceous (Taylor *et al.*, 2008). By the Middle Jurassic, the main gonyaulacoid–peridinioid lineages (under the subclass Peridiniphycidae) to which most known fossil dinoflagellates belong were already established. After the mid Jurassic, the appearance of new groups within the dominant Peridiniphycidae subclass involve only minor morphological changes, (*e.g.*, peridiniaceans differ from the earlier heterocapsaeans by the elimination of one apical plate boundary and the protoperidinaceans derive from peridinaciens via a reduction in the number of apical plates), contrasting with the major tabulation innovations that emerged in the Late Triassic–Early Jurassic (Fensome *et al.*, 1999). In general, no new important cyst types appear after the Mesozoic (Taylor *et al.*, 2008). The first freshwater fossil dinocysts, consisting of species of the ceratioid group, appeared in Barremian (Lower Cretaceous) deltaic ponds, having thus a much shorter record than dinocysts in marine facies (Martín-Closas, 2003). Differently from other groups, dinoflagellates do not seem to have been affected by species extinction at the Cretaceous–Tertiary boundary (K/T) (Macrae *et al.*, 1996), as all major lineages survived to this day (Taylor, 2004). However, regional evolution and extinctions of species during the late Cenozoic may have occurred, in connection to dramatic climatic variations at the onset of continental glaciations, as suggested by differences in cyst assemblages in mid-high latitudes of the Northern and Southern Hemispheres (De Vernal, 2009).

### 5.2.2. Dinocyst biozonations

Dinoflagellate cysts occur in a wide variety of marine sediments, from shales, clays and marls to sandstones and limestones (Sargeant, 1974). The circumstance that they can be found from inner neritic to pelagic settings makes dinocyst biostratigraphy particularly apt for correlations between proximal and distal marine sites (Pross *et al.*, 2010). Relative to calcareous microfossils (*e.g.*, foraminifera, calcareous nannoplankton), organic-walled cysts present the additional advantage that they do not suffer decalcification and are resistant to diagenetic processes as well as to mild thermal metamorphism (Sargeant, 1974). Relative to macrofossils, the analysis of dinocysts typically requires smaller amounts of material, remaining applicable to very small core samples (Pross, 2001; Sargeant, 1974). Dinoflagellates taxonomy is also more highly constrained than that of other palynomorphs, such as acritarchs and miospores (*e.g.*, angiosperm pollen), thus allowing for more robust approaches (Fensome, Crux, *et al.*, 2008). Taken together, these characteristics make organic-walled fossil dinocysts the prime candidates upon which to base a biostratigraphy of marine Mesozoic–Cenozoic strata.

Pioneer dinocyst-based biostratigraphic studies were largely the work of palynologists seeking a better understanding of petroleum systems (Williams *et al.*, 2004). An increased recognition of the usefulness of dinocysts ecobiostratigraphy in hydrocarbon exploration established it as routine tool in the past decades (Pross & Brinkhuis, 2005). Evidence that higher stratigraphic resolution can be obtained from dinocysts as compared to any other microfossil group has been reported for several oil and gas exploration sites at the central North Sea (Gradstein, Kristiansen, Loemo, & Kaminski, 1992). All earlier studies were however limited to local subsurface sections and did not include independent chronostratigraphic calibrations of dinocyst events (Williams *et al.*, 2004). Increased efforts towards more extensive studies, allowing for the correlation of multiple sections, (including reference surface sections and stratotypes) and for external chronostratigraphical controls (*e.g.*, biotic calibration to other fossil groups, such as foraminifers and planktonic nannofossils, or to macrofossils, magnetostratigraphy calibration, chemostratigraphic calibration) were thus developed, leading to the proposal of dinocyst biozonations for comprehensive regions and time intervals (Williams *et al.*, 2004).

A broad listing of dinocyst zonations for the Cretaceous–Cenozoic of the Northern Hemisphere and the Late Cretaceous–Paleogene of the Southern Hemisphere can be found in Williams *et al.* (2004), who also discuss remaining issues of calibration, particularly for the Paleogene in the Southern Ocean, and the problems faced by

Neogene zonation in higher latitudes of the Southern Hemisphere due to shortage of specimens (reflecting the destruction of cysts by oxygen-rich waters and/or the disappearance of cyst-producing dinoflagellates from the Antarctic realm during the Oligocen). Significant formal calibrated dinocyst zonation were provided, *e.g.*, for the Late Cretaceous–Early Oligocene and the Quaternary in the East Tasman Plateau (Brinkhuis, Sengers, Sluijs, Warnaar, & Williams, 2003), the Late Cretaceous and the Cenozoic of the Scotian Margin (Eastern Canada) (Fensome, Crux *et al.*, 2008), the northern European Turonian (Olde *et al.*, 2015), the upper Albian to lower Maastrichtian in the Barents Sea (Radmacher, Tyska, Mangerud, & Pearce, 2014), or the Eocene–Oligocen transition in the Southern Ocean (Sluijs *et al.*, 2003).

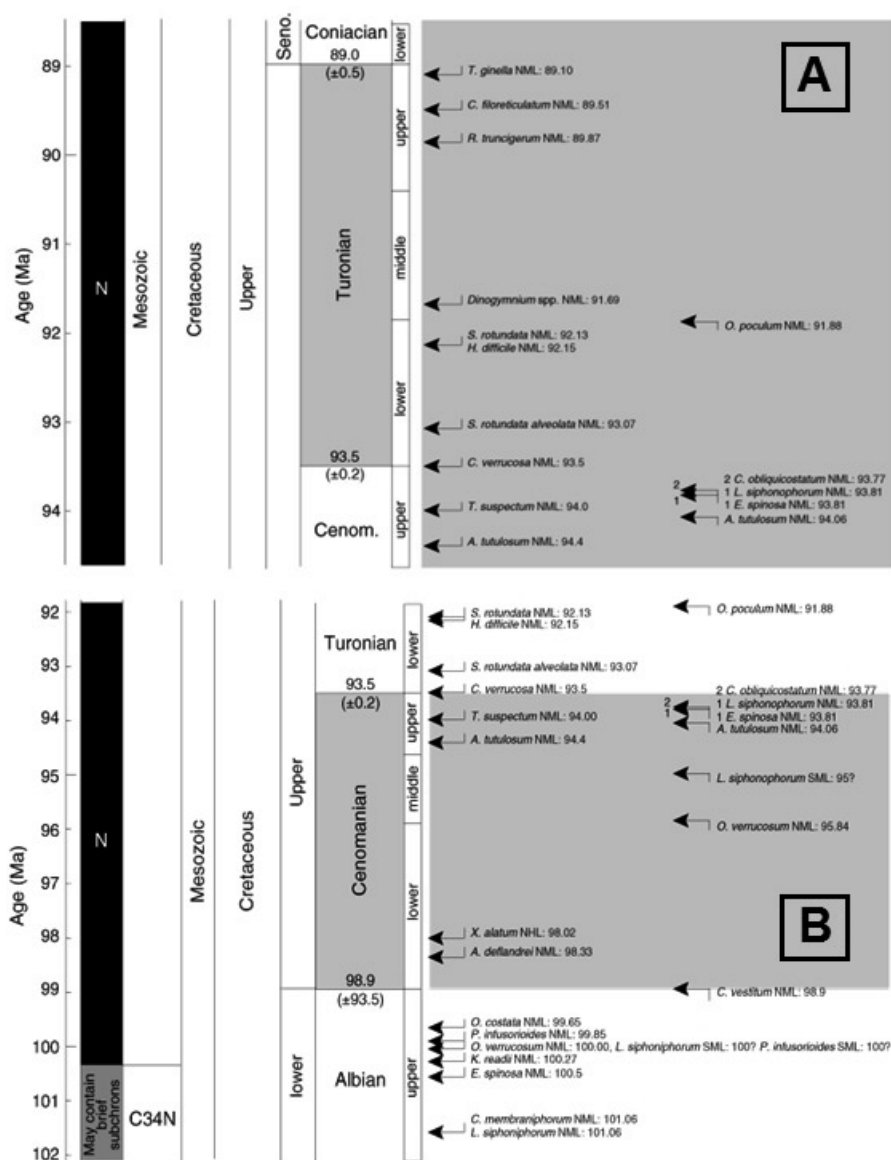


**Figure 15** - (A) Global dinoflagellates cyst events for the lower middle and upper Turonian provided in Williams *et al.* (2004). (B) Global dinoflagellates cyst events for the lower, middle and upper Cenomanian

provided in Williams *et al.* (2004). Retrieved from [http://www-odp.tamu.edu/publications/189\\_SR/107/107.htm](http://www-odp.tamu.edu/publications/189_SR/107/107.htm). MNL stands for Northern Hemisphere mid-latitudes. NML for Northern Hemisphere mid-latitudes and SHL for Southern Hemisphere high latitudes. First occurrences (FO): arrows with up bar; Last occurrences (LO): arrows with down bar.

Of special note is the global index of dinoflagellate cyst events published by Williams *et al.* (2004), which encompasses both the Northern and the Southern Hemispheres and can be used as a general reference for comparison in dinocyst stratigraphical research. Conducted under the framework of the Ocean Drilling Program (ODP), it compiled the results of numerous dinocyst studies with independent age control (to other microfossils and to palaeomagnetic ages) for the Northern Hemisphere and compared them with proposed zonations of the Southern Ocean and with the analysis of dinocyst data from two sites (offshore Tasmania, Southern Hemisphere) of the ODP Leg 189, for which magnetostratigraphic and biotic calibrations were also available. By collating the stratigraphic ranges of different *taxa*, they produced a sequence of dinocyst events in association with standard timescales for the Mesozoic (Gradstein and Ogg, 1996) and the Cenozoic (Berggren *et al.*, 1995), and extending from the Cenomanian (Late Cretaceous) to the Zanclean stage in the Neogene.

The stratigraphic ranges are conveyed through the indication of the First Occurrence (FO) and Last Occurrence (LO) for each *taxon* in mega-annum (Ma). Acknowledging the marked “provincialism” (geographical differentiation of dinocyst assemblages as a function of such factors as latitude/temperature) in the fossil record, first recognized in Mesozoic sediments (Pross & Brinkhuis, 2005), Williams *et al.* (2004) also add to the FO/LO of each *taxon* its assignment to high-, middle- or lower-latitudes in the Northern or Southern Hemispheres. Fig. 15 schematically illustrates the global dinoflagellate cyst events for the Turonian (A) and Cenomanian (B) stages of the Upper Cretaceous provided in Williams *et al.* (2004).

### 5.2.3. Dinocyst stratigraphic studies in Portugal (Mesozoic–Cenozoic)

As the present work specifically concerns a section of the Lusitanian Basin dating from the Lower to Middle Cenomanian, we provide in the following a brief overview of dinocyst biostratigraphic studies conducted in Portugal (also allowing in, by convenience, some references to the Iberian Peninsula), especially those focusing on the Lusitanian Basin. In a stratigraphic study of the Castilian Platform in Northern Spain, based on dinoflagellate cysts, Peyrot (2011) reported that, as regards the Cenomanian/Turonian (Upper Cretaceous) in the Iberian Peninsula, only one Portuguese

succession had been examined by Berthou, Foucher, Lecocq, and Moron (1980). In fact, at least one more study by Berthou and collaborators was concerned with Albian (Lower Cretaceous) and Cenomanian (Upper Cretaceous) dinocysts in different outcrops of the Lusitanian Basin (Lisbon Region) with a prime biostratigraphical focus (Berthou & Hasenboehler, 1982). A few significant biostratigraphical analyses based on dinoflagellate cysts have addressed Lower Cretaceous sections (Berriasian to Albian) in both the Lusitanian and the Algarve Basins: Berthou and Leereveld (1990); Heimhofer, Hochuli Burla, and Weissert (2007), Horikx, Heimhofer, Dinis, and Huck (2014). This latter study revised the stratigraphy of Albian strata in three sections of the Lusitanian Basin based on dinocyst assemblages with an independent chemostratigraphic calibration (strontium-isotope and carbon-isotope stratigraphy), allowing for a high-resolution and well-constrained stratigraphical model.

Most palynological studies allowing a room for the examination of dinocyst assemblages in Portuguese successions concern the Jurassic (more frequently Lower and Middle), *e.g.*: Barrón, Comas-Rengifo, and Duarte (2013) and Oliveira, Dino, Duarte, and Perilli (2007) focusing a Lower Jurassic section (Pliensbachian/Toarcian) of the Lusitanian Basin; Borges, Riding, Fernandes, and Pereira (2011) and Borges, Riding, Fernandes, Matos, and Pereira (2012), respectively addressing Pliensbachian to Kimmeridgian (mid-Lower to mid-Upper Jurassic) and Callovian (Middle Jurassic) stages in the Algarve Basin; Davies (1985), focusing the Sinemurian to Aalium interval (Lower to Middle Jurassic) in the central Lusitanian Basin; Doubinger, Adloff, and Palain (1970), affording a biostratigraphical analysis of the Lower Portuguese Mesozoic (Early Jurassic, reaching down to Late Triassic); Fernandes, Borges, Rodrigues, and Matos (2010), examining the Middle-Upper Jurassic (Callovian and Oxfordian stages) of the Algarve Basin at two offshore sites; Marques and Rocha (1988), addressing the Callovian of Eastern Algarve; Sousa (1998), focusing on the Oxfordian-Tithonian (Upper Jurassic) of the Lusitanian Basin. A few studies can also be found concerning the Cenozoic, *e.g.*: Castro (2010), focusing on the Tortonian (Late Miocene) deposits of the Lower Tagus basin; Castro, Borges, Pereira, Fernandes, and Pais (2013), addressing the biostratigraphical correlation between the Lower Tagus and the Algarve Basins on the basis of Miocene (Neogene) dinocysts assemblages; Gonçalves, Mendonça Filho, da Silva, Mendonça, and Flores (2014), covering the palynological content (dinocysts included) of a set of stratigraphic units ranging from Middle Jurassic to the Neogene in the Lower Tagus basin.

The degree to which dinoflagellate cysts were used with a proper biostratigraphic view in this array of studies is rather variable (exception made to the Cretaceous subset of studies, where this is invariably a primary focus), going from merely recognizing

their occurrence in the samples (*e.g.*, Gonçalves *et al.*, 2014), to according them a supplementary role as regards other palynomorphs (notably spores and pollens), to using them as major biostratigraphical constraints (with or without additional age controls). Stratigraphic ranges delimited by First and Last Occurrences (FO and FA) or First Common and Last Common Occurrences (FCO and LCO) of dinocyst *taxa* are offered in some studies, but not in many others. As regards the Upper Cretaceous, in particular the Cenomanian, Berthou *et al.* (1980) and Berthou and Hasenboehler (1982) emerge as the only available studies to the best of our knowledge, confirming the scarcity of dinocyst-calibrated stratigraphic models for the Portuguese successions corresponding to this geochronological span.

### 5.3 ECOLOGY AND PALAEOECOLOGY

Dinoflagellates are a highly diverse eukaryotic group which can be found in virtually any aquatic environment, from marine (around 90% of living species) to fresh water, predominantly in pelagic habitats, but also sometimes in sand (psammophilic dinoflagellates), ice or snow (Marret & Zonneveld, 2003; Taylor *et al.*, 2008). Forming a significant part of the phytoplankton, they are important as primary producers. While most of the over 2000 inventoried extant species are free-living, a small percentage are endosymbionts (*e.g.*, the *zooxanthellae*, associated with reef-forming corals) or parasites of other protists and animals (Taylor *et al.*, 2008).

Several characteristics of dinoflagellates favor their occurrence in a wide array of environments, noticeably among them (1) ability for directional swimming (as motile cells) and (2) diversity of trophic strategies (Hackett *et al.* 2004). In contrast to diatoms (see Smayda, 2002), controlled swimming allows dinoflagellates to position at distinct depths in the water column (vertical migrations) as a function of parameters such as, *e.g.*, nutrients concentration, light intensity, salinity, sea surface temperature or oxygen availability. Differential sensitivity to these parameters has moreover been found across individual species (Anderson & Stolzenbach, 1985; Hackett *et al.*, 2004).

As for nutrition, about half of dinoflagellates *taxa* are photo-synthetic and the other half heterotrophic, predating to a large extent on other protists, particularly diatoms. Most photosynthetic dinoflagellates are not actually autotrophic but mixotrophic, combining photosynthesis and heterotrophy. Capture and feeding behavior among heterotrophs can be highly variable, ranging from phagotrophy (non thecate cells that engulf their preys) to myzocytosis or pallium-feeding (Hoppenrath



& Saldarriaga, 2012; Jacobson & Anderson, 1986). Taken together, these ecologically relevant characteristics have allowed dinoflagellates as a group to globally exploit coastal waters, while at the same time exhibiting considerable habitat specialization at the level of individual species (Hackett *et al.*, 2004; Smayda, 2002; Taylor, 1987; Wall, Dale, Lohmann, & Smith, 1977).

As mentioned earlier, some proportion (around 10 to 20 %) of dinoflagellates produce dormant resistant cysts, mostly organic-walled (made of dinosporin, which resists decalcification), as part of their life-cycle. These cysts deposit on the bottom sediments, where they form seed banks available for the renewal of motile forms and become additionally prone to fossilization (Sargeant, 1974; Taylor *et al.*, 2008). The potential of the geographical distribution of dinocysts in the sediments for reconstructing salient environmental and climatic features of the upper water surfaces has been successfully demonstrated for neritic (*e.g.*, estuaries, epicontinental seas, continental shelves) and pelagic settings (*e.g.*, Marret & Zonneveld, 2003; Pross & Brinkhuis, 2005; Wall *et al.*, 1977), despite a number of acknowledged limitations (Dale, 1996; de Vernal & Marret, 2007; Wall *et al.*, 1977).

As reliably identified fossil organic-walled dinocysts are available from the Triassic onward, the prospect of reconstructing past environments and climates based on cysts distribution in ancient sediments was also opened thereby (Marret & Zonneveld, 2003; Pross & Brinkhuis, 2005). However, the palaeoecology of fossil cysts requires, as a precondition, detailed information on the relationships between present day environmental conditions and the distribution of modern cysts in recent sediments (Zonneveld *et al.*, 2013).

### **5.3.1. The ecological classification of organic-walled dinocysts: ground concepts**

The geographical distribution of modern dinocysts was initially the subject of separate regional studies (*e.g.*, western South Africa (Davey, 1971), North Atlantic Ocean (Williams, 1971)). In 1977, Wall *et al.* released a landmark study, based on 168 samples from fourteen geographical regions of mainly the North and South Atlantic oceans and adjacent seas, which set the basis for an ecological classification of dinoflagellates cysts as proxies to environmental-climatic factors characterizing different “water-types”, particularly sea surface temperature (SST) and salinity. Two main trends, relating to distance to the shore (estuarine, estuarine-neritic, neritic, neritic-oceanic and oceanic) and to latitude-climate (cool water of temperate zones, warm water of

tropical and subtropical zones) were identified in the distribution of marine cyst-based *taxa*. These two gradients have been consistently replicated in more recent and geographically broader studies, with sea surface temperature typically explaining the largest variance of species distributional data (Marret & Zonneveld, 2003; Zonneveld *et al.*, 2013; Taylor *et al.*, 2008).

Two other fundamental contributions of the Wall *et al.* (1977) paper involve the conceptual framework for an ecologically relevant interpretation of cysts distribution in the sediments and, related to it, the consideration of diversity signals within cyst assemblages, in addition to differences in species composition and the peak abundance of individual *taxa* (Pross & Brinkhuis, 2005).

Most organic-walled cyst producing dinoflagellates inhabit shallower-waters along continental margins characterized by unstable and unpredictable (i.e., displaying high seasonal variability and irregular recurrence of conditions) hydrographic regimes (Wall *et al.*, 1977; de Vernal & Marret, 2007). Consistent to what might be expected from an evolutionary adaptive standpoint, the most abundant *taxa* tend towards a cosmopolitan opportunistic distribution, exhibiting broad tolerance to salinity gradients (euryhaline properties), little thermal preference (eurythermic properties), slender differentiation along the inshore-offshore component and incipient speciation (limited to slight variations in features of cyst morphology, such as processes and spines) (Wall *et al.*, 1977).

These generalist *taxa*, due to their geographical ubiquity, are of reduced value to palaeological reconstructions. Those of greatest interest correspond to focused adaptations, at the species level, to stable sectors of the aquatic environments, typically occurring at the terminal/subterminal portions of the salinity and thermic regimes (Wall *et al.*, 1977). Examples of such stenotopic *taxa* are the stenohalines *Leptodinium*, adapted to fully saline ocean water, and *Gonyaulax apiculata*, found only in freshwater lake sediments (Wall *et al.*, 1977), or the stenothermics *Impagidinium Palidum*, adapted to cold ocean waters, and *Islandinium*, used as a marker of seasonal sea-ice cover (de Vernal & Marret, 2007). Fig. 16 illustrates these two sorts of adaptation to the thermic and salinity domains: generalist adaptation, tolerant to wide range variations and leading to cosmopolitan distributions (eurytopic *taxa*), and specialized adaptation to the terminal sectors of these domains, reflected in geographically restricted distribution patterns (stenotopic *taxa*).

While inshore-offshore and latitudinal distributional trends are primarily reflected in the peak abundance (or exclusive occurrence) of different *taxa* in their optimum environments, they are also manifest in changes of species associations (co-occurring species) both across environment-climatic units and along the transitional regions in

between them (e.g., estuarine-coastal or neritic-ocean transitions). This is consistent with the view that cysts assemblages arise from the combination of ecological groups through hydrographic mixing, so that species associations express the cumulative effects of individual *taxa* distributions (Wall *et al.*, 1977).

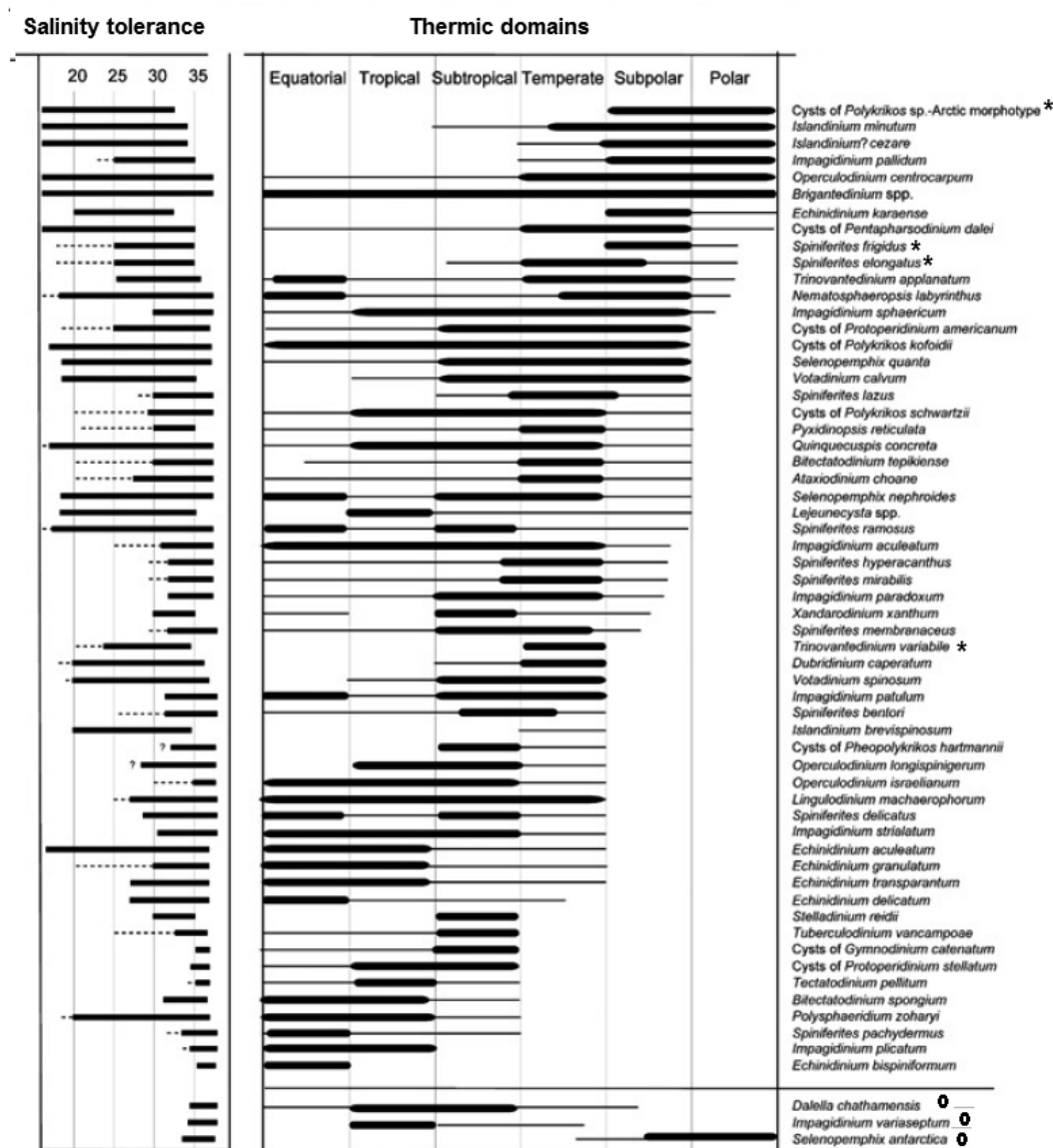


**Figure 16** - Diagrammatic representation of the distribution of a number of extant dinocysts in the sediments according to climatic regions (entailing distinct degrees of thermic-related tolerance) and of their corresponding salinity-related tolerance (slightly modified from de Vernal & Marret, 2007). The asterisk “\*” indicates *taxa* exclusively found in the northern Hemisphere; the “o” signals *taxa* only found in sediments of the southern Hemisphere.

In addition to these two indices, Wall *et al.* (1977) promoted a measure of species diversity (number of species in an assemblage after normalization to the sample size:

see Hurlbert, 1971), widely accepted among ecologists to reflect the amount of stress in ecosystems (higher diversity associating with lower stress). Inshore–offshore and latitudinal trends were again detected with the diversity index, showing seaward augmented diversity and an increase towards low latitudes (intertropical areas, with low seasonal temperature constraints) in both hemispheres. Less ecologically stressed environments were thus coincident overall with the more stable and predictable ones, and diversity was most often augmented by the occurrence of a small set of more stenotopic species in addition to a background of cosmopolitan species (Wall *et al.*, 1977).

Pearce (2000) proposed in this sense that a ratio of cyst species diversity to their absolute abundance be used as an index of environmental stability–predictability (SPI), with increasing values indicating higher stability. Also, considering its broad alignment with an inshore–offshore direction, the diversity index can be cautiously used as an indicator of shoreline proximity, changes in sea level and the occurrence of transgressive–regressive phases. As indicated by Pross & Brinkhuis (2005), dinocysts-based reconstruction of sea-levels has been chiefly based on (1) studies of assemblage composition and (2) studies of the diversity and abundance within assemblages.

### **5.3.2. Dinocysts-based environmental signals and new sets of environmental factors**

On the following of the Wall *et al.* (1977) paper, which laid down a framework for the use of dinocysts in palaeoceanographic studies, many regional studies of cysts distribution and their relation to environmental indices were conducted (for an extensive enumeration, covering the period from 1980 to early 2000–ths, see Marret & Zonnevel, 2003; see also de Vernal & Marret, 2007), and a first map of recent dinocysts in bottom sediments from the North Atlantic Ocean (and adjacent seas) was published by Harland in 1984. More updated databases were later provided for the North Atlantic Ocean (Rochon, de Vernal, Turon, Matthiessen, & Head, 1999; de Vernal *et al.*, 2001), leading to an Atlas of the world-wide distribution of modern organic-walled dinocysts, including the relationships of their relative abundance to surface-water parameters, released by Marret and Zonnevel in 2003. A new extended version of this Atlas, published by Zonneveld *et al.* in 2013 on the basis of information gathered from 2045 sites (comparing to 835 in the early version) affords, to the best of our knowledge, the most comprehensive source on extant dinocysts geographical distribution and its relation to environmental factors.

One noticeable feature of the more recent studies of dinocysts ecology is the enlargement of environmental parameters considered. Nitrates and phosphates (nutrients) concentrations, chlorophyll-*a* concentrations (indexing phytoplankton production), and bottom water oxygen concentrations (indexing the redox state of bottom waters) have thus also been included as environmental parameters in the Zonneveld *et al.* (2013) synthesis, in addition to more standard measures of annual and seasonal SST and salinity. New relationships between cysts assemblages and oxidation, an important taphonomic factor which differentially affects organic-walled cysts *taxa* (Zonneveld, Versteegh, & Kodrans-Nsiah, 2008), sea-surface productivity and trophic regimes could in that way be exploited and made available for use in palaeological reconstructions (see the species ecological classification on each environmental parameter proposed in Zonneveld *et al.* (2013).

Given the above said, the number of ecological signals to be derived from dinocysts assemblages has naturally grown. In 1996, Dale identified six cyst-based signals, relating to coastal versus oceanic waters, salinity, sea-level temperature, and sea-water productivity (including, *e.g.*, oceanic upwelling and coastal eutrophication), which all depended on the species composition of assemblages (Dale, 1996, 2001). A number of other signals may currently be added to the former, concerning, *e.g.*, benthic oxygenation and ventilation of water columns (see Pross, 2001), stratification of water masses and circulation of surface water (Pross & Brinkhuis, 2005), sea-ice coverage, SST seasonality, or transport mechanisms (de Vernal & Marret, 2007).

Furthermore, ecological signals have increasingly been linked to a network of specific indices (qualitative and/or quantitative) which often contribute to more than one type of signal. For instance, an increase in the proportion of heterotrophic species in cysts assemblages – commonly assessed by the ratio *Protoperidiniaceae*/*Gonyaulacaceae* (P/G, with P-cysts taken to be mostly heterotrophic, and G-cysts autotrophic) – may indicate changes in ocean upwelling intensity, augmented productivity unrelated to upwelling (due, *e.g.*, to SST changes) or eutrophication in systems without previous nutrients limitation (Dale, 2001); hence, additional indices, such as changes in cysts concentration and the concrete species associations (namely, low vs. high latitude *taxa*), need to be jointly considered in order to distinguish among the alternatives (Dale, 2001; de Vernal & Marret, 2007). Conversely, distance to the shoreline may be indicated by a prevalence of *taxa* with known oceanic/neritic distributions, changes in the diversity signal in the assemblages, or simply an increase/decrease of dinocysts abundance (cyst-producing dinoflagellates being mostly confined to coastlines, marked abundance speaks in favor of shoreline proximity) (Pross & Brinkhuis, 2005; de Vernal & Marret, 2007; Taylor *et al.*, 2008). Such indices

have been broadly used in reconstructing sea level changes (Pross & Brinkhuis, 2005). However, many parameters mediate the relationship between cysts distribution and the nearshore-offshore gradient (*e.g.*, water turbulence, water stratification, nutrients availability, long distance transport), calling on a cautious interpretation of results and on a multi-proxy approach to palaeoenvironmental inferences. For example, the impact of transport mechanisms on the assemblage might be evaluated with the (pollen + spores)/dinocyst ratio (Pol/Din), taken to reflect the terrestrial vs. marine origin of the organic flux (see de Vernal, 2009, and de Vernal & Marret, 2007, who refer to this ratio as a “continentality” index). An updated synthetic presentation and discussion of many of the environmental indices and ecological signals available from organic-walled dinocysts is provided by de Vernal & Marret (2007).

Pross & Brinkhuis (2005) indicate as two main advantages of using organic-walled dinocysts as (palaeo)environmental tracers (1) their sensitivity to even slight changes of several properties of surface waters (particularly temperature, where they compare favorably to most other microfossils), and (2) their abundance in neritic sediments, affording complementary information to that derived from offshore calcareous and siliceous fossil groups such as *c.* Even if much less studied, the potential (pala)ecological relevance of calcareous dinocysts in the sediments of open oceanic waters (Dale & Dale, 1992) has received growing attention as a source for the reconstruction of upper water conditions (especially productivity, stratification and surface water currents) in domains where organic-walled cysts are inexistent (Vink, 2004; Vink, Brune, Holl, Zonneveld, & Willems, 2002; Wendler, Gräfe & Willems, 2002; Wiese, Zobel, & Keupp, 2015). Freshwater dinoflagellate cysts have also known a regain in interest as ecological/environmental proxies. In an up to date review, Mertens, Rengefors, Moestrup, and Ellegaard (2012) documented their potential usefulness in palaeological reconstructions, namely as indicators of temperature, pH and productivity (despite the fact that only a few freshwater dinocysts have the potential to fossilize). De Vernal (2009) has accorded them a role in assessing the freshwater versus marine character of sediments, and thereby in the reconstruction of sea level changes.

### 5.3.3. Dinocysts-based palaeoecology

The palaeoecology of organic-walled dinocysts has been mostly studied in Quaternary marine sediments, due to the abundance of extant *taxa* allowing for an actuopalaeontological approach (Pross & Brinkhuis, 2005) and the use of robust

quantitative reconstruction methods, such as the Modern Analogue Technique (MAT: see deVernal, 2009; Simpson, 2007). Some of those studies, concerning in particular the late Quaternary, were specifically motivated by environmental goals, such as gaining a better understanding of eutrophication and pollution (Dale, 2001, 2009). The last interglacial period before the present one, corresponding to the Eemian stage in the Pleistocene, has been the focus of a considerable number of palaeoceanographic studies based on dinoflagellate cysts (*e.g.*, Head, 2007; Van Nieuwenhove, & Bauch, 2008). Dinocyst-based reconstructions of palaeoceanographic conditions and palaeoclimates in the Neogene, both during the Miocene (*e.g.*, Louwye, Foubert, Mertens, Van Rooij, & IODP Expedition 307 scientific party, 2008) and the Pliocene (*e.g.*, Head & Westphal, 1999), were also proposed. As for the Paleogene, important climatic events such as Earth's greenhouse-icehouse transition (*e.g.*, Pross & Brinkhuis, 2005; Sluijs, Pross, & Brinkhuis, 2005) and the Paleocene-Eocene thermal maximum (*e.g.*, Sluijs *et al.*, 2008) were addressed resorting to dinocyst studies (see also Pross, 2001, addressing the palaeo-oxygenation of epeiric settings in the Oligocene).

Mesozoic studies using organic-walled cysts as palaeoenvironmental tracers are scarcer. Most of the references included in Riding's (2012, 2013, 2014) compilation of the literature on Triassic, Jurassic, and earliest Cretaceous dinoflagellate cysts concern dinoflagellates taxonomy and biostratigraphy, with only residual examples of attempts at palaeoecological reconstructions. Moreover, for reasons related to the extensive nature of marine strata and the diversity of dinocysts of the Late Jurassic (Riding, 2012), most of the studies are focused on the Jurassic period, with little coverage of the Cretaceous.

Among the organic-walled cyst-based palaeoenvironmental studies of the Late Cretaceous (which includes the stratigraphic time interval of interest in our study, *i.e.* the Cenomanian Age), most deal with the palaeoceanographic conditions during the Cenomanian-Turonian transition. Noteworthy examples are Pearce, Karvis, and Tocher (2009), and Peyrot, Barroso-Barcenilla, and Susanne Feist-Burkhardt (2012), focusing, respectively, on a reference section in England and an outcrop in Central Spain. In addition to the Cenomanian/Turonian boundary, Lignum (2009) also affords palaeoenvironmental reconstructions of the Albian/Cenomanian boundary, and the mid-Cenomanian across several palaeogeographical regions. Examples of a few palaeological studies addressing other time intervals include Dodsworth (2016), focusing on the middle to upper Cenomanian, Skupien (2003), focusing on the upper Barremian-Albian ages of the Lower Cretaceous, and Pestchevitskaya (2008), focusing on a Berriasian to Barremian (Lower Cretaceous) section of the Siberia palaeobasin.





## METHOD AND PROCEDURES

### 6.1. SAMPLING

As a first required step, a stratigraphical profile was elaborated at the base of the south side of the Nazaré promontory, including a section with 13,5 meters and 49 strata encompassing alternate layers of marls and limestones with biostromes of *Ilymatogyra pseudoafricana* and a sequence of laminitic marly levels with *Gyrostrea ouremensis* (see section 3.4 in chapter 3 for details). Careful sedimentological analysis of the profile helped determine which layers afforded the most convenient lithology for sample collecting. The main criteria used were the type of granulometry (preferably thin) and the color of the sediment (a darker sediment would be preferred as it allows inferring a larger quantity of organic matter). The joint use of these criteria led to the selection of the marly levels in the profile as the most suitable ones, providing the array of layers from which the samples were then collected.

Samples were extracted from distinct marly levels, well separated apart in the profile, so as to provide a perspective on the distribution of dinoflagellates and other palynomorphs throughout the spanned time interval. Accordingly, samples were taken from layers more near the base, the middle and the top section of the profile. Furthermore, within each sampled layer, 2 or 3 samples were taken from the base, the middle (in case there were 3 samples) and the top of the layer. Accounting for the requirements of the subsequent laboratorial processing procedures, the amount of collected sediment for each sample was set to 200 grams.

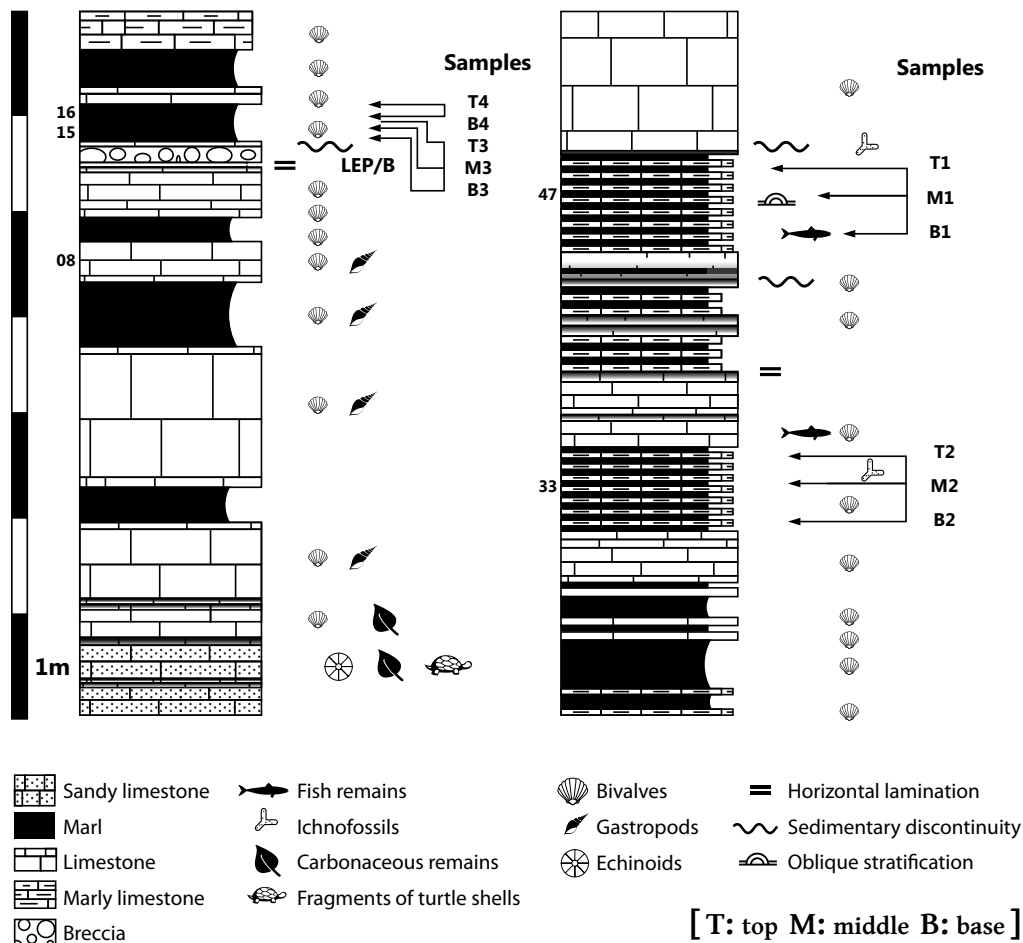


**Figure 17** – Correspondence between samples (11) and layers (4) in the stratigraphic column. **T**, **M**, and **B** respectively designate the top, middle and base sections in each layer.

A total of 11 distinct samples were taken from four distinct layers of the geological profile. The first three samples were taken from the base, middle and top of stratum n° 47 in the stratigraphic column. Three samples were similarly collected from the lower, middle and upper sections of stratum n° 33, and three other from the upper, middle and lower sections of stratum n° 15. The two final samples were taken from stratum n° 16. Given that this particular layer was only 10 cm thick, only two samples were collected, one from the base and one from the top (see Fig. 17).

Additional care was taken in keeping the sampling restricted to the inner sediments in each layer, avoiding the top sediments, typically more exposed and vulnerable to contamination. The collected sediments were placed in appropriate plastic bags which were properly identified and taken to the laboratory for analysis.

## 6.2. PALYNOLOGICAL PROCESSING

The fluxogram presented in the following (Fig. 18) summarizes the sequence of procedural stages leading from the sample collecting to the final palynological processing (Costa, 2015).

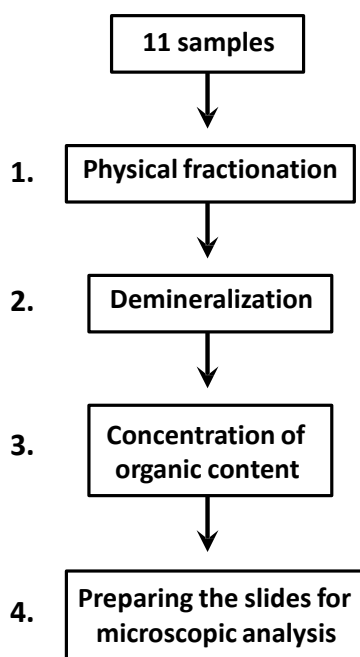


Figure 18 – Fluxogram of processing stages.

As noted by L. Castro (2006), «a good palynological procedure depends on the “know-how” of each researcher, astuteness and technique, along with some personal involvement. It is essential to have access to adequate equipment» (p. 87). Since I was given the opportunity to go through the laboratorial procedures in the Laboratory of Palynology of the LNEG, Porto, the standard palynological techniques of the LNEG were employed, which include consecutive treatments of the sampled material with chloridric and fluoridric acids. Several of these procedures have been the subject of careful descriptions in Borges (2012) and A description of the main features of these four processing stages is given below:

**Physical fractionation** - After being cleaned, samples were smashed into thinner particles (which potentiates the action of the acids) with a suitable hammer (Fig. 19). The resulting fragments were then washed in tap water in order to remove subsisting larger sized particles which might react violently to the acids.



**Figure 19** – Physical fractionation of the samples.

**Demineralization** – The fragments were placed in clearly identified teflon cups with large bottlenecks, which allow treatment with hydrochloric and hydrofluoric acids (see Fig. 20A and B). The sediment underwent several attacks with acids with different concentrations, in order for the mineral fraction to be progressively removed. This was performed in a laboratory hood that limited exposure to toxic fumes and facilitated the handling of the chemical products. Three consecutive acid attacks were applied:

- (1) With hydrochloric acid (for the elimination of carbonates): the samples were submitted to a 48 hours treatment with hydrochloric acid (20% concentration), which can be extended to 4 days, if necessary. The volume of hydrochloric acid used was always enough to cover all of the sediment, and effervescence had to cease completely before proceeding to the next treatment step. In case effervescence was excessive, a few drops of alcohol were added as a means to control it. The solution was then diluted with tap water (passing through a filtering system) and additionally filtered (15  $\mu\text{m}$  sieve) to remove any chlorides that may have formed. Before removing the fluid, the sample was left to decant for a minimum of 4 hours, allowing palynomorphs to deposit during that time;
- (2) With hydrofluoric acid (for the elimination of silicates): hydrofluoric acid (37% concentration) was added to the residue for a period of 6 to 10 days. This reaction generates a lot of heat, with the potential to damage the cups or even endanger the person who is conducting the procedure. For that reason, the cups were placed in cold water so that the resulting heat from the reaction dissipates. To boost the effect of the acid, they were then revolved periodically

(twice a day), the residue was subjected to successive decantations, and the acid renewed. After the sample was completely disaggregated, it was neutralized through consecutive decantations with water and subsequently filtered;

- (3) With hydrochloric acid (for the elimination of fluorides and sulfides): a hot attack with HCl was conducted to eliminate secondary minerals like insoluble fluorides and sulfides that might have resisted the previous treatments. The solution was boiled for about 5 minutes to eliminate the remaining mineral fraction. As in the previous stages, the remaining sediment was diluted, decanted and filtered (15  $\mu\text{m}$  filter) until the water became transparent and the acid was completely removed. In case a considerable mineral fraction subsisted after these procedures, the sample was again submitted to chemical treatment with HF for about 12 to 24 hours.

Following these three attacks, the remaining residue was cleaned with dispersant (for the elimination of thin mineral matter), washed and sieved (15  $\mu\text{m}$  sieve) (see Fig. 20C). In cases where leftovers of resistant minerals remained in the sediment, the treatment with hydrofluoric acid was repeated. When there was the further need to eliminate soluble organic matter (which hampers the observation of the lamina on the microscope), oxidation of the residue was induced, followed by a new cycle of washing and sieving, which concluded the demineralization stage.

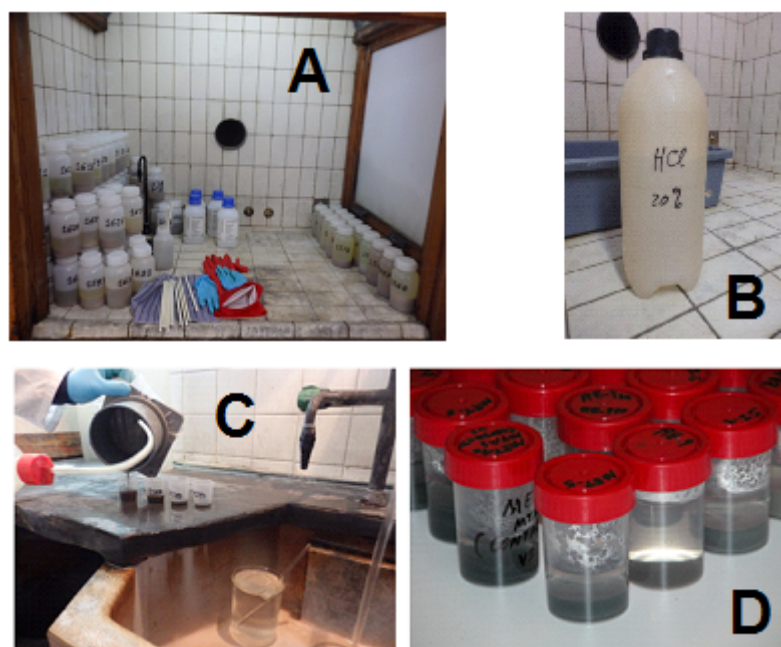


**Figure 20** – **A.** Teflon<sup>®</sup> bottles containing samples that are being treated with HF and HCl in the LNEG’s laboratory hood. **B.** HCl (20% concentration) used for the destruction of the mineral fraction. **C.** Washing and sieving. **D.** Storage of the concentrated organic residue in labeled vials.

**Concentration of the organic content** - In some samples, the resulting organic residue after the demineralization was scarce and a considerable mineral fraction had resisted the series of acid attacks. Two methods were then applied for the concentration of the organic residue. In samples with a really high mineral content, separation of the mineral and the organic fraction was achieved by using zinc chloride ( $\text{ZnCl}_2$ ), a high density liquid ( $2\text{gm}/\text{cm}^3$ ). The residues, placed in tubes, were centrifugated at 4000 r.p.m for 5 minutes (with a balanced weight per tube). After the supernatant water was eliminated, about 5 ml of  $\text{ZnCl}_2$  solution was added to each tube, which was then shaken and had their weight adjusted. A further 5 minutes centrifugation at 4000 r.p.m was performed, following which the supernatant, containing the concentrated organic residue, was removed with a pipette. The collected residue was examined under the microscope and, if no mineral fraction was detected, transferred to a beaker where the solution was neutralized with water. Otherwise, a new centrifugation cycle took place. After neutralization, the final residue was washed, filtered with a  $15\ \mu\text{m}$  sieve, and stored in small and properly labeled vials (Fig. 20D).

For samples with a low remaining mineral fraction, a second method was used. Concentration of the organic matter was then achieved by panning in a watch glass with water. The supernatant was removed with a pipette and the process repeated several times, so that all the organic matter could be removed. The recovered organic residue was then stored in properly identified small vials with water. A drop of diluted HCl was added to the vials in order to avoid fungal proliferation.

**Preparing the slides for microscopic analysis** - With the concentrated organic content moved to glass made beakers, a few drops of hydroxyethylcellulose (dispersant) were added to the solution to favor the dispersal of the palynomorphs at the time the lamellae were assembled. The solution was then manually agitated to become homogeneous and distributed by several lamellae with a pipette. These were placed in an appropriate greenhouse and left to dry at a constant temperature of  $30^\circ\text{C}$  (Fig. 21B).

The lamellae were labeled and assembled as microscope slides, using acrylic resin (Entelan<sup>®</sup>) as mounting medium. After a 2 hours rest, for the resin to settle and dry, the microscope slides were ready to be observed. As preliminary observations of the first slides revealed that the palynological content was not optimally visible, the practice was adopted of using a biological stain (Safranin) to highlight the structures of dinoflagellates and other palynomorphs. Several slides from each sample were thus prepared after first staining the organic fraction with Safranin for a period of 15 minutes to 4 hours (see Fig. 21A). These slides were then studied on a biological SMI microscope (Olympus BX40 e Camara Olympus C5050).

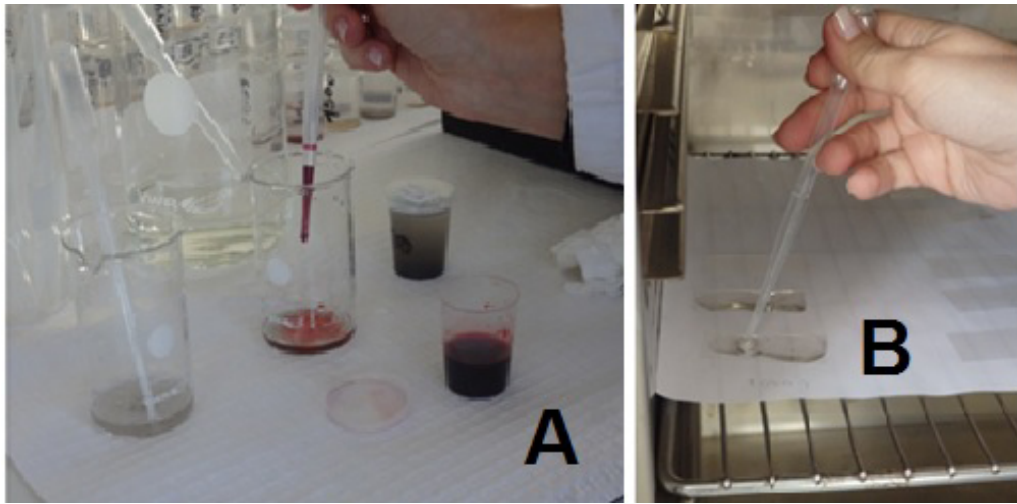


**Figure 21** – **A.**Organic fraction stained for 4 hours with Safranin. **B.** Assembly and drying of thin sections.

All samples, organic residues and slides are stored in the collections of LNEG, in S. Mamede de Infesta, Porto.





## Chapter 7

---

# PRESENTATION, ANALYSIS AND DISCUSSION OF RESULTS

### 7.1. GROUPS OF PALYNOMORPHS AND THEIR RELATIVE ABUNDANCE

Analysis of the palynological content of the samples disclosed the occurrence of distinct groups of palynomorphs, including 20 dinocysts *taxa*, 17 sporomorph *taxa* (of which 2 angiosperm and 9 gymnosperm pollen types, and 6 cryptogam spores), 4 *taxa* of green-blue algae, common to abundant microforaminiferal linings and a single acritarch specimen. One scolecodont, one specimen of *Diphyes* sp. and a few dinocyst type A were also recorded. The identified *taxa* of dinocysts, spores, angiosperm pollen, gymnosperm pollen and algae are alphabetically listed in Tables 2 and 3, along with their suprageneric affiliations and an associated code referring to their microphotographic illustration in the plates provided in Annex 1. Due to excessive fragmentation of the organic residual, two (T2 and T3) of the eleven samples were palynologically barren and are thus not considered in the following analyses.

The relative abundance of these distinct groups in each of the 9 positive samples is graphically represented in Fig. 22. These percentages were based on a counting of 157–233 palynomorphs/sample, with an average counting of 184 palynomorphs per sample. Samples are vertically arranged so as to reflect, from top to bottom, the location of the sampled layers in the stratigraphic column (number 1 corresponds to layers more towards the top, number 2 to layers near the middle, and numbers 4 and 3 to layers more towards the base of the profile). Within each layer, corresponding to a row, samples are also arranged in a top-down order, with T standing for the top,

M for the middle and B for the base of the corresponding layer.

**Table 2** – *Taxa* of found dinocysts. Suprageneric affiliations are given in the middle column. The rightmost column identifies the corresponding photomicrograph illustrations (“Pl.” stands for “plate”; the number before the colon identifies the plate; number(s) after the colon specify an image or a set of images in the plate).

<i>Taxa</i>	Botanical affinity	Figure
<b>Dinoflagellate cysts</b>		
<i>Canningia reticulata</i> (Cookson & Eisenack, 1960)	Areoligeraceae	Pl.1:1-2
<i>Canningia</i> sp.	Areoligeraceae	Pl.1:3-4 Pl.2: 1-4
<i>Epelidosphaeridia spinosa</i> (Cookson & Hughes, 1964)	Ovoidinioideae	Pl.17:1-5
<i>Florentinia mantellii</i> (Davey & Williams, 1966)	Cribopteridinioideae	Pl.3:1-2
<i>Florentinia</i> sp.	Cribopteridinioideae	Pl.3:3-4 Pl.4:1-3 Pl.5:1-5
<i>Heterosphaeridium</i> sp.	Gonyaulacales	Pl.6:1-2
<i>Impletosphaeridium</i> sp.	Gonyaulacales	Pl.7:1-6 Pl.8:1-5
<i>Oligosphaeridium pulcherrimum</i> (Deflandre & Cookson, 1955)	Leptodinioideae	Pl.9:1-2
<i>Oligosphaeridium</i> sp.	Leptodinioideae	Pl.10:1-2
<i>Palaeohystrichophora infusorioides</i> (Deflandre, 1935)	Palaeopteridinioideae	Pl.18:1-2
<i>Palaeohystrichophora</i> sp.	Palaeopteridinioideae	Pl.18:3-6
<i>Spinidinium</i> sp.	Deflandreoideae	Pl.19:1-6
<i>Spiniferites ramosus</i> (Ehrenberg, 1838)	Gonyaulacoideae	Pl.11:1-6 Pl.12:1-6
<i>Spiniferites</i> sp.	Gonyaulacoideae	
<i>Subtilisphaera</i> sp.	Palaeopteridinioideae	Pl.20:1-9 Pl.21:1-9 Pl.22:1-5
<i>Trithyrodinium suspectum</i> (Davey, 1969)	Deflandreoideae	Pl.23:1-7
<i>Trithyrodinium</i> sp.	Deflandreoideae	Pl.24:1-5
<i>Xenascus ceratioides</i> (Deflandre, 1933)	Ceratiaceae	Pl.13:1-3
<i>Xenascus</i> sp.	Ceratiaceae	Pl.13:4 Pl.14:1-5
<i>Xiphophoridium alatum</i> (Sarjeant, 1996)	Gonyaulacales	Pl.15:1-5 Pl.16:1-5

**Table 3** – *Taxa* of found spores, pollen grains and algae. Suprageneric affiliations are given in the middle column. The rightmost column identifies the corresponding photomicrograph illustrations.

<i>Taxa</i>	Botanical affinity	Figure
<b>Spores</b>		
<i>Cicatricosisporites</i> sp.	Pteridophyta (Schizaeaceae)	Pl.36:1-7
<i>Contignisporites cooksonii</i> (Dettmann, 1963)	Pteridophyta (Pteridaceae)	Pl.37:1-2
<i>Contignisporites</i> sp.	Pteridophyta (Pteridaceae)	Pl.37:3-4
<i>Patellasporites</i> sp.	Pteridophyta	Pl.38:1-12
<i>Plicatella</i> sp.	Pteridophyta (Schizaeaceae)	Pl.37:5-7
<i>Angiosperm pollen</i>		
<i>Afropollis jardinus</i> (Doyle <i>et al.</i> , 1982)	Uncertain	Pl.39:1
<i>Afropollis</i> sp.	Uncertain	Pl.39:2
<b>Gymnosperm pollen</b>		
<i>Alisporites</i> sp.	Coniferophyta (Pinaceae)	Pl.39:3-6
<i>Araucariacites australis</i> (Cookson & Couper, 1953)	Coniferophyta (Araucariaceae)	Pl.40:1
<i>Araucariacites</i> sp.	Coniferophyta (Araucariaceae)	Pl.40:2-4
<i>Classopollis brasiliensis</i> (Herngreen, 1975)	Coniferophyta (Cheirolepidiaceae)	Pl.41:1-9
<i>Classopollis jardinei</i> (Reyre <i>et al.</i> , 1970)	Coniferophyta (Cheirolepidiaceae)	Pl.41:10-11
<i>Classopollis</i> sp.	Coniferophyta (Cheirolepidiaceae)	Pl.41:12-13
<i>Corollina obidosensis</i>	Coniferophyta (incertae sedis)	Pl.40:5
<i>Corollina</i> sp.	Coniferophyta (Cheirolepidiaceae)	Pl.40:6
<i>Cycadopites</i> sp.	Cycadophyta	Pl.39:7-8
<i>Ephedripites</i> sp.	Ginkgophyta (Ephedraceae)	Pl.39:9
<b>Green and Blue-green Algae</b>		
<i>Botryococcus</i> sp.	Botryococcaceae	Pl.26:1-3
<i>Crassosphaera</i> sp.	Prasinophyceae	Pl.26:8
<i>Leiosphaeridia</i> sp.	Prasinophyceae	Pl.26:4-6
<i>Pterosmella</i> sp.	Prasinophyceae	Pl.26:7

The predominance of dinocysts over all other palynomorphs is clear in all samples, with a largest value of 85% in sample T1 (top layer) and a lowest value of 46% in M3 (in the base layer). Microforaminiferal linings and pollen grains alternate, depending on the samples, as the second most abundant group, with an advantage of microforaminifera in samples M1, B4 and B3, and of pollen grains in T1, B1, M2, T4 and M3 (equal representation in B2).

Spores occupy the following position, after dinocysts, pollen and microforaminiferal linings, in relative abundance, overcoming microforaminiferal linings in B1, B2 and T4 samples, and surpassing the percentage of pollen grains in B2 and B3. Except for samples B1 and M2, where they reach percentages of, respectively, 10% (overcoming microforaminiferal linings) and 7 % (matching the pollen percentage and again overcoming microforaminiferal linings), green-blue algae have only residual occurrence in a few other samples. The single recorded acritarch specimen represents 0,58% of the palynomorph content of sample B4.

A joint comparative appreciation of how these percentages vary across samples can be obtained from the stacked area chart of Fig. 23, which additionally affords a straightforward relation between samples and levels in the stratigraphic succession. The T2 and T3 barren samples (enclosed within brackets) are also located as regards the succession for convenience, but they have no corresponding values in the chart.

The largest reductions in dinocysts relative abundance (to 46 %) occur at M3 followed by B4 (57%) and B1 (58%). These reductions are related to somewhat distinct patterns of increase of other groups of palynomorphs: in M3 it is the relative increase of pollen grains and, although to a much lesser extent, of spores (i.e., the terrestrial component) that associates with the reduction in the percentage of dinocysts; in B4, an increase of the relative abundance of microforaminiferal linings (included in the aquatic-marine component) contributes as well to that reduction; and in B1, in addition to important relative increases of pollen and spores, increased relative abundance of both the algae and the microforaminiferal (aquatic component) is also associated with the diminished percentage of dinocysts.

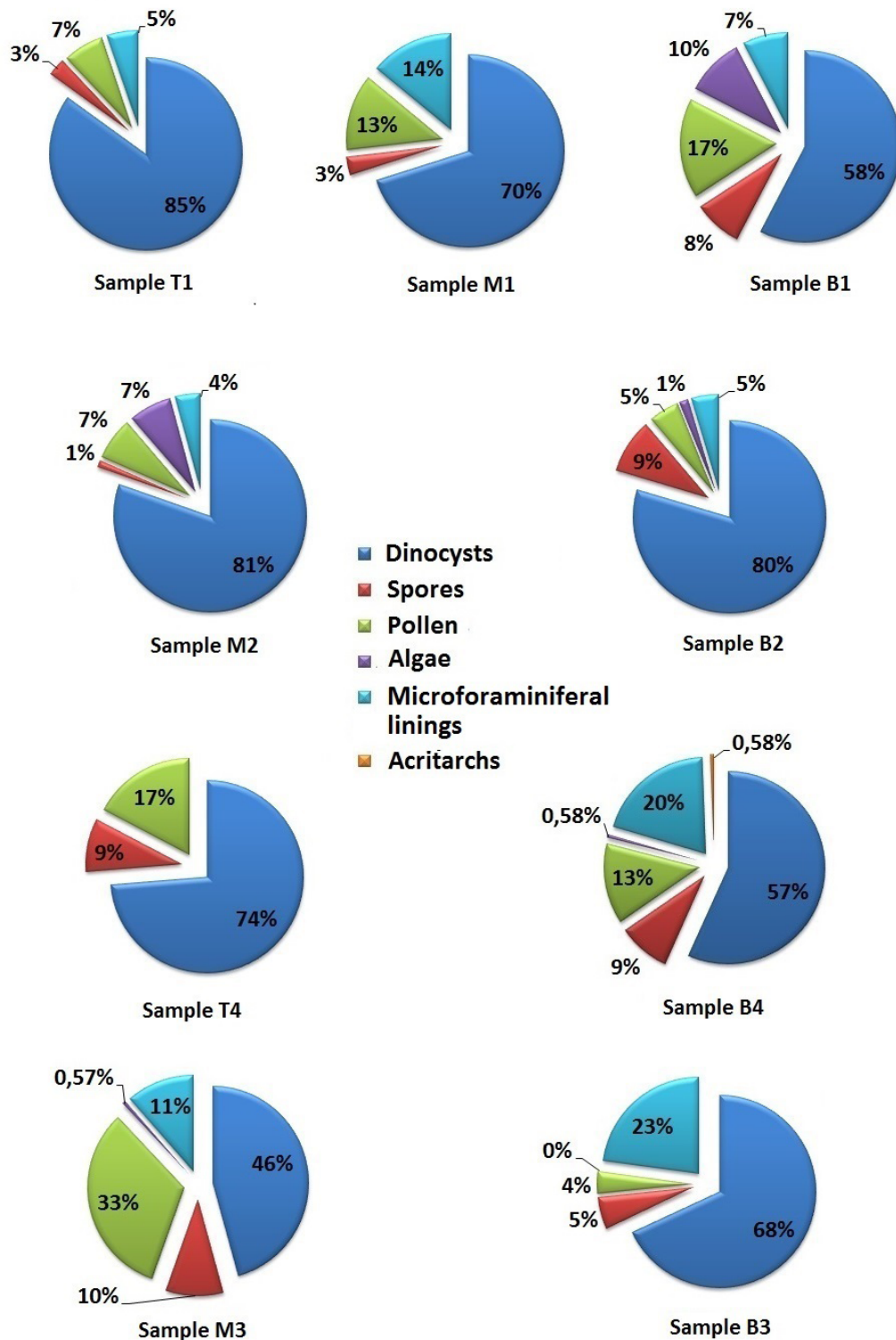


**Figure 22** – Pie charts showing the relative percentages of different categories of palynomorphs in each productive sample. These same data are resumed in aggregate form (100% stacked area chart, matched to the samples in the stratigraphic sequence) in figure 6.2.

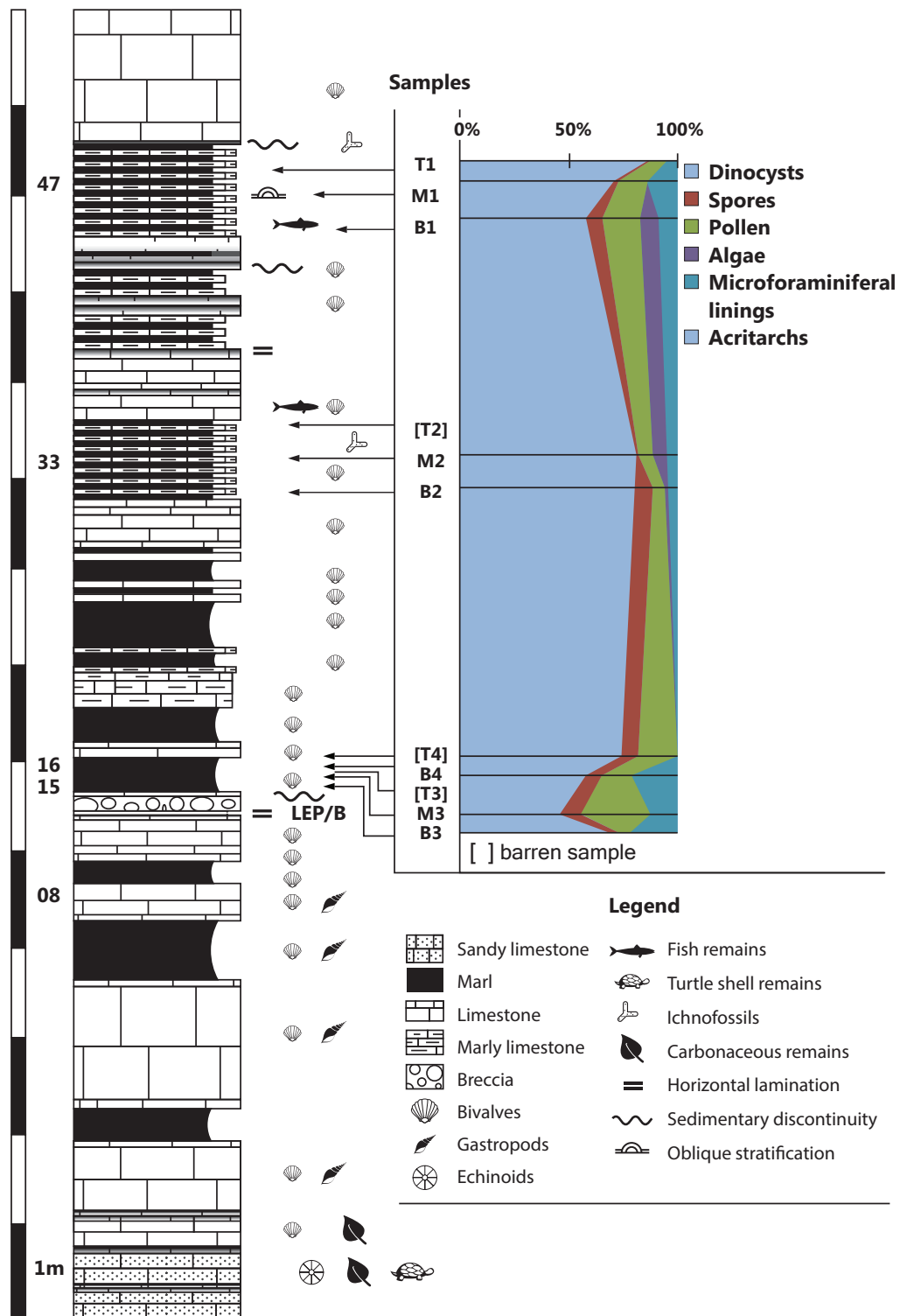


**Figure 23** – Integrated view of the palynomorph content of the samples. The colour schema of the stacked area chart allows comparing the proportions of distinct categories of palynomorphs across samples while keeping a reference to their location in the stratigraphic succession. The lines linking two consecutive sample-points correspond to linear interpolations and not to empirical data.

The marked predominance of *Botryococcus* sp., a freshwater alga, over the remaining algae in B1 (where it represents 89,4 % of the algae content) and in M2 (where it represents 100% of the algae content), the two samples with a larger fraction of green-blue algae, suggests a trend for a more positive balance of freshwater in palaeoenvironments associated with layers higher up in the succession (*e.g.*, proximal settings subjected to fluvial influence). The largest increases in dinocysts percentages occur in turn at T1 (to 85%) and M2 (to 81%): in T1 this is correlative of a decrease of all other groups; in M2, it associates primarily with a strong reduction of the spores content, accompanied by an also significant reduction of pollen grains (*i.e.*, it is chiefly correlative of a reduction of the terrestrial component).

## 7.2. RELEVANT PALYNOLOGICAL RATIOS

Several quantitative indexes of palaeoenvironmental and palaeoecological features have been proposed based on ratios between different types of palynomorphs (see point 4.3.2 above). Among them, one of the most common is the terrigenous versus marine ratio, computed as the sum of pollen grains and spores (representing the terrestrial influx) divided by the number of dinocysts (representing the marine influx) (de Vernal & Marret, 2007). Although complicated by a possible differential impact of oxidation conditions on the preservation of dinocysts and sporomorphs or by the importance of long-distance transport mechanisms (leading some authors to propose the exclusion of bisaccate pollen (*e.g.*, Fernández-Marrón, Gil, Gil-Cid, & Fonollá-Ocet, 2010), higher values of this ratio can be taken to signal greater proximity to the shoreline, the reason why Vernal and Marret (2007) termed it a “continentality” index. Graph A in Fig. 24 plots this ratio (on the ordinate) as a function of the productive samples (on the abscissa, ordered from the top to the bottom of the stratigraphic column). Values are in all cases below 1, reflecting the overall predominance of the marine influx. With the exception of sample M3, where the ratio approaches 1 (close to even contribution of terrestrial and marine fluxes), the remaining values are actually below 0.5, reflecting a marked dominance of the marine component.

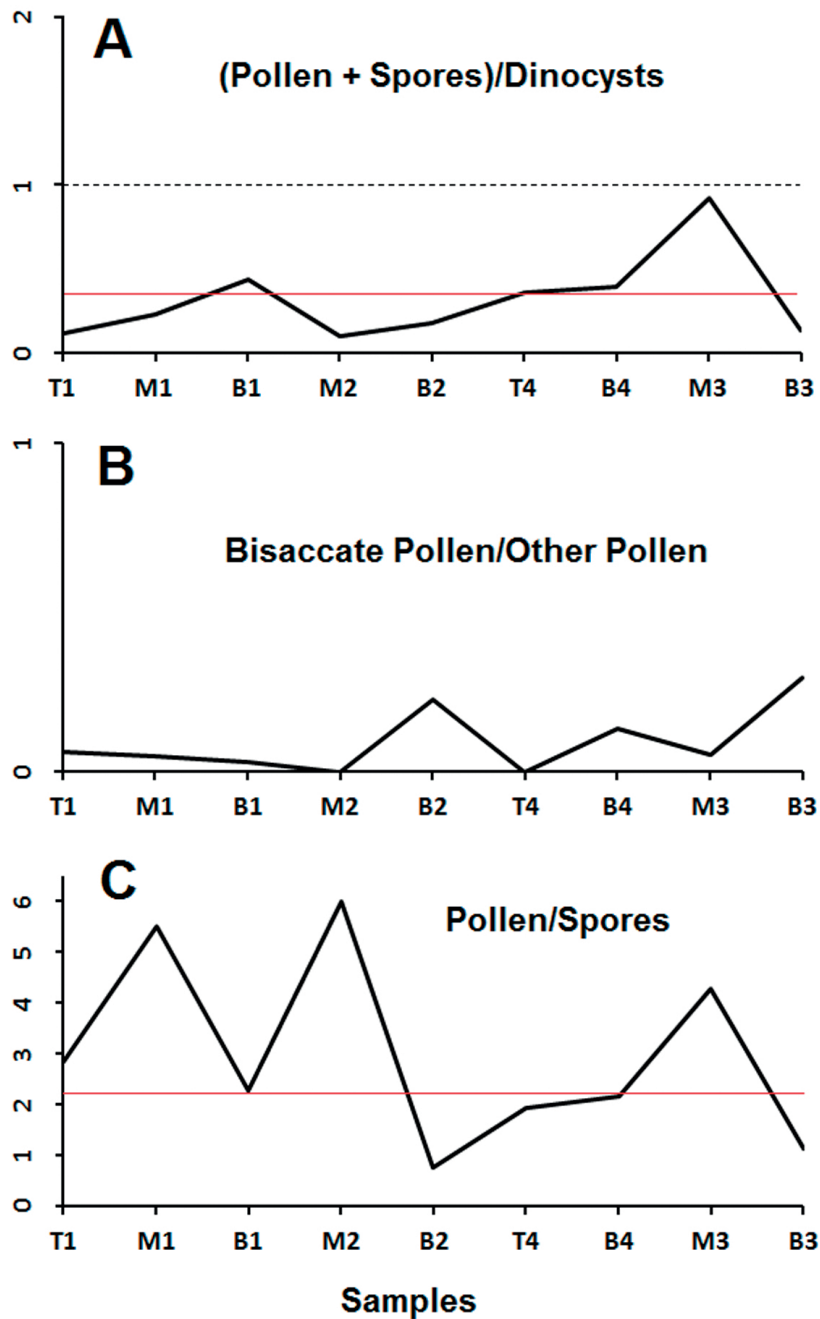


**Figure 24** – **A.** Changes of the pollen to dinocysts ratio [(pollen + spores)/dinocysts] across samples (on the abscissa, moving downward in the stratigraphic sequence). **B.** Ratio of bisaccate pollen to other pollen across the samples. **C.** Ratio of pollen to spores across the samples.



The red line helps to highlight a slight tendency for higher values of this ratio for samples located towards the bottom of the stratigraphic succession (T4 to B3, as compared to T1 to M2 or to B2).

Another proposed palynological ratio for evaluating increases/decreases in distance from seashore is the bisaccate pollen versus other pollen ratio (B:O). Due to their sac-like appendices, which make them more aero- and hydrodynamically efficient for long distance transport, bisaccate conifer pollen tends to increase their relative proportion as overall pollen concentration decreases with distance from the coastline (e.g., McCarthy, Mudie, Rochon, Gostlin, & Levac, 2000; Rochon & de Vernal, 1994; de Vernal, 2009). As any other single palynological ratio, this one may alternatively reflect factors other than an onshore-offshore gradient, such as changes in the plant communities at the source of the terrestrial influx. Graph B in Fig. 24 plots the B:O ratio as a function of the productive samples, ordered according to their location (from top to bottom) in the stratigraphic profile. Bisaccate pollen, represented in the examined samples by *Alisporites* sp., correspond in every sample to a small proportion of the pollen grains, which is reflected in the consistently low values of this ratio. A small trend for an increase of the B:O ratio in samples located more towards the bottom of the profile (to the right of M2 in the abscissa) can also be noticed, but still associated with rather low ratio values.

The ratio of pollen grains versus spores (P:S) has also been used as a proxy for distance to the shoreline, given the greater ease with which pollen can be wind or water-transported away from their origin (Batten, 1996), but mostly as a proxy for palynomorph oxidation. Since spores resist better to oxidation, the ratio P:S tends to be higher in environments of rapid sediment accumulation and burial (McCarthy *et al.*, 2000). The Graph C in Fig. 24 expresses this ratio (on the ordinate) as a function of the top-down succession of productive samples, on the abscissa. With the exception of sample B2, pollen predominate over spores in all samples, resulting in ratio values above 1. The red line helps detecting a trend for higher values in samples more towards the top of the profile, suggestive of higher rates of sediment accumulation than those associated with layers lower down in the succession.

One widely used dinocyst-based indicator for assessing primary productivity conditions, first documented by Lewis, Dodge, and Powell (1990), is the Peridinioids versus Gonyaulacoids ratio (P:G). The inferential basis for the use of this ratio rests on taking Peridinioids as a close approximation to heterotrophic dinoflagellate species (Pross & Brinkhuis, 2005). Evidence for that comes from an analogy with the prevailing feeding behaviour of modern Protoperidinioids and from Quaternary studies, leading several authors to question its relevance for Cretaceous studies (Dale

& Fjellså, 1994). Nevertheless, several externally calibrated studies (*e.g.*, using satellite data on primary productivity as a criterion) supported the potential usefulness of this ratio for productivity reconstruction (*e.g.*, Radi & deVernal, 2008). The dominance of peridinioid cysts in Cenomanian-Turonian assemblages is a common finding (Peyrot *et al.*, 2012), and has been linked to several other environmental controls besides primary productivity. For instance, the predominance of peridinioids in reduced salinity conditions has been contrasted with the predominance of gonyaulacoids and gymnodiods in normal marine salinity conditions (Harker, Sargeant, & Caldwell, 1990). Peridinioids comparative increase in nearshore conditions characterized by strong fluctuations in salinity and/or nutrient levels has also been signalled (Peyrot *et al.*, 2012). Moreover, peridinioid-dominated assemblages have been correlated with colder surface waters (and higher latitudes, Dale, 1985) and gonyaulacoid-dominated assemblages with warmer surface waters (Wall *et al.*, 1977). Finally, selective destruction of peridinioids by oxidation has been demonstrated in laboratory (Marret, 1993, Hopkins & McCarthy, 2002) and a reduced occurrence of peridinioids in oxidised sediments has been documented (Zonneveld, Hoek, Brinkhuis, & Willems, 2001). A decrease in the P:G ratio may thus reflect oxidation related processes such as rate of sedimentation, which differentially affect these two groups of cysts. Both the link of this ratio to primary productivity and to the rate of sedimentation open up the possibility of cautiously using it to estimate a nearshore-offshore gradient, with lower values of the ratio indicating more distal environments (de Vernal & Marret, 2007).

Graph A in Fig. 25 plots a simple ratio of number of Peridinioids/(number of Peridinioids + Gonyaulacoids) expressed as a relative percentage (0 to 100 %) as a function of the top-down succession of productive samples. A clear predominance of peridinioids is manifest by relative percentages well above 50% in all samples. . Given the aforesaid, this overall predominance is in itself suggestive of reduced or variable salinity, temperate/cold water, and high productivity associated with nearshore conditions (*e.g.*, lagoonal, estuarine or brackish).

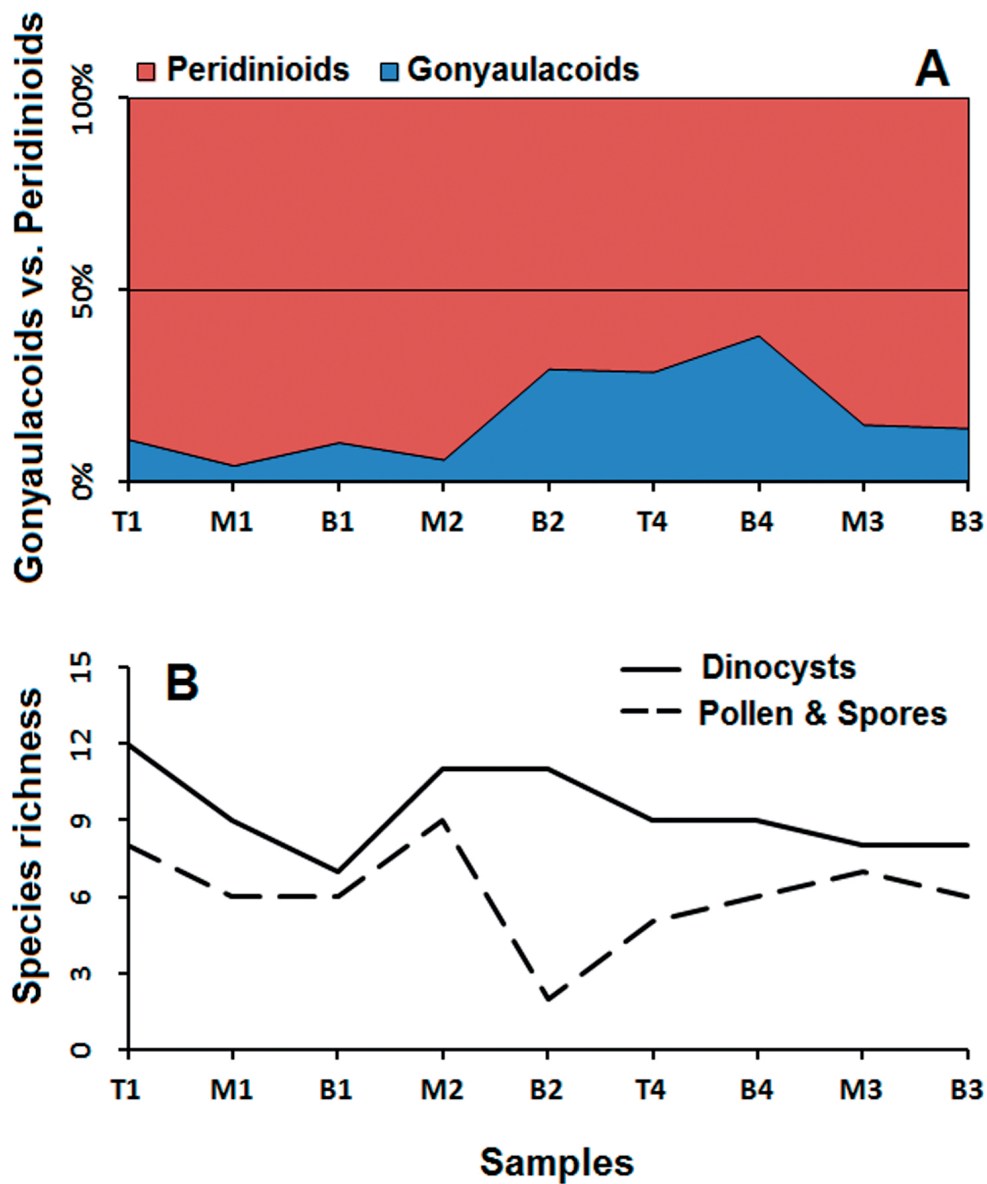


**Figure 25 – A:** 100% stacked area chart presenting the percentage of peridinioid and gonyaulacoid dinocysts across samples (on the abscissa, moving downward in the stratigraphic sequence). **B:** Dinocysts (dashed line) and pollen and spores (solid line) species richness across samples: richness was indexed simply by the number of species identified in a sample.

A trend for a comparative reduction in the proportion of peridinioids (correlative of an augmented proportion of gonyaulacoids) is apparent after M2, i.e., for samples collected at lower levels of the stratigraphic columns. Interpreted in light of a distal-proximal gradient, that would point to closer proximity to land at the top of the column, in agreement with the suggestions of the bissacate/other pollen ratio

(graph B in Fig. 25); considered from the standpoint of oxidation processes, to an increased rate of sedimentation/burial on the higher layers – in agreement with the suggestion of the Pollen/Spores ratio (graph C in Fig. 24). In this context, the increase of the terrestrial component in samples from the lower layers suggested by the (pollen + spore)/dinocyst ratio (graph A in Fig. 24) appears as either discrepant with the remaining indicators or as requiring explanation by factors other than higher proximity to land.

Other palynological-based signals have been proposed, namely regarding the inshore-offshore gradient, which are not based on quotients and can be used for cross-checking the indications arising from palynological ratios. Particularly in the case of dinocysts, highly indicative species (with marked preferences for specific environments) and assemblages' composition may afford useful signals, which will be dealt with in the following sections. After the Wall *et al.* (1977) paper, dinocysts diversity has come to be recognized in itself as a relevant palaeoenvironmental indicator, overall dependent on the stress in ecosystems, which is often related to shoreline proximity (Sluijs, Pross, & Brinkhuis, 2005). Dinocysts diversity has been found to typically increase offshore (particularly near the shelf edge, along slope-rise zones) and to decrease at more proximal settings, particularly in unstable and unpredictable (more ecologically stressed) estuarine/coastal habitats (Bradford & Wall, 1984; Goodman, 1979; Wall *et al.*, 1977). Graph B in Fig. 25 plots a straightforward measure of dinocysts diversity (the number of recorded distinct *taxa*, or species richness) as a function of the productive samples ordered from the top towards the bottom of the profile. An equivalent measure of diversity was also taken for the terrestrial component represented by spores and pollen grains and is additionally plotted for comparison (dashed line). The number of distinct dinocyst *taxa* in each sample is overall rather low (always below 15) and thus suggestive of a near shore, proximal setting, rather than open marine. In addition, it is quite constant, with only very small fluctuations between samples. A similar pattern is apparent for the pollen + spore diversity, with the exception of a somewhat noticeable fall in B2 (extending, to a lesser degree, to T4). Pollen + spore richness was always lower than dinocysts richness.

### 7.3. CHARACTERIZATION OF DINOCYST ASSEMBLAGES

*Subtilisphaera* sp. was by far the dominant *taxon* in all samples, accounting for around 71 % of the total of recorded dinocysts. Its representation across samples varied from a minimum of  $\approx 46$  % (sample T4) to a maximum of 88 % (sample B1). The second most abundant *taxa*, at a considerable distance from the third one, was *Spinidinium* sp., accounting for  $\approx 7$ % of the total number of dinocysts, and with percentages across samples varying in between  $\approx 2,5$  % (sample B2) and  $\approx 17,5$  % (sample T4). *Spiniferites ramosus* was the third most common *taxa*, with an overall representation of  $\approx 3,2$ %, varying from 0% (in M1 and B3) to  $\approx 15,5$ % (B4) across samples. The first two *taxa*, both peridinioids, which together account for more than 75 % of the entire dinocysts count, were recorded in all samples.

This pattern of species representation, graphically illustrated by the dinocyst percentage diagram in Fig. 26, reflects high dominance assemblages, with an overwhelming prevalence of the cosmopolitan species *Subtilisphaera* sp. An inverse relation between dominance and species diversity has been signalled by Goodman (1979), such that low dominance-high diversity assemblages reflect more offshore conditions and high dominance-low diversity assemblages more inshore conditions. The high dominance found in all samples thus converges with the low number of dinocysts *taxa* recorded (low diversity) in signalling an innershore marine setting. Moreover, assemblages including only a few dinocyst species and overwhelmingly dominated by one single *taxon* have been particularly associated with ecologically restricted nearshore and estuarine (brackish) environments (Li & Habib, 1996; McMinn, 1991), with relatively low energy and little water movement, leading to the suggestion that this may be the case here.

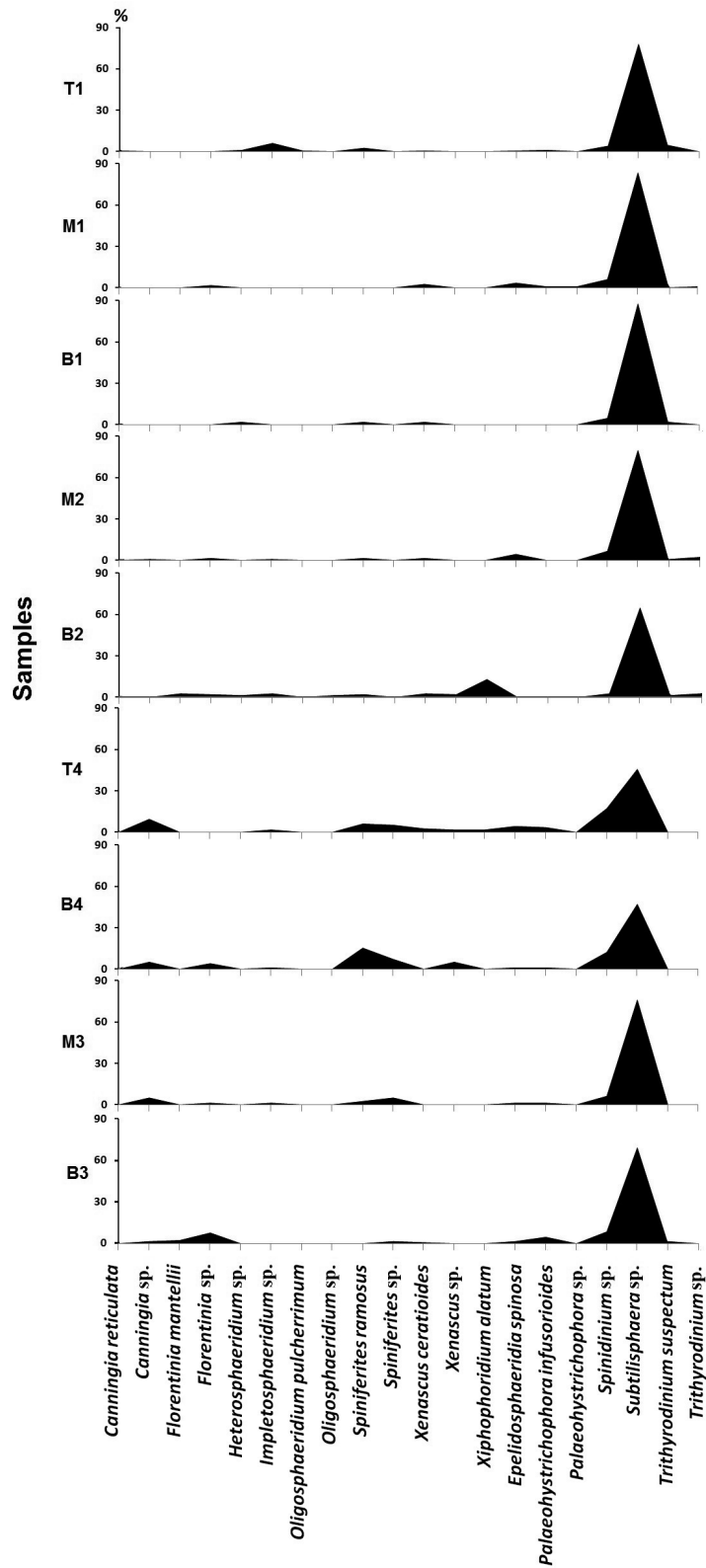


Figure 26 –Dinocyst percentage diagrams for the set of productive samples (ordered vertically as in the lithostratigraphic column).

Relatively small fluctuations of the percentage representation of each *taxon* across samples are apparent in Fig. 26. A comparatively higher peak of *Florentinia* sp. can be seen at B3, of *Spiniferites ramosus* at B4, of *Canningia* sp. and *Spinidinium* sp. at T4, of *Xiphophoridium alatum* at B2 or of *Heterosphaeridium* sp. at T1 sample. These fluctuations are associated with some degree of change in the species composition across samples and may involve either inverse or direct relations between the percentage representation of different species, which will be considered in the following sections.

Fig. 27 presents the relation across samples between the proportions of *Subtilisphaera* sp., the most abundant peridinioid cyst and the dominant *taxon* overall, and of *Spiniferites ramosus*, the most abundant gonyaulacoid (and third best represented *taxon*). An overall inverse relation can be noticed, whereby increases in the proportion of *Spiniferites ramosus* (gonyaulacoid) are accompanied by decreases in the proportion of *Subtilisphaera* sp. (peridinioid) and vice versa. A tendency for an enlarged representation of *Subtilisphaera* sp. on samples from higher layers indicates an increasing gradient of dominance towards the top of the succession (M2 to T1).

The ratio between the number of distinct peridinioid and distinct gonyaulacoid *taxa* was also computed for each sample and plotted on the same graph, with values on the left ordinate. This ratio allows examining whether the increased dominance of *Subtilisphaera* sp. at samples located higher in the stratigraphical succession goes along with an overall pattern favouring the occurrence of higher species richness of peridinioids over gonyaulacoids. As shown by the dashed line, this appears to be the case, with some trend for larger values of the ratio on the left part of the abscissa. This relative increase in species richness of the peridionoids concurs with the increased dominance of *Subtilisphaera* sp. and with the enlarged representation of peridinioids as a group (see Fig. 25A) to suggest augmented productivity and/or more reduced or variable salinity conditions of the palaeoenvironments associated with layers higher up in the succession.

Pearson correlations computed between all pairs of dinocyst *taxa* similarly indicate that an overall inverse relation between peridinioids and gonyaulacoids largely organizes the variation in species composition across samples. Statistically significant (at  $\alpha \leq 0.05$ , bilateral) negative correlations were found between *Subtilisphaera* sp. (dominant peridinioid) and the gonyaulacoids *Spiniferites ramosus* ( $r = -0.743$ ), *Canningia* sp. ( $r = -0.767$ ), *Spiniferites* sp. ( $r = -0.756$ ) and *Xenascus* sp. ( $r = -0.813$ ). Although they didn't reach the statistical significance criterion, the remaining correlations of *Subtilisphaera* sp. with other gonyaulacoids (excluding those occurring in less than three samples) were also negative, with two exceptions ( $r \approx 0$  for *Xenascus ceratioides* and  $r = 0.373$  for *Heterosphaeridium* sp.).

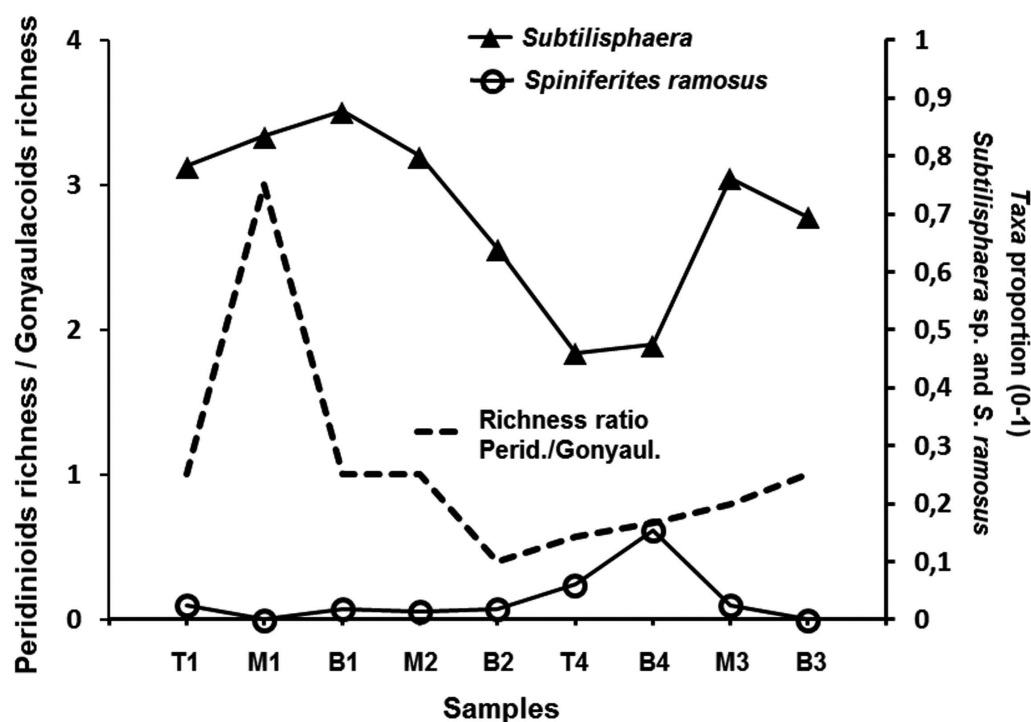


**Figure 27** – Full lines: changes in the proportion of the peridinioid *Subtilisphaera* sp. (the dominant *taxon*) and of *Spiniferites ramosus* (the most abundant gonyaulacoid and the third best represented *taxon*) across samples (ordered from top to bottom locations in the studied succession). Values should be read on the right vertical axis. Dashed line: ratio of the number of Peridinioids *taxa* (Peridinioids species richness) to the number of Gonyaulacoids *taxa* (Gonyaulacoids species richness) across samples. Values should be read on the vertical left axis.

Only one significant correlation, negative in sign,  $r = -0.774$ , was found between *Subtilisphaera* sp. and any of the other peridinioid cysts, involving *Spinidinium* sp., the second most ubiquitous and abundant *taxon* overall. Under the reservation that they were not statistically significant, negative correlations also occurred between *Subtilisphaera* sp. and *Palaeohystrichophora infusorioides*,  $r = -0.427$ , and *Epelidosphaeridia spinosa*,  $r = -0.140$ . These negative correlations may cautiously be taken to suggest a competitive relationship between the dominant *Subtilisphaera* sp. and some of the other peridinioid species. Positive non-significant correlations emerged in turn with *Trithyrodinium suspectum*,  $r = 0.373$ , and *Trithyrodinium* sp.,  $r = 0.171$  (because it only occurred in one sample, *Palaeohystrichophora* sp., was not considered). No significant correlations between peridinioid *taxa* other than the one involving *Subtilisphaera* sp. and *Spinidinium* sp. were found. All significant correlations found between gonyaulacoid species (6 correlations, after discarding species occurring in less than 3 samples) were positive, indicating that their percentage representations tended to



increase or decrease as a block. A significant negative correlation,  $r = -0.691$ , occurred between the gonyaulacoid *Heterosphaeridium* sp. and the peridinioid *Epelidosphaeridia spinosa*.

Another look at the distribution of dinocysts across samples is provided in Table 4, which classifies each *taxon* in terms of abundance (percentage of the total count of palynomorphs in each sample). Three classification categories were used, following the terminology and percentage criteria offered in Balme (1970): rare, for percentages  $< 1\%$ ; common, for percentages from 1.1 to 10%; abundant, for percentages  $> 10\%$ .

The absence of several gonyaulacoid *taxa* in T1, M1, B1 samples (e.g., *Canningia* sp., *Florentinia mantellii*, *Spiniferites* sp., *Xenascus* sp., *Xiphophoridium alatum*) reflects the signalled reduction in species richness of the gonyaulacoids in samples higher up in the succession (lowest values, of 2 and 4 *taxa* out of 13, occur at M1 and B1 respectively, and highest ones, of 10 and 7 *taxa*, occur at B2 and T4 respectively). Periodinioid *taxa*, in turn, have their highest species richness in T1 and M1, with 6 out of 7 *taxa* present). Using the rare (R) category to characterize dominance in dinocysts associations, the highest percentage of rare *taxa*, indexing higher dominance, occurs at T1 (58%) and the third highest value at M1 (37.5%), samples located higher in the stratigraphic succession. Considering now the abundant (A) and common (C) categories to characterize the prevalent species association, *Subtilisphaera* sp. (abundant in all samples), *Spinidinium* sp. (abundant in one sample and common in every other), *Spiniferites ramosus* (common in all seven samples where it occurs), *Xenascus ceratioides* (common in five out of seven samples where it occurs) and *Florentinia* sp. (common in five out of six samples where it occurs), appear as the most widely shared *taxa* across samples. Commonly represented in four out of seven and four out of five samples, respectively, the peridinioids *Epelidosphaeridia spinosa* and *Trithyrodinium suspectum* are also fairly transversal across assemblages.

**Table 4** – Stratigraphic distribution of dinocysts. Occurrences in each sample are classified as R-Rare (< 1%), C-Common (1.1 - 10 %) and A-Abundant (> 10%) (Balme, 1970).

		Dinocysts																				
Samples		<i>Canningia reticulata</i>	<i>Canningia sp.</i>	<i>Epelidosphaeridia spinosa</i>	<i>Florentinia mantellii</i>	<i>Florentinia sp.</i>	<i>Heterosphaeridium sp.</i>	<i>Impletosphaeridium sp.</i>	<i>Oligosphaeridium pulcherrimum</i>	<i>Oligosphaeridium sp.</i>	<i>Palaeohystrichophora infusorioides</i>	<i>Palaeohystrichophora sp.</i>	<i>Spiniferites sp.</i>	<i>Spiniferites ramosus</i>	<i>Spindinium sp.</i>	<i>Subtilisphaera sp.</i>	<i>Trithyrodinium suspectum</i>	<i>Trithyrodinium sp.</i>	<i>Xenascus ceratioides</i>	<i>Xenascus sp.</i>	<i>Xiphophoridium alatum</i>	
T1	R	R	R			R	C	R		R	R	C	C		A	C	R	R				
M1			C	C						R	R	C			A		R	C				
B1						C						C	C		A	C		C				
M2	R	C	C	C		R						C	C		A	R	C	C				
B2	R			C	C	C	C		C			C	C		A	C	A	C	C	A		
T4		C	C				C			C		A	C	C	A			C	C	C		
B4		C	R		C		R			R		C	C	C	A				C			
M3		C	R		R		R			R		C	C	C	A							
B3		C	C	C	C					C		C		C	A	C		R				

*Canningia sp.* and *Spiniferites sp.* contribute specifically to assemblages recorded in samples lower down in the section (B3, M3, B4, T4), where they are always common. They seldom co-occur with *Heterosphaeridium sp.* and *Trithyrodinium sp.*, which are restricted to higher-up samples (in between B2 and T1), the former being common in three out of three samples, and the latter common and abundant, respectively, in two out of five samples). *Xiphophoridium alatum* and *Xenascus sp.* only occur at lower to middle samples in the section, the former being restricted to T4 (where it is common) and B2 (where it becomes abundant), and the latter occurring commonly in samples B4, T4 and B2. These *taxa* with occurrences restricted to distinct sample ranges suggest that, in addition to a widely shared basic association comprising six or seven *taxa*, some degree of differentiation may be established between assemblages more towards the lower and more towards the upper parts of the succession.

The environmental preferences of dinocysts *taxa* have been recognized as important palaeoenvironmental and palaeoecological indicators. Despite the fact that many of the recorded species in this study are cosmopolitan and may be qualified as opportunistic, as is typical of most dinocysts assemblages (Wall *et al.*, 1977), remaining

differences in the degree of tolerance to variations in trophic, salinity or water depth conditions may still afford a basis for palaeoenvironmental inferences. As previously noticed, strong peridinioid dominance is a common finding in Cenomanian–Turonian assemblages (Peyrot, 2012), generally accepted as a signal of increased nutrient supply and/or reduced salinity under nearshore conditions (Wall *et al.*, 1977; Lewis *et al.*, 1990). However, while *Palaeohystricophora infusorioides* has currently emerged in those assemblages as the dominant cyst (Lignum, 2009; Pearce *et al.*, 2009; Peyrot *et al.*, 2011; Peyrot *et al.*, 2012), *Subtilisphaera* sp. is way far dominant in the present case. This difference plausibly reflects differences in ecological preferences, and may thus help highlighting characteristic features of the palaeoenvironment associated with the studied succession.

Affinities of *Subtilisphaera* sp. to salt marshy, intertidal (Skupien & Vacísek, 2002), deltaic (Carvalho, Bengtson, & Lana., 2016), estuarine and lagoonal low salinity environments (Jain & Millepied, 1975) have been suggested. Its strong dominance in unstable estuarine (Pedrão & Lana, 2000) and lagoonal (Ji, Meng, Yan, & Song, 2011) settings supports moreover a marked euryhaline character, allowing for rapid opportunistic proliferation at the onset of marine transgressions (Pedrão & Lana, 2000). *Palaeohystricophora infusorioides* has in turn been interpreted to show outer neritic, open marine affinities, with a predominance at offshore upwelling sites with high primary productivity (Pearce *et al.*, 2009; Peyrot, 2011; Skupien, 2007). Despite some tolerance for reduced salinity, which may account for its documented occurrence at nearshore environments (Habib & Miller, 1989), it displays a preference for close to normal salinity condition (Lignum, 2009). The overwhelming dominance of *Subtilisphaera* sp. in the present assemblages may thus be taken to suggest a restricted shallow marine to brackish environment, with either considerably reduced or variable salinity conditions. Its increased dominance at samples upward in the succession may additionally suggest a reinforcement of these conditions towards the top of the stratigraphic profile (i.e., an increasingly restricted, less open marine sedimentation environment).

This interpretation is overall consistent with the ubiquitous occurrence of *Spinidinium* sp., the second most abundant recorded *taxon*, which displays a preference for marginal marine environments (Sluijs, Brinkhuis, Williams, & Fensome, 2009; Willumsen & Vajda, 2010) and low salinity conditions, including those associated with fluvial freshwater input (Sluijs & Brinkhuis, 2009). Several other *taxa* in the assemblages exhibit akin tendencies:

- *Xenascus ceratioides*, whose relationship with restricted shallow marine (Tocher & Jarvis, 1987; Skupien & Mohammed, 2008) and low to varying salinity settings

- (Lister & Batten, 1988; Wilpshaar & Leereveld, 1994) appears well established;
- *Trithyrodinium* sp. and *Trithyrodinium suspectum*, typical occurrences of nearshore shallow marine environments with a sizeable terrestrial influx (Skupien & Mohammed, 2008) and often associated with marginal marine dinocysts genera, such as *Spinidinium* (Willumsen & Vajda, 2010);
  - *Canningia* sp. and *Canningia reticulata* which, within a general inner neritic propensity, have been related to lagoonal and restricted marine (Hunt, 1987; Peyrot, 2011, Skupien, 2007) varying salinity environments (Harris & Tocher, 2003; Skupien, 2007), though with a preference for hiposaline waters (Lignum, 2009);
  - *Oligosphaeridium pulcherrimum*, considered to be a euryhaline species with an affinity to reduced salinity nearshore environments (Harris & Tocher, 2003; Lebedeva, 2010; Lignum, 2009).

Although not much seems to be known about the palaeoecological preferences of *Impletosphaeridium* spp., except for an affinity to cold waters (Warny, Anderson, Londeix, & Bart, 2007), its recorded occurrence at a restricted infralittoral neritic marine environment (Borges, Riding, Fernandes, Matos, & Pereira, 2012) may be taken to suggest a propensity for nearshore shallow waters. Together with *Subtilisphaera* sp. and *Spininidium* sp. these *taxa* make up to 86 % of the total count of dinocysts.

Some of the other recorded *taxa* testify for distinct, open marine affinities. The stenohaline *Epelidosphaeridia spinosa* is widely regarded as a marker of offshore/oceanic environments (Harris & Tocher, 2003; Lignum, 2009); *Florentia* spp., in particular *Florentinia mantellii*, exhibit middle to outer-shelf affinities, with a leaning for outer environments (Omran, Soliman, & Mahmoud, 1990; Pearce, 2000; Peyrot *et al.*, 2011); the cosmopolitan *Heterosphaeridium* sp. has been credited with full marine affinities (Ellegaard, Lundholm, Ribeiro, Ekelund, & Andersen, 2008), preferential distribution in the inner to middle-shelf and a propensity for close to normal, slightly reduced salinity (Lignum, 2009). As mentioned above, *Palaeohystricophora infusorioides* also reveals outer neritic preferences, being often considered a marker of offshore upwelling zones (Pearce, 2000; Lignum, 2009, Peyrot *et al.*, 2011). The cosmopolitan species *Spiniferites ramosus*, corresponding to the most overall abundant gonyaulacoid (about 3% of the total dinocysts count), represents a special case. Despite recognized outer neritic affinities (Lignum, 2009, Mao & Lamolda, 1998, 1999; Peyrot, 2011), it displays broad tolerance to variations in primary productivity (from oligotrophic to eutrophic conditions), permanent or seasonal (*e.g.*, due to river discharges) reductions in water salinity and water temperature changes (Zonneveld *et al.*, 2013), and can thus be found in a wide range of habitats, including nearshore shallow-water environments (Carvalho *et al.*, 2016). Finally, *Xiphophoridium alatum* has shown no

palaeoenvironmental preferences as regards salinity or water-depth (Harris & Tocher, 2003).

Taken altogether, the overall composition of the assemblages is thus suggestive of a low salinity, possibly brackish setting, involving restricted shallow conditions consistent with lagoonal and/or tidal flat environments. The very low number of *taxa* presenting open marine, particularly outer neritic and oceanic affinities (4), and the scarcity of their percentage representation (excluding *Spiniferites ramosus*, due to its wide range of habitats, they account for about 6% of the total dinocysts sum) indicates a moderate degree of exposure to open marine influxes, possibly due to restricted (e.g., by barriers) tidal influx. The interpretation given above of the increasing dominance of *Subtilisphaera* sp. in samples higher up in the succession as a possible indication of a reinforcement of these palaeoenvironmental characteristics is to some extent supported by an upward increase in the representation of *Xenascus ceratioides*, *Trithyrodinium suspectum*, *Trithyrodinium* sp., *Canningia reticulata* and *Oligosphaeridium pulcherrimum*, and a better representation of *Palaeohystricophora infusorioides*, *Florentinia mantellii* and *Spiniferites* sp. at samples lower down in the succession (B3 to T4 or to B2), although the increased representation of *Canningia* sp. at samples lower in the succession would not be expected under this scenario (see Table 4).

Assemblages reflect a predominant Tethyan influence, signalled by the occurrence, among some of the best represented *taxa*, of species with a recognized Tethyan affinity, such as *Subtilisphaera* sp. (Arai, Neto, Lana, & Pedrão, 2000; Arai, 2014), *Spiniferites* spp. (Carvalho *et al.*, 2016), *Florentinia* spp. (Skupien & Vasicek, 2002), *Xenascus ceratioides* (Masure, Aumar, & Vrielynck, 2013). Only of few *taxa* exhibit high latitude affinities, such as *Xiphophoridium alatum* (Williams *et al.*, 2004), which nevertheless presents a cosmopolitan distribution (Masure *et al.*, 2013). In accordance with the lack of typically Temperate or Boreal species, several *taxa* exhibit preferences for warm water, such as *Trithyrodinium suspectum* (Willumsen & Vajda 2010), *Spiniferites* sp. (Prauss, 2002), *Oligosphaeridium pulcherrimum* and *Palaeohystricophora infusorioides* (Uwins & Batten, 1988). *Impletosphaeridium* sp. and *Heterosphaeridium* sp. appear in turn to prefer cooler water temperatures (Arai, 2007; Warny *et al.*, 2007). The absence of *Spiniferites* sp. and the decreased representation of *Palaeohystricophora infusorioides*, two *taxa* with a specific affinity for well oxygenated waters (Courtinat & Shaaf, 1990), at samples higher up in the succession, might signal upward decreasing oxygenation in the associated palaeoenvironmental. All in all, the most important palaeoenvironmental controls for the species composition of the assemblages and namely the overwhelming dominance of *Subtilisphaera* sp., seem to be nutrient availability under a restricted shallow water environment with reduced (and eventually varying) salinity.

## 7.4. CHARACTERIZATION OF OTHER PALYNOMORPHS ASSEMBLAGES

Table 5 provides a classification of sporomorphs, algae, microforaminiferal linings and acritarchs in terms of abundance (percentage of the total count of palynomorphs in the sample), based on the same criteria used above for dinocysts: R-Rare (< 1%), C-Common (1.1 - 10 %) and Abundant-A (> 10%).

**Table 5** – Stratigraphic distribution of spores, pollen, algae, foraminifera and acritarchs. R-Rare (< 1%), C-Common (1.1 - 10 %) and Abundant-A (> 10%).

Samples	Spores					Pollen						Algae			For.	Acr.								
	<i>Cicatricosisporites</i> sp.	<i>Contignisporites cooksonii</i>	<i>Contignisporites</i> sp.	<i>Pattelasporites</i> sp.	<i>Plicatella</i> sp.	<i>Afropollis jadinus</i>	<i>Afropollis</i> sp.	<i>Alisporites</i> sp.	<i>Araucaraacites australis</i>	<i>Araucaraacites</i> sp.	<i>Classopollis brasiliensis</i>	<i>Classopollis jariniei</i>	<i>Corollina obidocensis</i>	<i>Corollina</i> sp.	<i>Cycadopites</i> sp.	<i>Ephedripites</i> sp.	<i>Botryococcus</i> sp.	<i>Crassosphaera</i> sp.	<i>Leiosphaeridia</i> sp.	<i>Pterosmella</i> sp.	<i>Foraminifera</i>	<i>Acritarch</i>		
T1	R	R	R				R			C		R	C									C		
M1	R			C				R	C	C	C		C										A	
B1	C		R	C	C			R		C	A	C		C			C	R					C	
M2				C							C	R					C						C	
B2	R		C	C		R	R	C			C			R	C	R		R	C				C	
T4	C		R	C							C			A	R									
B4	R		R	C			C	C			A	C							R				A	R
M3				C			R	C		C	A	C					R						A	
B3	C	R		C				C			C												A	

*Spores*: the pteridophyte spore *Pattelasporites* sp., commonly found in several landscapes from the mid-Cretaceous Iberian Peninsula (Hasenboehler, 1981; Villanueva-Amadoz, 2009), was the only ubiquitous *taxa* across samples and also the most abundant, being common in all samples except T1 (where it becomes rare). It is followed by the also pteridophyte spore *Cicatricosisporites* sp., already recorded in the Cretaceous of Portugal (Rey, 1972), which can be found in many diverse environments, from marine to lagoonal and terrestrial (see: *Fossilworks: Gateway to the Paleobiology Database*, accessible at <http://www.fossilworks.org/>). Combined with the much larger representation of pollen grains versus spores (see Fig. 24C), the strong predominance of spores of pteridophytes, and the absence of bryophytes spores (more dependent on water for their reproduction) may signal a moderately humid palaeoclimate (Villanueva-Amadoz, Sender, Diez, Ferrer, & Pons, 2011).

*Pollen grains:* Gymnosperm pollen grains, particularly of the conyphera type, predominate, with *Classopollis* spp. (especially *Classopollis brasilliensis*) as the most ubiquitous and abundant. *Alisporites* is the only bisaccate pollen, much less represented than other pollen types (see also Fig. 24B), suggesting a low influence of transportation and a deposition close to the production site of the pollen grains. *Classopollis*-dominated assemblages have been interpreted as corresponding to coastal vegetation (Peyrot *et al.*, 2011). A similar association of conifer pollen, predominantly *Classopollis*, with spores of pterydophytes, chiefly *Pattelasporites*, has been reported for the Lower Cretaceous of the Lusitanian Basin (Mendes, Dinis, & Pais, 2014), and interpreted to indicate a warm, seasonally dry climate. This would agree, in the present case, with the tangentially rare representation of *Afropollis*, the only recorded type of angiosperms pollen, possibly associated with humid tropical climates (Doyle, Jardiné, & Doerenkam, 1982).

*Algae:* Among the recorded *taxa* of marine algae, *Leiosphaeridia* sp. (recorded at B1 and B2 samples) and *Pterosmella* sp. (recorded at B4) have been well correlated with shallowing phases in Jurassic studies (Tahoun & Mohamed, 2014), suggesting an overall shallow environment. The most abundant type, with common occurrence higher up in the succession (M2 and B1) is *Botryococcus* sp., a fresh-water/brackish alga (Guiry & Guiry, 2017; El Beialy, El Afty, Zavada, & Khoriby, 2010). Besides an overall indication of reduced salinity, possibly corresponding to a fluvial influence on the palaeoenvironment, its common occurrence higher up in the profile may indicate a reduction in salinity upwards. The prevalence of salinity reduced conditions is also supported by the presence of the other, prasynophyte-type algae, which typically signal lower salinity of surface waters and exhibit a preference for lagoonal to brackish environments (Skupien & Vasicek, 2002).

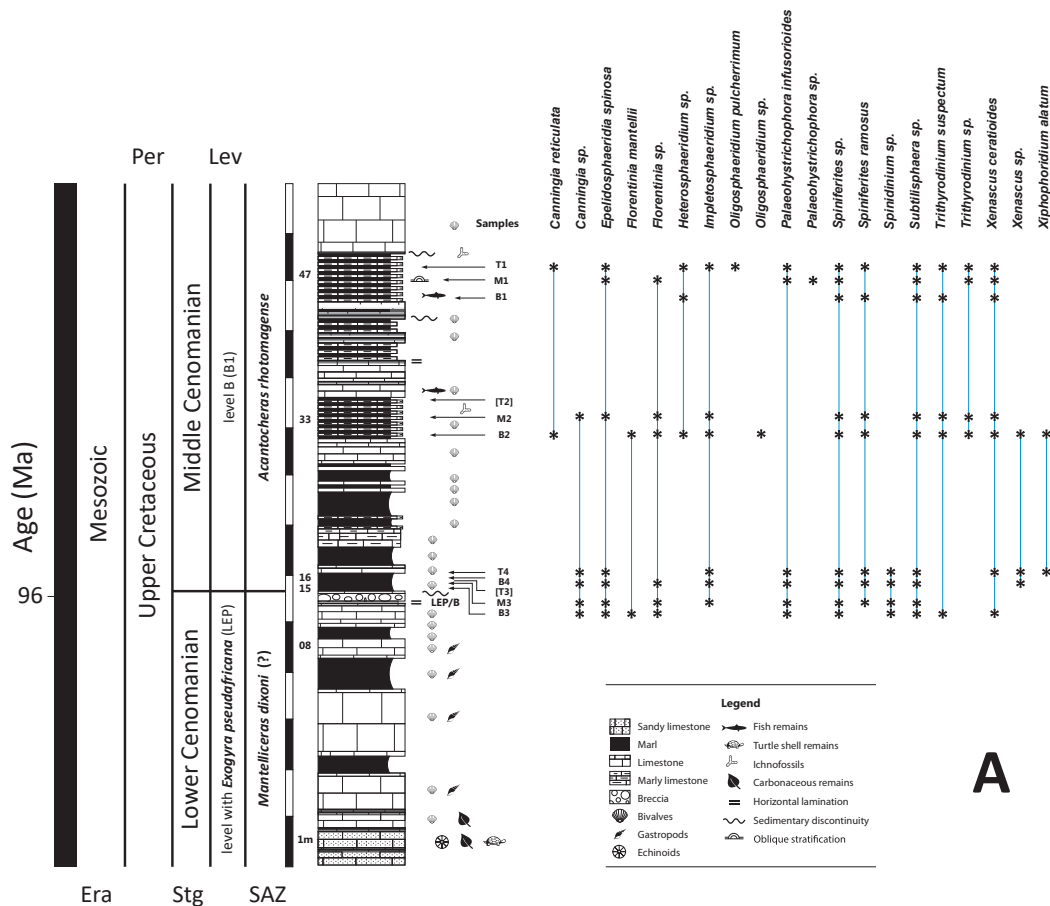
*Microforaminiferal linings:* Several studies have shown an increase in microforaminiferal linings in shallower waters (Melia, 1984; Powell, Dodge, & Lewis, 1990), allowing to interpret the common to abundant occurrence of microforaminifera across samples (with the single exception of T4, where no microforaminifera linings were recorded) as an indication of an overall shallow water palaeoenvironment. No particular shallowing trend upwards in the succession is suggested.

Taken overall, the study of the assemblages of palynomorphs other than dinocysts concurs with the same general indications of a shallow water nearshore palaeoenvironment with reduced salinity, possibly of a lagoonal/brackish type and allowing for some contribution of river freshwater input.

### 7.5. DINO CYSTS-BASED BIOSTRATIGRAPHY

The usefulness of dinocysts as biostratigraphic markers is highly dependent on the occurrence of biostratigraphically relevant species/genera, that is, *taxa* with a narrow chronostratigraphical range in between their first occurrence (FO) and their last occurrence (LO), allowing thereby for low resolution correlation. This was not the case of the studied assemblages, which individually do not add diagnostic value as regards the proposed age of the succession from late early Cenomanian to early middle Cenomanian on the basis of foraminifera, benthic faunas of invertebrates, and even ammonoid and vertebrate assemblages (e. g. Berthou, 1973, 1984; Berthou, Soares, & Lauerjat, 1979; Lauerjat, 1982; Callapez, 1998, 2008; Callapez *et al.*, 2014).

Fig. 28 illustrates the range of the recorded dinocysts *taxa* across samples with reference to the geological time scale (Gradstein *et al.*, 2012) (28A) and to the first (arrow with up bar) and/or last (arrow with down bar) occurrence of four *taxa* documented in this study and figuring among those selected in Williams *et al.* (2004) as of biostratigraphic interest to the Cenomanian (28B).





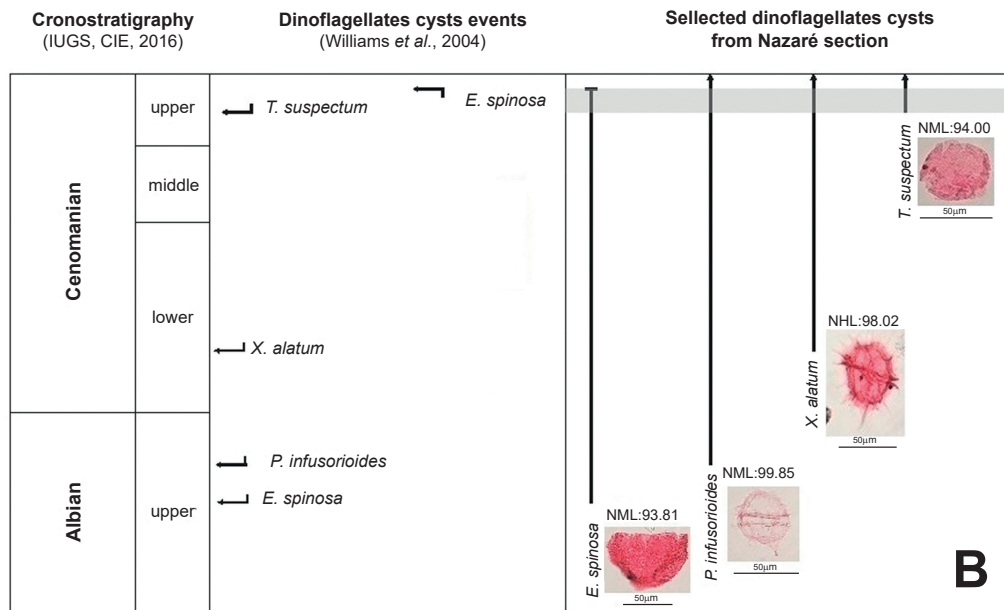


**Figure 28** – **A.** Stratigraphic ranges of dinocysts *taxa* identified in the sampled section. Age (Ma) refers to Gradstein *et al.*'s (2012) timescale for the Mesozoic. Per = Period, Stg = Stage, Lev = Level, SAZ = Standard Ammonite Zonation. **B.** First occurrence (FO: arrow with up bar) and last occurrence (LO: arrow with down bar) of *taxa* identified in the present study and selected as of biostratigraphic value for the Cenomanian by Williams *et al.* (2004). NHL = Northern Hemisphere high latitudes, NML = Northern Hemisphere mid-latitudes.

The correspondence between the stratigraphic column and the geological time scale in Fig. 28A was obtained through the alignment of the LEP/B discontinuity with the proposed onset of middle Cenomanian in Williams *et al.* (2004). Fig. 28B reproduces the FO and LO established in Williams *et al.* (2004) for the selected dinocysts *taxa* in the Cenomanian, affording thereby a comparative basis for possible biostratigraphic inferences.

Following Williams *et al.* (2004), *Xiphophoridium alatum* has its FO in the lower Cenomanian. In the present study it occurs for the first time in sample T4, where it is common. This may thus be taken to mean that, from sample T4 upward, the age of the succession cannot be inferior than the lower Cenomanian (which is consistent with a middle Cenomanian age, but does not add an independent calibration index to the existing ones). The Albian FO of *Palaeohystricophora infusorioides* and of *Epelidosphaeridia spinosa* (following Williams *et al.*, 2004) has even lesser biostratigraphical value: given that both *taxa* have their FO in the lowermost sample of the studied stratigraphical succession (B3), they may only indicate that the entire succession is postearly than Albian age. The LO of *Epelidosphaeridia spinosa* at the end of upper Cenomanian, still below the Cenomanian-Turonian transition (following Williams *et al.*, 2004), provides

a too coarse upper age limit for the studied succession, as its documented LO happens at the uppermost sample (T1). The possible inference is that the succession age is pre-Turonian (which, again, is consistent with the middle Cenomanian age already proposed, but does not afford any new specific calibration index to this datation).

The common occurrence of *Trithyrodinium suspectum* in several of the samples of the stratigraphic column, including the lowermost (B3) and uppermost (T1) ones, is a particular case. According to Williams *et al.* (2004), *Trithyrodinium suspectum* FO is referred to the middle of the upper Cenomanian (an indication already afforded in Williams & Bujak, 1985). The possible inference would then be that the studied succession is at least of upper Cenomanian age. In conclusion, the Nazaré section provided an age of middle upper Cenomanian to latest Cenomanian based on dinoflagellates cysts (Fig. 28B).

This result suggests an upper age for the Nazaré section than the robust middle Cenomanian age provided by numerous other micro and macro biostratigraphic markers (Callapez, 1998; Callapez *et al.*, 2014). Additional palynostratigraphic sampling in the studied section could provide additional relevant data, and eventually support the need for a revision of the FO of *Trithyrodinium suspectum* in Late Cretaceous in Iberia (while recognizing that no further evidence in the literature points in that direction).

## 7.6. COMPARISON WITH OTHER CRETACEOUS DINO CYSTS ASSEMBLAGES

Most studies of Upper Cretaceous dinocysts concern the upper Cenomanian and particularly the Cenomanian-Turonian boundary, given its association with the major biotic event known as OAE 2 or Bonarelli Event (Hart *et al.*, 2005; Pearce *et al.*, 2009; Barroso-Barcenilla *et al.*, 2011). Comparisons of the found dinocysts assemblages with coeval assemblages obtained in other studies (either specifically addressing or encompassing the late early and middle Cenomanian) in the same or distinct palaeogeographical realms are thus met with limited opportunities.

Two earlier studies conducted in Portugal which allow a comparison with the present one are those of Berthou *et al.* (1980) and Berthou & Hasenboehler (1982). They both investigate the Albian and Cenomanian dinocysts associations in the region of Lisbon (south of Nazaré) and distinguish furthermore between the early, middle and late Cenomanian stage. Besides the indication that dinocysts are considerably

more abundant in the Albian than in the Cenomanian in the studied region, Berthou *et al.* (1980) report that dinocysts occurrences were rare in both the early and middle Cenomanian, with *Trichodinium castaneum* as the single identified species. These findings diverge from those in the present study, where diverse and relatively well represented dinocyst *taxa* were found in samples corresponding in all likelihood to the middle Cenomanian, though not the very single *taxa* identified by Berthou *et al.* (1980) for this time interval (*Trichodinium castaneum*). This discrepancy might signal coeval diverging local sedimentological and palaeoenvironmental conditions at the Lisbon and Nazaré sectors.

The study of Berthou & Hasenboehler (1982) has provided a much larger diversity of *taxa* occurring during the early and middle Cenomanian (32 *taxa* ranging in the early and middle Cenomanian, although virtually all of them shared with Albian substages and many of them with the late Cenomanian one). A comparative summary of Berthou & Hasenboehler's (1982) reported *taxa* is given in Table 6 (middle column). All *taxa* shared with the present study are represented in bold: dominant *taxa* in a given Cenomanian substage and do not occurring in any other substages are additionally reported and signalled with two asterisks (\*\*), and *taxa* ceasing to occur after a given substage are marked with an asterisk (\*). *Taxa* within brackets ([ ]) are not of interest for the current comparison.

Nine of the 20 dinocysts *taxa* identified in the present study (i.e., 45%) were also reported in Berthou & Hasenboehler (1982). However, rather than being specific to one stage, they largely spread across the three Cenomanian substages. While all occurred at the middle Cenomanian, seven were also reported in the early Cenomanian and three in the late Cenomanian. With the exception of *Palaeohystrichophora infusorioides* identified only in the Cenomanian (across all substages), all other *taxa* also range across several Albian substages. Nevertheless, five of these shared *taxa* did not occur after the middle Cenomanian (*taxa* in bold followed by an asterisk), suggesting that the presently studied succession is below the basal upper Cenomanian, as already proved by other taxonomic groups.

However, no indications in the relevant literature support a key biostratigraphical value of these particular *taxa*, excepting *Epelidosphaeridia spinosa* for the whole Cenomanian (Williams & Bujak, 1985; Williams *et al.*, 2004). Concerning *Epelidosphaeridia spinosa*, its last occurrence is located by Williams *et al.* (2004) in late, not middle Cenomanian, which attributes it a diagnostic value as a pre-Turonian species, but not as regards a distinction between Cenomanian substages.

**Table 6** – Shared *taxa* (bold type) between the dinocysts assemblages of the present study and those from Cenomanian–Turonian sections of the Castilian Platform (Spain) and from Albian–Cenomanian sections of the Western Portuguese Basin (Lisbon region). *Taxa* listed for the present study are ordered from more to less abundant. The same happens with the first six *taxa* listed for the Spanish sections (accounting for > 75% of the counted dinocysts). All observed *taxa* at Nazaré are listed. As for the other sections, only *taxa* shared with the current study are reported, exception made to dominant or especially abundant *taxa* and *taxa* disappearing after a given Cenomanian substage (see the table footnote).

		Peyrot (2011) Peyrot <i>et al.</i> (2011) Peyrot <i>et al.</i> (2012)	Berthou & Hasenboehler (1982)	Present Study
Stratigraphic sections		Tamajon, Condemios, Fuentetoba, Puente de	Casal da Cova e Fontanelas	Nazaré
Turonian	Lower	<i>P. infusorioides</i> <i>Spiniferites ramosus</i> <i>Canningia reticulata</i> [ <i>E. phragmites</i> ] [ <i>T. castanea</i> ] <i>Xenascus ceratioides</i> $\Sigma > 75\%$		
	Upper	<i>Trithyrodinium suspectum</i> <i>Florentinia mantellii</i> <i>Florentinia</i> sp. <i>Spineferites</i> sp.	<i>P. Infusorioids</i> <i>X. ceratioides</i> <i>X. alatum</i> [ <i>T. castanea</i> ]	
Cenomanian	Middle		<i>P. infusorioides</i> <i>S. ramosus</i> <i>X. ceratioides</i> <i>X. alatum</i> <i>Florentinia</i> sp.* <i>Canningia</i> spp.* <i>Epelidosphaeridia spinosa</i> * <i>Oligosphaeridium</i> sp.* <i>O. pulcherrimum</i> * <i>Protoellips. corollum</i> **	<i>Subtilisphaera</i> sp.** <i>Spinidinium</i> sp. <i>Spiniferites ramosus</i> <i>Canningia</i> sp. <i>Florentinia</i> sp. <i>Xiphophoridium alatum</i> <i>Impletosphaeridium</i> sp. <i>Epelidosphaeridia spinosa</i> <i>Spiniferites</i> sp. <i>Trithyrodinium suspectum</i> <i>Xenascus ceratioides</i> <i>Palaeohystric. infusorioides</i> <i>Xenascus</i> sp. <i>Trithyrodinium</i> sp. <i>Florentinia mantellii</i> <i>Heterosphaeridium</i> sp. <i>Canningia reticulata</i> <i>Oligosphaeridium</i> sp. <i>O. pulcherrimum</i> <i>Palaeohystrichophora</i> sp.
	Lower		<i>P. infusorioides</i> <i>X. alatum</i> <i>Canningia</i> sp. <i>Oligosphaeridium</i> sp. <i>O. pulcherrimum</i> <i>Florentinia</i> sp. <i>Epelidosphaeridia spinosa</i> <i>Protoellips. corollum</i> ** <i>Spinid. vestitum</i> * <i>Exochosph. truncatum</i> *	

\*\* Dominant *taxon* not represented in any stage of another section; \**Taxa* which do not occur beyond the signaled substage; [ ] *Taxa* among the most abundant in Peyrot *et al.*, 2011.

One general indication of the Berthou & Hasenboehler's (1982) study, explicitly allowed by the authors (p. 761) and finally convergent with Berthou *et al.* (1980) and with the results of the present study is that, as far as the lower, middle and upper Cenomanian are concerned, dinocyst-based studies do not seem to add significantly to the biostratigraphic precisions in the studied regions. However, this does not mean that they cannot be useful for integrated biostratigraphic purposes with other taxonomic groups.

Another relevant indication supported by the fact that 65 % of the *taxa* in the current study, among which the dominant and the second most abundant genera, were absent from Berthou & Hasenboehler's (1982) samples, is that, again, coeval palaeoenvironmental conditions at the Lisbon and Nazaré regions were very likely divergent. This suggests that, in contrast to their seemingly reduced value for biostratigraphical purposes in the Cenomanian (at least in the studied settings of the WPCP), dinocyst-based studies may be important sources in assessing palaeoenvironmental conditions and palaeoecological communities, and differences among coeval distinct palaeogeographical regions.

In the left column of Table 6, a summary comparison with the findings of three dinocysts studies conducted at different sites of the Castilian Platform, Northern-Central Spain (Peyrot, 2011; Peyrot *et al.*, 2011, and Peyrot *et al.*, 2012) is presented. Although these studies were concerned with late Cenomanian-early Turonian stratigraphic intervals, not equivalent thus to the proposed late early-middle Cenomanian interval addressed in the current study, they still afford interesting possibilities for comparison. During the Late Cretaceous, the Iberian Subplate shared general tectonic, latitudinal, palaeogeographical and eustatic sea-level influences (Peyrot *et al.*, 2012; Segura *et al.*, 2014), which might reflect in some general affinities between dinocysts assemblages. In addition, the three Spanish studies involve distinct outcrop sections corresponding to an outer shelf to coastal and terrestrial transect (Peyrot, 2011; Peyrot *et al.*, 2011), opening the possibility for assemblages' comparisons across distinct palaeoenvironmental settings. Finally, assessing the extent to which *taxa* identified in the present study occur (or not) in the upper Cenomanian successions of settings with an overall akin palaeogeographic location (between the Tethyan and the Boreal Realms) affords additional means to evaluate the specificity of the recorded assemblages.

Despite differences in assemblage's diversities and composition, interpreted by the authors as expressing mainly the distal-proximal gradient, a transversal predominance of *Palaeohystrichophora infusorioides* and *Spiniferites ramosus* was found in all Spanish studies (Peyrot, 2011; Peyrot *et al.*, 2011; Peyrot *et al.*, 2012). This concurs with a

common dominance of *Palaeohystrichophora infusorioides* during the middle and late Cenomanian in most NW areas (Lignum, 2009), very often associated with *Spiniferites ramosus*, leading to the recognition of an Upper Cretaceous “Spiniferites–Palaeohystrichophora (S–P) Assemblage” (Prince, Jarvis, & Tocher, 1999), expressing eutrophic conditions of the middle shelf. As shown in Table 6 (left column), eight of the 20 *taxa* recorded in the present study (i.e., 40%) are represented in the late Cenomanian–early Turonian assemblages of the Castilian Platform (*taxa* in bold), with four of them among the six most abundant *taxa* in the Spanish studies (ordered by abundance and accounting for more than 75% of the total count). Conversely, 60% of the *taxa* in the present study are absent in the Castilian Platform assemblages, among which the largely dominant *Subtilisphaera* sp. and the second most ubiquitous and abundant *taxon* *Spinidinium* sp., expressing a rather different species composition (and namely, an important divergence as regards the P–S assemblage, which seems to provide the basic association in the Spanish samples). Given the interpretation of the P–S assemblage as a marker of eutrophic middle–shelf environments, the contrasting dominance of *Subtilisphaera* sp. in the present study, with reported affinities to restricted marginal low salinity environments, should be taken as a clear signal of a local palaeoenvironmental divergence. All three Spanish studies have used the dinocyst assemblages for palaeoenvironmental and palaeoecological inferences, but only one examined their value as biostratigraphic markers in the concerned stratigraphic interval (Peyrot, 2011), with limited results given by the absence of reliable late Cenomanian–early Turonian markers in the samples (p. 269). Of particular interest to the present study, none of the potentially useful biostratigraphical indications reported seems able to provide a distinctive signal of the late Cenomanian substage (i.e., simultaneously excluding earlier Cenomanian substages and the later Turonian age). These results appear to generalize the suggestion that Cenomanian dinocysts are much less useful for improving the resolution of stratigraphic datations than for palaeoenvironment reconstructions.

Finally, a last set of studies of Cenomanian dinocyst assemblages used for comparison were provided in Lignum (2009). These studies concern seven Cenomanian sections from NW Europe (Culver Cliff and Folkestone, UK, Vergons and Pont d’Issole, SE France, and Wunstorf, Ratssteinbruch and Gröbern, Northern Germany), selected so as to represent a Boreal–Tethyan transect (North Boreal represented by the German series, South Boreal by the UK sections, and Tethyan by the French sections) and a range of palaeoenvironments, namely as regards seawater depth. The Cenomanian interval being their proposed focus, most include samples taken from the standard European ammonite zones of *Mantelliceras dixonii*, corresponding to the

upper lower Cenomanian, and *Acanthoceras rothomagense* and *Acanthoceras jukesbrownei*, corresponding respectively to the lower and upper middle Cenomanian (Kennedy & Gale, 2006). These zones, particularly the *Acanthoceras rothomagense* one, offer a close stratigraphical equivalent to the beds with *Pterocera incerta*, or level B *sensu* Choffat (Callapez, 1998), from which the succession in the present study was selected, meaning that comparisons can be made with coeval assemblages.

Again, despite variations in species composition of the assemblages, *Palaeohystrichophora infusorioides* and *Spiniferites ramosus* (followed by *Chlamydochorella nyei*) predominated in most of the samples, with an increased representation of *Palaeohystrichophora infusorioides* during the early to early middle Cenomanian at several locations (Anglo-Paris, Vocontian and Lower Saxony basins), interpreted as the effect of increased nutrients supply to shelf areas (Lignum, 2009). In addition to *P. infusorioides* and *Spiniferites ramosus*, a few more taxa (*Epelidosphaeridium spinosa*, *Florentinia* sp., *Heterosphaeridium*, *Xenascus ceratioides*) were shared by Lignum's (2009) assemblages and those of the present study, which nevertheless differed greatly in composition from the former, both in terms of the recorded taxa and of the distinctive dominance of *Suptilisphaera* sp. and the significant proportion of *Spinidinium* sp.. As before, these differences are consistent with a specific local palaeoenvironment of the Nazaré's sector during the upper early-middle Cenomanian, departing from the inner to outer-shelf open marine environments represented in Lignum's (2009) samples. While the chief palaeoenvironmental controls of Cenomanian dinocysts assemblages appear to be sea-level, relative water depth and nutrient availability (Lignum, 2009), markedly reduced and/or variable salinity in a restricted shallow setting may have contributed an important additional control to the mid-Cenomanian assemblages in the Nazaré sector.

As reported by Lignum (2009), the most significant changes in dinocysts assemblages occurred at the Cenomanian/Turonian boundary, and cannot improve as such the resolution of Cenomanian substages (Lignum, 2009). Last occurrences of two species in the *Acanthoceras rothomagense* standard ammonite Zone (*Endoceratium dettmanniae* and *Impagidinium crassimuratum* subsp., none of them recorded in the present study) were documented, but remain of doubtful significance as useful mid-Cenomanian markers (Lignum, 2009). These results accord with and generalize the indications from the present study that Cenomanian dinocyst-based studies afford a valuable path for palaeoenvironmental and palaeoecological reconstructions, but not so much for additional biostratigraphical calibrations.





## Chapter 8

---

# FINAL DISCUSSION

This dissertation was aimed at providing an integrated stratigraphic and palynological study, with a particular focus on organic-walled dinocysts sampled from an upper lower-lower middle Cenomanian section located near the base of the carbonated succession exposed on the south face of the Nazaré promontory. This section comprises a partial record of the “Bellasian” stratigraphic units with *Ilymatogyra pseudaficana* and *Harpagodes incertus* (Callapez, 1998) (= “Level with *Exogyra pseudaficana*” and “Level with *Pterocera incerta*” *sensu* Choffat, 1900; Berthou, 1973; Rey, 1979). Except for the analysis of two samples collected by Moron (1981) at the detrital series beneath the first carbonate units, no other dinocysts studies have been conducted specifically at the site of Nazaré, to the best of our knowledge.

### 8.1. PALAEOENVIRONMENTAL AND PALAEOECOLOGICAL IMPLICATIONS

Drawing on the recognized potential of dinoflagellates cysts as palaeoenvironmental tracers (de Vernal & Marret, 2007; de Vernal & Rochon, 2011; Rochon, Eynaud, & de Vernal, 2008), one of the study’s purported goals was to contribute to a palaeogeographic reconstruction of the Nazaré sector during the early-middle Cenomanian. This particular section has been previously interpreted, based on the sedimentary *facies* and an extensive analysis of (mostly) macro invertebrate and

vertebrate faunas, as reflecting a transition from an inner-shelf carbonate platform (uppermost lower Cenomanian) to a more restricted lagoonal environment (basal middle Cenomanian) yielding benthic palaeocommunities dominated by the oyster *Gyrostrea ouremensis* (Callapez, 1998, 2004, 2008; Callapez *et al.*, 2014). An interesting prospect in this context is thus assessing the convergence of microbiotic data brought about by the study of dinocysts assemblages with the proposed regional palaeogeographic scheme (Callapez *et al.*, 2014), and whether further constraints to palaeoenvironmental interpretations can be obtained thereby.

Three structural features of the recorded dinocysts assemblages were: (1) high dominance, (2) low species diversity, and (3) a clear predominance of peridinioids over gonyaulacoids (with *Subtilisphaera* sp. alone representing over 70% of the total dinocysts count). As previously signaled, high dominance–low diversity assemblages are a common indicator of proximal innershore conditions (Goodman, 1979), with strong domination by one single *taxon*, as is the case here, often related to restricted nearshore and estuarine (brackish) low energy environments (Bradford & Wall, 1984; Li & Habib, 1996; McMinn, 1991). Dominance of peridinioid cysts, on the other hand, is an accepted proxy for reduced/variable salinity under nearshore conditions (Harker *et al.*, 1990) and/or abundant nutrient supply associated with upwelling zones or with enriched terrestrial input (Lewis *et al.*, 1990; Peyrot *et al.*, 2012; Wall *et al.*, 1977). All mentioned structural features thus converge in pointing towards a markedly nearshore, rather restricted, variable to low-saline, possibly brackish, environment with a rich nutrient supply, plausibly of terrestrial origin. This palaeoenvironment was in connection both with a large littoral/alluvial plain placed eastward, and the inner shelf sectors of a growing carbonate platform (Callapez, 2008).

The environmental preferences of the species/genera identified in the assemblages supported these indications and added further details. Diverging from the *Spiniferites-Palaeohystrichophora* (S-P) *Assemblage* (Prince *et al.*, 1999), predominant during middle-late Cenomanian times in Northwest Europe and reflecting middle to outer shelf eutrophic conditions, the by far dominant cyst was the strongly euryhaline *Subtilisphaera* sp., with reported affinities to restricted marine environments, including salt marshy, intertidal, deltaic, estuarine and lagoonal habitats (Carvalho *et al.*, 2016; Jain & Millepied, 1975; Ji *et al.*, 2011; Pedrão & Lana, 2000; Skupien & Vacísek, 2002). Consistent with this fact, specific preferences for marginal marine low salinity conditions, namely those associated with fluvial freshwater inflow, have been attributed to the ubiquitous and second most abundant *taxon*, *Spinidinium* sp. (Sluijs & Brinkhuis, 2009; Sluijs *et al.*, 2009; Willumsen & Vajda, 2010). Among the remaining *taxa*, several display an akin propensity towards restricted environments of low to

varying salinities, along with documented occurrences in diverse marginal marine and lagoonal habitats: *Xenascus ceratoides*, *Oligosphaeridium pulcherrimum*, *Trithyrodinium suspectum* and *Trithyrodinium* sp., *Canningia* sp. and *C. reticulata*, *Impletosphaeridium* spp. (Harris & Tocher, 2003; Hunt, 1987; Lebedeva, 2010; Lignum, 2009; Lister & Batten, 1988; Peyrot *et al.*, 2011; Skupien, 2007; Skupien & Mohammed, 2008; Tocher & Jarvis, 1987; Warny *et al.*, 2007; Willumsen & Vajda, 2010; Wilpshaar & Leereveld, 1994). The reduced representation ( $\approx 6\%$ ) of stenohaline *taxa* with open marine, and specifically outer neritic/oceanic, affinities (*Epelidosphaeridia spinosa*, *Florentinia* sp., *F. mantellii*, *Palaeohystricophora infusorioides*: see Harris & Tocher, 2003; Lignum, 2009; Omran *et al.*, 1990; Pearce, 2000; Peyrot *et al.*, 2011) accords with the preceding indications of a shallow nearshore palaeoenvironment, while simultaneously documenting some moderate degree of exposure to open marine influences, consistent with, *e.g.*, a restricted tidal influx.

Complementary indications from the other recorded palynomorphs are in line with those provided by dinoflagellate cysts. The occurrence of common to abundant microforamineferral linings is taken as an indication of shallow waters (Melia, 1984; Powell *et al.*, 1990). *Classopolis*-dominated assemblages of pollen grains, an indicator of coastal vegetation (Peyrot *et al.*, 2011), along with the scarce representation of bisaccate pollen, suggest a nearshore deposition, close to the production source. The presence of prasinophyte algae also suggests lower salinity of the surface water (Skupien & Vasicek, 2002), confirmed by the common occurrence of the fresh-water/brackish algae *Botryococcus* sp. in some samples (Guiry & Guiry, 2017; El Beialy *et al.*, 2010), which may additionally indicate local fluvial influences.

All taken together, the overall picture provided by the dinocysts-based analysis fits well the palaeoenvironmental interpretation of the middle Cenomanian of Nazaré based on the sedimentary and macro-faunal (invertebrate and vertebrate) evidence, namely the schematic reconstruction proposed by Callapez *et al.* (2014), articulating an idealized tidal flat model and a marginal marine lagoon partially separated from an open shelf environment by barrier shoals (see Fig. 29).

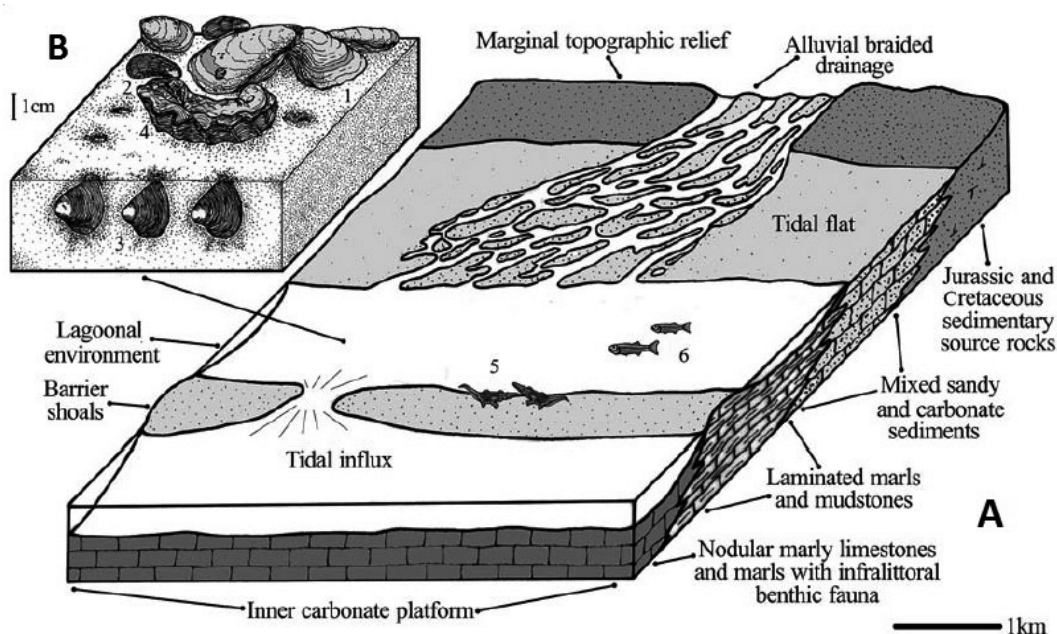


**Figure 29 - A.** Schematic palaeoenvironmental reconstruction for the Nazaré sector during the Middle Cenomanian (after Callapez *et al.*, 2014). The lagoonal environment is represented by oyster communities with *Gyrostrea ouremensis*, illustrated in **B.** and a vertebrate fauna including fishes, turtles and crocodyliforms.

Nevertheless, despite suggestions that these inferred palaeoenvironmental features may be somewhat reinforced at the top of the succession (*e.g.*, increased dominance of *Subtiliphaera* sp., increased representation of *taxa* with more nearshore affinities, absence or weakened representation of *taxa* with more offshore affinities: see section 7.3), no clear record of a lower Cenomanian open shelf environment, or of a transition into the suggested mid-Cenomanian lagoonal system, was obtained. This signals a limit of the present study, related to an uneven distribution of the samples across the stratigraphic succession. As a result of the criteria guiding the selection of the most suitable layers for sampling (thin granulometry and darker sediment: see section 6.1), the lowest sampled layers were actually close to the level of the LEP/B discontinuity, the accepted boundary between the lower and the middle Cenomanian. Undersampling of the “Level with *Exogyra pseudaficana*” strata may thus explain the lack of dinocyst-based evidence pointing to an open shelf environment (*e.g.*, a marked increase of stenohaline species and/or the occurrence of *P. infusorioides*-dominated assemblages), which may be available at layers lower down in the succession. This issue can only be addressed through future work. In any case, the present data suggest that a well developed restricted marginal marine setting was already in place at the very beginning of the mid-Cenomanian in the Nazaré sector.

## 8.2. BIOSTRATIGRAPHICAL IMPLICATIONS

Another purported goal of this study was to supplement local biostratigraphic analyses of the basal section of the carbonate formation (see Callapez, 1998, for a review of proposed biozonations), with data provided by the dinocysts assemblages. Results were rather limited, given the prevalence of species with a long chronostratigraphic range. Accepting that *Xiphophoridium alatum* has its FO during the lower Cenomanian and *Epelidosphaeridia spinosa* its LO of at the end of upper Cenomanian (following Williams *et al.*, 2004), still below the Cenomanian–Turonian transition, the pattern of occurrence of these two species in the samples suggests a lower to upper Cenomanian age of the studied stratigraphic succession (see Fig. 28A and B). The occurrence in several samples, including the lowermost one (M1), of *Trithyrodinium suspectum*, given its FO during the upper Cenomanian (following Williams *et al.*, 2004), suggests a late Cenomanian age for the succession, higher than the early to middle Cenomanian dating co-indicated by diverse other biostratigraphic markers (Callapez, 1998; Callapez *et al.*, 2014). Further palynostratigraphical sampling of the section would be needed for a better assessment of the occurrence profile of *Trithyrodinium suspectum*, making room for the possibility that a revision of its FO in the Late Cretaceous of Iberia might be required. Meanwhile, no other supporting evidence in the literature suggests that to be the case.

While allowing for a discussion of the overall age range of the succession, no relevant contributions for the distinction between Cenomanian substages (lower, middle, upper) came out of the dinocysts analysis. This concurs with the findings of several other studies where Cenomanian dinocysts assemblages were shown of limited value for improving the biostratigraphic resolution at the level of Cenomanian substages (Berthou & Hasenboehler, 1982; Lignum 2009; Peyrot, 2011).

## 8.3. COMPARATIVE VIEWS WITH OTHER CRETACEOUS DINOCYSTS ASSEMBLAGES

A further twofold goal of the study was to arrive at an exploratory view of the similarities and differences with dinocysts assemblages at stratigraphically equivalent regions in Northwest Europe, on the one hand, and at other Tethyan carbonate platforms from the Iberian microplate, which during the Late Cretaceous constituted a relatively independent tectonic block with a palaeogeographical location in between

the Protoatlantic and Mediterranean margins (Segura *et al.*, 2014).

The assemblages found at the Nazaré sector reflect a predominance of *taxa* with a recognized/probable Tethyan affinity, such as *Subtilishphaera* sp., *Florentinia* spp., *Spiniferites* spp., *Xenascus ceratioides* (Arai, 2014; Arai *et al.*, 2000; Carvalho *et al.*, 2016; Masure *et al.*, 2013; Skupien & Vasicek, 2002), and environmental preferences for warm water, such as *Spiniferites* sp., *O. pulcherrimum*, *P. infusorioides* (Prauss, 2002; Uwins & Batten, 1988), while also including species sometimes taken to reflect more northern, Protoatlantic influences, such as *Trithyrodinium suspectum* (Peyrot, 2011). Unlike assemblages of the Castilian Platform (Northern-Central Spain), where characteristic high latitude species such as *Isabelidinium acuminatum* were recorded, no *taxa* with a recognized specific Temperate-Boreal affinity were found at the Nazaré site.

The most general result of the comparisons with Cenomanian-Turonian Spanish assemblages (Peyrot, 2011; Peyrot *et al.*, 2011; Peyrot *et al.*, 2012) and with coeval assemblages from different parts of Northwest Europe (Lignum, 2009), which nearly all exhibited a predominance of *Palaeohystichophora infusorioides* and *Spiniferites ramosus*, was the suggestion of a rather specific local palaeoenvironment of the Nazaré sector during the late early-middle Cenomanian, departing from the widespread open shelf marine environments reflected in the studies used for comparison. This palaeocological specificity of Nazaré was further confirmed by comparisons with earlier studies of Albian-Cenomanian dinocysts in the region of Lisbon (Berthou *et al.*, 1980; Berthou & Hasenboehler, 1982: see section 7.6) and harmonizes well with the suggested role of local tectonics structures (close by diapiric structures of Caldas da Rainha and São Pedro de Moel acting as barriers) in sustaining the development of a marginal-marine lagoonal system in early-middle Cenomanian time (Callapez, 1998, 2008; Callapez *et al.*, 2014).

---

## REFERENCES

- Anderson, D.M., & Stolzenbach, K.D. (1985). Selective retention of two dinoflagellates in a well-mixed estuarine embayment: the importance of diel vertical migration and surface avoidance. *Marine Ecology Progress Series*, 25, 39–50.
- Antunes, M. (1979). Ensaio de síntese crítica acerca do Cretácico terminal e do Paleogénico de Portugal. *Ciências da Terra*, 5, 145–174.
- Antunes, M. (1986). Sobre a história da paleontologia em Portugal. *História e Desenvolvimento da Ciência em Portugal*, vol. 2. (pp. 773–814). Lisboa: Publicações do II centenário da Academia das Ciências de Lisboa.
- Arai, M. (2007). *Sucessão das associações de dinoflagelados (Protista, Pyrrhophyta) ao longo das colunas estratigráficas do Cretáceo das bacias da Margem Continental Brasileira: uma análise sob o ponto de vista paleoceanográfico e paleobiogeográfico* (PhD Thesis). Universidade Federal do Rio Grande do Sul, Porto Alegre.
- Arai, M. (2014). Aptian/Albian (Early Cretaceous) paleogeography of the South Atlantic: a paleontological perspective. *Brazilian Journal of Geology*, 44(2) 339–350. DOI: 10.5327/Z2317-4889201400020012
- Arai, M. Neto, J. B., Lana, C. C., & Pedrão, E. (2000). Cretaceous dinoflagellate provincialism in Brazilian marginal basins. *Cretaceous Research*, 21, 351–366.
- Barrón, E., Comas-Rengifo, M. J., & Duarte, L.V. (2013). Palynomorph succession of the Upper Pliensbachian–Lower Toarcian of the Peniche section (Portugal). *Comunicações Geológicas*, 100, Especial I, 55–61.

- Barroso-Barcenilla, F., Callapez, P. M., Soares, A., & Segura, M. (2011). Cephalopod associations and depositional sequences from the upper Cenomanian and lower Turonian of the Iberian Peninsula (Spain and Portugal). *Journal of Iberian Geology*, 37, 9-28.
- Batten, D. J. (1996). Palynofacies and petroleum potential. In J. Jansonius and D. C. McGregor (Eds.). *Palynology: Principles and Applications*, vol. 3 (pp 1065-1084). American Association of Stratigraphic Palynologists Foundation.
- Berggren, W. A., Kent, D. V., Swisher, C. C., III, & Aubry, M.-P. (1995). A revised Cenozoic geochronology and chronostratigraphy. In W.A. Berggren, D.V. Kent, M.-P. Aubry, and J. Hardenbol, (Eds.), *Geochronology, Time Scales and Global Stratigraphic Correlation*. Special Publication-SEPM (Society for Sedimentary Geology), 54, 129-212.
- Berthou, P.-Y. (1973). Le Cénomanién de l'Estremadure portugaise. *Memórias dos Serviços Geológicos de Portugal*, 23, 1-169.
- Berthou, P.-Y. (1984a). Albian-Turonian stage boundaries and subdivisions in the Western Portuguese Basin, with special emphasis on the Cenomanian-Turonian boundary in the Ammonite Facies and Rudist Facies. *Bulletin of the Geological Society of Denmark*, 33, 41-45.
- Berthou, P.-Y. (1984b). Répartition stratigraphique actualisée des principaux foraminifères benthiques du Crétacé moyen et supérieur du Bassin Occidental Portugais, *Benthos*, 83, 45-54.
- Berthou, P.-Y. (1984c). Zonation par les Ammonites du Cénomanién supérieur et du Turonien inférieur du Bassin Occidental Portugais. *Acta 1º Congresso Español de Geologia*, 1, 13-26.
- Berthou, P.-Y. (1984d). Résumé synthétique de la stratigraphie et de la paléogéographie du Crétacé moyen et supérieur du bassin occidental portugais. *Geonovas*, 7, 99-120.
- Berthou, P.-Y., Chancellor, G. & Lauerjat, J. (1985). Revision of the Cenomanian-Turonian Ammonite *Vascoceras* Choffat, 1898, from Portugal. *Comunicações dos Serviços Geológicos de Portugal*, 71(1), 55-79.
- Berthou, P.-Y., Foucher, J. C., Lecocq, B., & Moron, J. M. (1980). Aperçu sur les kystes de Dinoflagellés de l'Albien et du Cénomanién du Bassin occidental portugais. *Cretaceous Research*, 2, 125-141.



- Berthou, P.-Y., & Hasenboehler, B. (1982). Les kystes de Dinoflagellés de l'Albien et du Cénomaniens de la région de Lisbonne (Portugal). Répartition et intérêt stratigraphique. *Cuadernos Geología Ibérica*, 8, 761-779.
- Berthou, P.-Y., & Lauverjat, J. (1974). La limite Cénomaniens-Turonien dans la série portugaise à de l'embouchure du rio Mondego (Beira Litoral, Portugal). *Comptes Rendues de l'Académie des Sciences de Paris*, série D, 278, 1463-1466.
- Berthou, P.-Y., & Lauverjat, J. (1979). Essai de synthèse paléogéographique et paléobiostratigraphique du Bassin Occidental Portugais au cours du Crétacé supérieur. *Ciências da Terra*, 5, 121-144
- Berthou, P.-Y., & Leereveld, H. (1990). Stratigraphic implications of palynological studies on Berriasian to Albian deposits from western and southern Portugal. *Review of Palaeobotany and Palynology*, 66, 313-344.
- Berthou, P.-Y., Soares, A. F., & Lauverjat, J. (1979). Portugal. In Mid Cretaceous Events Iberian field Conference 77, guide, I.º partie. *Cuadernos de Geología Ibérica*, 5, 31-124.
- Borges, M. E. (2012). *Palinostratigrafia e isótopos estáveis do Jurássico da Bacia Algarvia e da Carrapateira* (PhD thesis). Universidade do Algarve, Faro.
- Borges, M. E., Riding, J. B., Fernandes, P., Matos, V., & Pereira, Z. (2012). Callovian (Middle Jurassic) dinoflagellate cysts from the Algarve Basin, southern Portugal. *Review of Palaeobotany and Palynology*, 170(1), 40-56.
- Borges, M. N., Riding, J. B., Fernandes, P., & Pereira, Z. (2011). Jurassic palynostratigraphy of the Algarve Basin and the Carrapateira Outlier, Southern Portugal, Work presented at the *44th annual meeting AASP*. Southampton, 2011.
- Borges, M. N., Riding, J. B., Fernandes, P., Pereira, Z., & Matos, V. (2011). New palynological data from the Ruivo-1 and Corvina wells, offshore Algarve Basin, Portugal – implications for future hydrocarbon exploration, Work presented at the *44th annual meeting AASP*. Southampton, 2011.
- Bradford, M. R., & Wall, D. A. (1984). The distribution of Recent organic-walled dinoflagellate cysts in the Persian Gulf, Gulf of Oman, and northwestern Arabian Sea. *Palaeontographica Abteilung B*, 192, p.16-84.

- Brinkhuis, H., Sengers, S., Sluijs, A., Warnaar, J., & Williams, G. L. (2003). Latest Cretaceous–earliest Oligocene and Quaternary dinoflagellate cysts, ODP Site 1172, East Tasman Plateau. In N. F. Exon, J. P. Kennett and M. J. Malone, (Eds.), *Proceedings ODP, Scientific Results*, 189 [Online]. Available from World Wide Web: [http://www-odp.tamu.edu/publications/189\\_SR/106/106.htm](http://www-odp.tamu.edu/publications/189_SR/106/106.htm)
- Bujak, J. P. & Williams, G. L. (1981). The evolution of dinoflagellates. *Canadian Journal of Botany*, 59, 2077–2087.
- Callapez, P.M. (1992). Estudo paleoecológico dos “*Calcários de Trouxemil*” (Cenomaniano–Turoniano) na região entre a Mealhada e Condeixa-a-Nova (Portugal Central). Monografia de Provas de Aptidão Pedagógica e Capacidade Científica. I.N.I.C. Coimbra.
- Callapez, P. M. (1998). *Estratigrafia e Paleobiologia do Cenomaniano-Turoniano: O significado do eixo da Nazaré-Leiria-Pombal* (PhD Thesis). Universidade de Coimbra, Coimbra.
- Callapez P. M. (1999). The Cenomanian–Turonian of the western Portuguese Basin. *EPA Workshop of Lisbon, field trip 2* (45 pp.).
- Callapez, P. M. (2001). Upper Cenomanian and Lower Turonian ammonite biostratigraphy of west–central Portugal. *Bulletin de la Société d’études de Sciences Naturelles d’Elbeuf*, 87, 63–68.
- Callapez, P.M. (2003). The Cenomanian–Turonian transition in West Central Portugal: ammonites and biostratigraphy. *Ciências da Terra*, 15, 53–70.
- Callapez, P.M., (2004). The Cenomanian–Turonian central West Portuguese carbonate platform. In J. Dinis, and P. P. Cunha (Eds.). *Cretaceous and Cenozoic events in the West Iberia margins. Field Trip Guidebook 2* (pp. 39–51). 23<sup>rd</sup> IAS Meeting of Sedimentology, Coimbra.
- Callapez P. M. (2008). Palaeogeographic evolution and marine faunas of the Mid-Cretaceous Western Portuguese carbonate platform. *Thalassas*, 24(1), 29–52.
- Callapez, P. M, Barroso–Barcenilla, F, Cambra–Moo, O., Ortega, F, Pérez–García, A., Segura, M., & Torices, A. (2014). Fossil assemblages and palaeoenvironments in the Cenomanian vertebrate site of Nazaré (West Central Portugal). *Neues Jahrbuch für Geologie und Paläontologie*, 273(2), 179–195.
- Callapez, P. M. & Soares, A. F. (2001). *Fósseis de Portugal: Amonóides do Cretácico superior (Cenomaniano-Turoniano)*. Museu Mineralógico e Geológico da Universidade de Coimbra. Coimbra: Ediliber Press.

- Carvalho, M. A., Bengtson, P., & Lana, C. C. (2016), Late Aptian (Cretaceous) paleoceanography of the South Atlantic Ocean inferred from dinocyst communities of the Sergipe Basin, Brazil, *Paleoceanography*, 31, 2–26. doi:10.1002/2014PA002772
- Castro, L. S. (2006). *Dinoflagelados e outros palinóforos do Miocénico do sector distal da Bacia do Baixo-Tejo* (PhD thesis). Universidade Nova de Lisboa, Lisboa.
- Castro, L. S. (2010). Palinologia do Tortoniano do sector distal da Bacia do Baixo Tejo (Península de Setúbal, Portugal). *E-Terra*, 17(6), 4p. <http://e-terra.geoport.pt>.
- Castro, L. S., Borges, M., Pereira, Z., Fernandes, P., & Pais, J. (2013). Miocene dinoflagellate cyst assemblages: preliminary correlation between the Lower Tagus and Algarve Basins (Portugal) [Abstract]. In *STRATI 2013: First International Congress on Stratigraphy: on the cutting edge of Stratigraphy*. Retrieved from <http://hdl.handle.net/10400.9/2148>
- Chancellor, G., Kennedy, W., & Hancock, J. (1994) Turonian ammonite faunas from central Tunisia. *Special Papers in Palaeontology*, 50, 1–118.
- Choffat, P. (1885). *Recueil de monographies stratigraphiques sur le Système Crétacique du Portugal - première étude* – Contrée de Cintra, de Bellas et de Lisbonne. Lisbonne : Section des Travaux Géologiques du Portugal.
- Choffat, P. (1886). Recueil d'études paléontologiques sur la Faune Crétacique du Portugal, 1 – Espèces nouvelles ou peu connues. *Memórias da Secção dos Trabalhos Geológicos de Portugal*, 17, 1–40.
- Choffat, P. (1897). Sur le Crétacique de la région du Mondego. *Comptes Rendus de l'Académie des Sciences de Paris*, 124, 422–424.
- Choffat, P. (1898). *Recueil d'études paléontologiques sur la Faune Crétacique du Portugal*, 2 (45 pp.). Lisbonne: Section des Travaux Géologiques du Portugal.
- Choffat, P. (1900). *Recueil de monographies stratigraphiques sur le Système Crétacique du Portugal – 2ème étude*. Le Crétacé supérieur au Nord du Tage. Lisbonne : Direction des Services Géologiques du Portugal.
- Choffat, P. (1901–1902). *Recueil d'études paléontologiques sur la Faune Crétacique du Portugal*, 3–4. Lisbonne: Direction des Services Géologiques du Portugal.

- Corrochano, A., Reis, R. P., & Armentero, I. (1998). Um paleocarso no Cretácico Superior do Sítio da Nazaré (Bacia Lusitânica, Portugal Central). Características, controlos e evolução. *Livro Guia das excursões do 5º Congresso Nacional de Geologia* (pp. 33–38). Lisboa.
- Costa, M. S. (2015). *Palinostratigrafia e maturação orgânica do Karoo da Bacia de Moatize-Minjova, Moçambique* (PhD thesis). Universidade Nova de Lisboa, Lisboa.
- Courtinat, B., & Schaaf, A. (1990). Les kystes de dinoflagellés enregistrent les variations d'oxygénation dans la zone photique. Le cas du Cénomaniens–Turonien du bassin vocontien, *Comptes. Rendus de l'Académie des Sciences de Paris, Série II*, 311, 699–704.
- Crosaz, R. (1975). Révision stratigraphique de la limite Cénomano–Turonienne de la région de Vila Nova de Ourém. *Comunicações dos Serviços Geológicos de Portugal*, 59, 243–252.
- Crosaz, R. (1976). Le Cénomaniens de la région de Vila Nova de Ourém (Portugal). Thèse du 3.º Cycle. Paris.
- Crosaz-Galletti, R. (1979). Étude stratigraphique et micropaléontologique du Cénomaniens calcaire de la région de Vila Nova de Ourém (Portugal). *Comunicações dos Serviços Geológicos de Portugal*, 65, 47–104.
- Cunha, P. (1992). *Estratigrafia e sedimentologia dos depósitos do Cretácico superior e Terciário de Portugal Central, a Leste de Coimbra* (PhD thesis). Universidade de Coimbra, Coimbra.
- Cunha, P., & Reis, R. P. (1995). Cretaceous sedimentary and tectonic evolution of the northern sector of the Lusitanian Basin (Portugal). *Cretaceous Research*, 16, 155–170.
- Dale, B., (1985). Dinoflagellate cyst analysis of Upper Quaternary sediments in core GIK 15530–4 from the Skagerrak. *Norsk Geologisk Tidsskrift*, 65, 97–102.
- Dale, B. (1996). Dinoflagellate cyst ecology: Modelling and geological applications. In J. Jansonius & D. C. McGregor (Eds.), *Palynology: Principles and Applications*, Vol. 5 (pp. 1249–1275). Dallas: AASP Foundation.
- Dale, B. (2001). The sedimentary record of dinoflagellate cysts: looking back into the future of phytoplankton blooms. *Scientia Marina*, 65(S2), 257–272.
- Dale, B. (2009). Eutrophication signals in the sedimentary record of dinoflagellate cysts in coastal waters. *Journal of Sea Research*, 61(1–2), 103– 113.

- Dale, B., & Dale, A. L. (1992). Dinoflagellate contributions to the deep sea. *Ocean Biocoenosis*, 5, 1-77.
- Dale, B., & Fjellså, A. (1994). Dinoflagellate cysts as paleoproductivity indicators: state of the art, potential and limits. In R. Zahn, T. F. Pedersen, M. A. Kaminski, and L. Laberie (Eds.), *Carbon cycling in the glacial ocean: constraints in the ocean's role in global change* (pp. 521-537). Berlin: Springer-Verlag.
- Davey, R. J. (1971). Palynology and palaeoenvironmental studies, with special reference to the continental shelf sediments of South Africa. In: A. Farinacci (Ed.), *Proceedings of the Second Planktonic Conference* (pp. 331-347). Roma: Tecnoscienza.
- Davies, E. H. (1985). The Miospore and Dinoflagellate Cyst Opperl-Zonation of the Lias of Portugal. *Palynology*, 9, 105-132.
- de Vernal, A. (2009). Marine palynology and its use for studying nearshore environments *IOP Conference Series: Earth and Environmental Science*, 5, 1-13. doi:10.1088/1755-1307/5/1/012002
- de Vernal, A., Henry, M., Matthiessen, J., Mudie, P. J., Rochon, A., Boessenkool, K. P., Voronina, E. (2001). Dinoflagellate cyst assemblages as tracers of sea-surface conditions in the northern North Atlantic, Arctic and sub-Arctic seas: the new 'n-677' data base and its application for quantitative palaeoceanographic reconstruction. *Journal of Quaternary Science*, 16, 681-698.
- de Vernal, A., & Marret, F. (2007). Organic-walled Dinoflagellate Cysts: Tracers of sea-surface conditions. In C. Hillaire-Marcel and A. de Vernal (Eds.), *Proxies in Late Cenozoic Paleoceanography* (pp. 371-408). Amsterdam, NL: Elsevier Science.
- de Vernal, A., & Rochon, A. (2011). Dinocysts as tracers of sea-surface conditions and sea-ice cover in polar and subpolar environments. *IOP Conference Series: Earth and Environmental Science*, 14. doi:10.1088/1755-1315/14/1/012007
- Dinis, J. L., & Cunha, P. P. (Eds.) (2004). *Cretaceous and Cenozoic events in the West Iberia margins. Field Trip Guidebook 2*. 23<sup>rd</sup> IAS Meeting of Sedimentology, Coimbra.
- Dinis, J. L., Lopes, F. C., Rodrigues, A. & Cunha, P. P. (2012). The "Nazaré fault". An illusion exposed by data analysis. *Conference Proceedings of the 7th Symposium on the Atlantic Iberian Margin (MIA 2012)* (p.43). Lisboa.
- Dinis, J. L., Rey, J., Cunha, P. P., Callapez, P. M., & Reis, R. P. (2008). Stratigraphy and allo-genic controls of the western Portugal Cretaceous: an updated synthesis. *Cretaceous Research*, 29, 772-780.

- Dinis, P.A., Dinis, J., Tassinari, C., Carter, A., Callapez, P., & Morais, M. (2015). Detrital zircon geochronology of the Cretaceous succession from the Iberian Atlantic Margin: palaeogeographic implications. *International Journal of Earth Sciences*, 105(3), 727-745.
- Dodge, J. D., & Greuet, C. (1987). Dinoflagellate ultrastructure and complex organelles. In F. J. R. Taylor (Ed.), *The biology of dinoflagellates. Botanical Monographs*, Vol. 21 (pp. 92-142) Oxford: Blackwell Scientific Publications.
- Dodsworth, P. (2016). Palynostratigraphy and palaeoenvironments of the Eagle Ford Group (Upper Cretaceous) at the Lozier Canyon outcrop reference section, west Texas, USA. *Palynology*, 40(3), 357-378.
- Doubinger, J., Adloff, M., & Palain, C. (1970). Nouvelles précisions stratigraphiques sur la série de base du Mésozoïque portugais. *Comptes Rendus de l'Académie des Sciences*, 270, 1770- 1772.
- Doyle, J. A., Jardiné, S., & Doerenkamp, A. (1982). Afropollis, a new genus of early angiosperm pollen, with notes on the Cretaceous palynostratigraphy and paleoenvironments of northern Gondwana. *Bulletin des centres de Recherche Exploration-Production Elf-Aquitaine*, 6(1), 39-117.
- El Beialy, S. Y., El Atfy, H. S., Zavada, M. S., Khoriby, E. M., & Abu-Zied, R. H. (2010). Palynological, palynofacies, paleoenvironmental and organic geochemical studies on the Upper Cretaceous succession of the GPTSW-7 well, North Western Desert, Egypt. *Marine and Petroleum Geology*, 27, 370-385.
- Ellegaard, M., Lundholm, N., Ribeiro, S., Ekelund, F., & Andersen, T. J. (2008). Long-term survival of dinoflagellate cysts in anoxic marine sediments. Abstract from *Eight International Conference on Modern and Fossil Dinoflagellates – Dino8*, Montreal, Canada.
- Evitt, W. R. (1985). *Sporopollenin Dinoflagellate Cysts: Their Morphology and Interpretation. Monograph Series 1*. Dallas: AASP Foundation.
- Fensome R. A., Crux, J. A., Gard, I. G., MacRae, R. A., Williams, G. L., Thomas, F. C., ..., Wach, G. (2008). The last 100 million years on the Scotian Margin, offshore eastern Canada: an event-stratigraphic scheme emphasizing biostratigraphic data. *Atlantic Geology*, 44, 93-126.
- Fensome, R. A., MacRae, R. A., & Williams, G. L. (1998). *DINOFLAJ*. Geological Survey of Canada, Open File 3653 [CD-ROM].

- Fensome, R. A., MacRae, R. A., & Williams, G. L., (2008). *DINOFLAJ2, Version 1*. American Association of Stratigraphic Palynologists, Data Series no. 1. Available from World Wide Web: [http://dinoflaj.smu.ca/wiki/Main\\_Page](http://dinoflaj.smu.ca/wiki/Main_Page).
- Fensome, R. A., Riding, J. B., & Taylor, F. J. (1996). Dinoflagellates. In J. Jansonius and D. C. McGregor (Eds.), *Palynology: Principles and Applications, Vol. 1* (pp. 107-169). Dallas: AASP Foundation.
- Fensome, R. A., Saldarriaga, J. F., & Taylor, M. F. R. (1999). Dinoflagellate phylogeny revisited: reconciling morphological and molecular based phylogenies. *Grana*, 38(2-3), 66-80. DOI: 10.1080/00173139908559216
- Fensome, R. A., Taylor, F. J., Norris, G., Sarjeant, W. A., Wharton, D. I., & Williams, G. L. (1993). A classification of living and fossil dinoflagellates. *Micropaleontology special papers*, 7. Hanover, PA: Sheridan Press.
- Fensome, R. A., & Williams, G. L. (2004). The Lentin and Williams Index of fossil dinoflagellates (2004 Edition). *American Association of Stratigraphic Palynologists, Contributions Series*, 42, 1-909.
- Fernandes, P., Borges, M. E., Rodrigues, B., & Matos, V. (2010.) A re-assessment of the organic maturation and palynostratigraphy of the wells Ruivo-1 and Corvina, offshore Algarve Basin, In *Abstracts of the II Central and North Atlantic Conjugate Margins Conference, Lisbon 2010, Vol. III* (pp. 111-115). Retrieved from <http://repositorio.lneg.pt/bitstream/10400.9/1278/1/34389.pdf>
- Fernández-Marrón, M. T., Gil, J., Gil-Cid, M. D., & Fonollá-Ocete, J. F. (2010). Précisions sur le patron d'empilement de dépôts du Cénomaniens-Turonien de Somolinos (Chaîne Ibérique, Espagne) d'après l'étude palynologique. *Geobios*, 43, 305-315.
- Figueroa, R. I., & Garcés, E. (2010). Dynoflagellate life cycles. Available from World Wide Web: [http://tolweb.org/notes/?note\\_id=5512](http://tolweb.org/notes/?note_id=5512) (the Tree of Life Web Project).
- Gaines, G., & Elbrächter, M. (1987). Heterotrophic nutrition. In F. J. R. Taylor (Ed.), *The biology of dinoflagellates, Botanical Monographs*. Vol. 21 (pp. 224-268). Oxford: Blackwell Scientific Publications.
- Gaines, G., & Taylor, F. J. (1985). Form and function of the dinoflagellate transverse flagellum. *The Journal of Protozoology*, 32(2), 290-296.

- Gale, A. S., Hardenbol, J., Hathway, B., Kennedy, W. J., Young, J. R., & Phansalkar, V. (2002). Global correlation of Cenomanian (Upper Cretaceous) sequences: evidence for Milankovitch control on sea level. *Geology*, 30, 291–294.
- Gocht, H. (1983). Morphogenetische Deutung und Bezeichnung ausgewählter Merkmale bei Dinoflagellaten-Zysten. *Neues Jahrbuch für Geologie und Paläontologie, Monatshefte*, 5, 257–276.
- Gómez, F. (2012). A checklist and classification of living dinoflagellates (Dinoflagellata, Alveolata). *CICIMAR Océanides*, 27(1), 65–140.
- Gonçalves, P. A., Mendonça Filho, J. G., da Silva, T. F., Mendonça, J. O., & Flores, D. (2014). The Mesozoic–Cenozoic organic facies in the Lower Tagus sub-basin (Lusitanian Basin, Portugal): Palynofacies and organic geochemistry approaches. *Marine and Petroleum Geology*, 52, 42–56.
- Goodman, D. K. (1979). Dinoflagellate “Communities” from the Lower Eocene Nanjemoy Formation of Maryland, U.S.A. *Palynology*, 3, 169–190.
- Gradstein, F. M., Kristiansen, I. L., Loemo, L., & Kaminski, M. A. (1992). Cenozoic foraminiferal and dinoflagellate biostratigraphy of the Central North Sea. *Micropaleontology*, 38(2), 101–137.
- Gradstein, F. M., & Ogg, J. (1996). A Phanerozoic time scale. *Episodes*, 19, 3–5.
- Gradstein, F. M., Ogg, J. G., & Hilgen, F. J. (2012). On The Geologic Time Scale. *Newsletters on Stratigraphy*, 45 (2), 171–188.
- Guiry, M. D. & Guiry, G. M. (2017). *AlgaeBase*. World-wide electronic publication, National University of Ireland, Galway.
- Habib, D., & Miller, J. A. (1989). Dinoflagellate species and organic facies evidence of marine transgression and regression in the Atlantic Coastal Plain. *Palaeogeography, Palaeoclimatology, Palaeoecology*, 74, 23–47.
- Hackett, J. D., Anderson, D. M., Erdner, D. L., & Bhattacharya, D. (2004). Dinoflagellates: a remarkable evolutionary experiment. *American Journal of Botany*, 91(10), 1523–1534. doi: 10.3732/ajb.91.10.1523
- Haq, B. U., Hardenbol, J., & Vail, P. R. (1988). Mesozoic and Cenozoic chronostratigraphy and cycles of sea-level change. In C. K. Wilgus, B. S. Hastings, C. C. Kendall, H. W. Posamentier, C. A. Ross, and J. C. Van Wagoner (Eds.), *Sea-Level changes: An integrated approach*, 42 (pp. 39–44). Society of Economic Paleontologists and Mineralogists Special Publication.



- Haq, B. U. (2014). Cretaceous eustasy revisited. *Global and Planetary Change*, 113, 44–58.
- Hancock, J. M., & Kauffman, E. G. (1979). The great transgressions of the Late Cretaceous. *Journal of the Geological Society*, 136(2): 175–186.
- Hardenbol, J., Thierry, J., Farley, M. B., Jacquin, T., de Graciansky, P.C., & Vail, P. R. (1998). Mesozoic and Cenozoic sequence chronostratigraphic framework of European basins, Chart 1, Mesozoic and Cenozoic sequence chronostratigraphic chart. In: P. C. Graciansky, J. Hardenbol, T. Jacquin, and P. Vail (Eds.), *Mesozoic and Cenozoic Sequence Stratigraphy of European Basins*. SEPM Special Publication, 60, Appendix.
- Harker, S. D., Sarjeant, W.A., & Caldwell, W. G. (1990), Late Cretaceous (Campanian) organic-walled microplankton from the interior plains of Canada, Wyoming and Texas: Biostratigraphy, palaeontology and palaeoenvironmental interpretation, *Palaeontographica Abteilung B*, 219, 1–243.
- Harris, A. J., & Tocher, B. A. (2003), Palaeoenvironmental analysis of Late Cretaceous dinoflagellate cyst assemblages using high-resolution sample correlation from the Western Interior Basin, USA. *Marine Micropaleontology*, 48, 127–148.
- Hart, M. B. (1990). Cretaceous sea level changes and global eustatic curves; evidence from SW England. *Proceedings of the Ussher Society*, 7, 268–272.
- Hart, M. B., Callapez, P. M., Fisher, J. K., Hannant, K., Monteiro, J. F., Price, G. D. & Watkinson, M. P. (2005). Micropalaeontology and stratigraphy of the Cenomanian/Turonian boundary in the Lusitanian Basin, Portugal. *Journal of Iberian Geology*, 31, 311–326.
- Hasenboehler, B. (1981). Etude Paléobotanique et Palynologique de l’Albien et du Cénomanién au Sud de l’accident de Nazaré (Province d’Estremadure, Portugal). *Mémoires des Sciences de la Terre*, 18–29 (317 pp.).
- Head, M. J. (2007). Last Interglacial (Eemian) hydrographic conditions in the southwestern Baltic Sea based on dinoflagellate cysts from Ristinge Klint, Denmark. *Geological Magazine*, 144, 987–1013.
- Head, M. J., & Westphal, H. (1999). Palynology and paleoenvironments of a Pliocene carbonate platform: the Clino core, Bhamas. *Journal of Paleontology*, 73(1), 1–25.
- Heimhofer, U., Hochuli P.A., Burla, S., & Weissert, H. (2007). New records of Early Cretaceous angiosperm pollen from Portuguese coastal deposits: Implications for the timing of the early angiosperm radiation. *Review of Palaeobotany and Palynology*, 144, 39–76.

- Hopkins, J. A., & McCarthy, F. M. (2002). Post-depositional palynomorph degradation in Quaternary shelf sediments: a laboratory experiment studying the effects of progressive oxidation. *Palynology*, 26, 167-184.
- Hoppenrath, M., & Saldarriaga, J. F. (2012). Dinoflagellates [Version 15 December 2012]. Available from wwb: <http://tolweb.org/Dinoflagellates/2445/2012.12.15> (the Tree of Life Web Project)
- Horikx, M., Heimhofer, U., Dinis, J., & Huck, S. (2014). Integrated stratigraphy of shallow marine Albian strata in the southern Lusitanian Basin of Portugal. *Newsletters on Stratigraphy*, 47, 85-106.
- Hunt, C. O. (1987). Dinoflagellate cyst and acritarch assemblages in shallow-marine and marginal-marine carbonates, the Portland Sand Portland Stone and Purbeck Formations (Upper Jurassic/Lower Cretaceous) of southern England and Northern France. In M. B. Hart, (Ed.), *The Micropalaeontology of Carbonate Environments* (pp.208-225). Chichester: Ellis Horwood, British Micropalaeontological Society Series.
- Hurlbert, S. H. (1971). The nonconcept of species diversity: a critique and alternative parameters. *Ecology*, 52(4), 577-586.
- Jacobson, D. M., & Anderson, D. M. (1986). Thecate heterotrophic dinoflagellates: feeding behavior and mechanisms. *Journal of Phycology*, 22, 249-258.
- Jacobson, D. M., & Anderson, D. M. (1992). Ultrastructure of the feeding apparatus and myonemal system of the heterotrophic dinoflagellate *Protoperidinium spinulosum*. *Journal of Phycology*, 28, 69-82.
- Jain, K. P., & Millepied, P. (1975). Cretaceous microplankton from Senegal Basin, W. Africa: Part II: Systematics and Biostratigraphy. *Geophytology*, 5, 209-213.
- Jeffrey, S. W., Sielicki, M., & Haxo, F. T. (1975). Chloroplast pigment patterns in dinoflagellates. *Journal of Phycology*, 11, 374-384.
- Ji, L., Meng, F., Yan, K., & Song, Z. (2011) The dinoflagellate cyst *Subtilisphaera* from the Eocene of the Qaidam Basin, northwest China, and its implications for hydrocarbon exploration. *Review of Palaeobotany and Palynology*, 167, 40-50.
- Kennedy, W. J., & Gale, A. S. (2006). The Cenomanian stage. *Proceedings of the Geologists' Association*, 117(2), 187-205.
- Kullberg, J. C. (2000). *Evolução tectónica Mesozóica da Bacia Lusitaniana* (PhD thesis). Universidade Nova de Lisboa, Lisboa.

- Kullberg, J. C., Moutherde, R., & Rocha, R. (1997). Réinterprétation de l'histoire stratigraphique et tectonique de la structure de Serra de El-Rei (Portugal). *Cahiers de l'Université Catholique de Lyon*, 10, 191–208.
- Kullberg, J. C., Rocha, R. B., Soares, A. F., Duarte, L. V., & Marques, J. F. (2014). Palaeogeographical Evolution of the Lusitanian Basin (Portugal) During the Jurassic. Part I: The Tectonic Constraints and Sedimentary Response, In R. Rocha, J. Pais, J. C. Kullberg and S. Finney (Eds.), *STRATI 2013* (pp. 665–672). Springer Geology. Doi: 10.1007/978-3-319-04364-7\_127
- Kullberg, J. C., Rocha, R. B., Soares, A. F., Rey, J., Terrinha, P., Callapez, P., & Martins, L. (2006). A Bacia Lusitaniana: Estratigrafia, Paleogeografia e Tectónica. In R. Dias, A. Araújo, P. Terrinha and J. C. Kullberg (Eds.). *Geologia de Portugal no contexto da Ibéria* (pp. 317–368). Évora: Universidade de Évora.
- Lauverjat, J. (1982). *Le Crétacé Supérieur dans le Nord du Bassin Occidental Portugais* (PhD thesis). Université Pierre et Marie Curie, Paris.
- Lebedeva, N. K. (2010). Palynofacies in Upper Cretaceous Sediments of Northern Siberia. *Stratigraphy and Geological Correlation*, 18, 5, 532–549.
- Lentin, J. K., & Williams, G. L. (1973). Fossil dinoflagellates: index to genera and species. *Geological Survey of Canada Paper n°. 73-42*, 1–176.
- Lentin, J. K., & Williams, G. L. (1975). Fossil dinoflagellates: index to genera and species. Supplement 1. *Canadian Journal of Botany*, 53(S1), 2147–2157.
- Lentin, J. K., & Williams, G. L. (1977). Fossil dinoflagellates: index to genera and species (1977 edition). *Bedford Institute of Oceanography, Report Series, BI-R-77-8*, 1–209.
- Lentin, J. K., & Williams, G. L. (1981). Fossil dinoflagellates: index to genera and species (1981 edition). *Bedford Institute of Oceanography, Report Series, BI-R-81-12*, 1–345.
- Lentin, J. K., & Williams, G. L. (1985). Fossil dinoflagellates: index to genera and species (1985 edition). *Canadian Technical Report of Hydrography and Ocean Sciences*, 60, 1–451.
- Lentin, J. K., & Williams, G. L. (1989). Fossil dinoflagellates: index to genera and species (1989 edition). *American Association of Stratigraphic Palynologists, Contributions Series*, 20, 1–473.

- Lentin, J. K., & Williams, G. L. (1993). Fossil dinoflagellates: index to genera and species (1993 edition). *American Association of Stratigraphic Palynologists, Contributions Series*, 28, 1-856 + i-viii.
- Lewis, J., Dodge, D., & Powell, A. J. (1990). Quaternary dinoflagellate cysts from the upwelling system offshore Peru, Hole 686B, ODP LEG 112. In E. Suess, R. von Huene *et al.* (Eds.), *Proceedings of the Ocean Drilling Program, Scientific Results*, 112, 323-328.
- Li, H., & Habib, D. (1996). Dinoflagellate stratigraphy and its response to sea level change in Cenomanian-Turonian sections of the Western Interior of the United States. *Palaios*, 11(1), 15-30. doi:10.2307/3515113
- Lignum, J. S. (2009). *Cenomanian (upper Cretaceous) palynology and chemostratigraphy: Dinoflagellate cysts as indicators of palaeoenvironmental and sea-level change* (PhD thesis). Kingston University London, UK.
- Lister, J. K., & Batten, D. J. (1988). Stratigraphic and palaeoenvironmental distribution of Early Cretaceous dinoflagellate cysts in the Hurlands Farm Borehole, West Sussex, England. *Palaeontographica, Abteilung B*, 210, 9-89.
- Louwye, S., Foubert, A., Mertens, K., Van Rooij, D., and the IODP Expedition 307 Scientific Party (2008). Integrated stratigraphy and palaeoecology of the lower and middle Miocene of Porcupine Basin. *Geological Magazine*, 145(3), 321-344. doi:10.1017/S0016756807004244.
- MacRae, R. A., Fensome, R. A., & Williams, G. L. (1996). Fossil dinoflagellate diversity, originations, and extinctions and their significance. *Canadian Journal of Botany*, 74(11), 1687-1694.
- Mao, S., & Lamolda, M. A. (1998). Quistes de dinoflagelados del Cenomaniense superior y del Turoniense inferior de Ganuza, Navarra, I – Paleontología sistemática. *Revista Española de Paleontología*, 13, 261-286.
- Mao, S., & Lamolda, M. A. (1999). Quistes de dinoflagelados del Cenomaniense superior y del Turoniense inferior de Ganuza, Navarra, II – Bioestratigrafía. *Revista Española de Paleontología*, nº extr. (Homenaje al Prof. J. Truyols), 195-203.
- Marques, B., & Rocha, R. B. (1988). O Caloviano do flanco norte do Guilhim (Algarve 599 oriental): bioestratigrafia e paleobiogeografia. *Ciências da Terra*, 9, 19-26.

- Marret, F. (1993). Les effets de l'acétolyse sur les assemblages de kystes de dinoflagellés. *Palynosciences*, 2, 267–272.
- Marret, F., & Zonneveld, K. A. (2003). Atlas of modern organic-walled dinoflagellate cyst distribution. *Review of Palaeobotany and Palynology*, 2507, 167–200.
- Martín-Closas, C. (2003). The fossil record and evolution of freshwater plants: A review. *Geologica Acta*, 1(4), 315–338.
- Masure, E., Aumar, A-M., & Vrielynck, B. (2013). World palaeogeography of Aptian and Late Albian dinoflagellates cysts: Implications for sea surface temperature gradient and palaeoclimate. In J. M. Lewis, F. Marret, and L. Bradley (Eds.), *Biological and Geological Perspectives of Dinoflagellates* (97–125). London: The Micropalaeontological Society, Special Publications.
- McCarthy, F. M., Mudie, P. J., Rochon, A., Gostlin, K. E., & Levac, E. (2000). Taphonomic problems in marine palynology and some possible solutions. Work presented at GeoCanada 2000 (Calgary University). Retrieved from [http://webapp1.dlib.indiana.edu/virtual\\_disk\\_library/index.cgi/2870166/FID3366/PDF/940.PDF](http://webapp1.dlib.indiana.edu/virtual_disk_library/index.cgi/2870166/FID3366/PDF/940.PDF)
- McMinn, A. (1991). Recent dinoflagellate cysts from estuaries on the central coast of New South Wales, Australia. *Micropaleontology*, 37, 269–287.
- McNeill, J., Barrie, F. R., Buck, W. R., Demoulin, V., Greuter, W., Hawksworth, D., ... Turland, N. J. (2012). International Code of Nomenclature for algae, fungi, and plants (Melbourne Code) adopted by the Eighteenth International Botanical Congress Melbourne, Australia, July 2011. *Regnum Vegetabile*, 154, 1–140.
- Medlin, L. K., & Fensome, R. A. (2013). Dinoflagellate macroevolution: some considerations based on an integration of molecular, morphological and fossil evidence. In J. M. Lewis, F. Marret, and L. Bradley (Eds.), *Biological and Geological Perspectives of Dinoflagellates* (263–274). The Micropalaeontological Society, Special Publications, London: Geological Society.
- Melia, M. B. (1984). The distribution and relationship between palynomorphs in aerosols and deep-sea sediments off the coast of northwest Africa. *Marine Geology*, 58, 345–371.
- Mendes, M. M., Dinis, J., & Pais, J. (2014). Lower Cretaceous Pollen–Spore and Mesofossil Associations of the Bombarral Formation (Lusitanian Basin, Western Portugal). In R. Rocha *et al.* (Eds.), *STRATI 2013* (pp. 1129–1133). Springer Geology. doi: 10.1007/978-3-319-04364-7\_216.

- Mertens, K. N., Rengefors, K., Moestrup, Ø., & Ellegaard, M. (2012). A review of recent freshwater dinoflagellate cysts: taxonomy, phylogeny, ecology and palaeocology. *Phycologia*, 51, 612–619. DOI: 10.2216/11-89.1
- Moldowan, J. M., & Talyzina, N. M. (1998). Biogeochemical evidence for dinoflagellate ancestors in the Early Cambrian. *Science*, 281(5380), 1168–70.
- Montenat, C., Guery, F., Jamet, M., & Berthou, P.-Y. (1988). Mesozoic evolution of the Lusitanian Basin: Comparison with the adjacent margin. *Proceedings of the Ocean Drilling Program, Scientific Results*, 103, 757–775.
- Moron, J. (1981). *Etude Paleobotanique et Palynologique du Cretace superieur du Bassin Occidental Portugais au Nord del 'accident de Nazare (Portugal)*. (PhD thesis). Université Pierre et Marie Curie, Paris.
- Morrill, L. C., & Loeblich III, A. R. (1983). Ultrastructure of the dinoflagellate amphiesma. *International Review of Cytology*, 82, 151–181.
- Netzel, H., & Dürr, G. (1984). Dinoflagellate cell cortex. In D. L. Spector (Ed.), *Dinoflagellates* (pp. 43–105). New York: Academic Press.
- Olde, K., Jarvis, I., Pearce, M., Uličný, D., Tocher, B., Trabucho-Alexandre, J., & Gröcke, D. (2015). A revised northern European Turonian (Upper Cretaceous) dinoflagellate cyst biostratigraphy: Integrating palynology and carbon isotope events. *Review of Palaeobotany and Palynology*, 213, 1–16.
- Oliveira, L. C., Dino, R., Duarte, L. V., & Perilli, N. (2007). Calcareous nannofossils and palynomorphs from Pliensbachian–Toarcian boundary in the Lusitanian Basin, Portugal. *Revista Brasileira de Paleontologia*, 10(1), 5–16.
- Omran, A. M., Soliman, H. A., & Mahmoud, M. S. (1990). Early Cretaceous palynology of three boreholes from northern Western Desert (Egypt). *Review of Palaeobotany and Palynology*, 66, 293–312.
- Pearce, M. A. (2000). *Palynology and Chemostratigraphy of the Cenomanian to Lower Campanian Chalk of Southern and Eastern England* (PhD thesis). Kingston University London, UK.
- Pearce, M. A., Jarvis, I., & Tocher, B. A. (2009). The Cenomanian–Turonian boundary event, OAE2 and palaeoenvironmental change in epicontinental seas: New insights from the dinocyst and geochemical records. *Palaeogeography, Palaeoclimatology, Palaeoecology* 280, 207–234

- Pedrão E., & Lana, C. C. (2000). Ecozona Subtilisphaera e seu registro nas bacias brasileiras. *Geociências*, V (Número Especial), 81–85.
- Pestchevitskaya, E. B. (2008). Lower Cretaceous palynostratigraphy and dinoflagellate cyst palaeoecology in the Siberian palaeobasin. *Norwegian Journal of Geology*, 88, 279–286.
- Peyrot, D. (2011). Late Cretaceous (Late Cenomanian–Early Turonian) dinoflagellate cysts from the Castilian Platform, northern Spain, *Palynology*, 35(2), 267–300, DOI:10.1080/01916122.2010.523987
- Peyrot, D., Barroso-Barcenilla, F., Barrón, E. & Comas-Rengifo, M. J. (2011). Palaeoenvironmental analysis of Cenomanian–Turonian dinocyst assemblages from the Castilian Platform (Northern Central Spain). *Cretaceous Research*, 32, 504–526.
- Peyrot, D., Barroso-Barcenilla, F., & Feist-Burkhardt, S. (2012). Palaeoenvironmental controls on late Cenomanian–early Turonian dinoflagellate cyst assemblages from Condemios (Central Spain). *Review of Palaeobotany and Palynology*, 180, 25–40.
- Pinheiro, L., Wilson, R., Reis, R. P., Whitmarsh, R. & Ribeiro, A. (1996). The western Iberia margin: a geophysical and geological overview. *Proceedings of the Ocean Drilling Program Scientific Research*, 149, 3–23.
- Powell, A. J., Dodge, D., & Lewis, J. (1990). Late Neocene to Pleistocene palynological facies of the Peruvian Continental Margin upwelling, LEG 112. In E. Suess, R. von Huene *et al.* (Eds.), *Proceedings of the Ocean Drilling Program, Scientific Results*, 112, 297–321.
- Prauss, M. L. (2012). The Cenomanian/Turonian Boundary event (CTBE) at Tarfaya, Morocco: Palaeoecological aspects as reflected by marine palynology. *Cretaceous Research*, 34, 233–256.
- Prince, I. M., Jarvis, & I., Tocher, B.A. (1999). High-resolution dinoflagellate cyst biostratigraphy of the Santonian–basal Campanian (Upper Cretaceous): new data from Whitecliff, Isle of Wight, England. *Rev. Palaeobot. Palynol.* 105, 143–169
- Pross, J., (2001). Paleo-oxygenation in Tertiary epeiric seas: evidence from dinoflagellate cysts. *Palaeogeography, Palaeoclimatology, Palaeoecology*, 166, 369–381.
- Pross, J., & Brinkhuis, H. (2005). Dinoflagellate cysts as paleoenvironmental indicators in the Paleogene: a synopsis of concepts. *Paläontologische Zeitschrift*, 79, 53–59.

- Pross, J., Houben, A. J. P., van Simaeys, S., Williams, G. L., Kotthoff, U., Coccioni, R., ... Brinkhuis, H. (2010). Umbria–Marche revisited: A refined magnetostratigraphic calibration of dinoflagellate cyst events for the Oligocene of the Western Tethys. *Review of Palaeobotany and Palynology*, 158, 213–235.
- Radi, T., & de Vernal, A. (2008). Dinocysts as proxy of primary productivity in mid-high latitudes of the Northern Hemisphere. *Marine Micropaleontology*, 68, 84–114.
- Radmacher, W., Tyszka, J., Mangerud, G., & Pearce, M. A. (2014). Dinoflagellate cyst biostratigraphy of the Upper Albian to Lower Maastrichtian in the southwestern Barents Sea. *Marine and Petroleum Geology*, 57, 109–121.
- Reis, R. P., Corrochano, A., & Armentero, I. (1997). El paleokarst de Nazare (Cretácico Superior de la Cuenca Lusitana, Portugal). *Geogaceta*, 22, 149–152.
- Reis, R. P., & Pimentel, N. (Eds.) (2010). Field-Trip Guidebook: Lusitanian Basin (Portugal). *CM 2010 abstracts, Vol. IX*. Lisbon, II Central & North Atlantic Conjugate Margins Conference.
- Rey, J. (1972). Recherches géologiques sur le Crétacé inférieur de l'Estremadura (Portugal). *Memórias dos Serviços Geológicos de Portugal*, N.S., 21, 1–477.
- Rey, J. (1992). Les unités litostratigraphiques du Crétacé inférieur de la région de Lisbonne. *Comunicações dos Serviços Geológicos de Portugal*, 78, 103–124.
- Rey, J. (2007). Stratigraphie séquentielle et séquences de dépôt dans le Crétacé inférieur du Bassin Lusitanien. *Ciências da Terra*, Volume Especial VI (120 pp.).
- Rey, J., Caetano, P. S., Callapez, P., & Dinis, J. (2009). Le Crétacé du Bassin Lusitanien (Portugal). Excursion du Groupe Français du Crétacé. GFC 2009, Série "Excursion" [available at <https://hal.archives-ouvertes.fr/hal-00452152>].
- Rey, J., & Dinis, J. L. (2004). Shallow marine to fluvial interplay in the Lower Cretaceous of central Portugal: Sedimentology, cycles and controls. In J. L. Dinis and P. Proença Cunha (Eds.), *Cretaceous and Cenozoic events in West Iberia margins, Field Trip Guidebook 2* (pp. 5–35). 23rd IAS Meeting of Sedimentology, Coimbra.
- Rey, J., Dinis, J. L., Callapez, P. M., & Cunha, P. P. (2006). *Da rotura continental à margem passiva. Composição e evolução do Cretácico de Portugal*. Cadernos de Geologia de Portugal, Lisboa: INETI.



- Ribeiro, A., Antunes, M. T., Ferreira, M. P., Rocha, R. B., Soares, A. F., Zbyszewski, ... Monteiro, J. H. (1979). *Introduction à la Géologie Générale du Portugal* (114 pp.). Lisboa: Serviços Geológicos de Portugal.
- Riding, J. B. (2012). A compilation and review of the literature on Triassic, Jurassic, and earliest Cretaceous dinoflagellate cysts. *American Association of Stratigraphic Palynologist Contributions Series*, 46 (119 p.). Dallas: American Association of Stratigraphic Palynologists Foundation.
- Riding, J. B. (2013). The literature on Triassic, Jurassic and earliest Cretaceous dinoflagellate cysts: supplement 1. *Palynology*, 37(2), 345-354.
- Riding, J. B. (2014). The literature on Triassic, Jurassic and earliest Cretaceous dinoflagellate cysts: supplement 2. *Palynology*, 38(2), 334-347.
- Rizzo, P.J. (1991). The enigma of the dinoflagellate chromosome. *Journal of Protozoology*, 38(3), 246-252.
- Rocha, R., Manuppella, G., Mouterde, R., Ruget, C., & Zbyszewski, G. (1981). Carta geológica de Portugal, escala 1/50.000. Notícia explicativa da folha 19-C-Figueira da Foz. Lisboa: Direcção geral Geral de Geologia e Minas, Serviços c de Portugal.
- Rocha, R. B., & Soares, A. F. (1984). Algumas reflexões sobre a sedimentação jurássica na orla meso-cenozóica ocidental de Portugal. *Memórias e Notícias*, 97, 133-142.
- Rochon, A., Eynaud, F., & de Vernal, A. (2008). Dinocysts as tracers of hydrographical conditions and productivity along the ocean margins: Introduction. *Marine Micropaleontology*, 68, 1-5.
- Rochon, A., & de Vernal, A. (1994). Palynomorph distribution in recent sediments from the Labrador Sea. *Canadian Journal of Earth Sciences*, 31, 115-127.
- Rochon, A., de Vernal, A., Turon, J.-L., Matthiessen, J., & Head, M. J. (1999). Distribution of recent dinoflagellate cysts in surface sediments from the North Atlantic Ocean and adjacent seas in relation to sea-surface parameters. *AASP Contribution Series*, 35, 1-152.
- Saporta, M. (1894). Flore fossile du Portugal. Nouvelles contributions à la flore mésozoïque accompagnées d'une notice stratigraphique par P. Choffat. *Memórias da Direcção dos Trabalhos Geológicos de Portugal* (288 pp.).
- Sarjeant, W. A. (1974). *Fossil and Living Dinoflagellates*. London, Academic Press,

- Sarjeant, W. A. (1982). Dinoflagellate cyst terminology: A discussion and proposals. *Canadian Journal of Botany*, 60(6), 922-945.
- Schnepf, E., & Elbrächter, M. (1992). Nutritional strategies in dinoflagellates: a review with emphasis on cell biological aspects. *European Journal of Protistology*, 28(1), 3-24.
- Segura, M., Barroso-Barcenilla, F., Callapez, P., García-Hidalgo, J. F., & Gil-Gil, J. (2014). Depositional sequences and ammonoid assemblages in the upper Cenomanian-lower Santonian of the Iberian Peninsula (Spain and Portugal). *Geological Acta*, 12(1), 19-27. Doi: 10.1344/105.000002056
- Simpson, G. (2007). Analogue Methods in Palaeoecology: Using the analogue Package. *Journal of Statistical Software*, 22(2), 1-29.
- Skupien, P. (2003). Dinoflagellate study of the Lower Cretaceous deposits in the Pieniny Klippen Belt (Rochovica section, Slovak Western Carpathians). *Bulletin of Geosciences*, 78(1), 67 – 82).
- Skupien, P. (2007). Upper Cretaceous dinoflagellates and palaeoenvironmental change of the Silesian basin (Outer Western Carpathians). *Geophysical Research Abstracts*, 9, 02355. SRef-ID: 1607-7962/gra/EGU2007-A-02355.
- Skupien, P., & Mohamed, O. (2008). Campanian to Maastrichtian palynofacies and dinoflagellate cysts of the Silesian Unit, Outer Western Carpathians, Czech Republic. *Bulletin of Geosciences* 83(2), 207–224.
- Skupien, P., & Vacísek, Z. (2002). Lower Cretaceous ammonite and dinocyst biostratigraphy and paleoenvironment of the Silesian Basin (outer western Carpathians). *Geologica Carpathica*, 53(3), 179-189.
- Sluijs, A., & Brinkhuis, H. (2009). A dynamic climate and ecosystem state during the Paleocene-Eocene Thermal Maximum: inferences from dinoflagellate cyst assemblages on the New Jersey Shelf. *Biogeosciences*, 6, 1755–1781.
- Sluijs, A., Brinkhuis, H., Stickle, C. E., Warnaar, J., Williams, G. L., & Fuller, M. (2003). Dinoflagellate cysts from the Eocene-Oligocene transition in the Southern Ocean: results from ODP Leg 189. In N. F. Exon, J. P. Kennett, and M. J. Malone, (Eds.), *Proceedings ODP, Scientific Results*, 189 [Online]. Available from World Wide Web: [http://www-odp.tamu.edu/publications/189\\_SR/104/104.htm](http://www-odp.tamu.edu/publications/189_SR/104/104.htm)
- Sluijs, A., Brinkhuis, H., Williams, G. L., Fensome, R. A. (2009). Taxonomic revision of some Cretaceous–Cenozoic spiny organic-walled peridiniacean dinoflagellate cysts. *Review of Palaeobotany and Palynology*, 154, 34–53.

- Sluijs, A., Pross, J., & Brinkhuis, H. (2005). From greenhouse to icehouse; organic-walled dinoflagellate cysts as paleoenvironmental indicators in the Paleogene. *Earth-Science Reviews*, 68, 281–315.
- Sluijs, A., Rohl, U., Schouten, S., Brumsack, H.-J., Sangiorgi, F., Damsté, J. S., & Brinkhuis, H. (2008). Arctic late Paleocene–early Eocene paleoenvironments with special emphasis on the Paleocene-Eocene thermal maximum (Lomonosov Ridge, Integrated Ocean Drilling Program Expedition 302). *Paleoceanography*, 23(1), PA1S11, 17 p. doi:10.1029/2007PA001495
- Smayda, T. J. (2002). Turbulence, watermass stratification and harmful algal blooms: an alternative view and frontal zones as ‘pelagic seed banks’. *Harmful Algae*, 1, 95–112.
- Soares, A. F. (1966). Estudo das formações pós-jurássicas das regiões de entre Sargento-Mor e Montemor-o-Velho (margem direita do Rio Mondego). *Memórias e Notícias*, 62, 1-343.
- Soares, A. F. (1968). Contribution à l’étude de la distribution des échinides du Crétacé supérieur du Portugal. Les échinides de la région entre Sargento-Mor et Montemor-o-Velho. *Memórias e Notícias*, 64, 1-20.
- Soares, A. F. (1972). Contribuição para o estudo do Cretácico em Portugal (o Cretácico superior da Costa de Arnes). *Memórias e Notícias*, 74, 1-56.
- Soares, A. F. (1980). A «Formação Carbonatada» na região do Baixo-Mondego. *Comunicações dos Serviços Geológicos de Portugal*, 66, 99-109.
- Sousa, L. (1998). Upper Jurassic, Upper Oxfordian-Tithonian, palynostratigraphy from the Lusitanian Basin, Portugal. *Memórias da Academia das Ciências de Lisboa: Classe de Ciências, Tomo XXXVII*, 49-77.
- Sousa, L., Rivas-Carballo, M. R., & Pais, J. (1999). Dinoflagelados, nomenclatura portuguesa. *Ciências da Terra*, 13, 35-37.
- Spector, D. L., Vasconcelos, A. C., & Triemer, R. E. (1981). DNA duplication and chromosome structure in the dinoflagellates. *Protoplasma*, 105(3-4), 185–194.
- Stover, L.W. (1975). Observations on some Australian Eocene dinoflagellates. *Geoscience and Man*, 11(1), 35-45.
- Tahoun, S. & Omar, M. (2014). Leiosphaeridia and Pterospermella acritarch genera as shallowing phase indicators in the early Jurassic, North Sinai, Egypt. *Arabian Journal of Geosciences* (published online). DOI 10.1007/s12517-014-1500-1.

- Taylor, F. J. (1987). Dinoflagellate ecology: General and marine ecosystems. In F. J. R.: Taylor (Ed.), *The biology of dinoflagellates. Botanical Monographs*, 21, 398–502.
- Taylor, F. J. (2004). Illumination or confusion? Dinoflagellate molecular phylogenetic data viewed from a primarily morphological standpoint. *Phycological Research*, 52, 308–324.
- Taylor, F. J., Hoppenrath, M., & Saldarriaga, J. F. (2008). Dinoflagellate diversity and distribution. *Biodiversity Conservation*, 17, 407–418.
- Tocher, B. A., & Jarvis, I. (1987). Dinoflagellate cysts and stratigraphy of the Turonian (Upper Cretaceous) chalk near Beer, southeast Devon, England. In M. B. Hart (Ed.), *Micropalaeontology of Carbonate Environments* (pp. 138–175). Chichester, U.K.: Ellis Horwood.
- Uwins, P. J., & Batten, D. J. (1988). Early to mid-Cretaceous palynology of northeast Libya. In A. El-Arnauti, B. Owens and B. Thusu (Eds.), *Subsurface Palynostratigraphy of North East Libya* (pp. 215–258). Benghazi: Garyounis University Publication.
- Van Nieuwenhove, N., & Bauch, H. A. (2008). Last interglacial (MIS 5e) surface water conditions at the Vøring Plateau (Norwegian Sea), based on dinoflagellate cysts. *Polar Research*, 27, 175–186. doi:10.1111/j.1751-8369.2008.00062.x
- Villanueva-Amadoz, U. (2009). *Nuevas aportaciones palinoestratigráficas para el intervalo Albiense-Cenomaniense en el Sector NE de la Península Ibérica. Implicaciones paleogeográficas y paleoclimáticas* (PhD dissertation). Universidad de Zaragoza, Spain.
- Villanueva-Amadoz, U., Sender, L. M., Diez, J. B., Ferrer, J., & Pons, D. (2011). Palynological studies of the boundary marls unit (Albian–Cenomanian) from northeastern Spain. Paleophytogeographical implications. *Geodiversitas*, 33(1), 137–176. DOI: 10.5252/g2011n1a7.
- Vink, A. (2004). Calcareous dinoflagellate cysts in South and equatorial Atlantic surface sediments: diversity, distribution, ecology and potential for palaeoenvironmental reconstruction. *Marine Micropaleontology*, 50, 43–88.
- Vink, A., Brune, A., Holl, C., Zonneveld, K. A., & Willems, H. (2002). On the response of calcareous dinoflagellates to oligotrophy and stratification of the upper water column in the equatorial Atlantic Ocean. *Palaeogeography, Palaeoclimatology, Palaeoecology*, 178, 53–66.

- Walker, L. M. (1984). Life histories, dispersal and survival in marine, planktonic dinoflagellates. In K. A. Steidinger and L. M. Walker (Eds.), *Marine Plankton Life Cycle Strategies* (pp. 19–34). Florida, USA: CRC Press.
- Wall, D., Dale, B., Lohmann, G. P., & Smith, W. K. (1977). The environmental and climatic distribution of dinoflagellate cysts in modern marine sediments from regions in the North and South Atlantic Oceans and adjacent areas. *Marine Micropaleontology*, 2, 121–200.
- Warny, S., Anderson, J. B., Londeix, L., & Bart, P. J. (2007). Analysis of the dinoflagellate cyst genus *Impletosphaeridium* as a marker of sea-ice conditions off Seymour Island, in Antarctica: An ecomorphological approach. In A. K. Cooper, C. R. Raymond *et al.* (Eds.), *Antarctica: A Keystone in a Changing World*. (4 pp.). USGS Open-File Report 2007-1047. doi:10.3133/of2007-1047.srp079
- Wendler, J., Gräfe, K.-U., & Willems, H. (2002). Palaeoecology of calcareous dinoflagellate cysts in the mid-Cenomanian Boreal Realm: Implications for the reconstruction of palaeoceanography of the NW European shelf sea. *Cretaceous Research*, 23, 213–229. doi:10.1006/cres.2002.0311
- Wiese, F., Zobel, K., & Keupp, H. (2015). Calcareous dinoflagellate cysts and the Turonian nutrient crisis – Data from the upper Turonian of the Lower Saxony Basin (northern Germany). *Cretaceous Research*, 56, 673–688.
- Williams, D. B. (1971). The occurrence of dinoflagellates in marine sediments. In B. M. Funnel and W. R. Riedel (Eds.), *Micropaleontology of the Oceans* (pp. 231–243). Cambridge: Cambridge University Press.
- Williams, G. L., Brinkhuis, H., Pearce, M. A., Fensome, R. A., & Weegink, J. W. (2004). Southern Ocean and global dinoflagellate cyst events compared: index events for the Late Cretaceous–Neogene. In N. F. Exon, J. P. Kennett, and M. J. Malone (Eds.), *Proceedings of the Ocean Drilling Program, Scientific Results, 189*, 1–98 [Online]. Available from World Wide Web: [http://www-odp.tamu.edu/publications/189\\_SR/VOLUME/CHAPTERS/107.PDF](http://www-odp.tamu.edu/publications/189_SR/VOLUME/CHAPTERS/107.PDF)
- Williams, G. L., & Bujak, J. P. (1985). Mesozoic and Cenozoic dinoflagellates. In H. M. Bolli, J. B. Saunders, and K. Nielsen (Coord.). *Plankton Stratigraphy* (pp. 847–1032). Cambridge, Cambridge University Press.
- Williams, G. L., & Fensome, R. A. (2016). Fossil Dinoflagellates: Nomenclatural Proposals in Anticipation of a Revised DINOFLAJ Database. *Palynology* 40(1), 137–143. doi: <http://dx.doi.org/10.1080/01916122.2015.1113209>

- Williams, G. L., Lentin, J. K., & Fensome, R. A. (1998) The Lentin and Williams Index of fossil dinoflagellates. 1998 edition. *American Association of Stratigraphic Palynologists, Contributions Series*, 34, 1-817.
- Willumsen, P. S., & Vajda, V. (2010). A new early Paleocene dinoflagellate cyst species, *Trithyrodinium partridgei*: its biostratigraphic significance and palaeoecology. *Alcheringa: An Australasian Journal of Palaeontology*, 34(4), 523-538. DOI: 10.1080/03115518.2010.519258
- Wilpshaar, M., & Leereveld, H. (1994). Palaeoenvironmental change in the Early Cretaceous Votocian Basin (SE France) reflected by dinoflagellate cysts. *Review of Palaeobotany and Palynology*, 84, 121-128.
- Wilson, R. (1988). Mesozoic development of the Lusitanian Basin, Portugal. *Revista de la Sociedad Geológica de España*, 1, 393-407.
- Wilson, R., Hiscott, R., Willis, M., & Gradstein, F. (1989). The Lusitanian Basin of west central Portugal; Mesozoic and Tertiary tectonic, stratigraphic and subsidence history. In A. J. Tankard and H. R. Balkwill (Eds.). *Extensional tectonics and stratigraphy of the North Atlantic margins. American Association of Petroleum Geologists Memoirs*, 46, 341-361.
- Zonneveld, K. A., Hoek, R., Brinkhuis, H., & Willems, H. (2001). Lateral distribution of organic walled dinoflagellates in surface sediments of the Benguela upwelling Region. *Progress in Oceanography*, 48, 25-72.
- Zonneveld, K. A., Marret, F., Versteegh, G., Bogus, K., Bonnet, S., Bouimetarhan, I., ... Young, M. (2013): Atlas of modern dinoflagellate cyst distribution based on 2405 data points. *Review of Palaeobotany and Palynology*, 191, 1-197. <http://dx.doi.org/10.1016/j.revpalbo.2012.08.003>.
- Zonneveld, K. A., & Pospelova, V. (2015). A determination key for modern dinoflagellate cysts. *Palynology*, 39(3), 387-409.
- Zonneveld, K. A., Versteegh, G., & Kodrans-Nsiah, M. (2008). Preservation and organic chemistry of Late Cenozoic organic-walled dinoflagellate cysts: a review. *Marine Micropaleontology*, 68, 179-197.

---

**APPENDIX**  
Plates 1 to 42

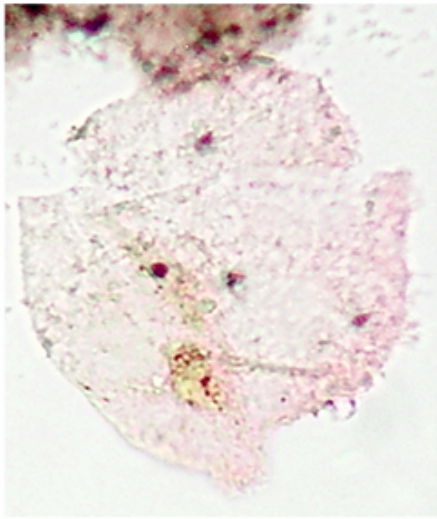
---

**Plate 1**

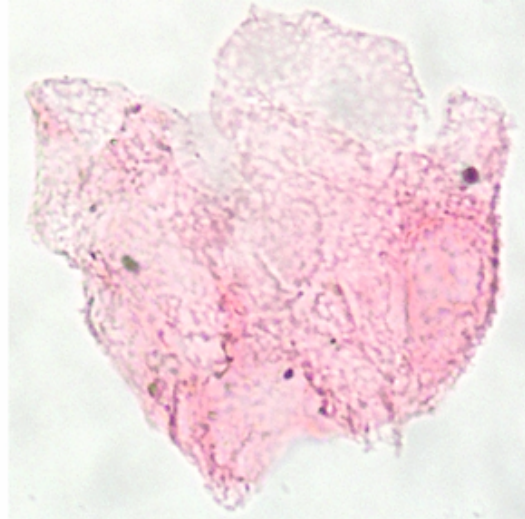
1. *Canningia reticulata* (Cookson and Eisenack, 1960) Helby, 1987; Nazaré Section, Sample T1, Slide T1.1
2. *Canningia reticulata* (Cookson and Eisenack, 1960) Helby, 1987; Nazaré Section, Sample B2, Slide B2.1 (stained for 15 minutes)
3. *Canningia* sp.; Nazaré Section, Sample B3, Slide 3B-1
4. *Canningia* sp.; Nazaré Section, Sample T4, Slide T4.1



APPENDIX

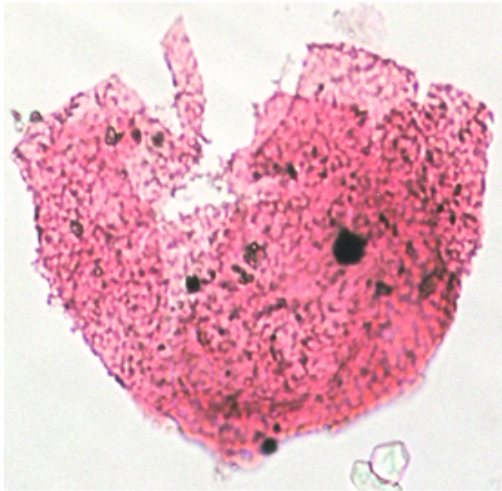


1

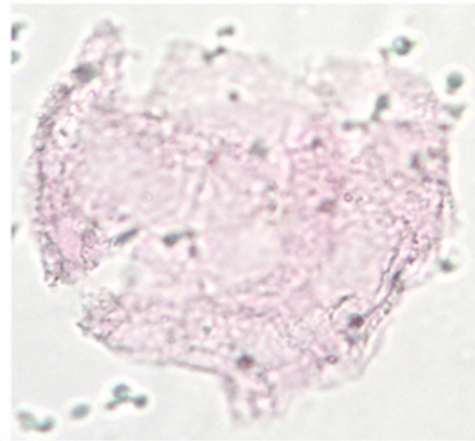


2

50µm



3



4

**Plate 2**

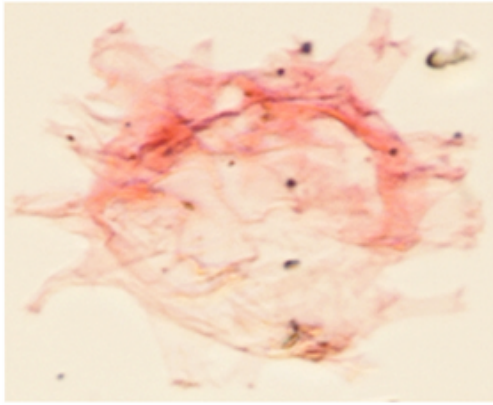
1. *Canningia* sp.; Nazaré Section, Sample T1, Slide T1.1
2. *Canningia* sp.; Nazaré Section, Sample M2, Slide M2.1
3. *Canningia* sp.; Nazaré Section, Sample T4, Slide T4.1
4. *Canningia* sp.; Nazaré Section, Sample T4, Slide T4.1



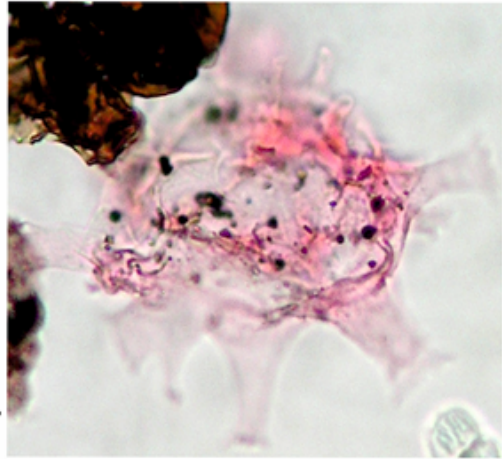
**Plate 3**

1. *Florentinia mantellii* (Davey and Williams, 1966) Davey and Verdier, 1973; Nazaré Section, Sample B2, Slide B2.1 (stained for 15 minutes)
2. *Florentinia mantellii* (Davey and Williams, 1966) Davey and Verdier, 1973; Nazaré Section, Sample B2, Slide B2.1 (stained for 15 minutes)
3. *Florentinia* sp.; Nazaré Section, Sample B2, Slide B2.1 (stained for 15 minutes)
4. *Florentinia* sp.; Nazaré Section, Sample B2, Slide B2.1 (stained for 15 minutes)

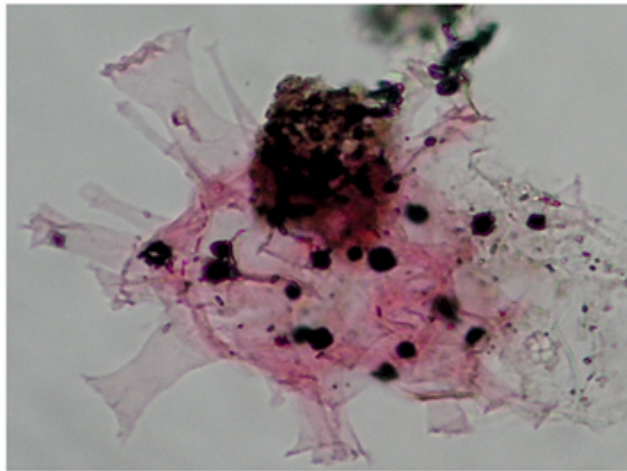
APPENDIX



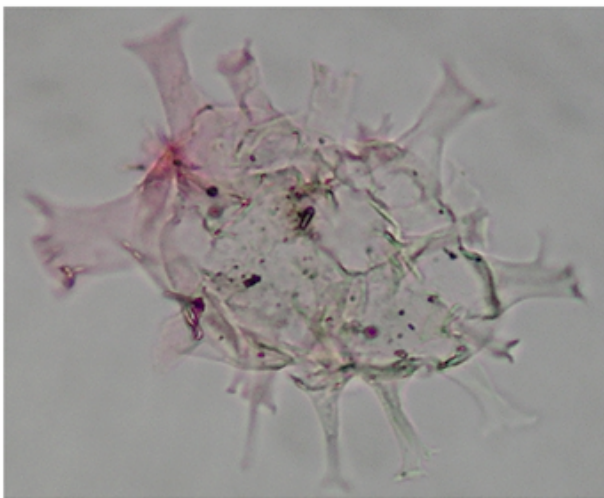
1



2



3

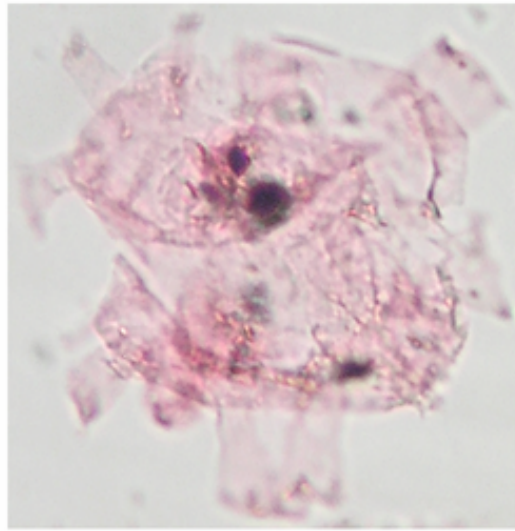


4

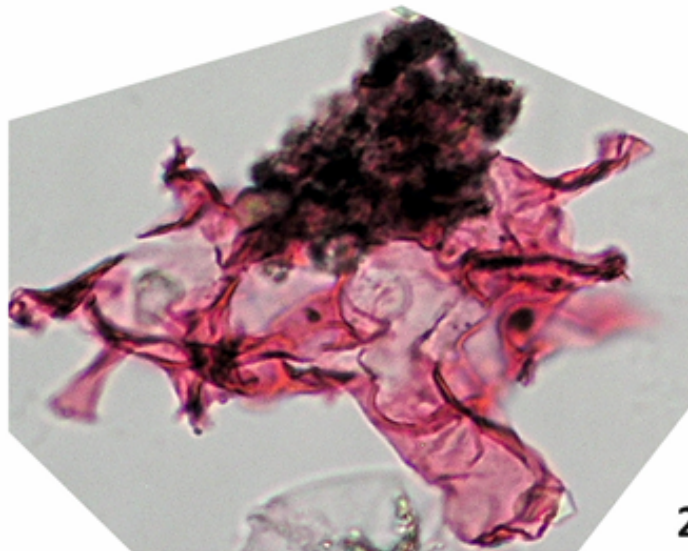
50µm

**Plate 4**

1. *Florentinia* sp.; Nazaré Section, Sample B3, Slide 3B-1 (stained for 15 minutes)
2. *Florentinia* sp.; Nazaré Section, Sample B2, Slide B2.1 (stained for 15 minutes)
3. *Florentinia* sp.; Nazaré Section, Sample B3, Slide 3B-1 (stained for 15 minutes)

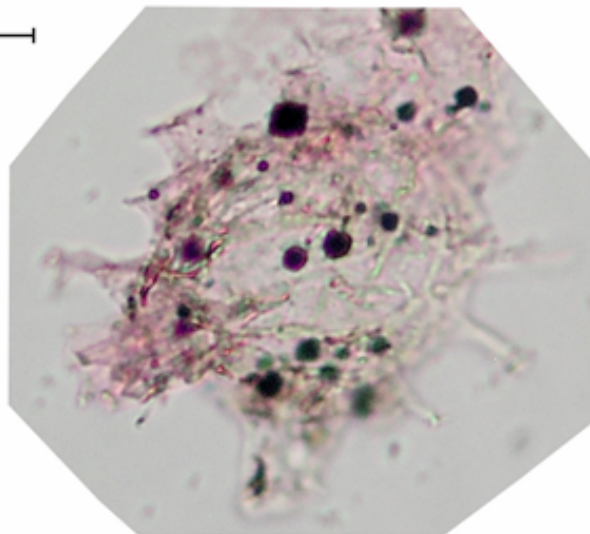


**1**



**2**

50µm



**3**

**Plate 5**

1. *Florentinia* sp. (Davey and Williams, 1966) Davey and Verdier, 1973; Nazaré Section, Sample B3, Slide 3B-1 (stained for 15 minutes)
2. *Florentinia* sp. (Davey and Williams, 1966) Davey and Verdier, 1973; Nazaré Section, Sample B3, Slide 3B-1 (stained for 15 minutes)
3. *Florentinia* sp. (Davey and Williams, 1966) Davey and Verdier, 1973; Nazaré Section, Sample B2, Slide 2B-2
4. *Florentinia* sp.; Nazaré Section, Sample B4, Slide B4.1
5. *Florentinia* sp.; Nazaré Section, Sample M1, Slide M1.1



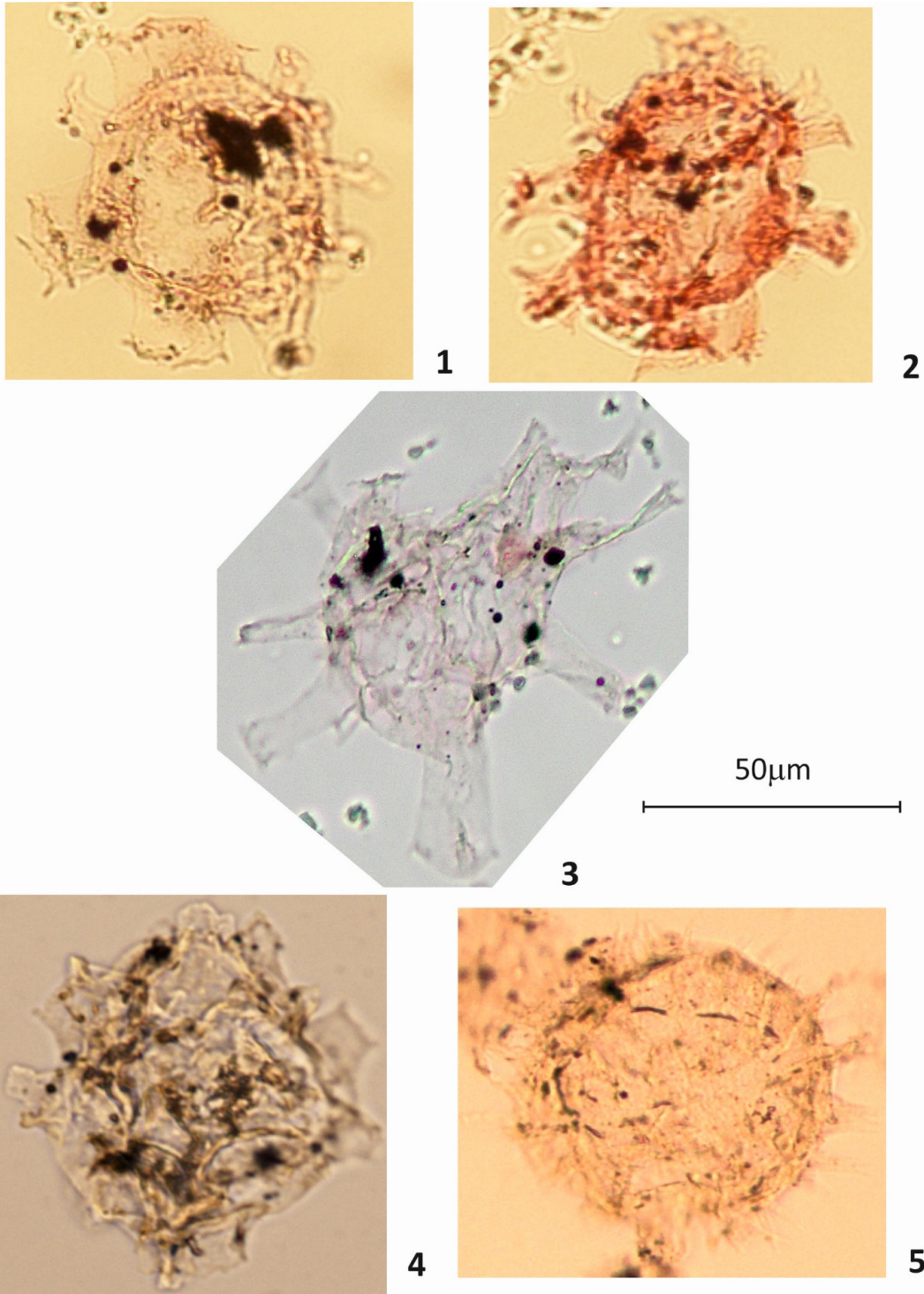
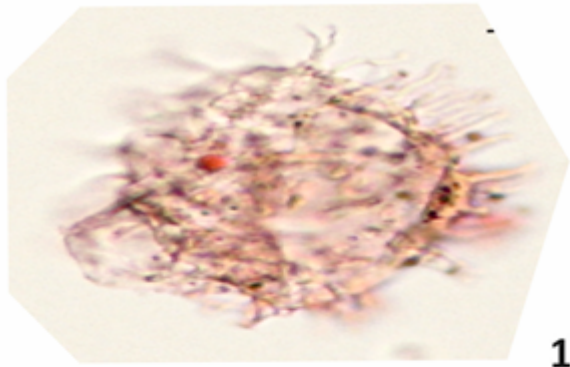


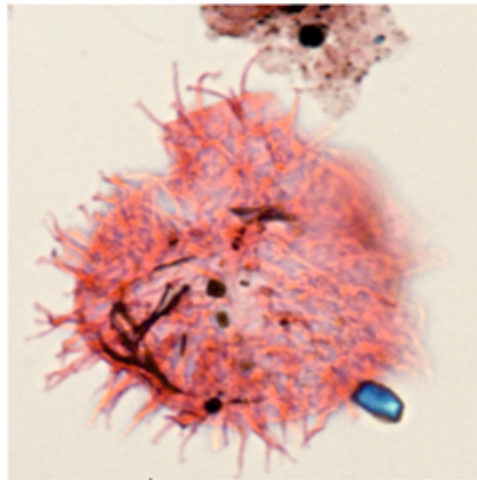
**Plate 6**

1. *Heterosphaeridium* sp.; Nazaré Section, Sample T1, Slide T1.1 (stained for 4 hours)
2. *Heterosphaeridium* sp.; Nazaré Section, Sample T1, Slide T1.1 (stained for 4 hours)



1

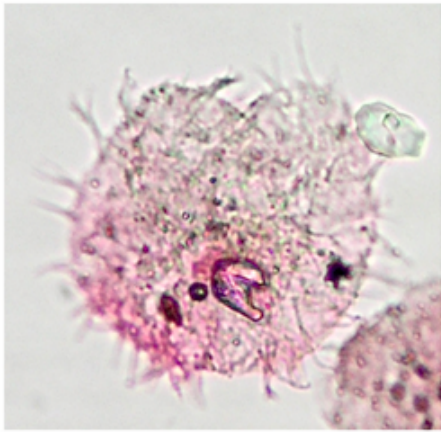
50µm



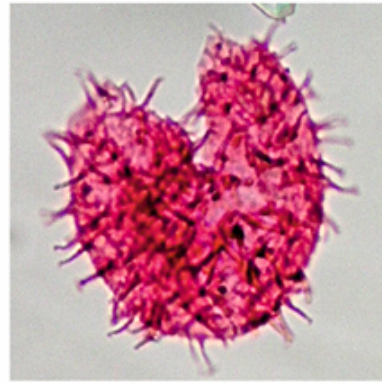
2

**Plate 7**

1. *Impletosphaeridium* sp.; Nazaré Section, Sample T1, Slide T1.1
2. *Impletosphaeridium* sp.; Nazaré Section, Sample T1, Slide T1.1
3. *Impletosphaeridium* sp.; Nazaré Section, Sample T1, Slide T1.1
4. *Impletosphaeridium* sp.; Nazaré Section, Sample T1, Slide T1.1
5. *Impletosphaeridium* sp.; Nazaré Section, Sample T1, Slide T1.1
6. *Impletosphaeridium* sp.; Nazaré Section, Sample T1, Slide T1.1 (stained for 4 hours)

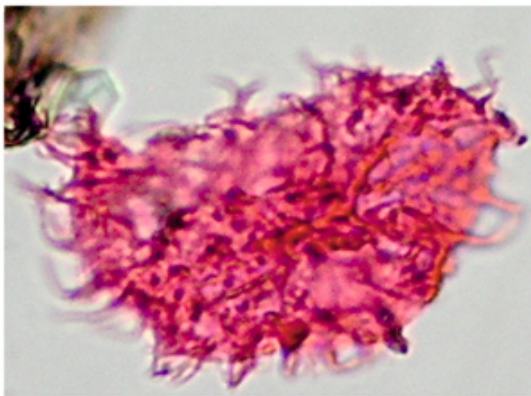


1

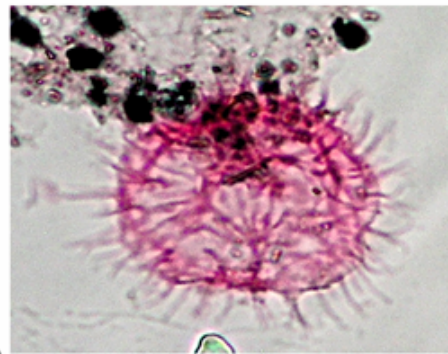


2

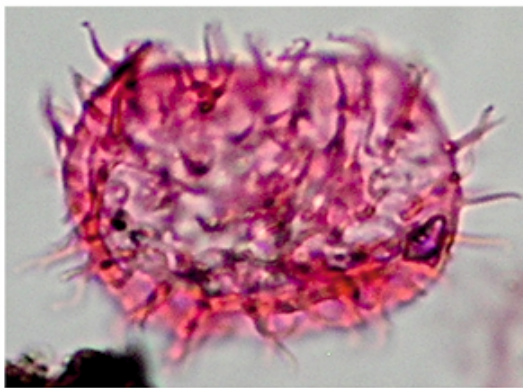
50µm



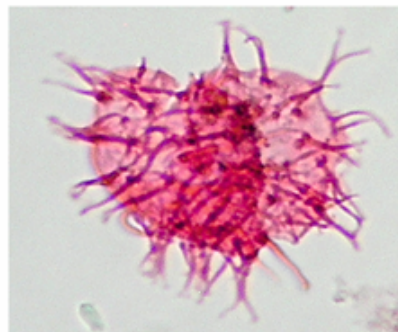
3



4



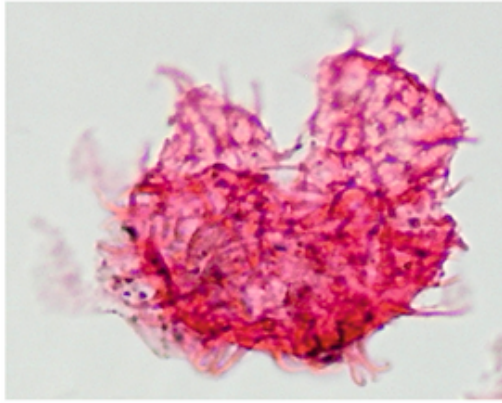
5



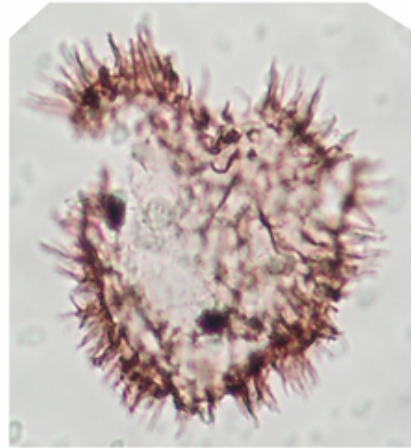
6

**Plate 8**

1. *Impletosphaeridium* sp.; Nazaré Section, Sample T1, Slide T1.1 (stained for 4 hours)
2. *Impletosphaeridium* sp.; Nazaré Section, Sample B2, Slide B2.1 (stained for 15 minutes)
3. *Impletosphaeridium* sp.; Nazaré Section, Sample T1, Slide T1.1
4. *Impletosphaeridium* sp.; Nazaré Section, Sample T1, Slide T1.1
5. *Impletosphaeridium* sp.; Nazaré Section, Sample T1, Slide T1.1

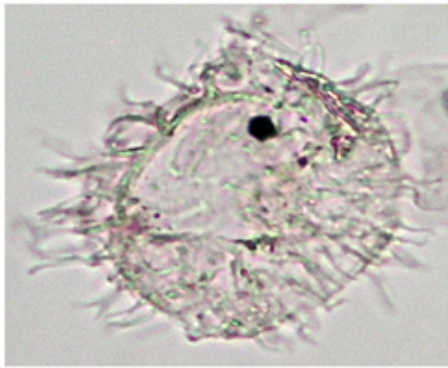


1

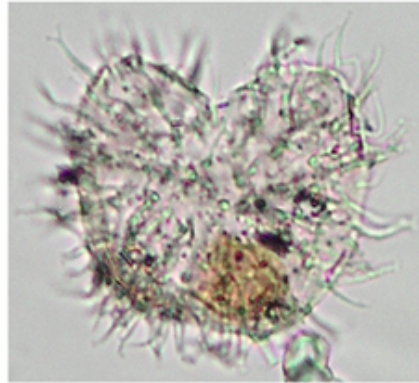


2

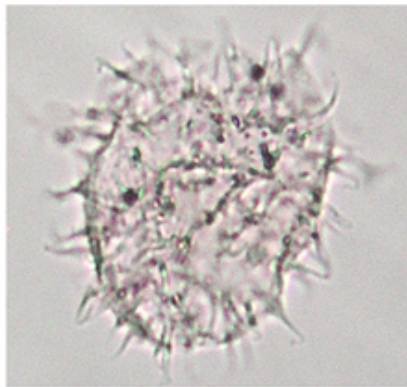
50µm



3



4



5

**Plate 9**

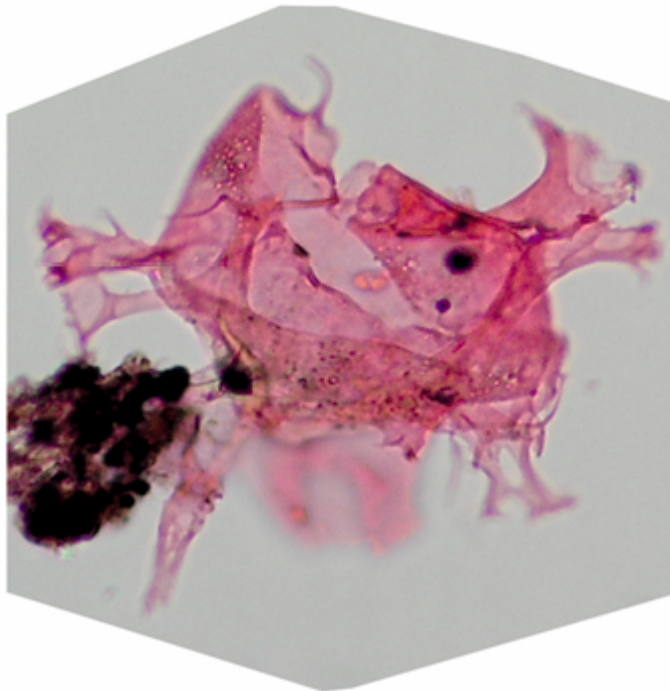
1. *Oligosphaeridium pulcherrimum* (Deflandre and Cookson, 1955) Fauconnier and Masure, 2004; Nazaré Section, Sample T1, Slide T1.1
2. *Oligosphaeridium pulcherrimum* (Deflandre and Cookson, 1955) Fauconnier and Masure, 2004; Nazaré Section, Sample T1, Slide T1.1 (stained for 4 hours)





1

50μm

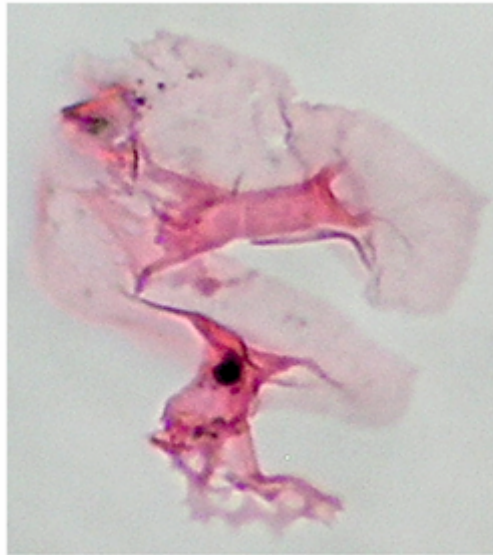


2

**Plate 10**

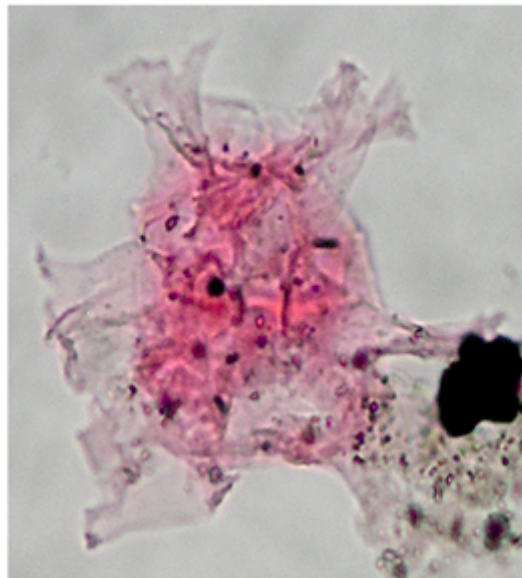
1. *Oligosphaeridium* sp.; Nazaré Section, Sample B2, Slide B2.1 (stained for 15 minutes)
2. *Oligosphaeridium* sp.; Nazaré Section, Sample B2, Slide B2.1 (stained for 15 minutes)

APPENDIX



1

50µm



2

**Plate 11**

1. *Spiniferites ramosus* (Ehrenberg, 1838) Davey and Williams, 1966; Nazaré Section, Sample T1, Slide T1.1 (stained for 15 minutes)
2. *Spiniferites ramosus* (Ehrenberg, 1838) Davey and Williams, 1966; Nazaré Section, Sample T1, Slide T1.1 (stained for 15 minutes)
3. *Spiniferites ramosus* (Ehrenberg, 1838) Davey and Williams, 1966; Nazaré Section, Sample T1, Slide T1.1 (stained for 15 minutes)
4. *Spiniferites ramosus* (Ehrenberg, 1838) Davey and Williams, 1966; Nazaré Section, Sample T1, Slide T1.1 (stained for 15 minutes)
5. *Spiniferites ramosus* (Ehrenberg, 1838) Davey and Williams, 1966; Nazaré Section, Sample T1, Slide T1.1 (stained for 15 minutes)
6. *Spiniferites ramosus* (Ehrenberg, 1838) Davey and Williams, 1966; Nazaré Section, Sample T1, Slide T1.1 (stained for 15 minutes)

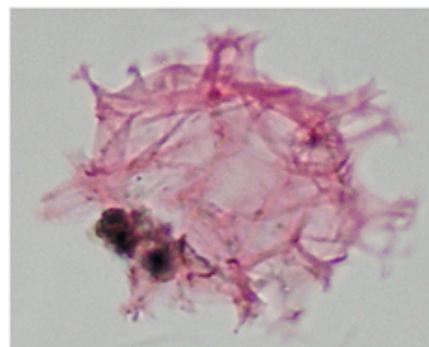
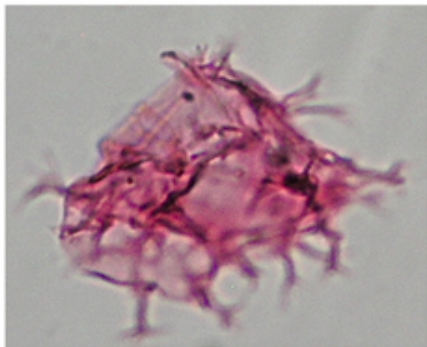
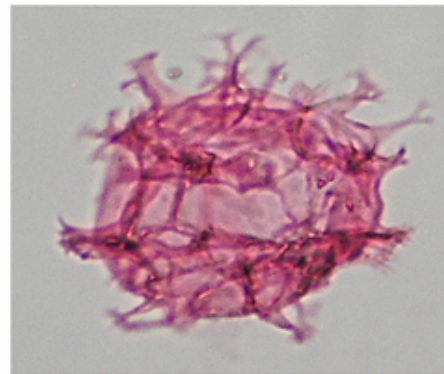
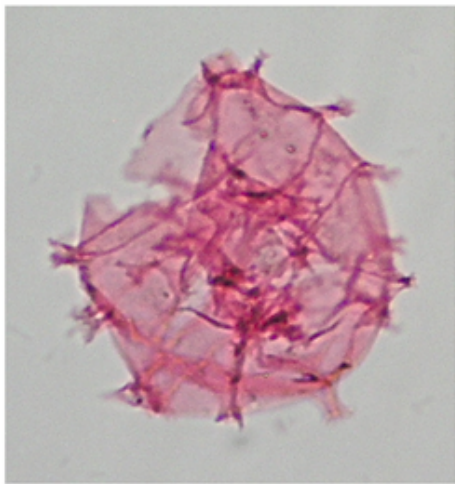
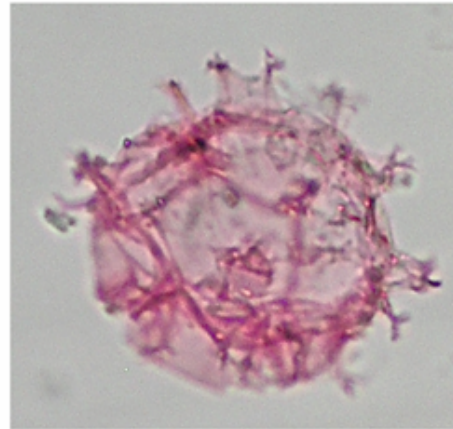
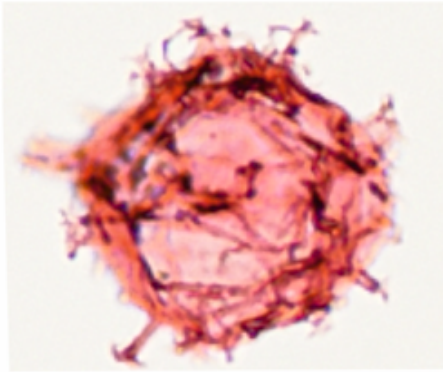
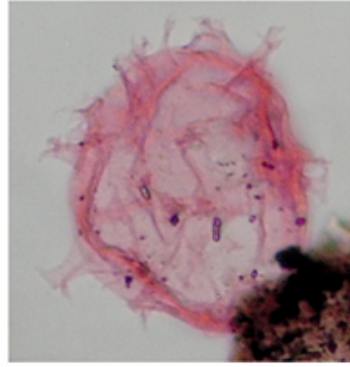


**Plate 12**

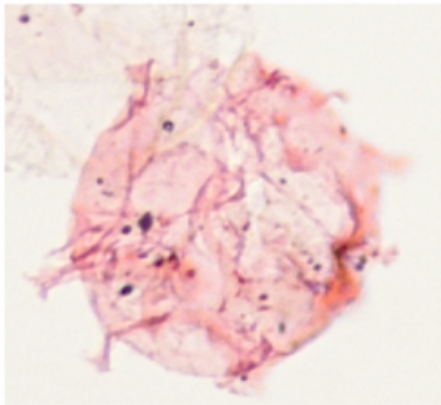
1. *Spiniferites ramosus* (Ehrenberg, 1838) Davey and Williams, 1966; Nazaré Section, Sample T1, Slide T1.1 (stained for 4 hours)
2. *Spiniferites ramosus* (Ehrenberg, 1838) Davey and Williams, 1966; Nazaré Section, Sample B2, Slide B2.1 (stained for 15 minutes)
3. *Spiniferites ramosus* (Ehrenberg, 1838) Davey and Williams, 1966; Nazaré Section, Sample T1, Slide T1.1 (stained for 4 hours)
4. *Spiniferites ramosus* (Ehrenberg, 1838) Davey and Williams, 1966; Nazaré Section, Sample T1, Slide T1.1 (stained for 15 minutes hours)
5. *Spiniferites ramosus* (Ehrenberg, 1838) Davey and Williams, 1966; Nazaré Section, Sample T1, Slide T1.1 (stained for 4 hours)
6. *Spiniferites ramosus* (Ehrenberg, 1838) Davey and Williams, 1966; Nazaré Section, Sample T1, Slide T1.1 (stained for 15 minutes)



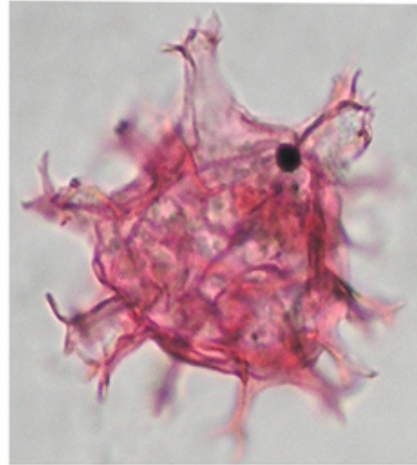
1



2

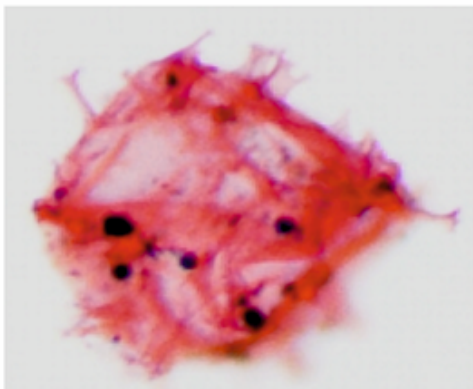


3

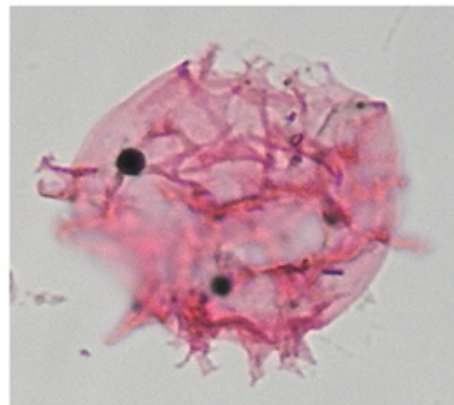


4

50µm



5

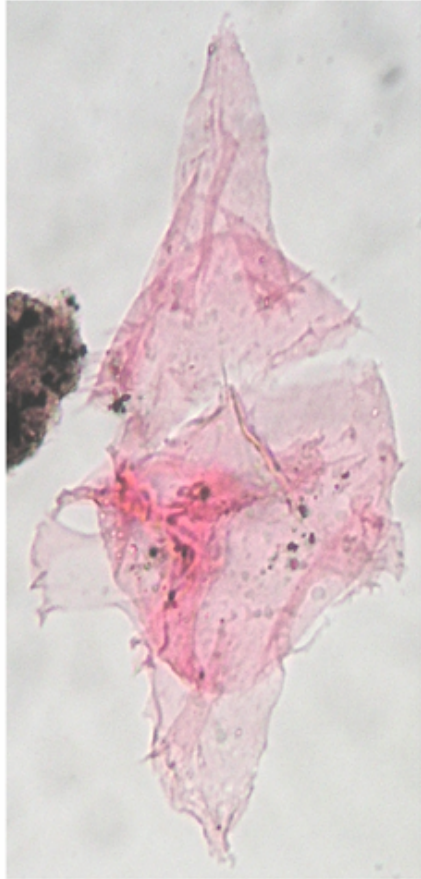


6

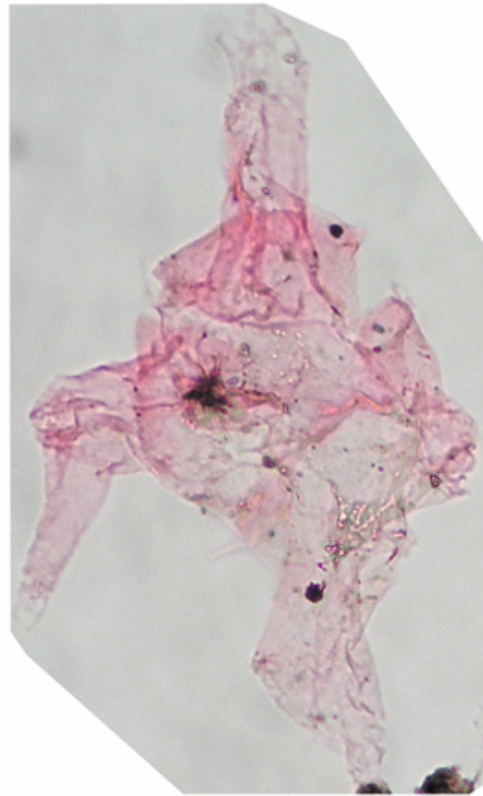
**Plate 13**

1. *Xenascus ceratioides* (Deflandre, 1937) Lentin and Williams, 1973; Nazaré Section, Sample B2, Slide B2.1 (stained for 15 minutes)
2. *Xenascus ceratioides* (Deflandre, 1937) Lentin and Williams, 1973; Nazaré Section, Sample B2, Slide B2.1 (stained for 15 minutes)
3. *Xenascus ceratioides* (Deflandre, 1937) Lentin and Williams, 1973; Nazaré Section, Sample T1, Slide T1.1
4. *Xenascus* sp.; Nazaré Section, Sample B2, Slide B2.1 (stained for 15 minutes)



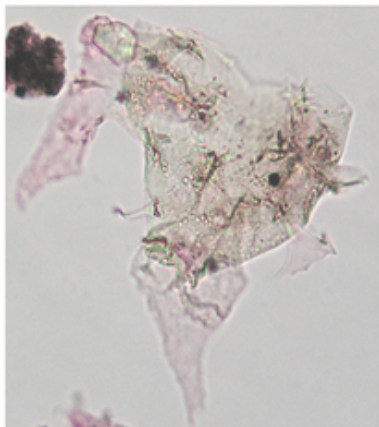


1

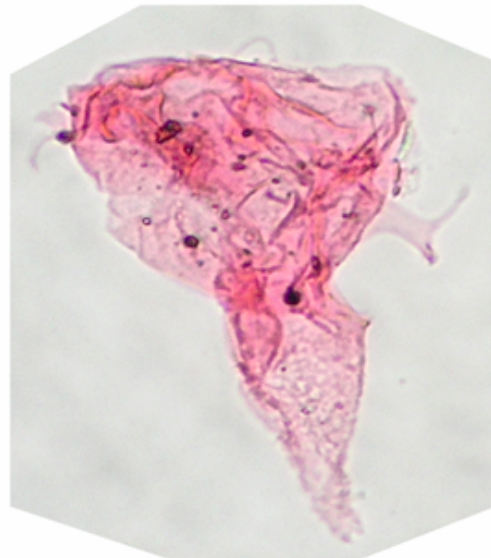


2

50µm



3



4

**Plate 14**

1. *Xenascus* sp.; Nazaré Section, Sample B2, Slide B2.1 (stained for 15 minutes)
2. *Xenascus* sp.; Nazaré Section, Sample T1, Slide B2.1 (stained for 15 minutes)
3. *Xenascus* sp.; Nazaré Section, Sample T1, Slide T1.1 (stained for 4 hours)
4. *Xenascus* sp.; Nazaré Section, Sample B2, Slide B2.1 (stained for 15 minutes)
5. *Xenascus* sp.; Nazaré Section, Sample B2, Slide 2B-2 (stained for 15 minutes)

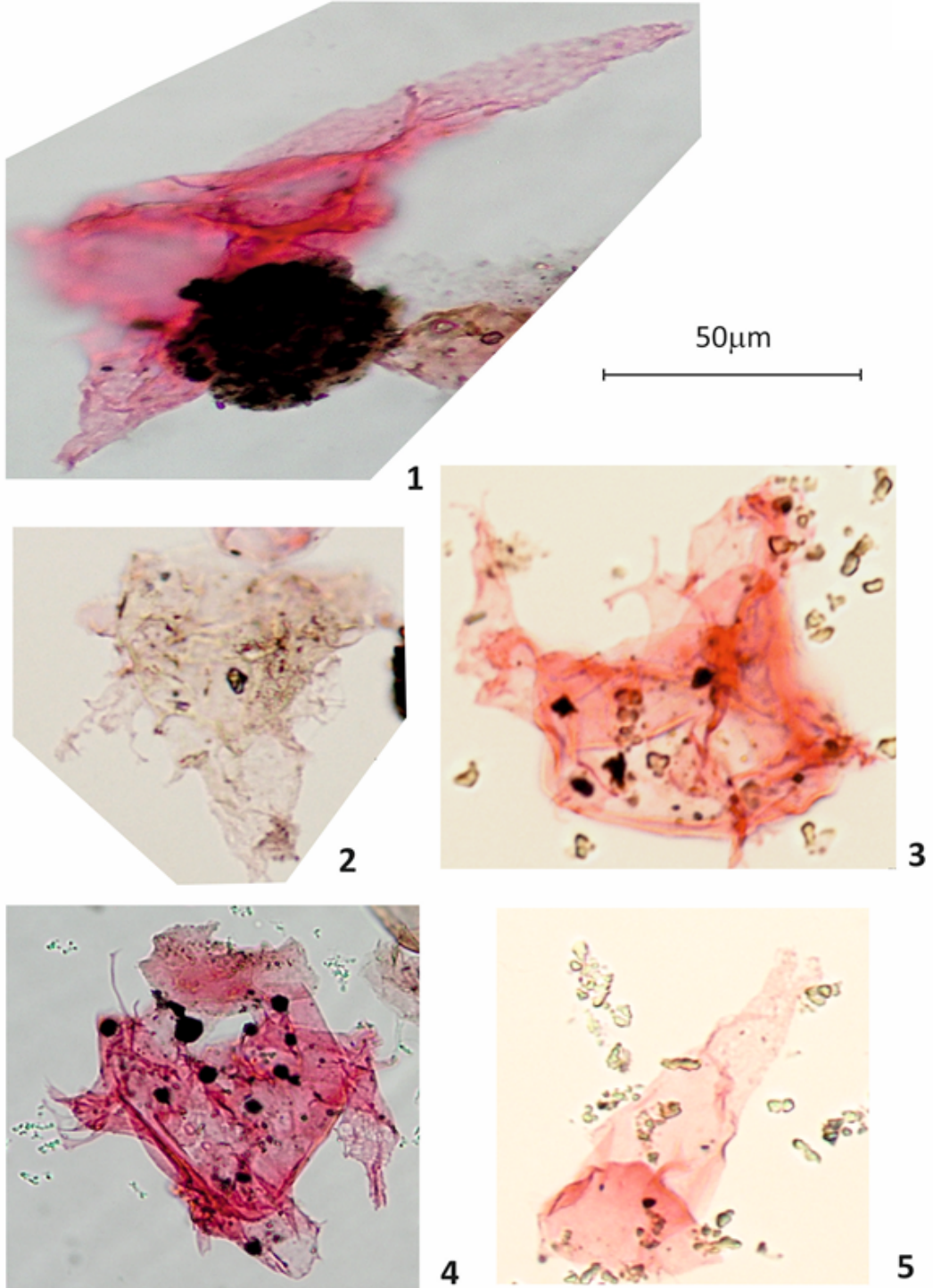
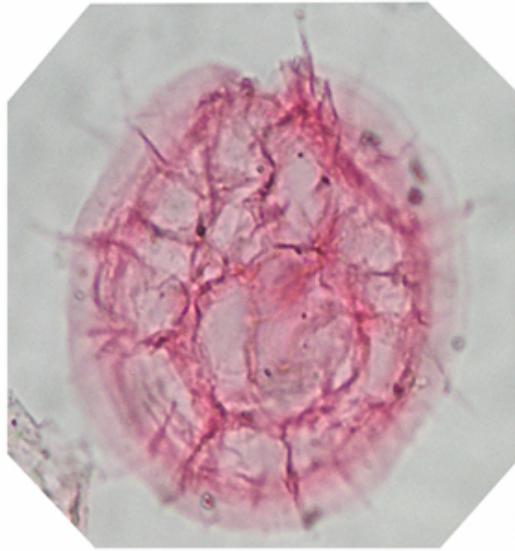


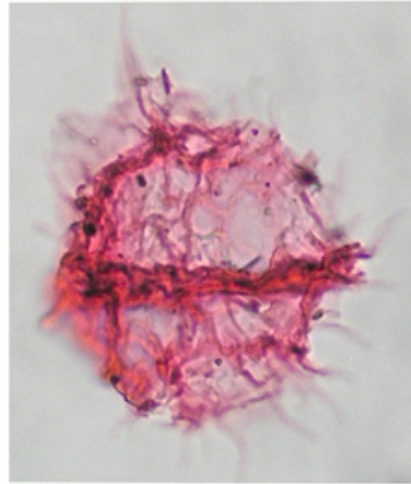
**Plate 15**

1. *Xiphophoridium alatum* (Cookson and Eisenack, 1962) Sarjeant, 1966; Nazaré Section, Sample B2, Slide B2.1 (stained for 15 minutes)
2. *Xiphophoridium alatum* (Cookson and Eisenack, 1962) Sarjeant, 1966; Nazaré Section, Sample B2, Slide B2.1 (stained for 15 minutes)
3. *Xiphophoridium alatum* (Cookson and Eisenack, 1962) Sarjeant, 1966; Nazaré Section, Sample B2, Slide B2.1 (stained for 15 minutes)
4. *Xiphophoridium alatum* (Cookson and Eisenack, 1962) Sarjeant, 1966; Nazaré Section, Sample B2, Slide B2.1 (stained for 15 minutes)
5. *Xiphophoridium alatum* (Cookson and Eisenack, 1962) Sarjeant, 1966; Nazaré Section, Sample B2, Slide B2.1 (stained for 15 minutes)

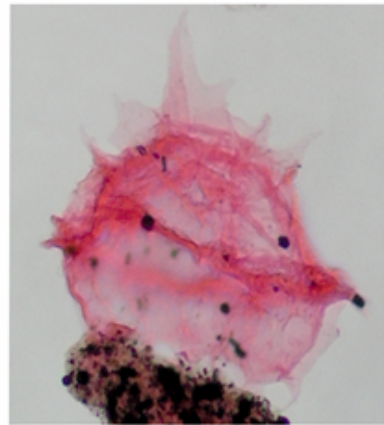


1

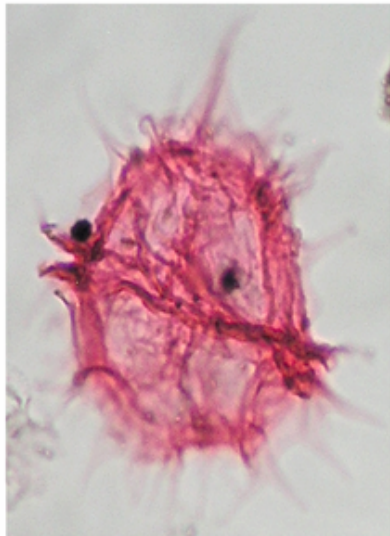
50µm



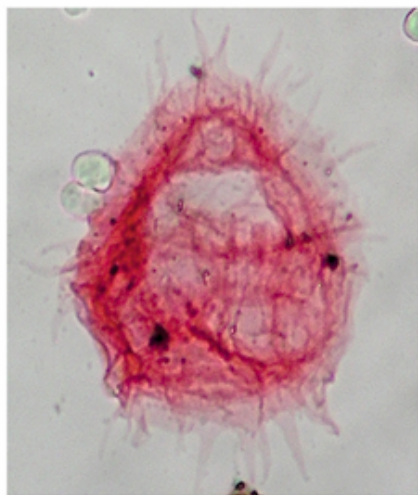
3



4



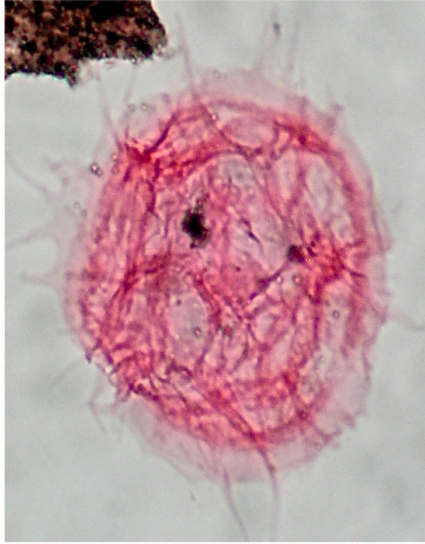
2



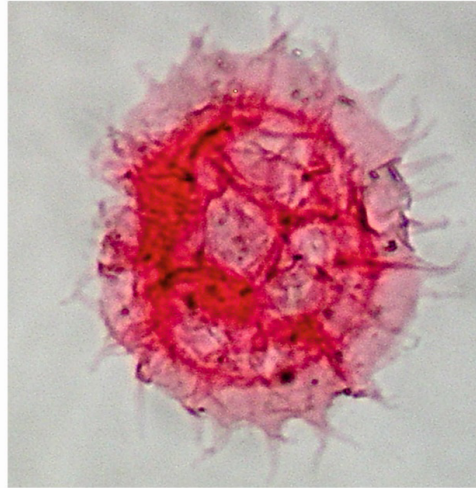
5

**Plate 16**

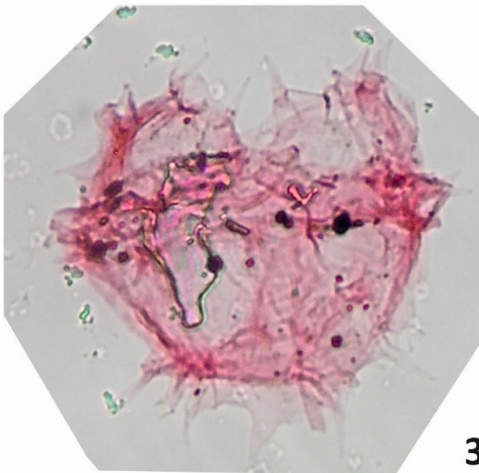
1. *Xiphophoridium alatum* (Cookson and Eisenack, 1962) Sarjeant, 1966; Nazaré Section, Sample B2, Slide B2.1 (stained for 15 minutes)
2. *Xiphophoridium alatum* (Cookson and Eisenack, 1962) Sarjeant, 1966; Nazaré Section, Sample B2, Slide B2.1 (stained for 15 minutes)
3. *Xiphophoridium alatum* (Cookson and Eisenack, 1962) Sarjeant, 1966; Nazaré Section, Sample B2, Slide 2B-2 (stained for 15 minutes)
4. *Xiphophoridium alatum* (Cookson and Eisenack, 1962) Sarjeant, 1966; Nazaré Section, Sample B2, Slide B2.1 (stained for 15 minutes)
5. *Xiphophoridium alatum* (Cookson and Eisenack, 1962) Sarjeant, 1966 (contains pyrite remains); Nazaré Section, Sample B2, Slide B2.1 (stained for 15 minutes)



1



2

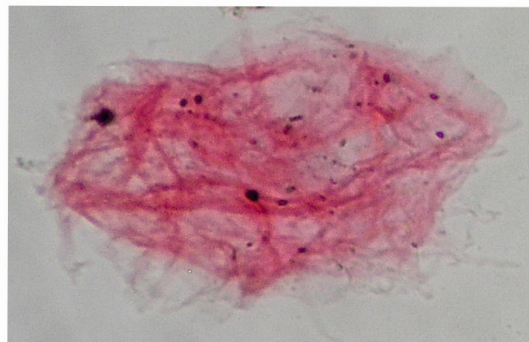


3



4

50µm

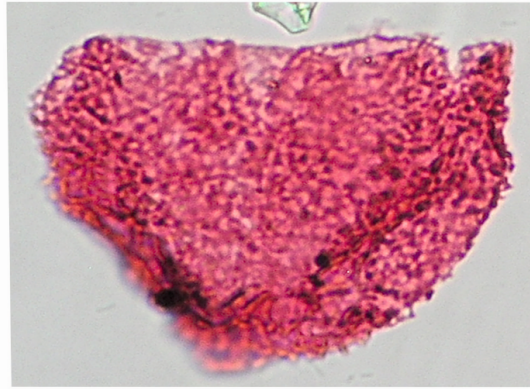


5

**Plate 17**

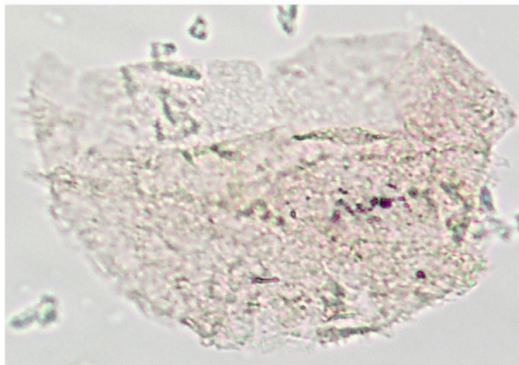
1. *Epelidosphaeridia spinosa* (Cookson and Hughes, 1964) Davey, 1969; Nazaré Section, Sample T1, Slide T1.1 (stained for 15 minutes)
2. *Epelidosphaeridia spinosa* (Cookson and Hughes, 1964) Davey, 1969; Nazaré Section, Sample B3, Slide 3B-1 (stained for 15 minutes)
3. *Epelidosphaeridia spinosa* (Cookson and Hughes, 1964) Davey, 1969; Nazaré Section, Sample B3, Slide 3B-1 (stained for 15 minutes)
4. *Epelidosphaeridia spinosa* (Cookson and Hughes, 1964) Davey, 1969; Nazaré Section, Sample T1, Slide T1.1 (stained for 15 minutes)
5. *Epelidosphaeridia spinosa* (Cookson and Hughes, 1964) Davey, 1969; Nazaré Section, Sample M2, Slide 2M.1





1

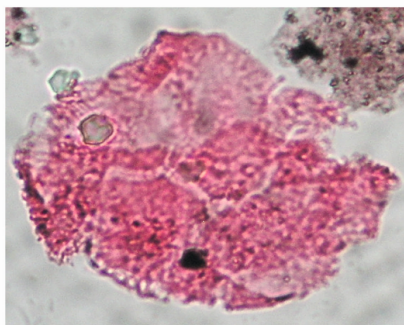
50µm



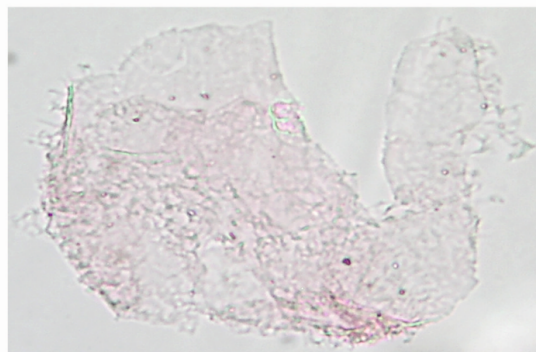
2



3



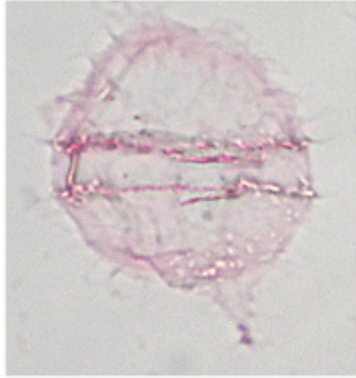
4



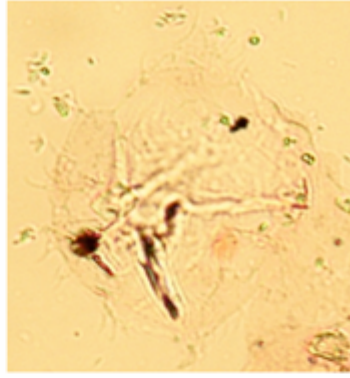
5

**Plate 18**

1. *Palaehystrichophora infusorioides* (Deflandre, 1935) Aurisano, 1989; Nazaré Section, Sample T1, Slide T1.1
2. *Palaehystrichophora infusorioides* (Deflandre, 1935) Aurisano, 1989; Nazaré Section, Sample B3, Slide 3-B (stained for 15 minutes)
3. *Palaehystrichophora* sp.; Nazaré Section, Sample B3, Slide 3B-1 (stained for 15 minutes)
4. *Palaehystrichophora* sp.; Nazaré Section, Sample B3, Slide 3B-1 (stained for 15 minutes)
5. *Palaehystrichophora* sp.; Nazaré Section, Sample B3, Slide 3B-1 (stained for 15 minutes)
6. *Palaehystrichophora* sp.; Nazaré Section, Sample B3, Slide 3B-1 (stained for 15 minutes)

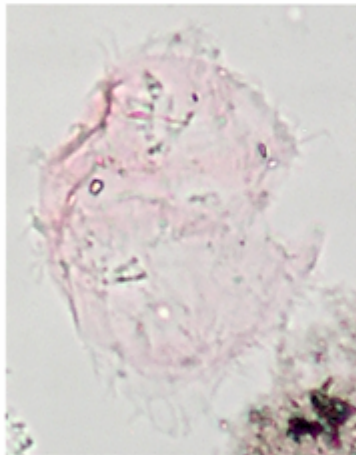


1

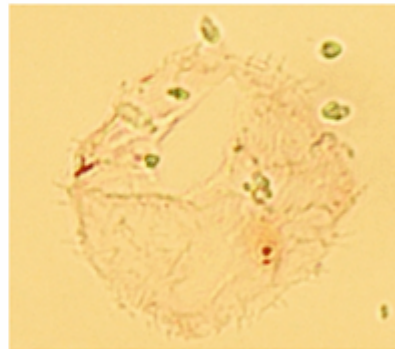


2

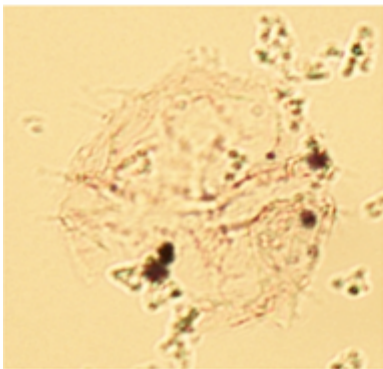
50µm



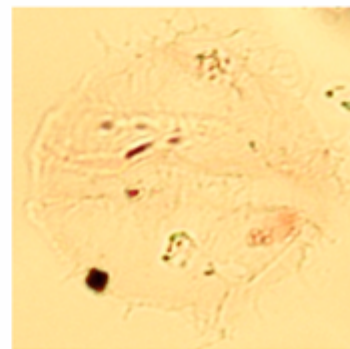
3



4



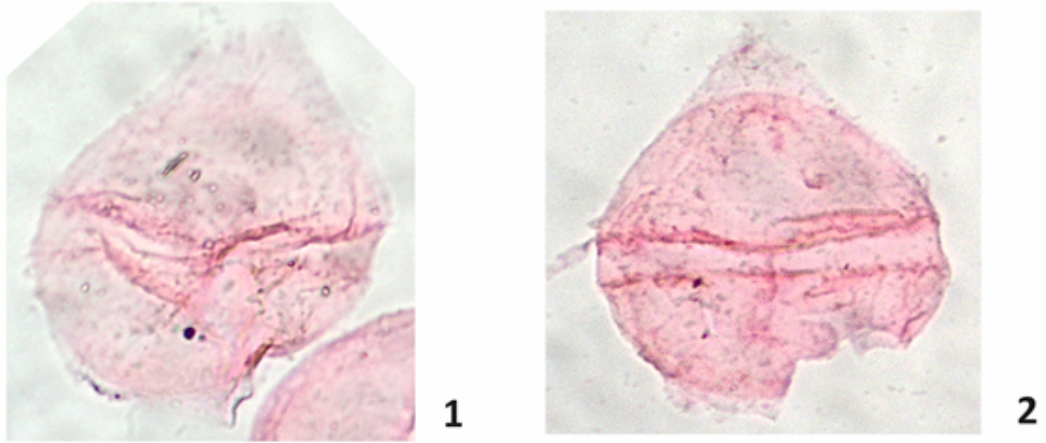
5



6

**Plate 19**

1. *Spinidinium* sp.; Nazaré Section, Sample T1, Slide T1.1 (stained for 15 minutes)
2. *Spinidinium* sp.; Nazaré Section, Sample T1, Slide T1.1 (stained for 15 minutes)
3. *Spinidinium* sp.; Nazaré Section, Sample T1, Slide T1.1 (stained for 15 minutes)
4. *Spinidinium* sp.; Nazaré Section, Sample B3, Slide 3B-1 (stained for 15 minutes)
5. *Spinidinium* sp.; Nazaré Section, Sample B3, Slide 3B-1 (stained for 15 minutes)
6. *Spinidinium* sp.; Nazaré Section, Sample B4, Slide B4.1



50µm

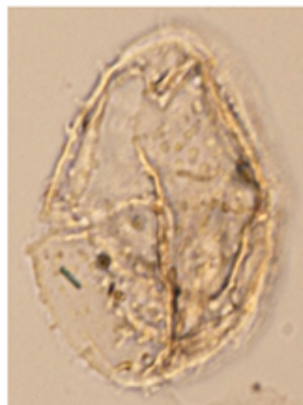
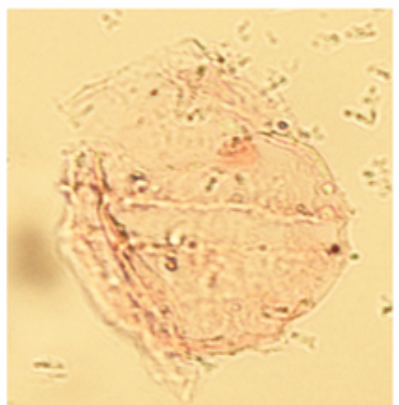
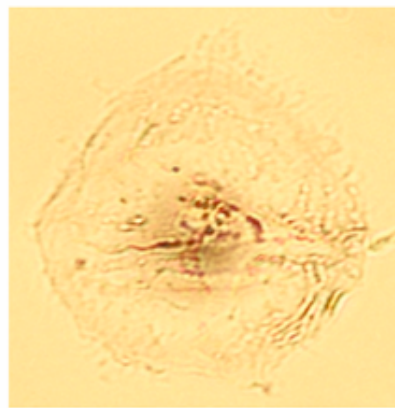
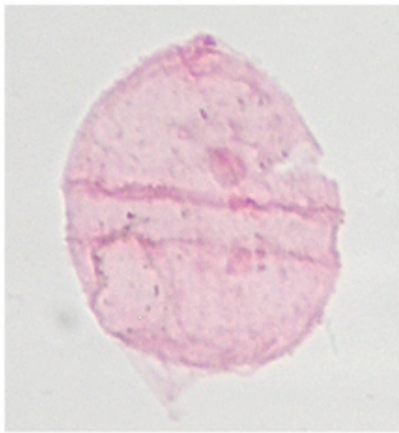


**Plate 20**

1. *Subtilisphaera* sp.; Nazaré Section, Sample T1, Slide T1.1 (stained for 4 hours)
2. *Subtilisphaera* sp.; Nazaré Section, Sample T1, Slide T1.1 (stained for 4 hours)
3. *Subtilisphaera* sp.; Nazaré Section, Sample T1, Slide T1.1 (stained for 4 hours)
4. *Subtilisphaera* sp.; Nazaré Section, Sample T1, Slide T1.1 (stained for 4 hours)
5. *Subtilisphaera* sp.; Nazaré Section, Sample T1, Slide T1.1 (stained for 15 minutes)
6. *Subtilisphaera* sp.; Nazaré Section, Sample T1, Slide T1.1 (stained for 4 hours)
7. *Subtilisphaera* sp.; Nazaré Section, Sample T1, Slide T1.1 (stained for 4 hours)
8. *Subtilisphaera* sp.; Nazaré Section, Sample T1, Slide T1.1 (stained for 4 hours)
9. *Subtilisphaera* sp.; Nazaré Section, Sample T1, Slide T1.1 (stained for 4 hours)

APPENDIX

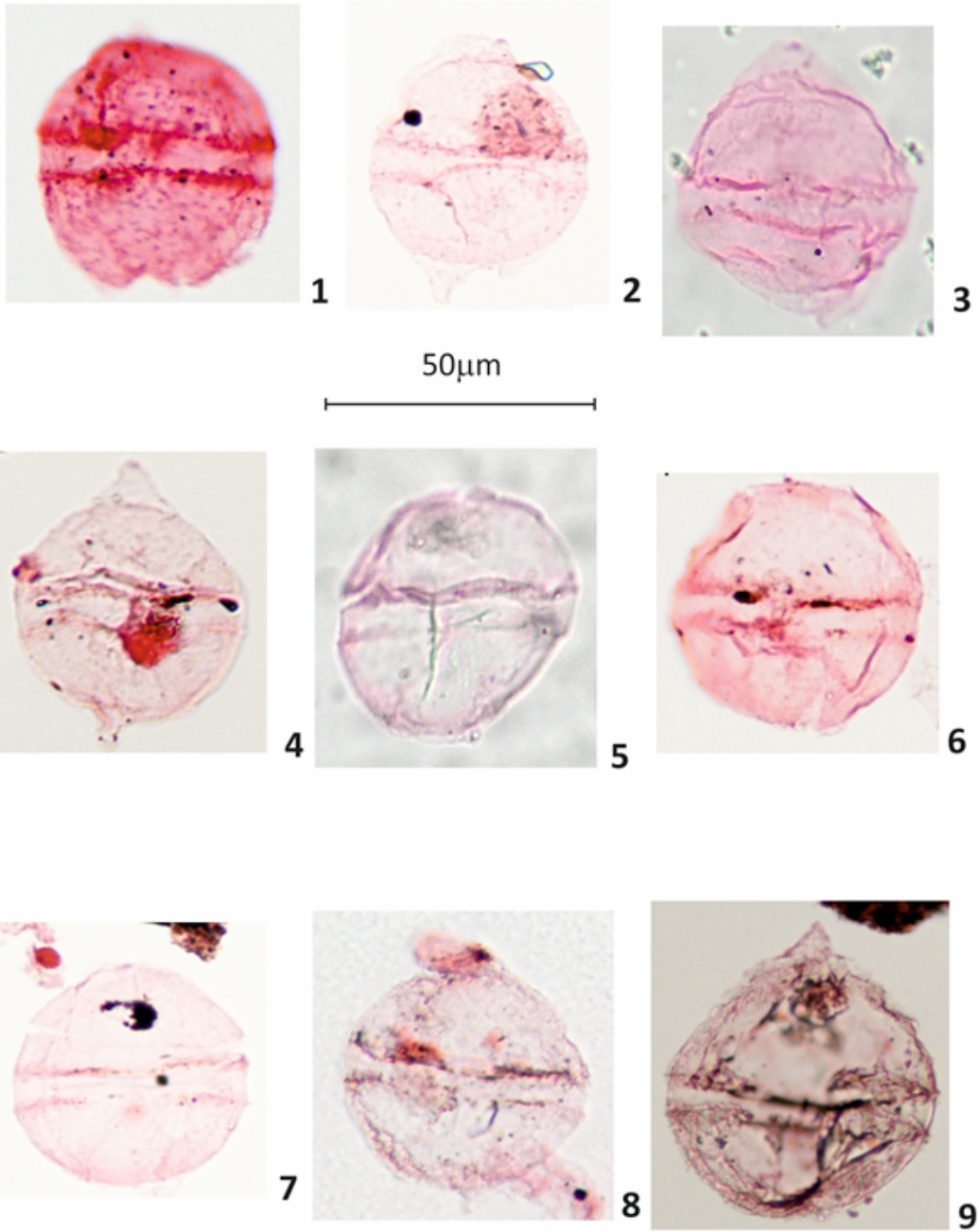
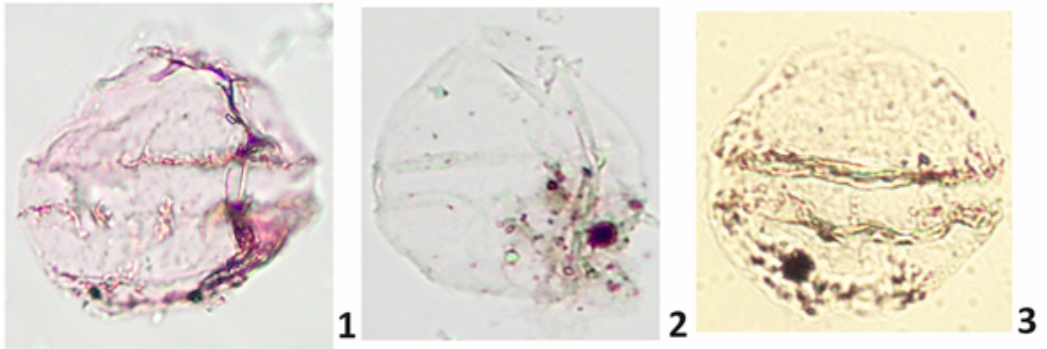


**Plate 21**

1. *Subtilisphaera* sp.; Nazaré Section, Sample B3, Slide 3B-1 (stained for 15 minutes)
2. *Subtilisphaera* sp.; Nazaré Section, Sample T1, Slide T1.1
3. *Subtilisphaera* sp.; Nazaré Section, Sample M2, Slide M2.1
4. *Subtilisphaera* sp.; Nazaré Section, Sample T1, Slide T1.1
5. *Subtilisphaera* sp.; Nazaré Section, Sample T1, Slide T1.1 (stained for 15 minutes)
6. *Subtilisphaera* sp.; Nazaré Section, Sample B2, Slide B2.2 (stained for 4 hours)
7. *Subtilisphaera* sp.; Nazaré Section, Sample T1, Slide T1.1 (stained for 15 minutes)
8. *Subtilisphaera* sp.; Nazaré Section, Sample T1, Slide T1.1 (stained for 15 minutes)
9. *Subtilisphaera* sp.; Nazaré Section, Sample T1, Slide T1.1 (stained for 15 minutes)



APPENDIX



50µm

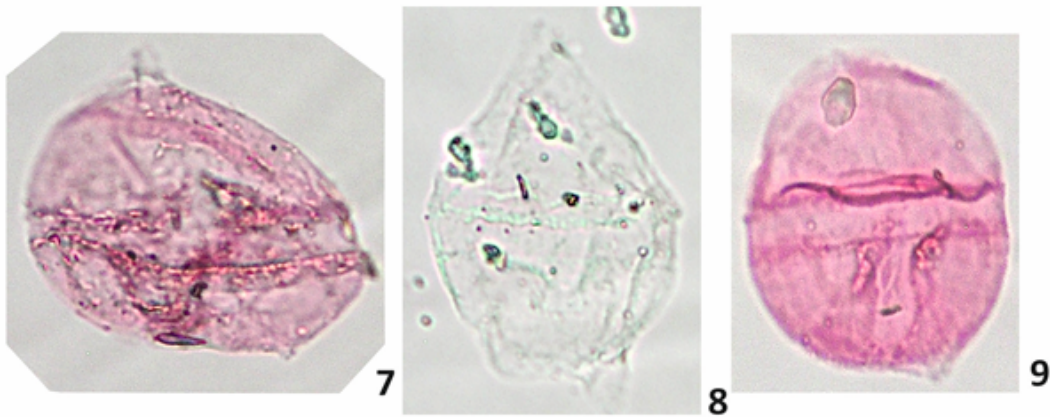
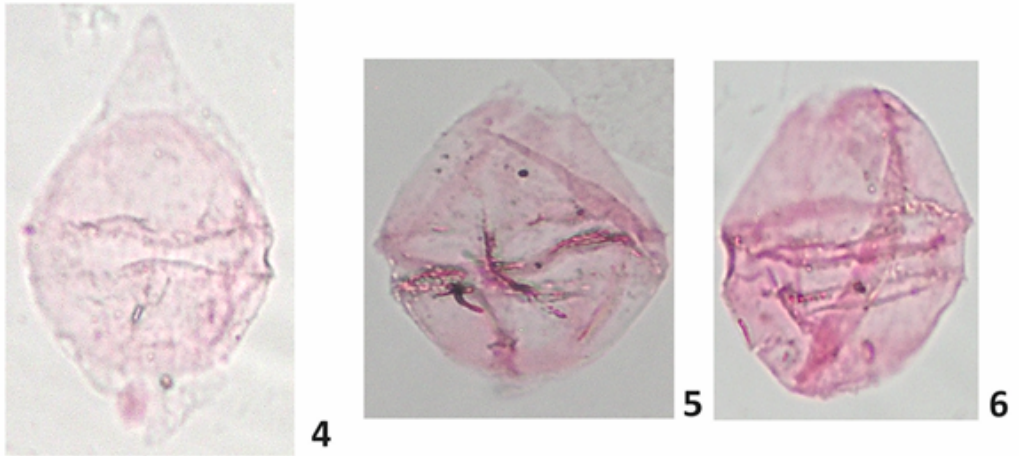
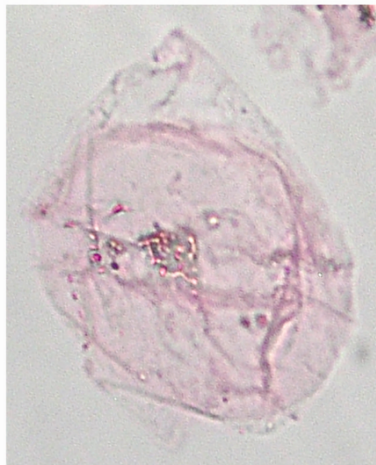


**Plate 22**

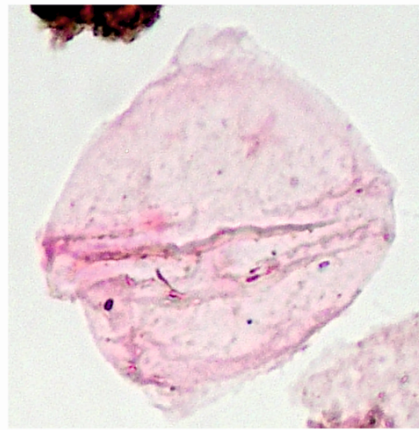
1. *Subtilisphaera* sp.; Nazaré Section, Sample T1, Slide T1.1 (stained for 15 minutes)
2. *Subtilisphaera* sp.; Nazaré Section, Sample T1, Slide T1.1 (stained for 15 minutes)
3. *Subtilisphaera* sp.; Nazaré Section, Sample T1, Slide T1.1 (stained for 4 hours)
4. *Subtilisphaera* sp.; Nazaré Section, Sample T1, Slide T1.1 (stained for 15 minutes)
5. *Subtilisphaera* sp.; Nazaré Section, Sample T1, Slide T1.1 (stained for 15 minutes)



1



2



3



4



5

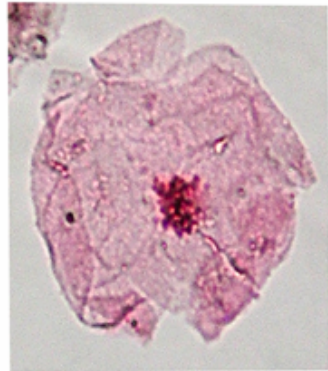
50μm



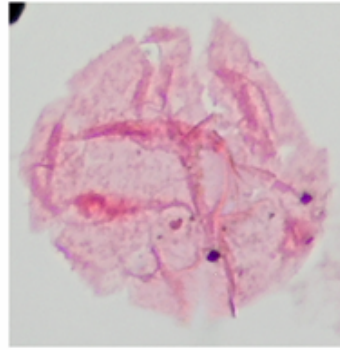
**Plate 23**

1. *Trithyrodinium suspectum* (Manum and Cookson, 1964) Davey, 1969; Nazaré Section, Sample T1, Slide T1.1 (stained for 4 hours)
2. *Trithyrodinium suspectum* (Manum and Cookson, 1964) Davey, 1969; Nazaré Section, Sample T1, Slide T1.1 (stained for 15 minutes)
3. *Trithyrodinium suspectum* (Manum and Cookson, 1964) Davey, 1969; Nazaré Section, Sample T1, Slide T1.1 (stained for 15 minutes)
4. *Trithyrodinium suspectum* (Manum and Cookson, 1964) Davey, 1969; Nazaré Section, Sample T1, Slide T1.1 (stained for 4 hours)
5. *Trithyrodinium suspectum* (Manum and Cookson, 1964) Davey, 1969; Nazaré Section, Sample T1, Slide T1.1 (stained for 15 minutes)
6. *Trithyrodinium suspectum* (Manum and Cookson, 1964) Davey, 1969; Nazaré Section, Sample T1, Slide T1.1 (stained for 15 minutes)
7. *Trithyrodinium suspectum* (Manum and Cookson, 1964) Davey, 1969; Nazaré Section, Sample T1, Slide T1.1 (stained for 15 minutes)

APPENDIX

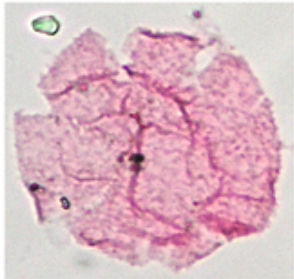


1

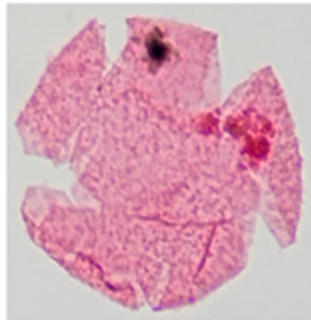


2

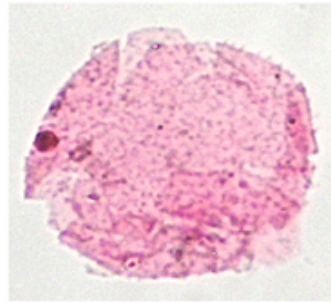
50µm



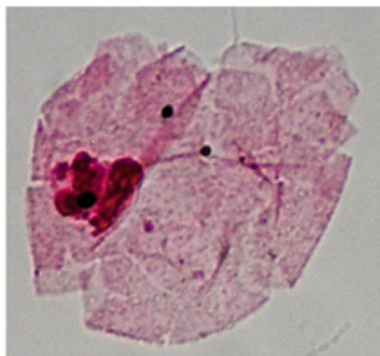
3



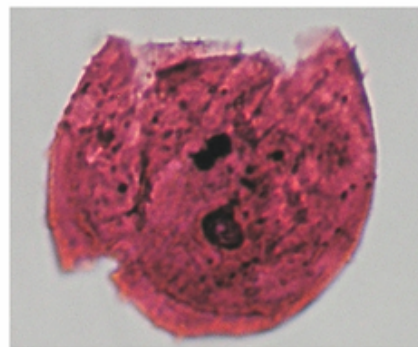
4



5



6

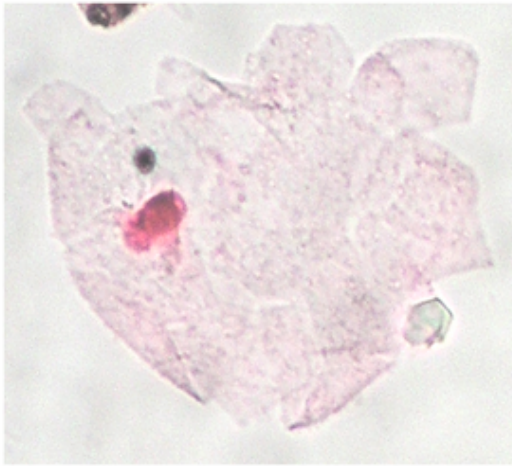


7

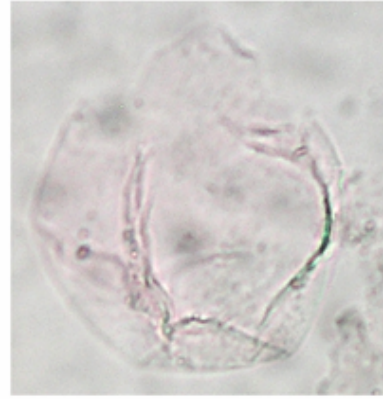
**Plate 24**

1. *Trithyrodinium* sp.; Nazaré Section, Sample B2, Slide B2.1 (stained for 15 minutes)
2. *Trithyrodinium* sp.; Nazaré Section, Sample T1, Slide T1.1
3. *Trithyrodinium* sp.; Nazaré Section, Sample B1, Slide 1B.4 (stained for 15 minutes)
4. *Trithyrodinium* sp.; Nazaré Section, Sample M2, Slide 2M.1
5. *Trithyrodinium* sp.; Nazaré Section, Sample B2, Slide B2.1 (stained for 15 minutes)

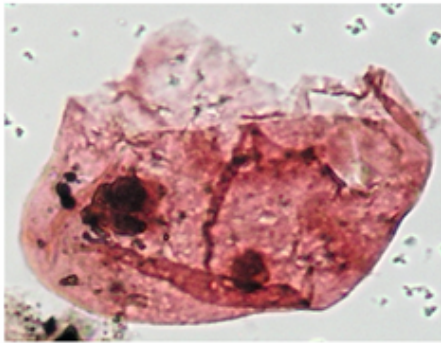
APPENDIX



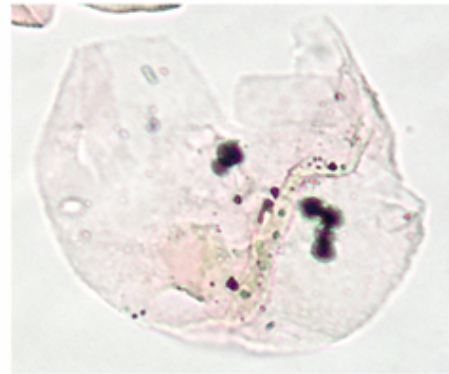
1



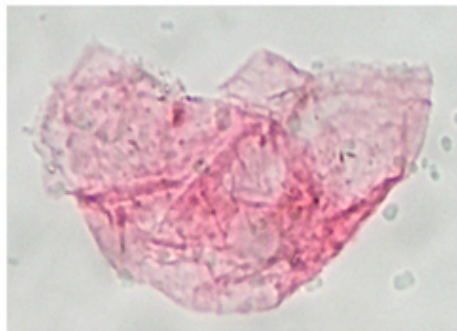
2



3



4



5

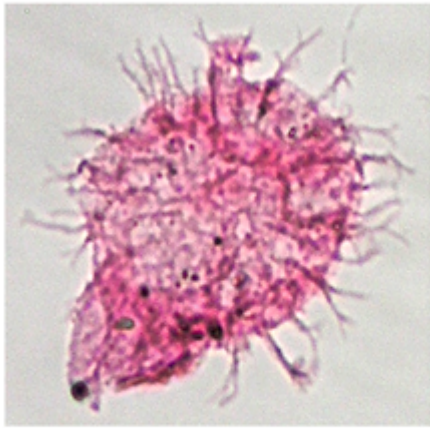
50μm



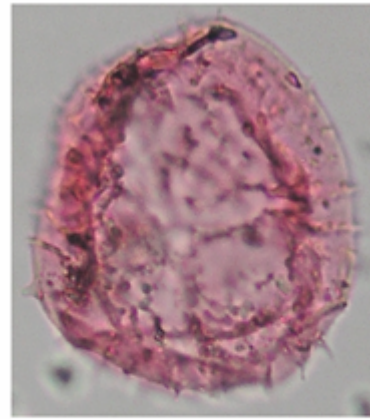
**Plate 25**

1. *Diphyes* sp.; Nazaré Section, Sample T1, Slide T1.1 (stained for 15 minutes)
2. Dinocyst type A; Nazaré Section, Sample B4, Slide B4.1
3. Dinocyst type A; Nazaré Section, Sample B4, Slide B4 (stained for 15 minutes)
4. Dinocyst type A; Nazaré Section, Sample B4, Slide B4.1

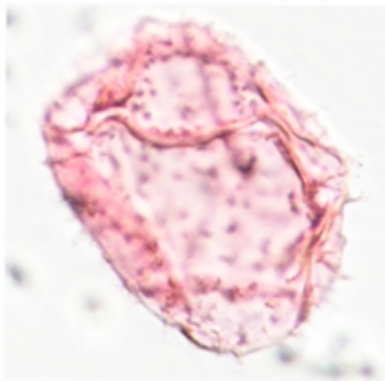




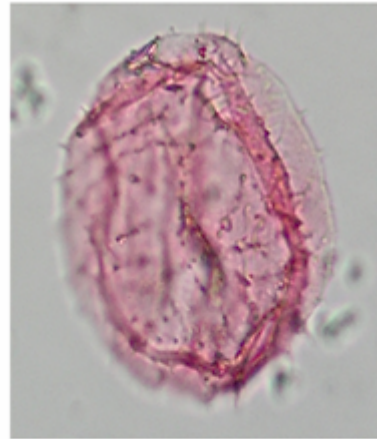
1



2



3



4

50μm



**Plate 26**

1. *Botryococcus* sp. (Compound colony showing connecting strands and cells); Nazaré Section, Sample B1, Slide B1.3 (stained for 15 minutes)
2. *Botryococcus* sp. (Compound colony showing connecting strands and cells); Nazaré Section, Sample B1, Slide B1.1 (stained for 15 minutes)
3. *Botryococcus* sp. (Compound colony showing connecting strands and cells); Nazaré Section, Sample B1, Slide B1\_1B-1 (stained for 15 minutes)
4. *Leiosphaeridia* sp.; Nazaré Section, Sample B2, Slide B2.1 (stained for 15 minutes)
5. *Leiosphaeridia* sp.; Nazaré Section, Sample B2, Slide B2.1 (stained for 15 minutes)
6. *Leiosphaeridia* sp.; Nazaré Section, Sample B1, Slide B1.4 (stained for 15 minutes)
7. *Pterospmella* sp.; Nazaré Section, Sample B4, Slide B4.1 (stained for 15 minutes)
8. *Crassosphaera* sp.; Nazaré Section, Sample B2, Slide B2.2 (stained for 15 minutes)

APPENDIX

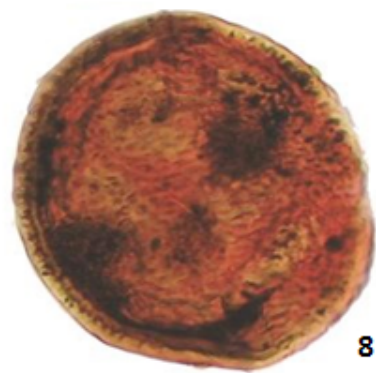
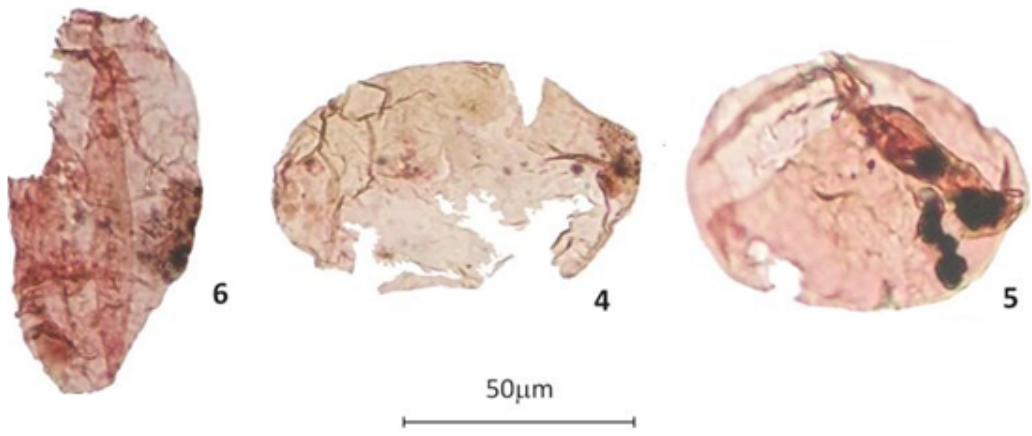
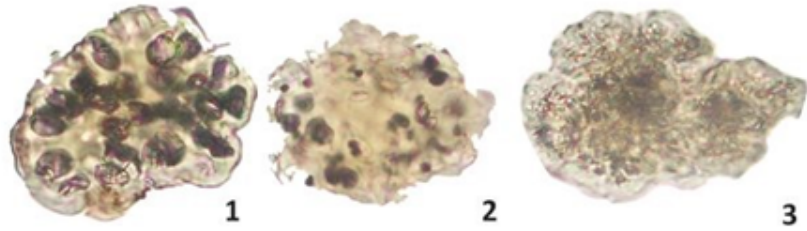


**Plate 27**

1. Microforaminiferal linings (Single chamber); Nazaré Section, Sample B3, Slide B3.1 (stained for 15 minutes)
2. Microforaminiferal linings (Uniserial); Nazaré Section, Sample B2, Slide B2.1 (stained for 4 hours)
3. Microforaminiferal linings (Biserial); Nazaré Section, Sample B3, Slide B3.1 (stained for 15 minutes)
4. Microforaminiferal linings (Biserial); Nazaré Section, Sample B3, Slide B3.1 (stained for 15 minutes)
5. Microforaminiferal linings (Biserial); Nazaré Section, Sample B3, Slide B3.1 (stained for 15 minutes)

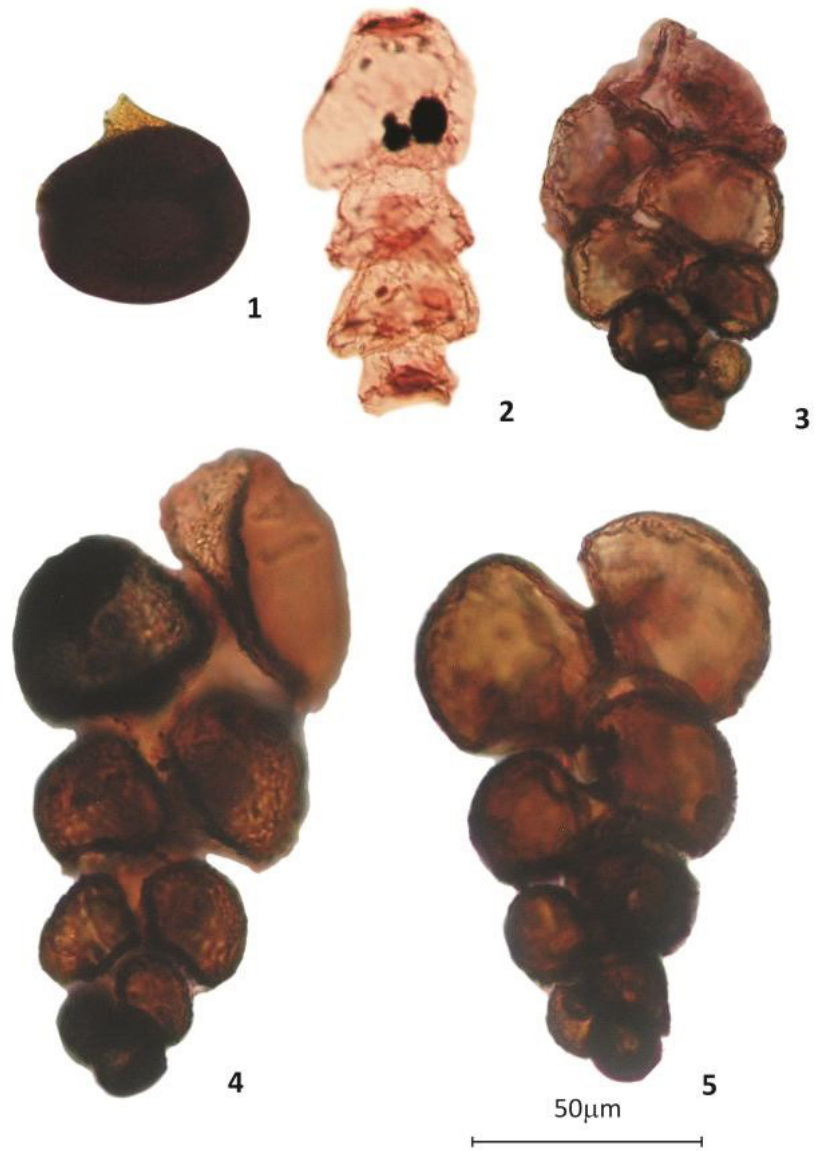


**Plate 28**

1. Microforaminiferal linings (Compound, coiled uniserial); Nazaré Section, Sample B4, Slide B4.1 (stained for 15 minutes)
2. Microforaminiferal linings (Planispiral, laterally appressed); Nazaré Section, Sample T1, Slide T1.1 (stained for 4 hours)
3. Microforaminiferal linings (Compound, coiled biserial); Nazaré Section, Sample B3, Slide B3.1 (stained for 15 minutes)
4. Microforaminiferal linings (Compound, coiled biserial); Nazaré Section, Sample B3, Slide B3.1 (stained for 15 minutes)

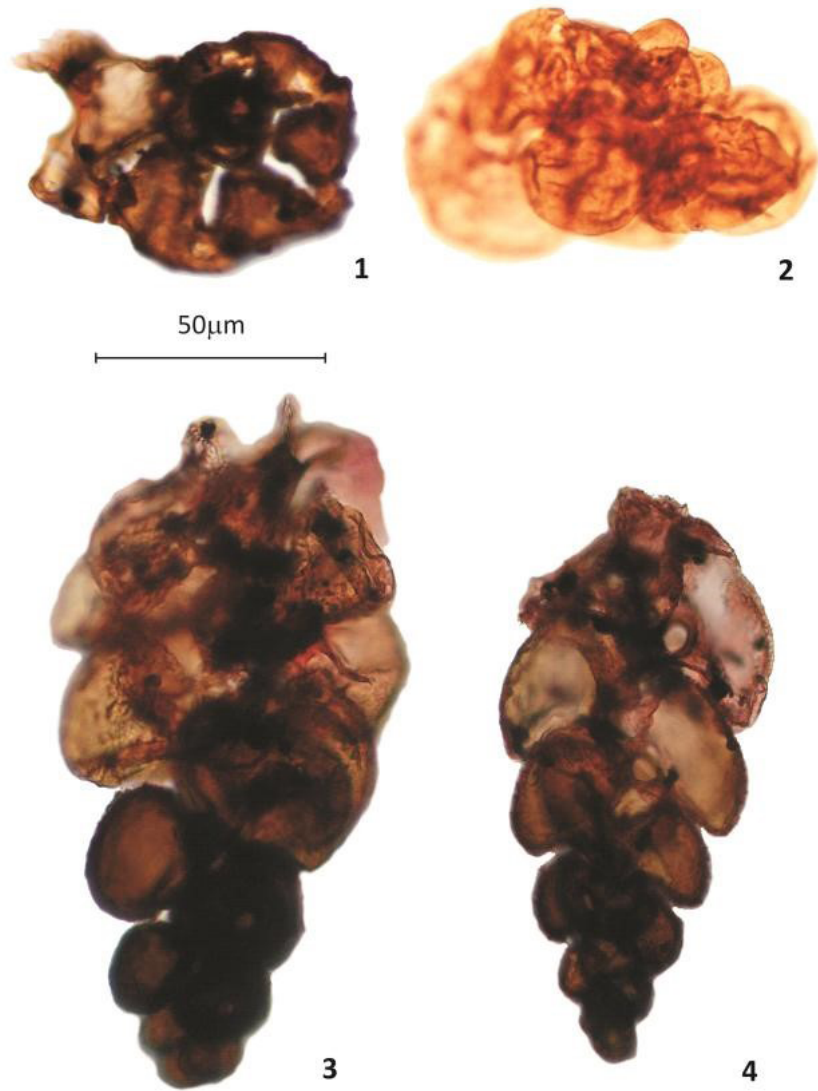


**Plate 29**

1. Microforaminiferal linings (Coiled Trochospiral, chambers overlap); Nazaré Section, Sample B3, Slide B3.1 (stained for 15 minutes)
2. Microforaminiferal linings (Coiled Trochospiral, chambers overlap); Nazaré Section, Sample B1, Slide B1.2 (stained for 15 minutes)
3. Microforaminiferal linings (Coiled Trochospiral, chambers overlap); Nazaré Section, Sample B1, Slide B1.4 (stained for 15 minutes)
4. Microforaminiferal linings (Coiled Trochospiral, chambers overlap); Nazaré Section, Sample B3, Slide B3.1 (stained for 15 minutes)
5. Microforaminiferal linings (Coiled Trochospiral, chambers overlap); Nazaré Section, Sample B2, Slide B2.2 (stained for 15 minutes)



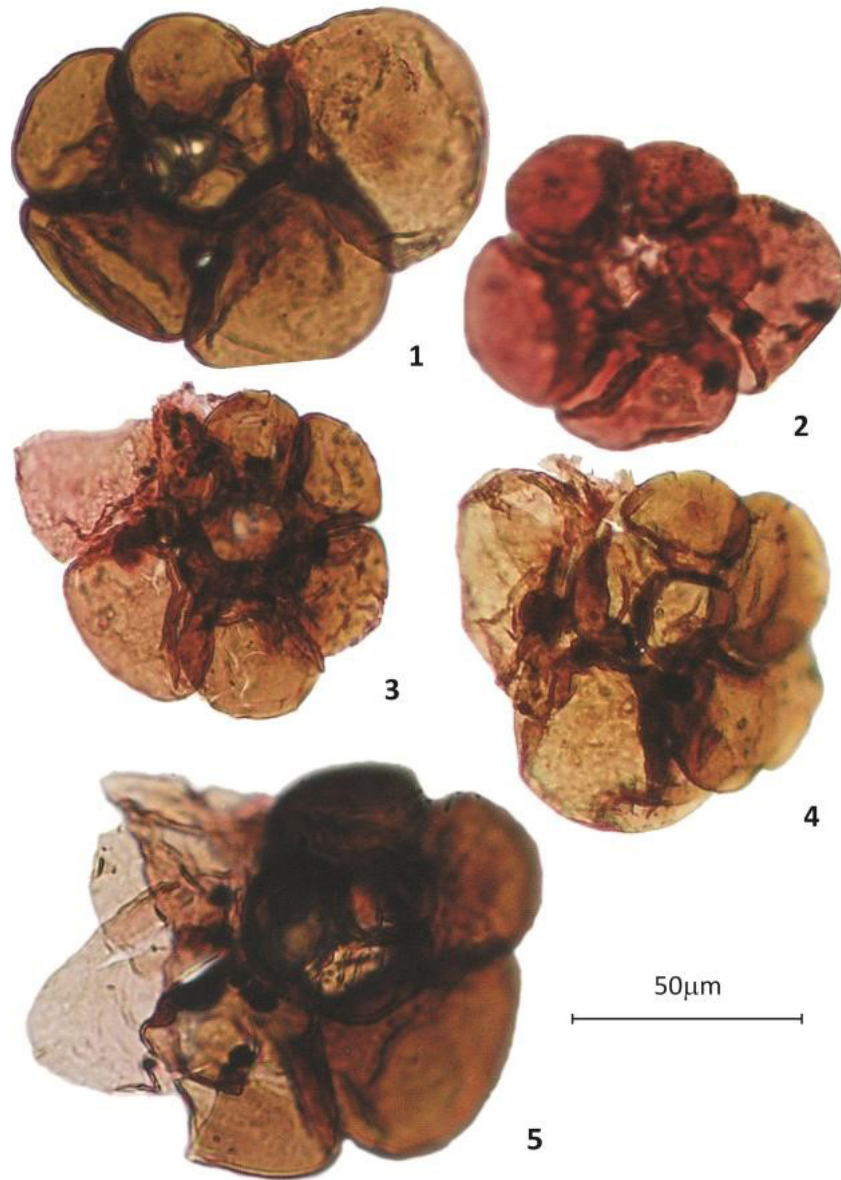


**Plate 30**

1. Microforaminiferal linings (Coiled Trochospiral, chambers overlap); Nazaré Section, Sample B1, Slide B1.1 (stained for 15 minutes)
2. Microforaminiferal linings (Coiled Trochospiral, laterally appressed); Nazaré Section, Sample B2, Slide B2.1 (stained for 15 minutes)
3. Microforaminiferal linings (Coiled planispiral, chambers discrete); Nazaré Section, Sample T1, Slide T1.1 (stained for 4 hours)
4. Microforaminiferal linings (Coiled planispiral, chambers discrete); Nazaré Section, Sample B1, Slide B1.2 (stained for 15 minutes)

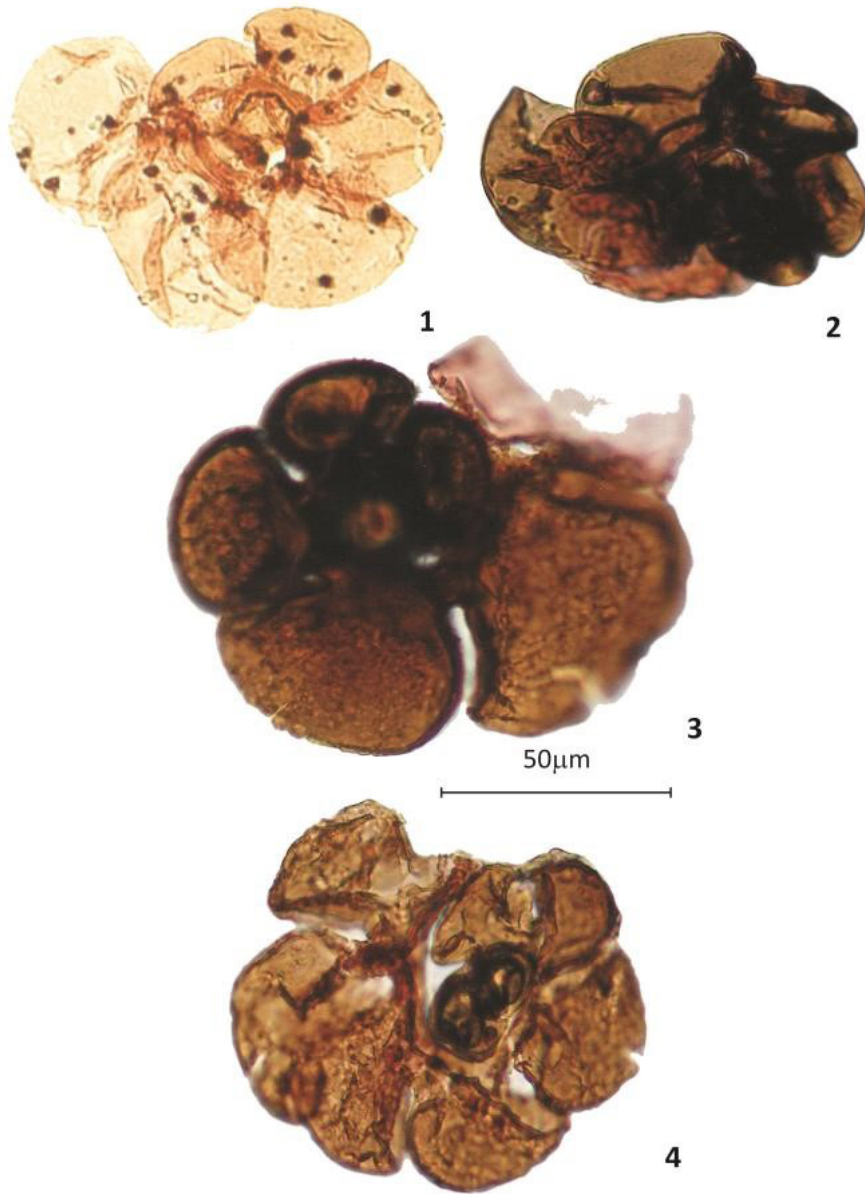


**Plate 31**

1. Microforaminiferal linings (Coiled planispiral, chambers discrete and separate);  
Nazaré Section, Sample T1, Slide T1.1 (stained for 4 hours)
2. Microforaminiferal linings (Coiled planispiral, chambers discrete and separate);  
Nazaré Section, Sample T1, Slide T1.1 (stained for 4 hours)
3. Microforaminiferal linings (Coiled planispiral, chambers discrete and separate);  
Nazaré Section, Sample B3, Slide B3 (stained for 4 hours)
4. Microforaminiferal linings (Coiled planispiral, chambers discrete and separate);  
Nazaré Section, Sample B3, Slide B3 (stained for 4 hours)



50µm

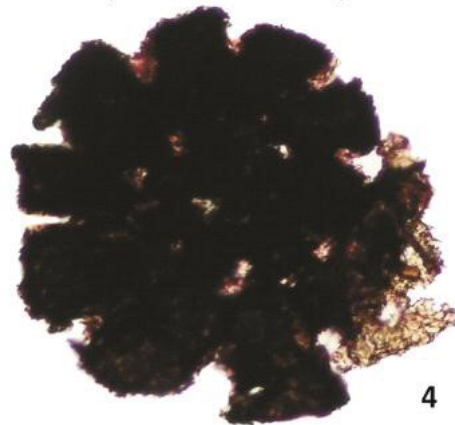


**Plate 32**

1. Scolecodont; Nazaré Section, Sample B2, Slide 2B-2 (stained for 15 minutes)
2. Spiny acritarch; Nazaré Section, Sample B4, Slide B4 (stained for 15 minutes)

50µm



**1**



**2**

**Plate 33**

1. Plant - derived cuticle (cuticle with stoma); Nazaré Section, Sample B2, Slide B2.2 (stained for 4 hours)
2. Plant - derived cuticle (cuticle with stoma); Nazaré Section, Sample B2, Slide B2.1 (stained for 4 hours)



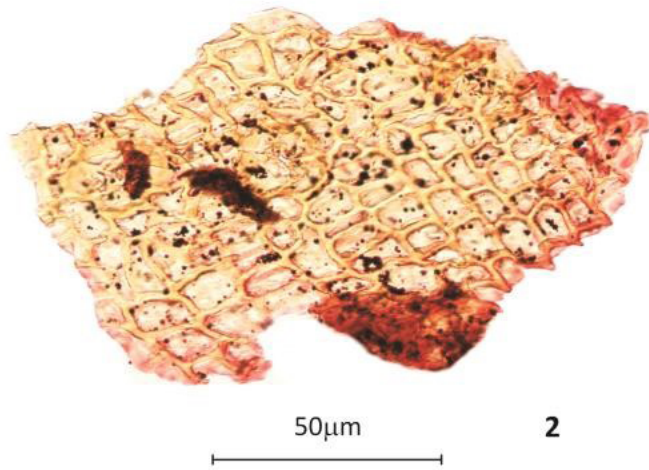
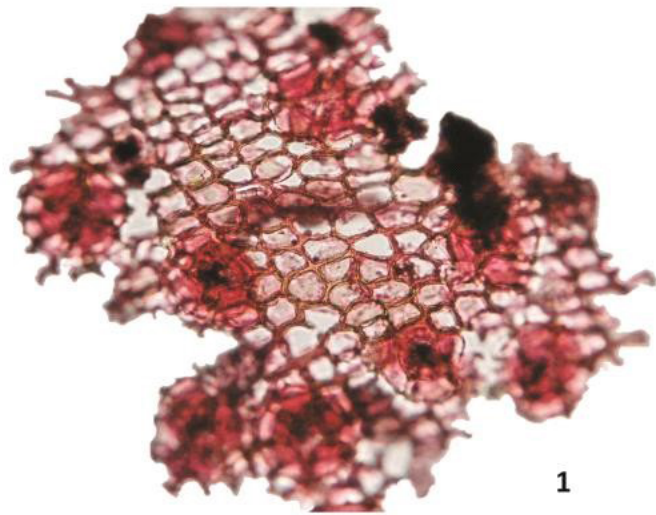


**Plate 34**

1. Plant - derived cuticle; Nazaré Section, Sample B2, Slide B2.4 (stained for 4 hours)
2. Plant - derived cuticle; Nazaré Section, Sample T1, Slide T1.1 (stained for 4 hours)
3. Plant - derived cuticle; Nazaré Section, Sample B2, Slide B2.2 (stained for 4 hours)
4. Plant - derived cuticle; Nazaré Section, Sample T1, Slide T1.1 (stained for 4 hours)
5. Plant - derived cuticle; Nazaré Section, Sample M2, Slide M2.1 (stained for 4 hours)

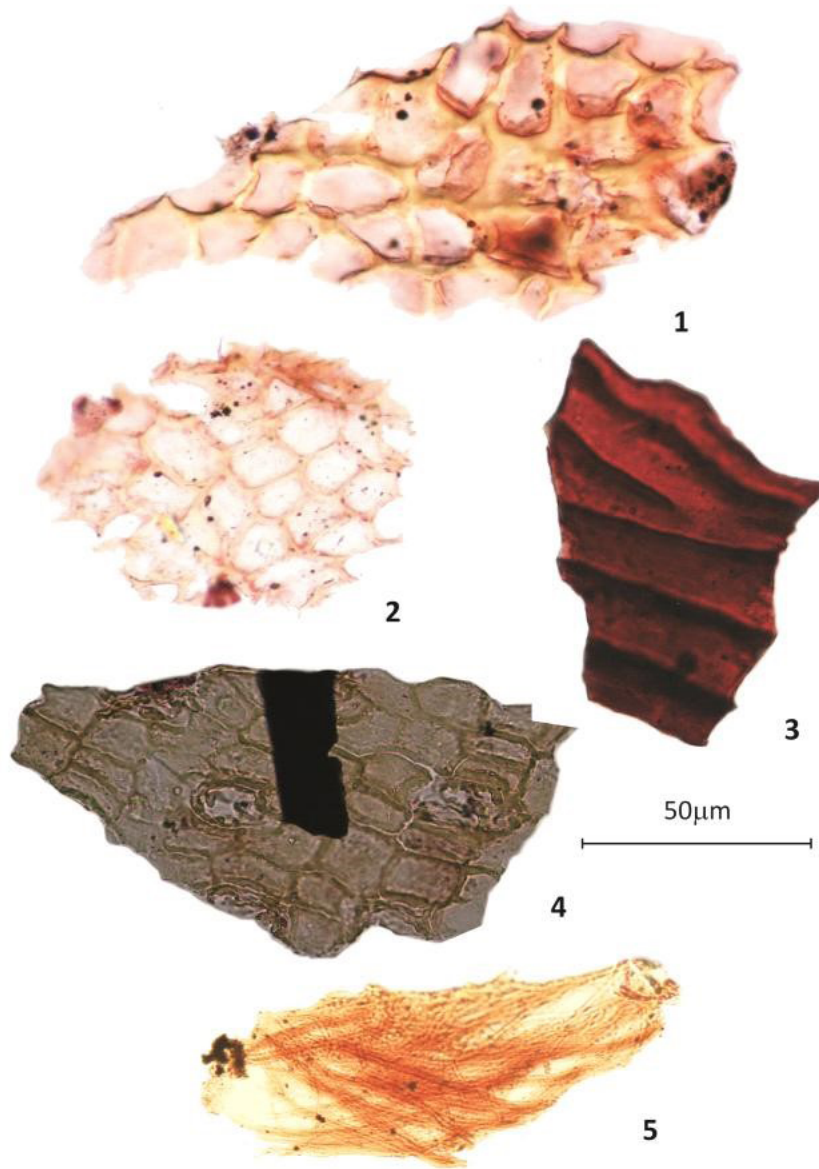


**Plate 35**

1. Plant - derived cuticle; Nazaré Section, Sample B2, Slide B2.2 (stained 4 hours)
2. Plant - derived cuticle; Nazaré Section, Sample T1, Slide T1.1 (stained 4 hours)
3. Plant - derived cuticle; Nazaré Section, Sample B3, Slide B3.1
4. Animal? - derived cuticle; Nazaré Section, Sample T1, Slide T1.1

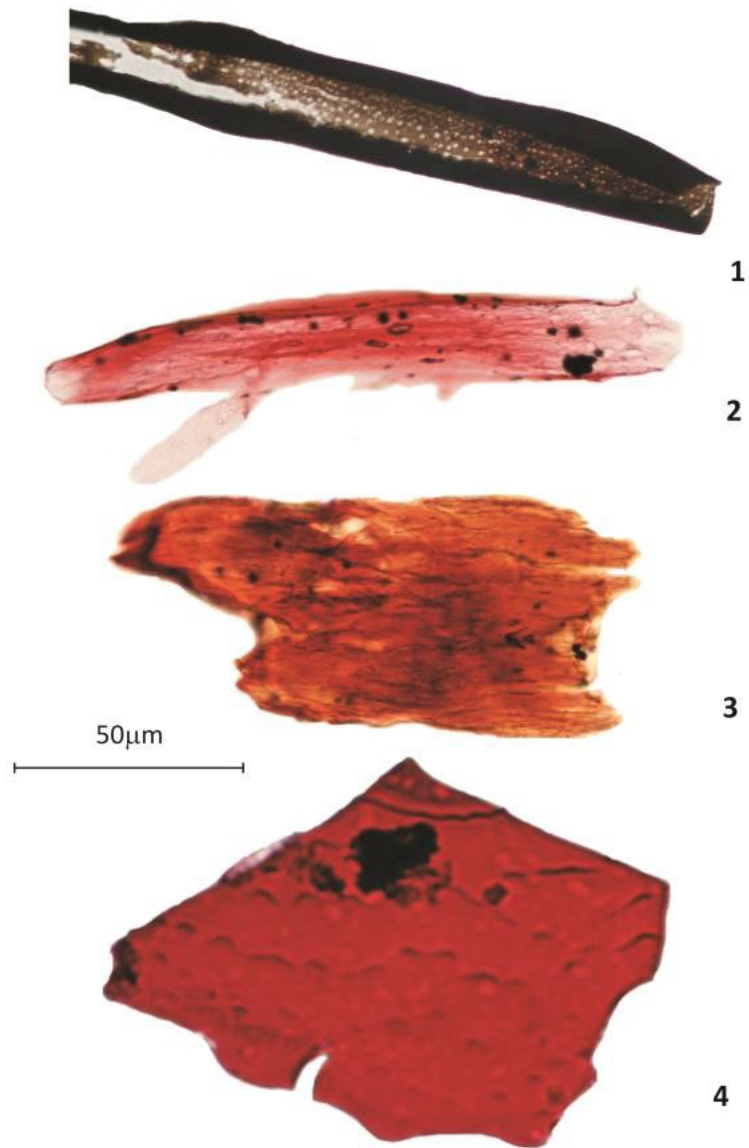


**Plate 36**

1. *Cicatricosisporites* spp.; Nazaré Section, Sample B3, Slide B 3.1 (stained for 15 minutes)
2. *Cicatricosisporites* spp.; Nazaré Section, Sample T1, Slide T1.1a (stained for 15 minutes)
3. *Cicatricosisporites* spp.; Nazaré Section, Sample T1, Slide T1.1c (stained for 15 minutes)
4. *Cicatricosisporites* spp.; Nazaré Section, Sample B2, Slide 2.1 (stained for 15 minutes)
5. *Cicatricosisporites* spp.; Nazaré Section, Sample B1, Slide B 1.1 (stained for 15 minutes)
6. *Cicatricosisporites* spp.; Nazaré Section, Sample B1, Slide B 1.4 (stained for 15 minutes)
7. *Cicatricosisporites* spp.; Nazaré Section, Sample B1, Slide B 1.1 (stained for 15 minutes)

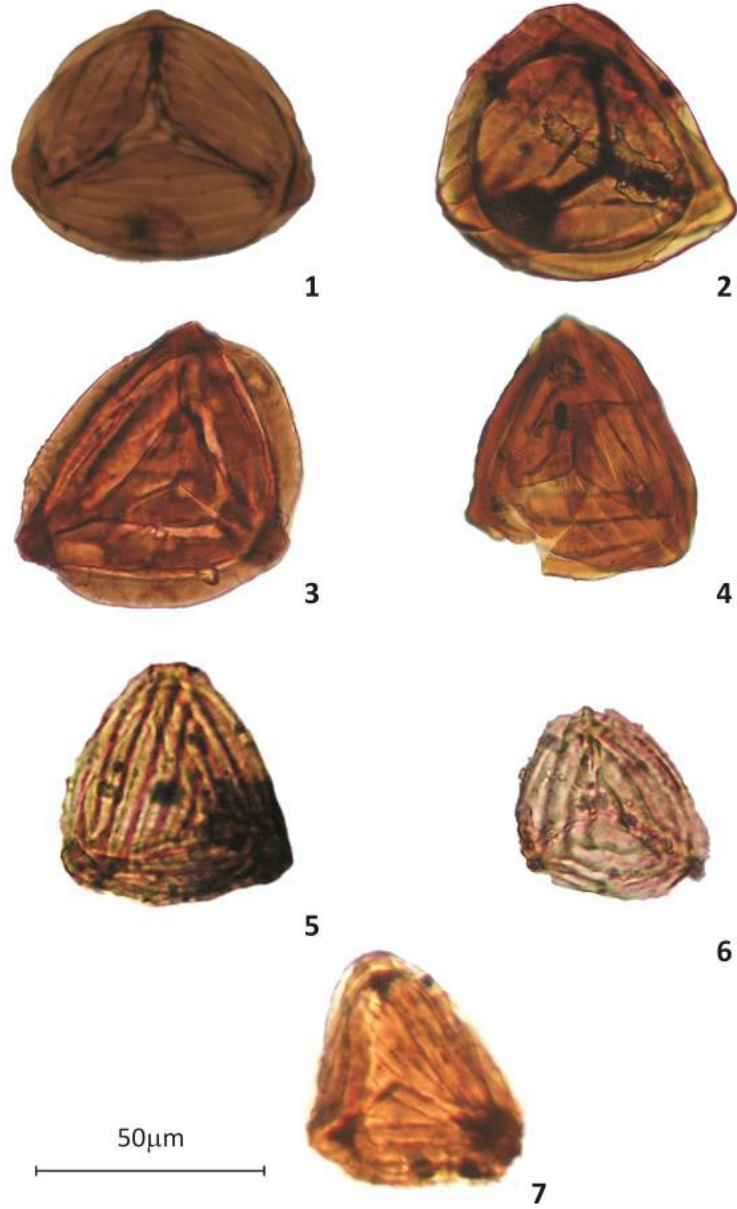


**Plate 37**

1. *Contignisporites cooksonii* (Balme 1957) Dettmann 1963; Nazaré section, Sample T1, Slide T 1.1 (stained for 15 minutes)
2. *Contignisporites cooksonii* (Balme 1957) Dettmann 1963; Nazaré Section, Sample B2, Slide B2.1 (stained for 15 minutes)
3. *Contignisporites* sp.; Nazaré Section, Sample B1, Slide B 1.4 (stained for 15minutes)
4. *Contignisporites* sp.; Nazaré Section, Sample B2, Slide B 2.1 (stained for 15 minutes)
5. *Plicatella* sp.; Nazaré Section, Sample T1, Slide T1.1 (stained for 15 minutes)
6. *Plicatella* sp.; Nazaré Section, Sample B1, Slide B1.1 (stained for 15 minutes)
7. *Plicatella* sp.; Nazaré Section, Sample B1, Slide B1.2 (stained for 15 minutes)



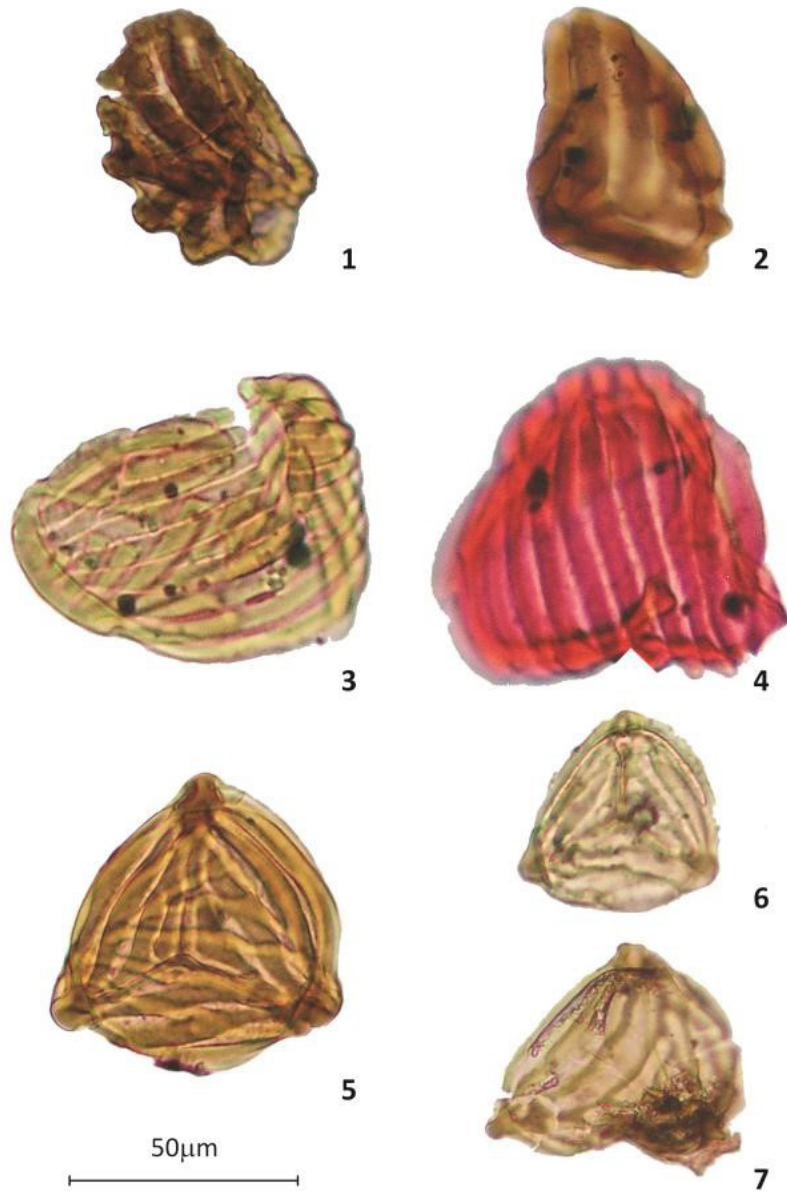


**Plate 38**

1. *Patellasporites* sp.; Nazaré Section, Sample B 2, Slide B 2.1 (stained for 15 minutes)
2. *Patellasporites* sp.; Nazaré Section, Sample B 3, Slide B 3.1 (vermelha)
3. *Patellasporites* sp.; Nazaré Section, Sample B 2, Slide B 2.1 (stained for 15 minutes)
4. *Patellasporites* sp.; Nazaré Section, Sample T 1, Slide T 1.1 (stained for 15 minutes)
5. *Patellasporites* sp.; Nazaré Section, Sample B 2, Slide B 2.2 (stained for 15 minutes)
6. *Patellasporites* sp.; Nazaré Section, Sample B 2, Slide B 2.1 (stained for 15 minutes)
7. *Patellasporites* sp.; Nazaré Section, Sample B 2, Slide B 2.1 (stained for 15 minutes)
8. *Patellasporites* sp.; Nazaré Section, Sample B 2, Slide B 2.1 (stained for 15 minutes)
9. *Patellasporites* sp.; Nazaré Section, Sample B 1, Slide B 1.2 (stained for 15 minutes)
10. *Patellasporites* sp.; Nazaré Section, Sample B 4, Slide B 4.1 (stained for 15 minutes)
11. *Patellasporites* sp.; Nazaré Section, Sample B 1, Slide B 1.2 (stained for 15 minutes)
12. *Patellasporites* sp.; Nazaré Section, Sample B 2, Slide B 2.1 (stained for 15 minutes)

APPENDIX

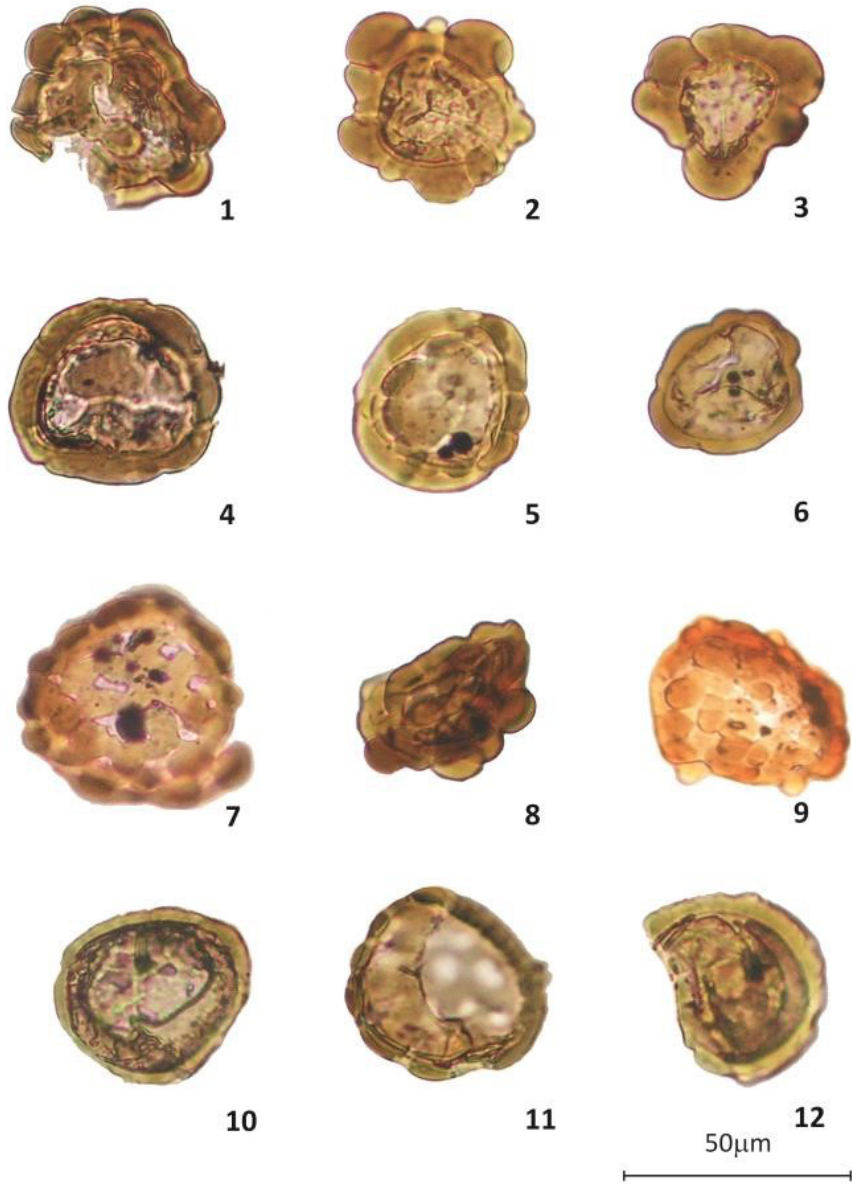


**Plate 39**

1. *Afropollis jardinus* (Brenner) Doyle, Doerenkamp and Jardiné, 1982; Nazaré Section, Sample B2, Slide B2.1 (stained for 15 minutes)
2. *Afropollis* sp.; Nazaré Section, Sample B 2, Slide B2.1 (stained for 15 minutes)
3. *Alisporites* sp.; Nazaré Section, Sample B 3, Slide 3B-1 (stained for 15 minutes)
4. *Alisporites* sp.; Nazaré Section, Sample B 2, Slide B2.1 (stained for 15 minutes)
5. *Alisporites* sp.; Nazaré Section, Sample B 2, Slide B2.1 (stained for 15 minutes)
6. *Alisporites* sp.; Nazaré Section, Sample T 1, Slide T1.1 (stained for 4h)
7. *Cycadopites* sp.; Nazaré Section, Sample B 2, Slide B2.1 (stained for 15 minutes)
8. *Cycadopites* sp.; Nazaré Section, Sample B 2, Slide B2.1 (stained for 15 minutes)
9. *Ephedripites* sp.; Nazaré Section, Sample B 2, Slide B2.1 (stained for 15 minutes)

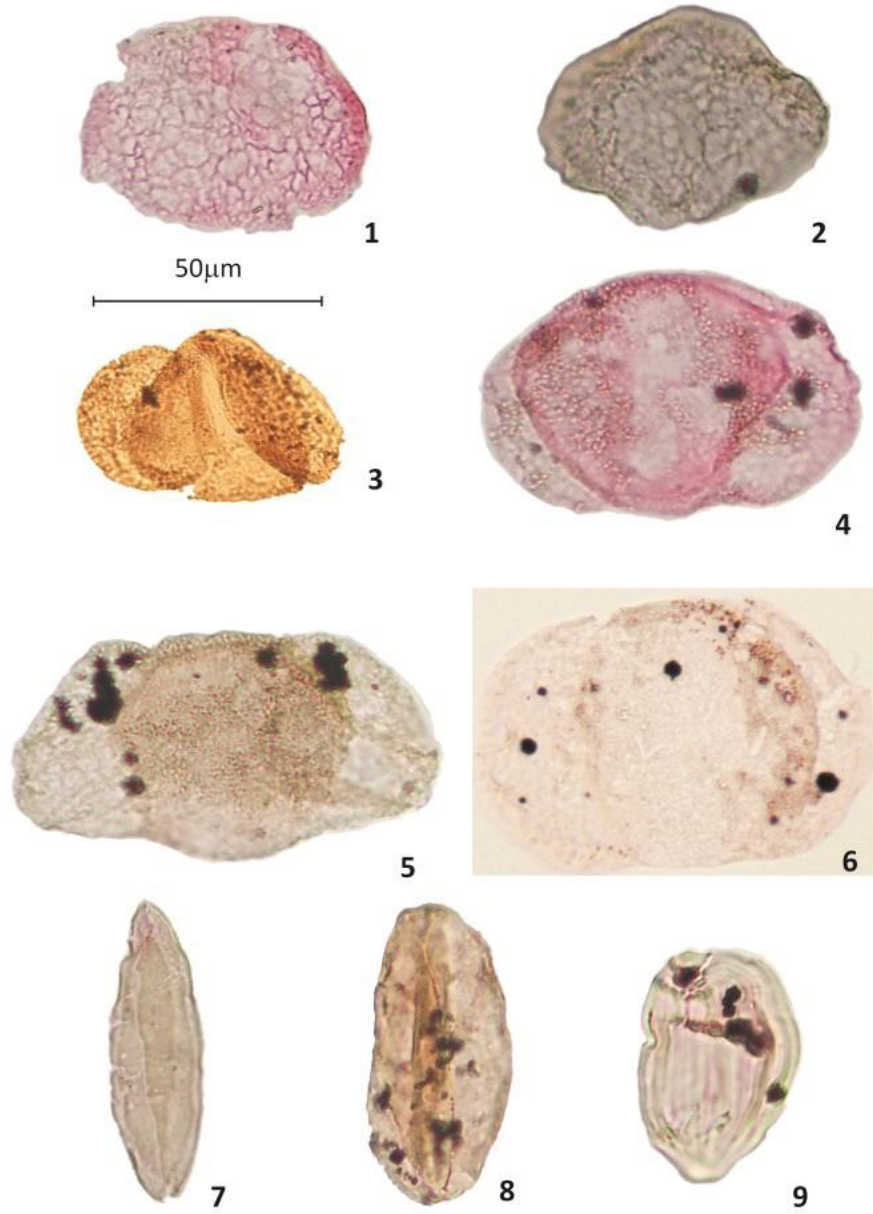


**Plate 40**

1. *Araucariacites australis* (Cookson 1947); Nazaré Section, Sample T 1, Slide T1.1 (stained for 4h)
2. *Araucariacites* sp., Nazaré Section, Sample T 1, Slide T1.1 (stained for 4h)
3. *Araucariacites* sp., Nazaré Section, Sample M 1, Slide M1.1 (stained for 4h)
4. *Araucariacites* sp., Nazaré Section, Sample T 1, Slide T1.1 (stained for 4h)
5. *Corollina obidosensis* (Groot and Groot, 1962); Nazaré Section, Sample T 1, Slide T1.1 (stained for 4h)
6. *Corollina* sp. Tetrad; Nazaré Section, Sample B 2, Slide B2.1 (stained for 15 minutes)

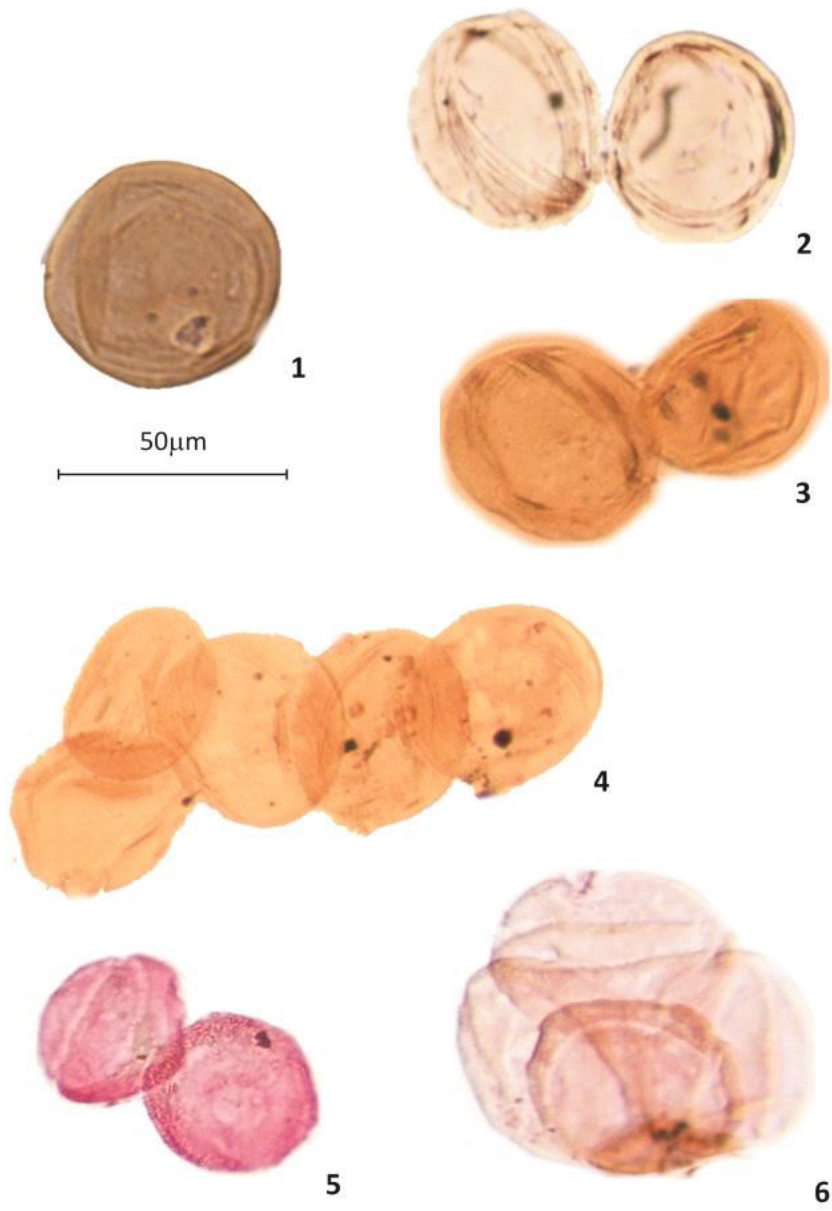


**Plate 41**

1. *Classopollis brasiliensis* (Hernegreen 1975); Nazaré Section, Sample B 1, Slide B1.3 (stained for 15 minutes)
2. *Classopollis brasiliensis* (Hernegreen 1975); Nazaré Section, Sample B 1, Slide B1.2 (stained for 15 minutes)
3. *Classopollis brasiliensis* (Hernegreen 1975); Nazaré Section, Sample B 1, Slide B1.1 (stained for 15 minutes)
4. *Classopollis brasiliensis* (Hernegreen 1975); Nazaré Section, Sample B 1, Slide B1.4 (stained for 15 minutes)
5. *Classopollis brasiliensis* (Hernegreen 1975); Nazaré Section, Sample B 1, Slide B1.3 (stained for 15 minutes)
6. *Classopollis brasiliensis* (Hernegreen 1975); Nazaré Section, Sample B 1, Slide B1.4 (stained for 15 minutes)
7. *Classopollis brasiliensis* (Hernegreen 1975); Nazaré Section, Sample B 1, Slide B1.2 (stained for 15 minutes)
8. *Classopollis brasiliensis* (Hernegreen 1975); Nazaré Section, Sample B 1, Slide B1.2 (stained for 15 minutes)
9. *Classopollis brasiliensis* (Hernegreen 1975); Nazaré Section, Sample B 2, Slide B2.1 (stained for 15 minutes)
10. *Classopollis jardinei* (Reyre, Kieser and Pujl 1970); Nazaré Section, Sample M 2, Slide M2.1 (stained for 15 minutes)
11. *Classopollis* cf. *jardinei* (Reyre, Kieser and Pujl 1970); Nazaré Section, Sample B 1, Slide B1.1 (stained for 15 minutes)
12. *Classopollis* sp. Tetrad; Nazaré Section, Sample B 1, Slide B 1.4 (stained for 15 minutes)
13. *Classopollis* sp. Tetrad; Nazaré Section, Sample B 1, Slide B 1.1 (stained for 15 minutes)



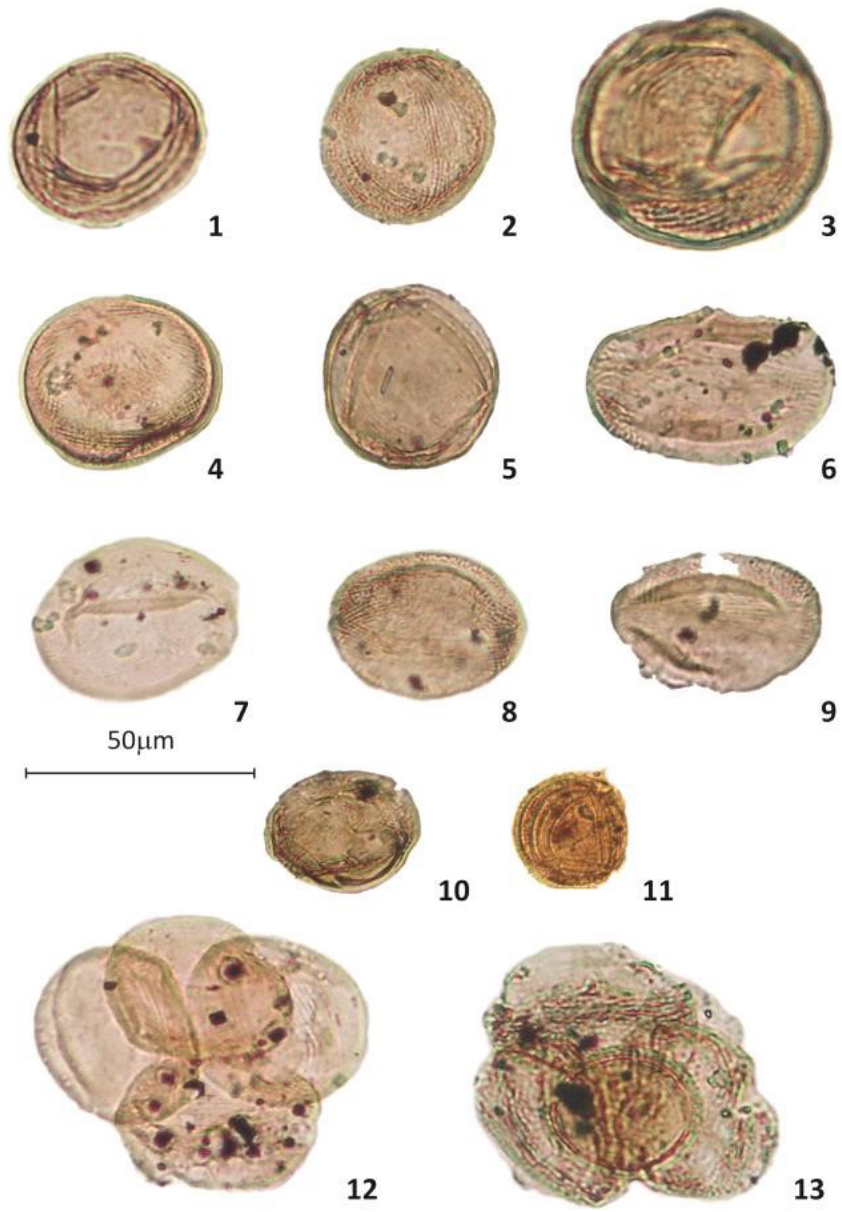
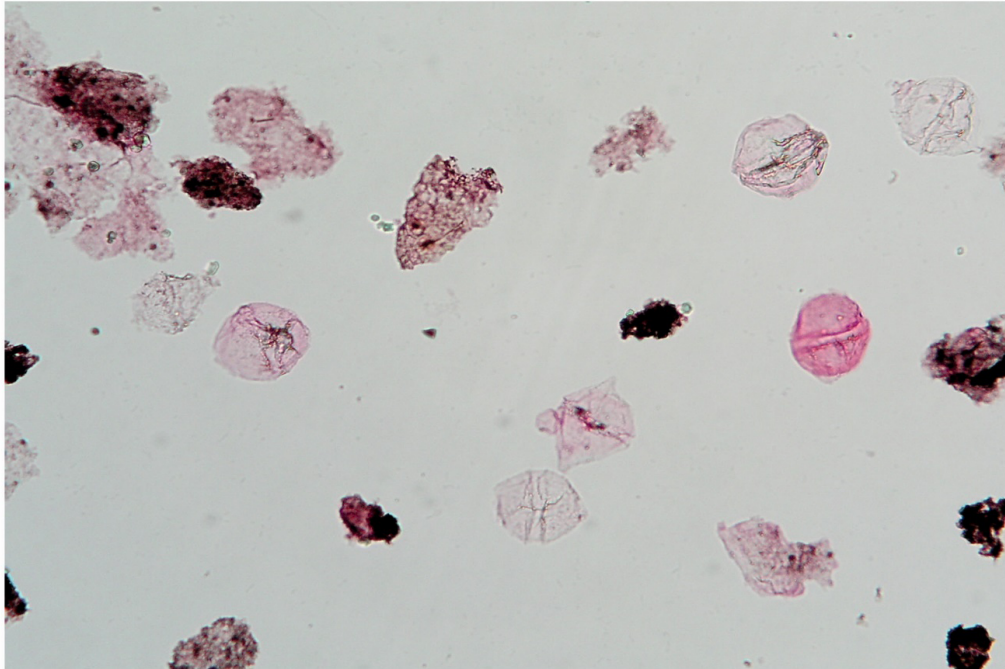


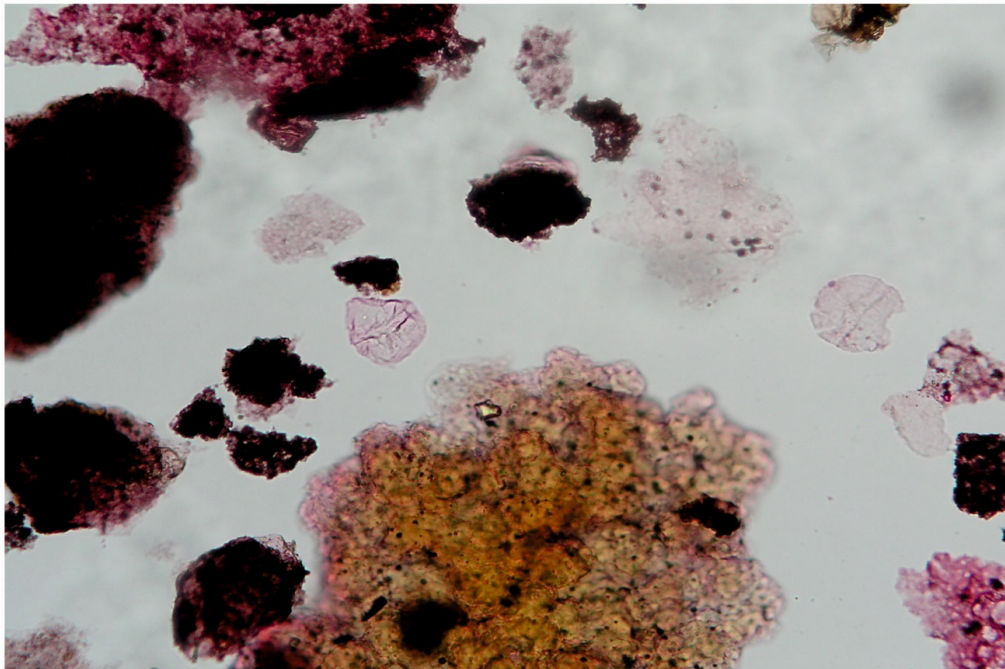
**Plate 42**

1. General view of Sample T1, Slide T1.1 (stained for 4 hours) - large numbers of *Subtilisphaera* sp.
2. General view of sample T1, Slide T1.1 (stained 4 hours) - *Subtilisphaera* sp. and *Botryococcus* sp.



1

50µm



2